Automated Digital Microscope for Detection of Schistosomiasis and Soil-Transmitted Helminth Infection

Oyibo, P.O.

DOI
10.4233/uuid:09032422-9c20-4482-874a-afa97432e349

Publication date
2025

Document Version
Final published version

Citation (APA)
Oyibo, P. O. (2025). *Automated Digital Microscope for Detection of Schistosomiasis and Soil-Transmitted Helminth Infection*. [Dissertation (TU Delft), Delft University of Technology].
https://doi.org/10.4233/uuid:09032422-9c20-4482-874a-afa97432e349

Important note
To cite this publication, please use the final published version (if applicable).
Please check the document version above.

Automated Digital Microscope for Detection of Schistosomiasis and Soil-Transmitted Helminth Infection

PROSPER OBARO OYIBO

Automated Digital Microscope for Detection of Schistosomiasis and Soil-Transmitted Helminth Infection

Automated Digital Microscope for Detection of Schistosomiasis and Soil-Transmitted Helminth Infection

Dissertation

for the purpose of obtaining the degree of doctor
at Delft University of Technology
by the authority of the Rector Magnificus,
Prof. dr. ir. T.H.J.J. van der Hagen,
chair of the Board for Doctorates
to be defended publicly on
Tuesday 2 September 2025 at 10:00 o'clock

by

Prosper Obaro OYIBO

Masters of Science in Control Engineering,
Ahmadu Bello University, Zaria, Nigeria
born in Orhuwhorun, Nigeria

This dissertation has been approved by the promotors.

Composition of the doctoral committee:

Rector Magnificus,	chairperson
Prof. dr. ir. G. Vdovin,	Delft University of Technology, *promotor*
Prof. dr. ir. J.C. Diehl,	Delft University of Technology, *promotor*
Prof. dr. W.A. Oyibo,	University of Lagos, Nigeria, *promotor*

Independent members:

Prof. dr. ir. M.B. van Gijzen	Delft University of Technology
Prof. dr. J.J. van Hellemond	Erasmus Medical Center
Prof. dr. E. Spezi	Cardiff University, United Kingdom
Dr. S.M. Jacob	Federal Ministry of Health, Nigeria
Prof. dr. A.R. Balkenende,	Delft University of Technology, reserve member

This research was funded by the Dutch Research Council (NWO-WOTRO), grant number W 07.30318.009 through the inclusive diagnostics for poverty related diseases in Nigeria and Gabon (INSPiRED) Project.

Keywords: Schistosomiasis, Soil-Transmitted Helminthiasis, Digital Microscopy, Deep Learning, Computer Vision
Printed by: ProefschriftMaken

ISBN 978-94-6510-803-2

An electronic copy of this dissertation is available at https://repository.tudelft.nl/.

To my dearest dad, Engr. John E. Oyibo, my loving mum, Mrs. Roseline E. Oyibo, my beloved wife, Oluwaseun, and my precious daughter, Oviereya — for your unwavering love, support, and inspiration.

CONTENTS

SUMMARY

The global burden of schistosomiasis and soil-transmitted helminth (STH) infections is substantial, with millions at risk, particularly in sub-Saharan Africa. Traditional diagnostic methods using optical microscopy are labour intensive, operator dependent, and often inaccessible in remote areas. This thesis focuses on the development and validation of an AI-based digital microscope, the Schistoscope, designed to enhance the diagnosis of these infections, particularly in resource-limited settings. The aim is to bridge existing diagnostic gaps by developing an automated system that reduces reliance on skilled personnel, enhances diagnostic accuracy, and improves accessibility.

The research integrates innovations in hardware design, digital imaging, and artificial intelligence (AI) to create an affordable, efficient, and accurate diagnostic tool that addresses the limitations of traditional microscopy. The primary objectives include designing and developing cost-effective digital microscope prototypes, integrating AI algorithms for automated detection and classification of parasite eggs, and validating the diagnostic performance of the system through field studies. The development process began with two low-cost digital microscope prototypes: the Raspberry Pi-based Schistoscope and the smartphone-based Schistoscope. Both designs focused on affordability, portability, and ease of use, with key innovations such as the integration of 3D-printed components and locally sourced materials to ensure sustainability and ease of maintenance in endemic regions.

Subsequent iterations led to the development of the Schistoscope 5.0, which featured significant improvements in imaging quality, automation, and user interface. The device incorporates a whole slide imaging system with an advanced autofocusing algorithm, enhancing image clarity and diagnostic accuracy. A cornerstone of the thesis is the integration of AI for automated detection and quantification of *Schistosoma haematobium* and intestinal helminth eggs. The diagnostic framework employs deep learning models, particularly convolutional neural networks (CNNs), to perform semantic segmentation and object detection. Key components include the DeepLabV3 with a MobileNetV3 backbone, used for semantic segmentation of Schistosoma haematobium eggs, effectively distinguishing eggs from background artifacts, and the EfficientDet model, applied for the detection of intestinal helminth eggs, including *Ascaris lumbricoides*, *Trichuris trichiura*, hookworm, and *Schistosoma mansoni*.

The models were trained on robust datasets collected from field sam-

ples, with extensive image annotation to ensure accuracy. The diagnostic system demonstrated high sensitivity and specificity, meeting the World Health Organisation's target product profiles for schistosomiasis and STH control programs. Comprehensive field validation studies were conducted in Nigeria and Gabon to assess the real-world performance of the Schistoscope. These studies compared the device's diagnostic accuracy with conventional microscopy and composite reference standards incorporating real-time PCR and UCP-LF CAA. In Nigeria, the study also focused on the usability and acceptability of the Schistoscope among healthcare workers, demonstrating high acceptance rate of both the semi- and fully automated modes. In Gabon, the diagnostic performance was assessed on fresh and banked urine samples, with the Schistoscope demonstrating comparable accuracy to traditional microscopy, alongside the added benefits of automation and reduced diagnostic time.

Key findings highlight improved diagnostic accuracy, with the Schistoscope achieving high precision and sensitivity in detecting schistosomiasis and STH infections. The integration of AI reduced the need for skilled personnel, thereby enhancing automation and efficiency. The device's cost-effectiveness is underscored by the use of affordable materials and open-source hardware/software, making it accessible for low-resource settings. Field readiness was confirmed through validation under real-world conditions, attesting to the device's robustness and reliability.

Despite these advancements, the research identified several challenges and limitations. Some images were affected by sub-optimal autofocusing, impacting diagnostic accuracy in certain cases. The AI models require further training on more diverse datasets to improve generalisation across different environmental conditions. Additionally, operational challenges such as mechanical issues in the autofocusing mechanism were noted, necessitating further hardware refinements.

Building on these successes and lessons learned, future research will focus on hardware and software refinement to improve mechanical stability and AI model robustness. The Schistoscope will be adapted for the diagnosis of other parasitic diseases, with enhanced field validation through extensive trials in diverse settings. Sustainable deployment strategies will explore local manufacturing options to reduce costs and improve accessibility. Furthermore, the development of cloud-based data storage and analysis systems will support large-scale public health initiatives.

In conclusion, this thesis demonstrates that the integration of AI with digital microscopy can revolutionise the diagnosis of schistosomiasis and STH infections. The Schistoscope not only matches traditional microscopy in diagnostic accuracy but also offers significant advantages in terms of automation, cost-effectiveness, and field applicability. By addressing key challenges in parasitic disease diagnostics, this research contributes to global efforts in controlling and eliminating neglected tropical

diseases (NTD), with the potential to improve health outcomes in some of the world’s most vulnerable populations. Therefore, accelerating the achievement of the elimination targets as enshrined in the WHO’s NTD Road Map, 2021-2030 in resource-limited settings.

SAMENVATTING

De wereldwijde ziektelast veroorzaakt door schistosomiasis en van bodem overgedragen helminth-infecties is aanzienlijk, waarbij miljoenen mensen risico lopen, vooral in Sub-Sahara Afrika. Traditionele diagnostische methoden die gebruik maken van optische microscopie zijn arbeidsintensief, afhankelijk van getraind personeel en vaak ontoegankelijk in afgelegen gebieden. Dit proefschrift richt zich op de ontwikkeling en validatie van een op AI-gebaseerde digitale microscoop, de Schistoscope, ontworpen met als doel om de diagnose van deze infecties te verbeteren, met name in gebieden met beperkte middelen. Het doel is om bestaande diagnostische problemen te overkomen door het ontwikkelen van een geautomatiseerd systeem dat de afhankelijkheid van geschoold personeel vermindert, de diagnostische nauwkeurigheid verbetert en de toegankelijkheid vergroot.

Het onderzoek integreert innovaties op het gebied van hardware ontwerp, digitale beeldvorming en kunstmatige intelligentie (AI) om een betaalbaar, efficiënt en nauwkeurig diagnostisch hulpmiddel te creëren dat de beperkingen van traditionele microscopie overkomt. De primaire doelstellingen zijn het ontwerpen en ontwikkelen van kosteneffectieve digitale microscoopprototypes, het integreren van AI-algoritmen voor geautomatiseerde detectie en classificatie van parasieteneieren, en het valideren van de diagnostische prestaties van het systeem via veldstudies. Het ontwikkelingsproces ving aan met twee goedkope digitale microscoopprototypes: de op Raspberry Pi gebaseerde Schistoscope en de op smartphone gebaseerde Schistoscope. Beide ontwerpen waren gericht op betaalbaarheid, draagbaarheid en gebruiksgemak, met als innovatie de integratie van 3D-geprinte componenten en lokaal beschikbare materialen om de duurzaamheid en eenvoudig onderhoud in endemische gebieden te waarborgen. Vervolgiteraties hebben geleid tot de ontwikkeling van de Schistoscope 5.0, die aanzienlijke verbeteringen demonstreerde in beeldkwaliteit, automatisering en gebruikersinterface. Het apparaat beschikt over een whole-slide imaging systeem met een geavanceerd autofocussysteem, wat de beeldhelderheid en diagnostische nauwkeurigheid verbetert. Een belangrijke bijdrage van dit proefschrift is de integratie van AI voor geautomatiseerde detectie en kwantificering van Schistosoma haematobium en intestinale helminth-eieren. Het diagnostisch kader maakt gebruik van deep learning modellen, met name convolutionele neurale netwerken (CNN's), voor semantische segmentatie en objectdetectie. Belangrijke componenten zijn

de DeepLabV3 met een MobileNetV3-backbone, gebruikt voor semantische segmentatie van Schistosoma haematobium-eieren, waarbij eieren effectief worden onderscheiden van achtergrondartefacten, en het EfficientDet-model, toegepast voor de detectie van intestinale helmintheieren, waaronder Ascaris lumbricoides, Trichuris trichiura, maanwormen en Schistosoma mansoni.

De modellen zijn getraind op robuuste datasets die zijn verzameld uit veldmonsters, met omvangrijke beeldannotatie om de nauwkeurigheid te waarborgen. Het diagnostisch systeem toonde een hoge gevoeligheid en specificiteit, waarmee het voldoet aan de productprofielen van de Wereldgezondheidsorganisatie voor zogenaamde controleprogramma's voor schistosomiasis en STH. Uitgebreide veldvalidatiestudies zijn uitgevoerd in Nigeria en Gabon om de prestaties van de Schistoscope in de praktijk te beoordelen. Deze studies vergeleken de diagnostische nauwkeurigheid van het apparaat met conventionele microscopie en met real-time PCR en UCP-LF CAA. In Nigeria richtte de studie zich ook op het gebruiksgemak en de acceptatie van de Schistoscope onder zorgverleners, waarbij een hoge acceptatiegraad van zowel de semi- als de volledig geautomatiseerde modi werd aangetoond. In Gabon werd de diagnostische prestatie beoordeeld op verse en opgeslagen urinemonsters, waarbij de Schistoscope vergelijkbare nauwkeurigheid toonde als traditionele microscopie, naast de extra voordelen van automatisering en verkorte diagnosetijd.

De bevindingen benadrukken verbeterde diagnostische nauwkeurigheid, waarbij de Schistoscope een hoge precisie en gevoeligheid behaalde bij de detectie van schistosomiasis en STH-infecties. De integratie van AI verkleinde de behoefte aan geschoold personeel, waardoor de automatisering en efficiëntie werden verbeterd.

De kosteneffectiviteit van het apparaat wordt onderstreept door het gebruik van betaalbare materialen en open-source hardware/software, waardoor het toegankelijk is voor omgevingen met beperkte middelen. De geschiktheid voor gebruik in het veld werd bevestigd door validatie onder werkelijke werkomstandigheden, hetgeen de robuustheid en betrouwbaarheid van het apparaat aantoont. Ondanks deze vooruitgang, identificeerde het onderzoek ook verschillende uitdagingen en beperkingen. Sommige beelden werden beïnvloed door suboptimale autofocus, wat in bepaalde gevallen de diagnostische nauwkeurigheid negatief beïnvloedde. De AI-modellen vereisen verdere training op meer diverse datasets om de generaliseerbaarheid naar andere omgevingsomstandigheden te verbeteren. Bovendien werden er operationele uitdagingen, zoals mechanische problemen in het autofocussysteem, vastgesteld, wat verdere hardware verbeteringen noodzakelijk maakt. Voortbouwend op deze successen en geleerde lessen zal toekomstig onderzoek zich moeten richten op hardware- en softwareverbeteringen om de mechanische stabiliteit en de robuustheid van AI-modellen verder te verbeteren.

De Schistoscope kan worden aangepast voor de diagnose van andere parasitaire ziekten, met verbeterde veldvalidatie door uitgebreide proeven in verschillende gebruiksomgevingen. Duurzame implementatiestrategieën zullen de lokale productie opties verkennen om de kosten te verlagen en de toegankelijkheid te verbeteren. Bovendien zal de ontwikkeling van op de cloud gebaseerde gegevensopslag- en analysesystemen grootschalige volksgezondheidsinitiatieven ondersteunen.

Tot slot toont dit proefschrift aan dat de integratie van AI met digitale microscopie, de diagnose van schistosomiasis en STH-infecties revolutionair kan verbeteren. De Schistoscope evenaart niet alleen de traditionele microscopie in diagnostische nauwkeurigheid, maar biedt ook aanzienlijke voordelen op het gebied van automatisering, kosteneffectiviteit en toepasbaarheid in het veld. Door belangrijke uitdagingen in de diagnostiek van parasitaire ziekten aan te pakken, draagt dit onderzoek bij aan de wereldwijde inspanningen om verwaarloosde tropische ziekten te bestrijden en uit te roeien, met het potentieel om de gezondheidsresultaten te verbeteren in enkele van ’s werelds meest kwetsbare bevolkingsgroepen. Daarom versnelt het de verwezenlijking van de eliminatiedoelen zoals vastgelegd in de WHO’s NTD Routekaart 2021-2030 in omgevingen met beperkte middelen.

1

INTRODUCTION

This chapter provides an overview of schistosomiasis and soil-transmitted Helminth infections, examining transmission pathways, clinical and programmatic impact, and current treatment and control strategies. The emphasis is on the critical role of accessible, timely, and regular diagnostics in disease management, control, and elimination, underscoring the limitations of traditional microscopy in resource-limited regions where diagnostic sensitivity, specificity, and affordability remain significant barriers. The motivation, aim, objectives, and structure of this thesis conclude this chapter.

1

1.1. NEGLECTED TROPICAL DISEASES

Neglected tropical diseases (NTDs) comprise a diverse range of conditions caused by various pathogens, including viruses, bacteria, parasites, fungi, and toxins. These diseases have profound health, social and economic impacts, particularly in impoverished communities in tropical regions, although some NTDs extend beyond these areas. More than 1 billion people are affected by NTDs, with approximately 1.6 billion people in need of preventive and curative interventions [1]. NTDs encompass a wide array of diseases, such as Buruli ulcer, Chagas disease, dengue and chikungunya, dracunculiasis, echinococcosis, foodborne trematodiases, human African trypanosomiasis, leishmaniasis, leprosy, lymphatic filariasis, mycetoma, chromoblastomycosis, and other deep mycoses, as well as noma, onchocerciasis, rabies, scabies and other ectoparasitoses, schistosomiasis, soil-transmitted helminthiases, snakebite envenoming, taeniasis/cysticercosis, trachoma, and yaws. However, this research specifically focuses on schistosomiasis and soil-transmitted helminthiases.

1.1.1. SCHISTOSOMIASIS

The World Health Organisation (WHO) reports that in 2020, approximately 240 million people in 78 countries needed preventive chemotherapy for schistosomiasis, and more than 90% of those affected reside in Africa, particularly in sub-Saharan regions [2–4]. Schistosomiasis is transmitted through contact with freshwater contaminated with *Schistosoma (S.)* parasites. This makes activities involving freshwater, such as swimming, bathing, fishing, or even farming in irrigated fields, common transmission opportunities in endemic regions. Schistosomiasis exists in two primary forms: intestinal and urogenital. Intestinal schistosomiasis is caused mainly by *S. mansoni*, *S. mekongi*, *S. japonicum*, *S. intercalatum*, and *S. guineensis*, while *S. haematobium* is responsible for urogenital schistosomiasis [3]. Of these six species, *S. mansoni* and *S. haematobium* are the most widespread [4]. Continued exposure to infested water - due to the absence of piped water, lack of bridges across streams, poor health communication, and inadequate vector control - remains a key driver of infection, sustaining the reservoir of disease.

The clinical impacts of schistosomiasis vary: *S. mansoni* often leads to liver inflammation, malnutrition, and stunted growth in children, whereas *S. haematobium* is associated with haematuria, painful urination, urinary tract infections, and in severe cases, bladder and kidney damage, lesions in the cervix of women with Female Genital Schistosomiasis (FGS), as well as high infertility rates in regions with high schistosomiasis prevalence [4, 5]. Although preventable and treatable, schistosomiasis persists and improved diagnostic capabilities could enable timely intervention,

particularly for small-scale farming and fishing communities [2, 6]. Efforts to eliminate schistosomiasis as a major public health problem continue as part of the broader fight against neglected tropical diseases [3, 4, 7–9]. In 2022, the WHO released updated guidelines for the prevention and control of schistosomiasis, recommending an integrated approach that includes the extension of preventive chemotherapy to all individuals at risk from age two in areas with a prevalence of at least 10%, as well as improving sanitation, access to treatment, and vector control [2, 10]. This guideline also recommended case management (detection of cases and treatment) in areas with low prevalence. Effective diagnosis is essential for early diagnosis and treatment and for assessing intervention success, tracking disease reduction, and monitoring parasite transmission. Accessible and accurate diagnostics are crucial for surveillance and treatment efforts [2, 3, 11]. Although new diagnostic tools are being developed, challenges in sensitivity, specificity, and affordability continue to hinder the effective diagnosis of schistosomiasis [2, 3, 11].

1.1.2. SOIL TRANSMITTED HELMINTH INFECTIONS

Soil-transmitted helminth (STH) infections pose a significant public health and economic burden and are often associated with poverty [12]. Approximately 1.5 billion people are currently infected with STHs worldwide, with the primary causes being *Ascaris lumbricoides*, *Trichuris trichiura*, hookworm species (*Necator americanus* and *Ancylostoma duodenale*), and *Strongyloides stercoralis* [13, 14].

Transmission occurs when parasitic worm eggs from improperly disposed human feces contaminate soil and water sources. This occurs in settings with poor and inadequate sanitation. Infections arise through direct contact of the skin with contaminated soil or water during daily activities such as farming or through play for children. Ingestion can also occur by consuming unwashed or undercooked vegetables or, in some cases, contaminated water. Symptoms of STH infections range from diarrhea, abdominal pain, and general discomfort to anemia [14, 15].

Since the mid-1980s, mass chemotherapy programs have been the primary approach to combating STH infections globally. These programs have reduced the prevalence and intensity of infections; however, low-intensity infections with high re-infection rates remain problematic, and transmission persists [16]. The persistence of STH has led the WHO to emphasize the critical role of diagnostics in achieving the goal of eliminating these infections as a public health issue by 2030 [17].

Various diagnostic techniques are used for STH detection, including microscopy-based methods (e.g., direct wet mount and Kato-Katz (KK) method), tube spontaneous sedimentation technique (TSET),

McMaster, Mini-FLOTAC, and formol-ether concentration, as well as immunodiagnostic-based methods (e.g., ELISA) and DNA-based methods (e.g., quantitative polymerase chain reaction [qPCR] and loop-mediated isothermal amplification) [18, 19]. However, these methods differ in terms of sensitivity, cost, simplicity, and practicality. Despite advances in diagnostic technology, the WHO continues to recommend the Kato-Katz microscopy method for the diagnosis of STH due to its simplicity, ease of use in the field and affordability [20].

1.2. RESEARCH PROBLEM

The diagnosis of schistosomiasis and soil-transmitted helminth infections in resource-limited settings remains challenging due to the reliance on a labor-intensive microscopy technique that requires skilled personnel and is prone to variability in accuracy. Existing automated microscopy-based diagnostic tools for diagnosing these infections are inefficient with automated slide scanning systems that capture and focus on irrelevant areas of the slide, thus require optimization to minimize scanning time by targeting only diagnostically relevant parts of sample slides. Furthermore, there is a critical need for a robust and automated helminth egg detection system that can handle the complexities of field-captured images, such as artifacts, transparent, and overlapping eggs, to improve both accuracy and efficiency. This research aims to address these challenges by developing and validating a digital microscope with a comprehensive automated diagnosis framework. This diagnostic framework will integrate deep learning and refined segmentation techniques for the enhanced detection and quantification of *Schistosoma* eggs in urine samples and will be extended to the detection and classification of multiple intestinal helminth species in Kato-Katz fecal smears. The goal is to create a reliable, affordable and easy-to-use system that meets the WHO's diagnostic target product profiles, thereby supporting schistosomiasis and STH control and elimination efforts, reducing diagnostic errors, increasing speed, and enhancing accessibility in low-resource environments.

1.3. RESEARCH MOTIVATION

The motivation for this research is driven by the urgent need for accessible, accurate and affordable diagnostic tools to combat schistosomiasis and soil-transmitted helminth infections, particularly in low-resource settings where the burden of these diseases is highest. Current diagnostic methods, such as conventional microscopy, are limited by their dependency on skilled personnel, high operational costs, and limited sensitivity, especially to detect low-intensity infections. These limitations hinder effective disease monitoring, control and

treatment in under-served areas, which face significant logistical and financial barriers to access to healthcare.

Advances in portable digital microscopy and AI-based diagnostic technologies offer a promising path to address these challenges. Using AI-driven automation, portable digital devices, and locally manufacturable components, there is potential to create high-throughput, accurate diagnostic tools that can operate independently of extensive infrastructure and trained personnel. This research aims to bridge the gap between traditional and innovative diagnostic approaches by developing, validating, and optimizing an AI-integrated digital microscope to meet these requirements, supporting a reliable and efficient diagnosis of schistosomiasis and STHs even in the most resource-constrained environments.

Through this work, we seek to establish a scalable community-centered diagnostic tool that aligns with the WHO's goals for disease control and elimination. By ensuring that the device meets the sensitivity, specificity, and usability requirements for field deployment, this research will help to strengthen local health systems, expand access to diagnostics, and ultimately improve patient outcomes in endemic regions. This thesis is motivated by a commitment to advancing global health equity by providing sustainable diagnostic solutions tailored to the needs of communities most affected by neglected tropical diseases.

1.4. AIM AND OBJECTIVES

1.4.1. RESEARCH AIM

The aim of this thesis is to develop, validate and assess a low-cost, locally manufacturable digital microscope that integrates AI-based detection algorithms and advanced autofocusing and scanning techniques for the accurate detection and quantification of *S. haematobium* and intestinal helminth infections in resource-limited settings, evaluating its field applicability, usability, and diagnostic performance against conventional methods using fresh and banked samples.

1.4.2. RESEARCH OBJECTIVES

The objectives of this thesis are as follows:

1. To develop a low-cost, automated digital microscope for the registration and detection of helminth eggs in both urine and fecal samples.
2. To evaluate the usability and acceptability of the automated digital microscope by comparing its effectiveness with conventional microscopy among healthcare workers and medical students in low-resource settings.

3. To design and implement a Perturb and Observe (P&O) autofocusing algorithm and an optimized whole slide scanning procedure to improve image quality, diagnostic accuracy, and scanning efficiency in the automated digital microscope.
4. To develop and assess automated helminth egg detection algorithms, including the two-stage AI-based diagnostic framework and deep learning models, for accurately detecting and classifying *S. haematobium* and intestinal helminth eggs in both urine and stool samples.
5. To evaluate the diagnostic performance of the automated digital microscope in detecting and quantifying of *S. haematobium* eggs in field-collected urine samples, and to compare its accuracy with conventional microscopy and a composite reference standard (CRS) comprising PCR and UCP-LF CAA.
6. To assess the potential of the automated digital microscope for retrospective analysis by evaluating its performance on freshly collected and banked urine samples in resource-limited settings.

1.4.3. RESEARCH HYPOTHESIS

This research is guided by the following hypotheses:

1. The developed automated digital microscope, with its modular and locally manufacturable design, will demonstrate diagnostic accuracy, usability, and operational feasibility comparable to or exceeding traditional microscopy for detecting *S. haematobium* and intestinal helminth eggs in resource-limited settings.
2. The integrated imaging components, including the perturb and observe (P&O) autofocusing algorithm, optimized scanning procedures, and AI-based detection models, will significantly improve diagnostic accuracy, processing speed, and egg quantification, meeting or exceeding WHO diagnostic standards for schistosomiasis and STH diagnostics.
3. The Edge AI implementation of the Schistoscope, combining the two-stage diagnostic framework with deep learning-based classification, will achieve high sensitivity, specificity, and user acceptability, enabling reliable field deployment and effective diagnostic performance in both fresh and banked samples.

1.5. THESIS STRUCTURE

This thesis is structured as a series of published articles, arranged in the order in which the research was conducted, supplemented by integrative

chapters including an introduction, literature review, and conclusion to provide a coherent narrative. The original format of each published article has been maintained to allow a straightforward correlation with their source papers. All articles are available under green open access through the TU Delft Research Portal at research.tudelft.nl, with direct links included in the bibliography entries. This format not only showcases our research productivity through peer-reviewed publications but also validates the quality, relevance, and originality of the work, providing tangible evidence of our contributions to the scientific understanding of neglected tropical disease diagnosis.

1. Chapter 2 provides a comprehensive review of the literature on diagnostic tools for the quantitative diagnosis of helminth infections. They are categorized according to three stages: sample preparation, microscopic imaging, and automated identification of helminth eggs.

2. Chapter 3 discusses the development and design of two low-cost digital microscope prototypes, Raspberry Pi-based (Schistoscope RP) and smartphone-based (Schistoscope SP), aimed at diagnosing urinary schistosomiasis in resource-limited settings.

3. Chapter 4 presents a low-cost, automated diagnostic device (Schistoscope 5.0) for detecting *S. haematobium* eggs in urine, with the aim of providing a viable solution for point-of-care diagnostics in low-resource settings.

4. Chapter 5 presents a study on the usability and user acceptance of the developed automated digital microscope (Schistoscope 5.0) among healthcare workers and medical students in low-resource settings.

5. Chapter 6 explores a field-based evaluation of the automated digital microscope (Schistoscope 5.0) as a diagnostic tool for *S. haematobium* in Nigeria. The study compares the device's performance in both semi- and fully automated modes with conventional light microscopy, especially in resource-limited areas where schistosomiasis remains prevalent and traditional diagnostic approaches are challenging.

6. Chapter 7 explores the optimization of the autofocusing and whole slide scanning systems of the automated digital microscope (Schistoscope 5.0) for efficient and accurate diagnosis of parasitic diseases, particularly *S. haematobium* in sub-Saharan Africa.

7. Chapter 8 details the development and implementation of a two-stage diagnostic framework for the automated detection and counting of S*S. haematobium* eggs in urine samples from field settings using the automated digital microscope (Schistoscope 5.0).

8. Chapter 9 presents a comprehensive validation study of the automated digital microscope (Schistoscope 5.0) for diagnosing *S. haematobium* infections in Gabon. The diagnostic performance of the Schistoscope was compared with that of conventional microscopy and a composite reference standard (CRS) that incorporates real-time PCR and UCP-LF CAA. Conducted in two parts, Study A assessed fresh samples, while Study B evaluated banked samples stored for two years.

9. Chapter 10 discusses the development of an artificial intelligence system for automated detection and classification of intestinal helminth eggs in Kato-Katz stool smears, specifically designed to run on the edge computing system of the automated digital microscope (Schistoscope 5.0) .

10. Chapter 11 presents a summary and reflections on chapters 2 to 10. Each section captures the essential insights, achievements, and implications drawn from the individual chapters. Provides a critical reflection on the impact and limitations of the research, and a robust and comprehensive conclusion to the thesis.

1.6. CONTRIBUTION SUMMARY

This thesis presents the development and validation of an automated digital microscopy system for the detection of schistosomiasis and STH infections, with a focus on delivering affordable and scalable diagnostics for resource-limited settings. Although this research is part of a larger collaborative effort, my specific contributions are detailed below:

1. **Review of Existing Diagnostic Tools**
   - Conducted an extensive literature review to assess the current state of digital microscopy and AI-based diagnostics for schistosomiasis and STH detection.
   - Identified gaps in existing diagnostic techniques, particularly the limitations of traditional microscopy in sensitivity, accessibility, and automation.
   - Analyzed and identified performance trade-offs between Schistoscope RP & SP designs.
   - Formulated the research problem and objectives based on a critical analysis of existing methodologies.

2. **Conceptualization and Development of Schistoscope 5.0**
   - Led the design, development, and refinement of Schistoscope 5.0, a low-cost, AI-integrated digital microscope optimized for Schistosomiasis and STH diagnosis.

- Engineered a modular optical system and an automated sample stage, ensuring robustness and reproducibility for field deployment.

3. **Development of AI-Based Diagnostic Frameworks**
   - Created a *S. haematobium* (SH) dataset, comprising 12,051 field-of-view (FoV) images captured from 103 independent urine samples collected in field settings.
   - Created an STH and *S. mansoni* dataset consisting of over 3,000 FoV images containing parasite eggs, extracted from more than 300 fecal smears prepared using the Kato-Katz technique in field settings.
   - Developed an automated detection pipeline for urogenital schistosomiasis using UNET deep learning architecture .
   - Developed a 2-staged diagnostic frame work for urogenital schistosomiasis using DeepLabV3-MobileNetV3 deep learning architecture and a region based segmentation approach.
   - Developed an object detection and classification model for *S. mansoni* and STH eggs using EfficientDet deep learning architecture .
   - Trained, validated, and optimized AI models using annotated microscopy datasets, improving diagnostic sensitivity and specificity.
4. **Optimization of Autofocusing and Whole-Slide Imaging**
   - Designed and implemented an adaptive Perturb & Observe autofocusing algorithm, improving image clarity and diagnostic precision.
   - Developed an automated whole-slide scanning approach, enhancing the system's ability to analyze large sample areas in a shorter time.
5. **Validation of Schistoscope 5.0**
   - Led on-site validation studies in Nigeria and Gabon, coordinating data collection and testing under real-world clinical conditions.
   - Performed statistical analysis that compared the diagnostic performance of Schistoscope 5.0 and traditional microscopy using precision, sensitivity, and specificity metrics.
   - Conducted surveys to assess user experience and feasibility of deploying Schistoscope 5.0 in low-resource healthcare settings in Nigeria.

My work directly contributes to bridging the gap between traditional microscopy and AI-driven diagnostics, demonstrating how affordable, portable AI-enhanced microscopes can significantly improve disease detection, surveillance, and treatment strategies in endemic regions. This research not only advances the automation and accuracy of schistosomiasis and STH diagnostics, but also lays the foundation for scalable AI-powered solutions in global health.

REFERENCES

[1] World Health Organisation. *Neglected tropical diseases – GLOBAL*. 2024. url: https://www.who.int/health-topics/neglected-tropical-diseases#tab=tab_1 (visited on 11/02/2024).

[2] World Health Organization. *WHO guideline on control and elimination of human schistosomiasis*. World Health Organization, 2022. isbn: 9789240041608. url: https://iris.who.int/handle/10665/351856.

[3] World Health Organization. "34th meeting of the International Task Force for Disease Eradication, 34ˆè reunion du Groupe spécial international pour l'éradication des maladies, 19–20 Septembre 2022". In: *Weekly Epidemiological Record* 98.04 (2022), pp. 41–50. url: https://iris.who.int/handle/10665/365721.

[4] O. P. Aula, D. P. McManus, M. K. Jones, and C. A. Gordon. "Schistosomiasis with a focus on Africa". In: *Tropical Medicine and Infectious Disease* 6.3 (2021), p. 109. doi: 10.3390/tropicalmed6030109.

[5] C. Yohana, J. S. Bakuza, S. M. Kinung, B. A. Nyundo, and P. F. Rambau. "The trend of schistosomiasis related bladder cancer in the lake zone, Tanzania: a retrospective review over 10 years period". In: *Infect Agent Cancer* 18.10 (2023), pp. 1–10. doi: 10.1186/s13027-023-00491-1.

[6] R. H. Mnkugwe, O. S. Minzi, S. M. Kinungohi, A. A. Kamuhabwa, and E. Aklillu. "Efficacy and safety of praziquantel for treatment of schistosoma mansoni infection among school children in Tanzania". In: *Pathogens* 9.1 (2019), p. 28. doi: 10.3390/pathogens9010028.

[7] K. G. Weerakoon, G. N. Gobert, P. Cai, and D. P. McManus. "Advances in the diagnosis of human schistosomiasis". In: *Clin Microbiol Rev* 28.4 (2015), pp. 939–967. doi: 10.1128/CMR.00137-14.

[8] K. G. Weerakoon, C. A. Gordon, and D. P. McManus. "DNA diagnostics for schistosomiasis control". In: *Trop Med Infect Dis* 3.3 (2018), pp. 1–20. doi: 10.3390/tropicalmed3030081.

[9] C. Kokaliaris, A. Garba, M. Matuska, R. N. Bronzan, D. G. Colley, A. M. Dorkenoo, U. F. Ekpo, F. M. Fleming, M. D. French, A. Kabore, J. B. Mbonigaba, N. Midzi, P. N. M. Mwinzi, E. K. N'Goran, M. R. Polo, M. Sacko, L.-A. Tchuem Tchuenté, E. M. Tukahebwa, P. A. Uvon, G. Yang, L. Wiesner, Y. Zhang, J. Utzinger, and P. Vounatsou. "Effect of preventive chemotherapy with praziquantel on schistosomiasis among school-aged children in sub-Saharan Africa: a spatiotemporal modelling study". In: *The Lancet Infectious Diseases* 22.1 (Jan. 2022), pp. 136–149. doi: 10.1016/S1473-3099(21)00090-6.

[10] O. Ally, B. N. Kanoi, L. Ochola, S. G. Nyanjom, C. Shiluli, G. Misinzo, and J. Gitaka. "Schistosomiasis diagnosis: Challenges and opportunities for elimination". In: *PLOS Neglected Tropical Diseases* 18.7 (2024), e0012282. doi: 10.1371/journal.pntd.0012282.

[11] World Health Organization. *Diagnostic target product profiles for monitoring, evaluation and surveillance of schistosomiasis control programmes*. World Health Organization, 2021. isbn: 9789240031104. url: https://iris.who.int/handle/10665/344813.

[12] P. Hotez. "Hookworm and poverty". In: *Ann. N. Y. Acad. Sci.* 1136.1 (2008), pp. 38–44. doi: 10.1196/annals.1425.000.

[13] World Health Organization. *Soil-transmitted helminth infections*. Aug. 2023. url: https://www.who.int/news-room/fact-sheets/detail/soil-transmitted-helminth-infections (visited on 09/26/2024).

[14] P. M. Jourdan, P. H. L. Lamberton, A. Fenwick, and D. G. Addiss. "Soil-transmitted helminth infections". In: *The Lancet* 391.10117 (2018), pp. 252–265. doi: 10.1016/S0140-6736(17)31930-X.

[15] J. Bethony, S. Brooker, M. Albonico, S. M. Geiger, A. Loukas, D. Diemert, and P. J. Hotez. "Soil-transmitted helminth infections: ascariasis, trichuriasis, and hookworm". In: *The lancet* 367.9521 (2006), pp. 1521–1532. doi: 10.1016/S0140-6736(06)68653-4.

[16] J. P. Webster, D. H. Molyneux, P. J. Hotez, and A. Fenwick. "The contribution of mass drug administration to global health: past, present and future". In: *Phil. Trans. R. Soc. B* 369.1645 (2014), p. 20130434. doi: 10.1098/rstb.2013.0434.

[17] World Health Organization. *2030 targets for soil-transmitted helminthiases control programmes*. World Health Organization, 2020. isbn: 9789240000315. url: https://iris.who.int/handle/10665/330611.

[18] M. Mbong Ngwese, G. Prince Manouana, P. A. Nguema Moure, M. Ramharter, M. Esen, and A. A. Adégnika. “Diagnostic Techniques of Soil-Transmitted Helminths: Impact on Control Measures”. In: *Trop. Med. Infect. Dis.* 5.2 (2020), p. 93. doi: 10.3390/tropicalmed5020093.

[19] R. Tello, A. Terashima, L. A. Marcos, J. Machicado, M. Canales, and E. Gotuzzo. “Highly effective and inexpensive parasitological technique for diagnosis of intestinal parasites in developing countries: spontaneous sedimentation technique in tube”. In: *Int J Infect Dis* 16.6 (2012), e414–e416. doi: 10.1016/j.ijid.2011.12.017.

[20] N. Cure-Bolt, F. Perez, L. A. Broadfield, B. Levecke, P. Hu, J. Oleynick, M. Beltrán, P. Ward, and L. Stuyver. “Artificial intelligence-based digital pathology for the detection and quantification of soil-transmitted helminths eggs”. In: *PLOS Neglected Tropical Diseases* 18.9 (2024), e0012492. doi: 10.1371/journal.pntd.0012492.

2

REVIEW OF QUANTITATIVE DIAGNOSTIC TOOLS

In this chapter, we have comprehensively reviewed sample preparation devices, portable digital microscopes, and automated detection procedures essential for diagnosing schistosomiasis and soil-transmitted helminth (STH) infections. Sample preparation techniques, including urine filtration, fecal thick smear, sedimentation, and flotation methods, have been refined for simplicity, cost-effectiveness, and applicability in field settings. Portable digital microscopes, from handheld models to smartphone-based setups and fully automated digital systems, offer promising pathways for diagnostics in resource-limited areas, enabling real-time data sharing and remote diagnosis. Automated detection and identification methodologies, spanning machine learning and deep learning approaches, address the labor intensity and operator dependency of manual examination. Machine learning methods established initial frameworks for feature extraction and parasite classification, but the complex variability in real-world samples shifted focus to deep learning models, which excel in handling complex images with artifacts. However, challenges such as dataset diversity, model robustness, and hardware costs persist. Bridging the gap between these innovative tools and practical field applications requires improving data quality and model generalization, optimizing device affordability, and fostering adaptability to field conditions. Progress in these areas will be crucial to creating scalable, effective diagnostic solutions, ultimately advancing control efforts and evaluations of treatment efficacy in schistosomiasis and STH-endemic regions.

2.1. INTRODUCTION

Diagnostic techniques for schistosomiasis and STH infections are generally divided into qualitative and quantitative approaches. Qualitative techniques determine whether the urine or fecal sample of a patient is positive for the targeted helminth infection, while quantitative techniques assess the intensity of the infection [1]. Although there are multiple techniques for examining urine and fecal samples [1–6], they often have operational limitations, such as high cost, complexity, low sensitivity, and/or reproducibility. Quantitative methods, which involve the careful preparation of samples prior to microscopic examination, are widely used to visualise and quantify helminth eggs. This approach ensures high reliability and diagnostic accuracy, as microscopic examination also provides a standardized measure (e.g., eggs/mL for urine or eggs per gram of feces - EPG), which is critical for assessing infection prevalence and intensity in control programs or drug efficacy assessments.

The quantitative diagnosis of schistosomiasis and soil-transmitted helminth infections involves three primary stages: sample preparation, microscopic imaging, and identification of helminth eggs. In this chapter, we first review the tools available for the preparation of urine and fecal samples. Next, we discuss portable microscopic imaging devices that have been developed or adapted for the field diagnosis of helminth infections. Lastly, we examine recent advances in artificial intelligence (AI) algorithms for automated detection and identification of helminth eggs in urine and fecal samples using machine learning and deep learning models. Specifically, we analyze these tools from a technological perspective, detailing the motivations behind their development, as well as their advantages, benefits, and intended contributions. Finally, we discuss their limitations, challenges, and diagnostic gaps. This review aims to provide researchers with insights into developing accessible, reliable, and affordable point-of-care diagnostic tools for helminth infections.

2.2. SAMPLE PREPARATION TECHNIQUES

2.2.1. URINE FILTRATION TECHNIQUES

Urine filtration devices are essential tools in diagnosing *Schistosoma (S.) haematobium* infections (urogenital schistosomiasis). This technique is widely adopted due to its simplicity, affordability, and high specificity, making it suitable for use in low-resource settings where the burden of the disease is high.

The filtration device typically consists of a plastic filter holder containing a polycarbonate, nylon, or paper filter with pore sizes ranging from 12 to 20 μm. During sample preparation, a standard 10 mL urine

sample is pushed through the filter using a syringe [7]. Eggs of *S. haematobium* (approximately 150 by 60 µm in size) present in the urine are retained in the filter, which is then mounted on a microscope slide and, in some cases, stained for a clear visualisation of the eggs under microscopy.

Urine filtration has shown high sensitivity, which is particularly effective in diagnosing infections in school-aged children, a group especially vulnerable to schistosomiasis, and is recommended by the WHO for detecting *S. haematobium* [8]. However, a significant barrier to the use of this technique is the cost of the filtration equipment and its limited availability in rural areas, where it is most needed. For example, Millipore schistosome filtration devices cost more than $2 per filter. However, less expensive filtration kits are being developed and their accuracy is evaluated compared to the established, but costly, Millipore device [7]. Lowering these costs could significantly expand testing and monitoring capabilities in resource-limited settings.

In addition, researchers have explored the use of locally available materials, such as paper products (paper towels, newspaper and paper from a student workbook) [9], coffee filters, and chiffon, for urine filtration. Although these materials can filter urine while retaining eggs, the resulting images often suffer from background interference, reducing egg visibility.

A specialized microfiltration device for isolating schistosome eggs in urine was developed by Xiao *et al.* [3]. This device employs a linear array of microfluidic traps to capture schistosome eggs with a trapping efficiency 100% at a flow rate of 300 µl/min. The trapped eggs can be recovered for downstream analysis or preserved in situ for whole-mount staining. However, completing the filtration procedure in under 10 minutes would require a flow rate of 3000 µl/min, reducing the trapping efficiency to 83%.

2.2.2. FECAL THICK SMEAR TECHNIQUES

The fecal thick smear method, which uses a cellophane cover to examine helminth eggs in stool, was initially introduced by Kato [10] and has since been evaluated and modified by various researchers [11–15]. However, this method requires a precision balance to accurately weigh the fecal sample, making the quantitative determination of egg counts challenging in field settings.

To address this, Layrisse, Martínez-Torres, and Ferrer-Farias [16] designed a volumetric device that estimates stool weight using a 1 mL plastic syringe cut 3 mm from its tip. A metal retaining ring around the plunger limits displacement, maintaining consistent volume. Additional components - a 3 mm diameter bolt and nut calibrator and a 2x2 mm steel collar - ensure constant plunger displacement and, consequently,

uniform stool volume. Although low-cost and reusable, this design is labor intensive to clean, potentially leading to cross-contamination of fecal samples with helminth eggs.

To simplify this process, Katz, Chaves, and Pellegrino [17] introduced a disposable 1.37 mm thick cardboard with a 6 mm center hole, allowing standardized fecal sample volumes for quantitative thick smear methods. The sample weights obtained using this technique demonstrated statistical uniformity within acceptable limits, with a high correlation between *S. mansoni* egg counts per gram and traditional weighing methods. The WHO has since integrated this cardboard-based device into the Kato-Katz test kit, which includes an applicator stick, screen, and template. This kit is widely used in mass surveys because of its reliability, low cost, and simplicity.

However, the Kato-Katz method examines a relatively small stool sample (typically 41.7 mg), which limits its analytical sensitivity in low-intensity infections (fewer than 100 EPG). Increased sampling with the Kato-Katz method can enhance sensitivity, but this approach incurs additional costs and labor [4]. Furthermore, the Kato-Katz technique cannot process watery stool samples and is affected by the variability of stool composition. These limitations can be addressed by employing concentration methods, such as sedimentation or flotation techniques, to improve the detection of parasites.

2.2.3. SEDIMENTATION TECHNIQUES

Sedimentation techniques operate on the principle that when a liquid with a density lower than the parasite eggs is applied to a stool sample, the eggs separate from the fecal material and, being heavier, settle at the bottom of the container [1]. This separation can occur spontaneously or with the aid of centrifugation. The laboratory use of centrifugation for sedimentation was first introduced by Telemann [18], where centrifugal force was applied to a mixture containing ether (as solvent), hydrochloric acid and fecal material to isolate specific portions of the feces containing intestinal parasites [18]. Since then, techniques and procedural parameters have been modified, with adjustments for added simplicity or improved performance [19–24].

The effectiveness of spontaneous sedimentation for detecting *S. mansoni* eggs was noted by Lutz [25], showing a 20% improvement compared to direct examination [26]. This method can be scaled for large sample sets using parasitological kits such as Paratest and Coprotest, with contamination minimized by using disposable components and handling samples in a closed system [27, 28]. However, the extended sedimentation time limits its applicability in high-throughput laboratory environments. Furthermore, spontaneous sedimentation does not adequately separate debris from parasites, resulting in dense smears

filled with impurities, which can reduce diagnostic sensitivity [5].

Later, a layering technique that leverages differential segmentation gradients was adapted to recover *S. mansoni* eggs from stool samples [29, 30]. This was accomplished by introducing a saline solution through an aerating stone at the bottom of a flask containing a homogenized fecal sample. Building on this approach, Coelho *et al.* [31] developed a saline gradient device comprising two interconnected cylindrical plastic columns. The reservoir column, with a capacity of 50 ml, is placed above a separating column that holds 10 mL of liquid. The columns are connected by a rubber hose with a roller clamp, and an aquarium aerating stone, sealed with silicon, is fixed at the bottom of the separating column. The separating column also has an upper drainage hose. As the 3% saline solution flows slowly and continuously from the reservoir to the separating column that contains the fecal sample, it suspends and discharges low-density waste, clearing the sediment at the bottom. The eggs, with their higher density, remain on the surface of the porous plate.

The saline gradient device provides high sensitivity, handles large sample sizes (0.5–1g), and produces clean sediments, facilitating the rapid identification of eggs under bright-field microscopy. However, it is primarily suitable for *S. mansoni* eggs and carries the risk of losing parasites in the liquid medium, as well as potential morphological alterations of the structures of the parasite eggs during processing.

2.2.4. FLOTATION-BASED TECHNIQUES

Flotation techniques are based on the principle that when liquids with a density higher than that of parasite eggs are applied to a sample, the eggs become lighter and rise to the surface of the solution. This method was first reported by Bass [32] to detect hookworm eggs. Spontaneous flotation can be performed with a saturated solution with a density ranging from 1.18 to 1.27 g/mL, depending on the reagent. Willis [33] demonstrated the recovery of light helminth eggs in sodium chloride solution (NaCl, 1.20 g/mL). However, this technique is less suitable for recovering dense eggs and protozoa due to issues such as crystal formation in the fecal smear and osmotic damage to protozoa in saturated solutions.

Centrifugal flotation with zinc sulfate (1.18 g/mL) recovered twice as many eggs compared to direct examination, leading to its increased use as a reference method for intestinal parasite surveys [5]. The Wisconsin technique [34] involves floating eggs in salt solution by centrifuging on a swinging bucket rotor. After centrifugation, the eggs are collected in the meniscus, transferred to a coverlip, and counted by light microscopy [35]. This method is particularly effective for recovering nematode eggs, especially when detecting low egg counts. However, inefficiencies can

occur due to errors in the transfer of eggs from the centrifugation tube to the microscope slide, affecting precision in high egg counts [36].

Various other techniques concentrate parasite eggs into a single microscopic field of view to facilitate counting. In the McMaster technique, the sample is added to a flotation solution and placed in a McMaster chamber [37]. The chamber setup uses a base slide and a top slide, printed with a grid, to measure egg concentration. The technique has seen numerous modifications [38–42] to improve aspects such as fecal sample weight, volume of flotation solution, centrifugation time and speed, and flotation duration of the sample [43].

The FLOTAC device features two 5 mL flotation chambers, which allow up to 1 g of stool to be analyzed [44]. Inspired by McMaster and Wisconsin methods, FLOTAC provides counts for large fecal samples, offering greater sensitivity and precision for the detection of intestinal helminth eggs compared to traditional methods [44]. However, the time and labor intensive nature of FLOTAC, together with its reliance on laboratory equipment, limits its accessibility in resources-constrained settings [44]. The Mini-FLOTAC [45] is a portable adaptation of FLOTAC. It consists of a base, a reading disk with two 1 mL flotation chambers, and an optional microscope adapter. Unlike FLOTAC, Mini-FLOTAC does not require centrifugation equipment, making it suitable for field and low-resource settings. However, its sensitivity is lower than that of FLOTAC, and for high-accuracy applications, FLOTAC remains preferable.

The results of flotation methods are traditionally recorded on paper. For real-time monitoring of the prevalence and intensity of helminth infections, digital solutions are preferable. The FECPAK system, based on a modified McMaster technique [46], uses a tube with a central pillar to collect parasite eggs in a single viewing area. The captured images are stored digitally, allowing the data to be processed or uploaded for future reference [14]. Despite the advantage of digital storage, FECPAK exhibits lower sensitivity and egg recovery rates [15].

The lab-on-a-disk (LOD) platform [35], designed to isolate and image parasite eggs, uses a disk (10 cm diameter) that fits in a commercial mini-centrifuge. It features two identical flotation chambers, enabling balanced centrifugation and efficient egg collection. The device forms a monolayer of parasite eggs within a precise height chamber, improving the image accuracy. However, around 30% eggs were lost during injection, mainly due to sample transfer problems and dead volume within the Luer-lock adapter. Improvements in design using computational fluid dynamics simulations are necessary to enhance egg capture efficiency.

A primary limitation of flotation-based methods is that factors such as the type of fixative (e.g. formalin, sodium acetate-acetic acid-formalin), the duration of preservation, and the selection of flotation solutions can affect the recovery of helminth eggs, affecting the overall accuracy of

these methods.

2.3. PORTABLE DIGITAL MICROSCOPES

Portable microscopy was first introduced in 1932 by John Norris McArthur, a pioneering clinical researcher, and was further advanced in clinical applications by the Wellcome Trust initiative, which led to the development of the Newton NM1 microscope [47–49]. Recent advances in opto-mechanics and opto-electronics have significantly transformed biomedical optics, enabling the redesign of optical imaging technologies such as conventional light microscopes into integrated, miniaturized, and portable formats for use at the point of care (POC). Zhu *et al.* [50] reviewed cutting-edge optical imaging technologies with potential impacts on global health, although these technologies are more readily accessible in high-income countries. Infectious diseases remain endemic in many low-income countries, raising the need for affordable, user-friendly optical imaging solutions. Consequently, handheld and mobile phone microscopes have been developed for the diagnosis of neglected tropical diseases (NTD), with several reviews highlighting their application in both field and laboratory settings [47, 51, 52]. However, more recently, Meulah *et al.* [53] employed an adapted technology readiness level (TRL) scale aligned with the WHO target product profile (TPP) for soil-transmitted helminths (STH) and schistosome infections, to classify the developmental stages of optical devices, assessing their readiness for practical use in field settings. Despite these reviews, the focus on technology design remains limited. This section discusses various portable microscope designs for imaging helminth eggs, examining their strengths and limitations from an engineering design perspective.

The Readiview handheld microscope from Meade Instruments Corporation (Irvine, CA) is a lightweight, low-cost (under 0.25 kg) monocular microscope with few moving parts and a LED light source, priced at approximately $70. Stothard *et al.* [54] evaluated its optical quality to examine Kato-Katz fecal smears, noting that it is a convenient photomicrography platform. At 80× or 160× magnification, trained users can identify *S. mansoni* eggs, though the lack of a mechanical stage may lead to duplicate or missed fields during examination due to manual slide movement. However, it is suitable for the detection of schistosome eggs for the confirmation of infection.

Bogoch *et al.* [55] converted an iPhone 4S into a microscope by mounting a 3 mm ball lens with double-sided tape over the phone camera. With a small space between the lens and the sample slide and illumination from a handheld flashlight, this setup achieved 50–60× magnification. However, manual slide manipulation limits precision and image quality is lower than that of conventional microscopes, making

species differentiation challenging. Smaller eggs like those of *T. trichiura* were harder to detect, reducing sensitivity for certain helminths.

Coulibaly *et al.* [56] tested two experimental portable microscopes on Kato-Katz slides: the mobile phone-mounted reversed-lens, CellScope, and the Newton NM1 Portable Field Microscope. The CellScope consists of a 3D-printed attachment fitted over an iPhone 5s. It uses the light source of the phone, but requires manual movement for sample scanning, which impacts egg count accuracy due to lack of structural support. However, the Newton NM1 is a commercially available handheld microscope, lightweight (under 500 g), with objective lenses (10x, 40x, 100x) and an XY translation stage, providing a more stable platform. Although it costs $650, it offers a long battery life (300 hours on three AAA batteries) and allows digital imaging with a mobile phone camera, adding versatility but increasing cost [57, 58].

Digital microscopy offers advantages over conventional microscopy, including real-time data sharing and remote diagnosis, and the potential for automated diagnosis via digital image analysis. Holmström *et al.* [59] used a compact, cloud-connected digital microscope constructed from low-cost smartphone camera components. It includes a 5-megapixel CMOS sensor, LED light sources for both bright-field and fluorescent imaging, and an image resolution of approximately 1.23 µm. The device is USB-connected and controlled via MATLAB software, capturing images that can be stitched into virtual slides for deep learning analysis of stool samples.

The FECPAKG2 platform uses the MICRO-I device to capture digital images of helminth eggs concentrated within the FECPAKG2 cassette [60]. This system enables technicians to view, count, and store images online, eliminating the need for microscopists on site. Cloud-based storage allows quality control and the potential for automated egg counting, which could improve throughput and reduce labor costs [61].

Li *et al.* [62] adapted a fully automated microscopy system in a cost-effective design using 3D printed housings, a CMOS sensor, and low-cost lenses. The system achieves high resolution (1.55 µm), though it has a limited field of view. Sample scanning and image acquisition are automated using LabVIEW, reducing manual labor and supporting whole-slide imaging.

A benchtop imaging system for field experiments was developed by Sukas *et al.* [35], using a Sony 5100 camera with a Samyang 100 mm macrolens and halogen lighting. This setup allows for transmitted light imaging, and Wi-Fi connectivity allows remote control via tablet. Despite the $1420 cost, the system offers high-resolution imaging and is suitable for field use.

Agbana *et al.* [63] developed a low-cost microscope that uses a smartphone camera with a reverse lens setup to capture high-magnification images of *Schistosoma haematobium* eggs in urine

samples, emphasizing affordability, local production and adaptability for settings limited by resources. Building on similar principles, Dacal *et al.* [64] introduced a 3D printed adapter that aligns a smartphone camera with a conventional microscope eyepiece, effectively transforming the setup into a digital microscope. This compact design retains traditional microscope functionality while allowing easy image digitization and sharing through a custom Android app. For point of care diagnosis, Armstrong *et al.* [65] designed a smartphone-based microscope featuring a specialized disposable cartridge. The cartridge filters and concentrates schistosome eggs from urine, aligning them within the field of view for easy imaging with the reversed lens optics of the smartphone, achieving sufficient magnification and resolution for effective detection.

Meanwhile, Ward *et al.* [66] created a flexible and low-cost whole-slide imaging (WSI) scanner using modular and readily available components, focused on delivering high-quality data capture at a price below $2,000. Advancing automation in digital microscopy, Oyibo *et al.* [67] presented the Schistoscope, an affordable digital microscope with an optical system modeled after a standard light microscope. It incorporates a robust illumination setup and a 4x magnification objective adjustable up to 20x, projecting the image to a Raspberry Pi camera sensor. The automated Z-axis focus and X-Y stage movements of the Schistoscope allow for precise autofocus and slide scanning, ensuring reliable image capture for diagnostic applications. A commercially available single-slide automated scanner and microscope similar to the Schistoscope is the AiDx Assist Makau-Barasa *et al.* [68]. Its optical train includes a 4$\times$ microscope objective with a numerical aperture (NA) of 0.10 and a working distance of 18.0 mm, paired with a Sony IMX 178 CMOS sensor (6.41 Mpix, 3088 $\times$ 2076 pixels) that registers a pixel size of 2.40 μm. This multidiagnostic device is capable of detecting microfilaria, *S. haematobium*, and *S. mansoni* eggs in blood, urine and stool samples, respectively.

A primary challenge with mobile phones and handheld microscopes remains the manual manipulation of samples, leading to undercounting of eggs. Some portable microscope designs address this by incorporating XY stages and motorized autofocus. Advanced designs integrate image digitization and real-time data sharing for remote diagnosis and automated analysis via AI. However, cost constraints persist, limiting widespread adoption in low-resource settings.

2.4. AUTOMATED DETECTION AND IDENTIFICATION OF HELMINTH EGGS

Human parasitic infections are typically diagnosed by identifying parasitic organisms in feces, urine, blood, or tissue samples using

specific diagnostic methods [69]. Following sample preparation, trained specialists examine the prepared slides to detect parasitic organisms, most often helminth eggs or protozoa cysts. Upon identifying these organisms, experts assess their size, shape, and count to determine the species of parasites, severity of infection, and appropriate treatment [70]. However, samples frequently contain artifacts such as urine crystals, large food debris, amorphous particles, or undigested plant cells in fecal samples, complicating the interpretation of microscopy images. Consequently, manual microscopic examination is both labor intensive and time consuming. Its accuracy can also be influenced by the skill and experience of the examiner, which is particularly problematic in regions with limited access to trained personnel. To overcome these challenges, AI algorithms for the automated identification of parasitic components and clinical diagnosis of helminth infections are increasingly vital. These automated detection and identification methods are generally divided into two main categories: deep learning-based and machine learning-based approaches.

2.4.1. MACHINE LEARNING-BASED METHODS

The early work of Yang *et al.* [70] marked one of the first applications of computer vision for identifying and classifying helminth eggs in fecal samples. They introduced an automated fecal examination system that extracted morphometric features—shape, shell smoothness, and size—from microscopy images, using an Artificial Neural Network (ANN) for the initial separation of eggs from artifacts, followed by a secondary ANN for species classification. Building on this, Avci and Varol [71] employed a multiclass support vector machine (MCSVM) classifier for parasite classification using invariant moments from pre-processed images.

Following this foundational research, Bruun, Kapel, and Carstensen [72] applied matched filters for detection, with linear and quadratic discriminant analysis to classify features such as autocorrelation and scattering intensity under dark-field illumination. In a similar vein, Suzuki *et al.* [73] used ellipse matching and the image foresting transform for segmentation, with object recognition achieved through an optimum path forest classifier. Further advancements by Zhang *et al.* [74] introduced the Cascaded-Automatic Segmentation (CAS) approach for segmenting *S. japonicum* eggs in fecal samples, using Radon-like feature enhancement, Randomized Hough transform for elliptical detection, and final segmentation with an Active Contour Model.

In a related approach, Li *et al.* [75] used phase coherence technology for contour extraction and applied SVM classification based on shape and texture characteristics. Liu *et al.* [76] advanced this by combining morphological segmentation, clustering, and neural networks for a

refined analysis. Wang *et al.* [77] implemented edge detection on grayscale and B-channel images, followed by morphological processing, and extracted six morphological features for SVM classification.

For increased accuracy, Wang *et al.* [78] applied threshold segmentation using inscribed and circumscribed circles to exclude overlapped impurities, followed by feature extraction using LBP-uniform, Gabor, HOG, GLCM and Haar. SVM classifiers with HOG features achieved the best accuracy. Tchinda *et al.* [79] employed active contours and the Hough transform for segmentation, followed by feature reduction through principal component analysis and classification using a probabilistic neural network.

Machine learning-based methods established foundational techniques for feature extraction and classification, utilising SVMs, ANNs, and contour detection. Despite demonstrating effectiveness, these approaches often struggled with complex samples laden with various artifacts, leading to a shift toward deep learning methodologies.

2.4.2. DEEP LEARNING-BASED METHODS

The complexity of microscopic images, especially in field samples, paved the way for deep learning approaches. Peixinho *et al.* [80] introduced ConvNet-based feature extraction combined with a linear SVM to improve the detection of fecal parasite eggs. Subsequent work by Du *et al.* [81] furthered this with an object detection model using morphological methods to extract candidates, followed by the PCA-Inception-v3 architecture for recognition, demonstrating high precision and adaptability across images.

With advances in CNN architectures, Li *et al.* [62] developed a system using a CNN based on U-Net trained on annotated images to accurately distinguish eggs from background debris. Building on this model, Li *et al.* [82] proposed FecalNet, leveraging ResNet152 and a feature pyramid network to fully automate detection. More recent work by Kitvimonrat *et al.* [83] compared three object detectors: Faster R-CNN, RetinaNet, and CenterNet, finding that RetinaNet is the most effective for parasite egg identification.

Other studies expanded these methods to *S. haematobium* egg detection in urine samples, despite the challenges of field-captured images with various artifacts. Early on, Hassan and Al-Hity [84] used thresholding of cross-correlation coefficients for isolated *S. haematobium* egg detection, although performance in noisy images was limited. Later, Armstrong *et al.* [65] addressed this with transfer learning, comparing RetinaNet, MobileNet, and EfficientDet, with RetinaNet performing well in isolated egg detection and debris rejection, although the clump artifacts remained challenging. Complementing these methods, Oyibo *et al.* [85] developed a two-stage diagnosis framework, which

consists of semantic segmentation of *S. haematobium* eggs using the DeepLabv3-MobileNetV3 deep convolutional neural network and a refined segmentation step using the ellipse fitting approach to approximate eggs with an automatically determined number of ellipses.

In parallel, applications targeting intestinal helminth detection progressed. Alva *et al.* [86] employed logistic regression with geometric and brightness features, while Viet, ThanhTuyen, and Hoang [87] introduced Faster R-CNN for stool sample analysis. Yang *et al.* [88] presented Kankanet, an ANN-based mobile application for egg recognition, although dataset limitations affected its performance. Later, delas Peñas *et al.* [89] applied a tiny YOLO model, which demonstrated real-time processing potential but limited accuracy for soil-transmitted helminths.

Subsequent models integrated deep learning-based segmentation and object detection, such as Deep Belief Networks by Roder *et al.* [90] and SSD-MobileNet by Dacal *et al.* [64], which improved remote analysis capabilities, particularly for *T. trichiura*. With improved speed and precision, YOLOv5 [91] outperformed traditional approaches, while Nakasi, Aliija, and Nakatumba [92] and Lim *et al.* [93] found deep learning methods such as AlexNet and GoogleNet to be more effective for segmentation tasks.

Recent models emphasized the robustness of classification. For example, Khairudin *et al.* [94] explored classifiers such as k-NN, SVM, and Ensemble, with features that include Hu's invariant moments and GLCM. Subsequent innovations by Lee *et al.* [95] and Libouga *et al.* [96] proposed integrated platforms and modified U-Net models to improve helminth egg detection accuracy, although challenges in data set diversity continued. YOLOv4-Tiny [97] and Faster R-CNN [98] further demonstrated enhanced accuracy in high-magnification stool images.

Efforts to develop large datasets, such as the collection of KK stool smears by Ward *et al.* [66], underscored the issue of class imbalance. Concurrently, Acula *et al.* [99] and Caetano, Santana, and de Lima [100] explored CNN architectures and AdaBoost classifiers for species detection in limited datasets. Most recently, Jaya Sundar Rajasekar *et al.* [101] found that YOLOv8 with an SGD optimizer outperformed previous models, and Lundin *et al.* [102] employed two CNNs to classify soil-transmitted helminth (STH) eggs, although sample level counts were consistently higher than the results of manual microscopy.

Deep learning models, particularly those using CNNs architectures, have proven more adept at handling complex, high-variability images. These approaches also support automation, providing potential solutions for field applications in regions with limited access to trained personnel. However, challenges remain, notably in the limitations of the dataset, the variability in image quality, and the generalization between different types of samples.

For a reliable real-world application, future research must focus

on expanding the diversity of the dataset to include images with overlapping eggs, various impurities, and artifacts, ensuring robust model performance across settings. The studies reviewed here confirm the promise of deep learning in the advancement of automated diagnosis, underscoring the need for adaptable, data-rich solutions to support diagnostics in diverse environmental and clinical contexts.

2.5. CONCLUSION

Although traditional methods and newer automated technologies have contributed valuable tools for the diagnosis of parasitic diseases, there is a critical need to improve the cost, accessibility, and robustness of datasets. The future of effective parasite diagnostics in low-resource settings lies in the seamless integration of affordable, portable sample preparation and imaging devices with advanced AI-based analysis. This thesis aims to enhance the diversity of helminth image datasets, improve the accuracy of automated helminth detection models, and optimize the efficiency and affordability of digital microscope devices. These advances are crucial for developing scalable diagnostic solutions to meet the growing demand in real-world applications within endemic regions.

REFERENCES

[1] K. Jaromin-Gleń, T. Kłapeć, G. Łagód, J. Karamon, J. Malicki, A. Skowrońska, and A. Bieganowski. “Division of methods for counting helminths’ eggs and the problem of efficiency of these methods”. In: *Ann Agric Env. Med* 24.1 (2017), pp. 1–7. doi: 10.5604/12321966.1233891.

[2] K. O. Abosalif, A. A. Ahmed, I. M. Shammat, A. S. Aljafari, A. A. Afifi, and C. J. Shiff. “A Comparative Study of Three Conventional Methods for Diagnosis of Urinary Schistosomiasis”. In: *Journal of The Faculty of Science and Technology* 6 (2019), pp. 48–61. doi: 10.52981/jfst.vi6.603.

[3] Y. Xiao, Y. Lu, M. Hsieh, J. Liao, and P. K. Wong. “A microfiltration device for urogenital schistosomiasis diagnostics”. In: *PLoS ONE* 11.4 (2016), e0154640. doi: 10.1371/journal.pone.0154640.

[4] V. Silva-Moraes, L. M. Shollenberger, L. M. V. Siqueira, W. Castro-Borges, D. A. Harn, R. F. Q. E. Grenfell, A. L. T. Rabello, and P. M. Z. Coelho. “Diagnosis of Schistosoma mansoni infections: what are the choices in Brazilian low-endemic areas?” In: *Mem. Inst. Oswaldo Cruz* 114 (2019), e180478. doi: 10.1590/0074-02760180478.

[5] F. A. Soares, A. D. N. Benitez, B. M. D. Santos, S. H. N. Loiola, S. L. Rosa, W. B. Nagata, S. V. Inácio, C. T. N. Suzuki, K. D. S. Bresciani, A. X. Falcão, and J. F. Gomes. “A historical review of the techniques of recovery of parasites for their detection in human stools”. In: *Rev. Soc. Bras. Med. Trop.* 53 (2020). doi: 10.1590/0037-8682-0535-2019.

[6] M. Mbong Ngwese, G. Prince Manouana, P. A. Nguema Moure, M. Ramharter, M. Esen, and A. A. Adégnika. “Diagnostic Techniques of Soil-Transmitted Helminths: Impact on Control Measures”. In: *Trop. Med. Infect. Dis.* 5.2 (2020), p. 93. doi: 10.3390/tropicalmed5020093.

[7] T. W. Gyorkos, M. Ramsan, A. Foum, and I. S. Khamis. “Efficacy of new low-cost filtration device for recovering Schistosoma haematobium eggs from urine”. In: *Journal of Clinical Microbiology* 39.7 (July 2001), pp. 2681–2682. doi: 10.1128/JCM.39.7.2681-2682.2001.

[8] World Health Organisation. *Schistosomiasis*. 2024. url: https://www.who.int/news-room/fact-sheets/detail/schistosomiasis (visited on 09/26/2024).

[9] R. K. Ephraim, E. Duah, J. R. Andrews, and I. I. Bogoch. "Ultra-low-cost urine filtration for Schistosoma haematobium diagnosis: a proof-of-concept study". In: *American Journal of Tropical Medicine and Hygiene* 91.3 (Sept. 2014), pp. 544–546. doi: 10.4269/ajtmh.14-0221.

[10] K. Kato. "Comparative examinations". In: *Jpn J Parasitol* 3 (1954), p. 35.

[11] K. Kato. "A correct application of the thick-smear technique with cellophane paper cover. A pamphlet. 9p., 1960 (In Japanese)". In: *Jpn. J Med Sci Biol* 19.1 (1966), pp. 59–64.

[12] N. Katz, P. M. Z. Coelho, and J. Pellegrino. "Evaluation of Kato's quantitative method through the recovery of Schistosoma mansoni eggs added to human feces". In: *J. Parasitol.* 56.5 (1970).

[13] Y. Komiya and A. Kobayashi. "Evaluation of Kato's thick smear technic with a cellophane cover for helminth eggs in feces". In: *Jpn. J. Med. Sci. Biol.* 19.1 (1966), pp. 59–64.

[14] L. K. Martin and P. C. Beaver. "Evaluation of Kato thick-smear technique for quantitative diagnosis of helminth infections". In: *Am. J. Trop. Med. Hyg.* 17.3 (1968), pp. 382–391. doi: 10.4269/ajtmh.1968.17.382.

[15] G. Chaia, A. B. Q. Chaia, J. McAullife, N. Katz, and D. Gasper. "Coprological diagnosis of schistosomiasis. II. Comparative study of quantitative methods". In: *Rev. Inst. Med. Trop. São Paulo* 10.6 (1968).

[16] M. Layrisse, C. Martínez-Torres, and H. Ferrer-Farias. "A simple volumetric device for preparing stool samples in the cellophane thick-smear technique". In: *Am. J. Trop. Med. Hyg.* 18.4 (1969), pp. 553–554.

[17] N. Katz, A. Chaves, and J. Pellegrino. "A simple device for quantitative stool thick-smear technique in Schistosomiasis mansoni". In: *Rev. Inst. Med. Trop. Sao Paulo* 14.6 (1972), pp. 397–400.

[18] W. Telemann. "Eine methode zur erleichterung der auffindung von parasiteneiern in den faeces". In: *DMW-Dtsch. Med. Wochenschr.* 34.35 (1908), pp. 1510–1511. doi: 10.1055/s-0028-1135692.

[19] M. M. Manser, A. C. S. Saez, and P. L. Chiodini. “Faecal parasitology: concentration methodology needs to be better standardised”. In: *PLoS Negl. Trop. Dis.* 10.4 (2016), e0004579. doi: 10.1371/journal.pntd.0004579.

[20] L. S. Ritchie. “An ether sedimentation technique for routine stool examinations”. In: *Bull. U. S. Army Med. Dep.* 8.4 (1948).

[21] J. Maldonado and J. Acosta-Matienzo. “A Comparison of fecal examination procedures in the diagnosis of schistosomiasis mansoni”. In: *Exp. Parasitol.* 2.3 (1953), pp. 294–310. doi: 10.1016/0014-4894(53)90040-X.

[22] P. A. Collender, A. E. Kirby, D. G. Addiss, M. C. Freeman, and J. V. Remais. “Methods for quantification of soil-transmitted helminths in environmental media: current techniques and recent advances”. In: *Trends Parasitol.* 31.12 (2015), pp. 625–639. doi: 10.1016/j.pt.2015.08.007.

[23] K. H. Young, S. L. Bullock, D. M. Melvin, and C. L. Spruill. “Ethyl acetate as a substitute for diethyl ether in the formalin-ether sedimentation technique”. In: *J. Clin. Microbiol.* 10.6 (1979), pp. 852–853. doi: 10.1128/jcm.10.6.852-853.1979.

[24] L. S. Garcia, M. Arrowood, E. Kokoskin, G. P. Paltridge, D. R. Pillai, G. W. Procop, N. Ryan, R. Y. Shimizu, and G. Visvesvara. “Laboratory diagnosis of parasites from the gastrointestinal tract”. In: *Clin. Microbiol. Rev.* 31.1 (2018). doi: 10.1128/CMR.00025-17.

[25] A. O. Lutz. “Schistosomum mansoni e a schistosomatose segundo observações feitas no Brasil”. In: *Mem. Inst. Oswaldo Cruz* 11.1 (1919), pp. 121–155. doi: 10.1590/S0074-02761919000100006.

[26] W. A. Hoffman, J. A. Pons, and J. L. Janer. “The sedimentation-concentration method in schistosomiasis mansoni”. In: *Puerto Rico Journal of Public Health and Tropical Medicine* 9.3 (1934), pp. 283–291.

[27] V. Amato Neto, R. Campos, P. L. Pinto, L. Matsubara, L. M. Braz, A. Miyamoto, R. Foster, S. A. do Nascimento, H. B. de Souza, and A. A. Moreira. “Evaluation of the usefulness of the Coprotest for parasitologic examination of feces”. In: *Rev. Hosp. Clin.* 44.4 (1989), pp. 153–5.

[28] C. R. Mendes, A. T. Teixeira, R. A. Pereira, and L. C. Dias. “A Comparative Study Of The Parasitological Techniques: Kato-katz And Coprotest”. In: *Rev. Soc. Bras. Med. Trop.* 38.2 (2005), pp. 178–180. doi: 10.1590/s0037-86822005000200010.

[29] W. B. Rowan and A. L. Gram. “Quantitative recovery of helminth eggs from relatively large samples of feces and sewage”. In: *J. Parasitol.* 45.6 (1959), pp. 615–622.

[30] L. S. Ritchie and L. A. Berrios-Duran. “A simple procedure for recovering schistosome eggs in mass from tissues”. In: *J. Parasitol.* 47.3 (1961), pp. 363–365.

[31] P. M. Z. Coelho, A. D. Jurberg, Á. A. Oliveira, and N. Katz. “Use of a saline gradient for the diagnosis of schistosomiasis”. In: *Mem. Inst. Oswaldo Cruz* 104.5 (Aug. 2009), pp. 720–723. doi: 10.1590/S0074-02762009000500010.

[32] C. C. Bass. “The diagnosis of hookworm infection with special reference to the examination of feces for eggs of intestinal parasites”. In: *Arch Diag* 3 (1910), pp. 231–236.

[33] H. H. Willis. “A simple levitation method for the detection of hookworm ova”. In: *Med. J. Aust.* 2.18 (1921). doi: 10.5694/j.1326-5377.1921.tb60654.x.

[34] P. D. Cox and A. C. Todd. “Survey of gastrointestinal parasitism in Wisconsin dairy cattle”. In: *J. Am. Vet. Med. Assoc.* 141.6 (1962), pp. 706–709.

[35] S. Sukas, B. Van Dorst, A. Kryj, O. Lagatie, W. De Malsche, and L. J. Stuyver. “Development of a Lab-on-a-Disk Platform with Digital Imaging for Identification and Counting of Parasite Eggs in Human and Animal Stool”. In: *Micromachines* 10.12 (2019), p. 852. doi: 10.3390/mi10120852.

[36] T. G. Egwang and J. O. Slocombe. “Evaluation of the Cornell-Wisconsin centrifugal flotation technique for recovering trichostrongylid eggs from bovine feces”. In: *Can. J. Comp. Med.* 46.2 (1982), pp. 133–137.

[37] H. M. Gordon and H. V. Whitlock. “A new technique for counting nematode eggs in sheep faeces”. In: *J. Counc. Sci. Ind. Res.* 12.1 (1939), pp. 50–52.

[38] H. V. Whitlock. “Some modifications of the McMaster helminth egg-counting technique and apparatus”. In: *J. Counc. Sci. Ind. Res. Aust.* 21.3 (1948), pp. 177–180.

[39] R. Brink. “A simple McMaster egg counting procedure for trichostrongylid eggs in cattle faeces”. In: *Tijdschr. Diergeneeskd.* 96.13 (1971), pp. 859–862.

[40] S. A. Henriksen and K. Aagaard. “A simple flotation and McMaster method (author’s transl)”. In: *Nord. Vet. Med.* 28.7–8 (1976), p. 392.

[41] J. J. Mines. “Modifications of the McMaster worm egg counting method”. In: *Aust. Vet. J.* 53.7 (1977), pp. 342–343. doi: 10.1111/j.1751-0813.1977.tb00247.x.

[42] J. P. Raynaud, J. C. Leroy, M. Virat, and J. A. Nicolas. “A polyvalent egg count technique by dilution and sedimentation in water, flotation in a high sd solution (DSF) and counting in Mac Master slide. Note 1-Interest, justification and description”. In: *Rev. Med. Veterinaire* (1979).

[43] A. Pereckiene, V. Kaziūnaite, A. Vysniauskas, S. Petkevicius, A. Malakauskas, M. Sarkūnas, and M. A. Taylor. “A comparison of modifications of the McMaster method for the enumeration of Ascaris suum eggs in pig faecal samples”. In: *Vet. Parasitol.* 149.1–2 (2007), pp. 111–116. doi: 10.1016/j.vetpar.2007.04.014.

[44] G. Cringoli, L. Rinaldi, M. P. Maurelli, and J. Utzinger. “FLOTAC: new multivalent techniques for qualitative and quantitative copromicroscopic diagnosis of parasites in animals and humans”. In: *Nat. Protoc.* 5.3 (2010), pp. 503–515. doi: 10.1038/nprot.2009.235.

[45] G. Cringoli, L. Rinaldi, M. Albonico, R. Bergquist, and J. Utzinger. “Geospatial (s) tools: integration of advanced epidemiological sampling and novel diagnostics”. In: *Geospatial Health* 7.2 (2013), pp. 399–404. doi: 10.4081/gh.2013.97.

[46] M. H. Rashid, M. A. Stevenson, S. Waenga, G. Mirams, A. J. D. Campbell, J. L. Vaughan, and A. Jabbar. “Comparison of McMaster and FECPAK G2 methods for counting nematode eggs in the faeces of alpacas”. In: *Parasit. Vectors* 11.1 (2018), p. 278. doi: 10.1186/s13071-018-2861-1.

[47] A. Vasiman, J. R. Stothard, and I. I. Bogoch. “Mobile phone devices and handheld microscopes as diagnostic platforms for malaria and neglected tropical diseases (NTDs) in low-resource settings: a systematic review, historical perspective and future outlook”. In: *Advances in Parasitology* 103 (2019), pp. 151–173. doi: 10.1016/bs.apar.2018.09.001.

[48] K. Dunning and J. R. Stothard. “From the McArthur to the millennium health microscope (MHM): future developments in microscope miniaturization for international health”. In: *Microsc Today* 15.2 (2007), pp. 18–21.

[49] R. J. Kreindler. “The Nm1 (Newton Microscopes): Part 2 of 2”. In: *-Depth Exam. Comp. Folded-Opt. Des. Micscape Mag.* (2013).

[50] H. Zhu, S. O. Isikman, O. Mudanyali, A. Greenbaum, and A. Ozcan. “Optical imaging techniques for point-of-care diagnostics”. In: *Lab on a Chip* 13.1 (2013), pp. 51–67. doi: 10.1039/c2lc40864c.

[51] J. Rajchgot, J. T. Coulibaly, J. Keiser, J. Utzinger, N. C. Lo, M. K. Mondry, J. R. Andrews, and I. I. Bogoch. “Mobile-phone and handheld microscopy for neglected tropical diseases”. In: *PLoS Neglected Tropical Diseases* 11.7 (2017), e0005550. doi: 10.1371/journal.pntd.0005550.

[52] M. A. Saeed and A. Jabbar. “Smart diagnosis of parasitic diseases by use of smartphones”. In: *Journal of Clinical Microbiology* 56.1 (2018), e01469–17. doi: 10.1128/JCM.01469-17.

[53] B. Meulah, M. Bengtson, L. Van Lieshout, C. H. Hokke, A. Kreidenweiss, J. C. Diehl, A. A. Adegnika, and T. E. Agbana. “A Review on Innovative Optical Devices for the Diagnosis of Human Soil-Transmitted Helminthiasis and Schistosomiasis: From Research and Development to Commercialization”. In: *Parasitology* 150.2 (2023), pp. 137–149. doi: 10.1017/S0031182022001664.

[54] J. R. Stothard, N. B. Kabatereine, E. M. Tukahebwa, F. Kazibwe, W. Mathieson, J. P. Webster, and A. Fenwick. “Field evaluation of the Meade Readiview handheld microscope for diagnosis of intestinal schistosomiasis in Ugandan school children”. In: *Am. J. Trop. Med. Hyg.* 73.5 (2005), pp. 949–955. doi: 10.4269/ajtmh.2005.73.949.

[55] I. I. Bogoch, J. R. Andrews, B. Speich, J. Utzinger, S. M. Ame, S. M. Ali, and J. Keiser. “Mobile phone microscopy for the diagnosis of soil-transmitted helminth infections: A proof-of-concept study”. In: *The American Journal of Tropical Medicine and Hygiene* 88.4 (2013), pp. 626–629. doi: 10.4269/ajtmh.12-0742.

[56] J. T. Coulibaly, M. Ouattara, M. V. D’Ambrosio, D. A. Fletcher, J. Keiser, J. Utzinger, E. K. N’Goran, J. R. Andrews, and I. I. Bogoch. “Accuracy of mobile phone and handheld light microscopy for the diagnosis of schistosomiasis and intestinal protozoa infections in Côte d’Ivoire”. In: *PLoS Neglected Tropical Diseases* 10.6 (2016), e0004768. doi: 10.1371/journal.pntd.0004768.

[57] J. R. Stothard, B. Nabatte, J. C. Sousa-Figueiredo, and N. B. Kabatereine. “Towards malaria microscopy at the point-of-contact: an assessment of the diagnostic performance of the Newton Nm1 microscope in Uganda”. In: *Parasitology* 141.14 (2014), p. 1819. doi: 10.1017/S0031182014000833.

[58] I. I. Bogoch, J. T. Coulibaly, J. R. Andrews, B. Speich, J. Keiser, J. R. Stothard, E. K. N'goran, and J. Utzinger. "Evaluation of portable microscopic devices for the diagnosis of Schistosoma and soil-transmitted helminth infection". In: *Parasitology* 141.14 (2014), pp. 1811–1818. doi: 10.1017/S0031182014000432.

[59] O. Holmström, N. Linder, B. Ngasala, A. Mårtensson, E. Linder, M. Lundin, H. Moilanen, A. Suutala, V. Diwan, and J. Lundin. "Point-of-care mobile digital microscopy and deep learning for the detection of soil-transmitted helminths and *Schistosoma haematobium*". en. In: *Global Health Action* 10.sup3 (June 2017), p. 1337325. doi: 10.1080/16549716.2017.1337325.

[60] I. R. Cooke, C. J. Laing, L. V. White, S. J. Wakes, and S. J. Sowerby. "Analysis of menisci formed on cones for single field of view parasite egg microscopy". In: *J. Microsc.* 257.2 (2015), pp. 133–141. doi: 10.1111/jmi.12192.

[61] B. Jiménez, C. Maya, G. Velásquez, F. Torner, F. Arambula, J. Barrios, and M. Velasco. "Identification and quantification of pathogenic helminth eggs using a digital image system". In: *Experimental Parasitology* 166 (2016), pp. 164–172. doi: 10.1016/j.exppara.2016.04.016.

[62] Y. Li, R. Zheng, Y. Wu, K. Chu, Q. Xu, M. Sun, and Z. J. Smith. "A low-cost, automated parasite diagnostic system via a portable, robotic microscope and deep learning". In: *J. Biophotonics* 12.9 (2019), e201800410. doi: 10.1002/jbio.201800410.

[63] T. Agbana, G. Y. Van, O. Oladepo, G. Vdovin, W. Oyibo, and J. C. Diehl. "Schistoscope: Towards a locally producible smart diagnostic device for Schistosomiasis in Nigeria". In: *2019 IEEE Global Humanitarian Technology Conference (GHTC)*. Seattle, WA, USA, 2019, pp. 1–8. doi: 10.1109/GHTC46095.2019.9033049.

[64] E. Dacal, D. Bermejo-Peláez, L. Lin, E. Álamo, D. Cuadrado, Á. Martínez, A. Mousa, M. Postigo, A. Soto, E. Sukosd, A. Vladimirov, C. Mwandawiro, P. Gichuki, N. A. Williams, J. Muñoz, S. Kepha, and M. Luengo-Oroz. "Mobile microscopy and telemedicine platform assisted by deep learning for the quantification of Trichuris trichiura infection". In: *PLoS neglected tropical diseases* 15.9 (2021). doi: 10.1371/journal.pntd.0009677.

[65] M. Armstrong, A. R. Harris, M. V. D'Ambrosio, J. T. Coulibaly, S. Essien-Baidoo, R. K. D. Ephraim, J. R. Andrews, I. I. Bogoch, and D. A. Fletcher. "Point-of-care sample preparation and automated quantitative detection of schistosoma haematobium using mobile phone microscopy". In: *American Journal of Tropical*

Medicine and Hygiene 106.5 (2022), pp. 1442–1449. doi: 10.4269/ajtmh.21-1071.

[66] P. Ward, P. Dahlberg, O. Lagatie, J. Larsson, A. Tynong, J. Vlaminck, M. Zumpe, S. Ame, M. Ayana, V. Khieu, Z. Mekonnen, M. Odiere, T. Yohannes, S. V. Hoecke, B. Levecke, and L. J. Stuyver. "Affordable artificial intelligence-based digital pathology for neglected tropical diseases: A proof-of-concept for the detection of soil-transmitted helminths and Schistosoma mansoni eggs in Kato-Katz stool thick smears". In: *PLoS neglected tropical diseases* 16.6 (2022), e0010500. doi: 10.1371/journal.pntd.0010500.

[67] P. Oyibo, S. Jujjavarapu, B. Meulah, T. Agbana, I. Braakman, A. van Diepen, M. Bengtson, L. van Lieshout, W. Oyibo, G. Vdovine, and J. C. Diehl. "Schistoscope: An Automated Microscope with Artificial Intelligence for Detection of Schistosoma haematobium Eggs in Resource-Limited Settings". In: *Micromachines* 13.5 (2022), p. 643. doi: 10.3390/mi13050643.

[68] L. Makau-Barasa, L. Assefa, M. Aderogba, D. Bell, J. Solomon, R. O. Urude, O. J. Nebe, J. A-Enegela, J. G. Damen, S. Popoola, J. C. Diehl, G. Vdovine, and T. Agbana. "Performance evaluation of the AiDx multi-diagnostic automated microscope for the detection of schistosomiasis in Abuja, Nigeria". In: *Scientific Reports* 13.1 (Sept. 2023), p. 14833. doi: 10.1038/s41598-023-42049-6.

[69] L. R. Ash and T. C. Orihel. *Atlas of Human Parasitology*. 5th. American Society of clinical pathologists, 2007. isbn: 978-0891891673.

[70] Y. S. Yang, D. K. Park, H. C. Kim, M. H. Choi, and J. Y. Chai. "Automatic identification of human helminth eggs on microscopic fecal specimens using digital image processing and an artificial neural network". In: *IEEE Transactions on Biomedical Engineering* 48.6 (2001), pp. 718–730. doi: 10.1109/10.923789.

[71] D. Avci and A. Varol. "An expert diagnosis system for classification of human parasite eggs based on multi-class SVM". In: *Expert Systems with Applications* 36.1 (2009), pp. 43–48. doi: 10.1016/j.eswa.2007.09.012.

[72] J. M. Bruun, C. M. Kapel, and J. M. Carstensen. "Detection and classification of parasite eggs for use in helminthic therapy". In: *2012 9th IEEE International Symposium on Biomedical Imaging (ISBI)*. Barcelona, Spain, 2012, pp. 1627–1630. doi: 10.1109/ISBI.2012.6235888.

[73] C. T. Suzuki, J. F. Gomes, A. X. Falcao, J. P. Papa, and S. Hoshino-Shimizu. “Automatic segmentation and classification of human intestinal parasites from microscopy images”. In: *IEEE Trans. Biomed. Eng.* 60.3 (2012), pp. 803–812. doi: 10.1109/TBME.2012.2187204.

[74] J. Zhang, Y. Lin, Y. Liu, Z. Li, Z. Li, S. Hu, Z. Liu, D. Lin, and Z. Wu. “Cascaded-Automatic Segmentation for Schistosoma japonicum eggs in images of fecal samples”. In: *Comput. Biol. Med.* 52 (2014), pp. 18–27. doi: 10.1016/j.compbiomed.2014.05.012.

[75] Z. Li, H. Gong, W. Zhang, L. Chen, J. Tao, L. Song, and Z. Wu. “A robust and automatic method for human parasite egg recognition in microscopic images”. In: *Parasitol. Res.* 114.10 (2015), pp. 3807–3813. doi: 10.1007/s00436-015-4611-z.

[76] L. Liu, H. Lei, J. Zhang, Y. Yuan, Z. Zhang, J. Liu, Y. Xie, G. Ni, and Y. Liu. “Automatic identification of human erythrocytes in microscopic fecal specimens”. In: *J. Med. Syst.* 39.11 (2015), p. 146. doi: 10.1007/s10916-015-0334-z.

[77] W. Wang, M. Si, F. Chen, H. Liu, and X. Jiang. “Study on recognition method of label-free red and white cell using fecal microscopic image”. In: *Proceedings of the 2018 6th International Conference on Bioinformatics and Computational Biology*. Chengdu, China, 2018, pp. 95–100. doi: 10.1145/3194480.3198909.

[78] X. Wang, L. Liu, X. Du, J. Zhang, J. Liu, G. Ni, R. Hao, and Y. Liu. “Leukocyte recognition in human fecal samples using texture features”. In: *J. Opt. Soc. Am. A* 35.11 (2018), pp. 1941–1948. doi: 10.1364/JOSAA.35.001941.

[79] B. S. Tchinda, M. Noubom, D. Tchiotsop, V. Louis-Dorr, and D. Wolf. “Towards an automated medical diagnosis system for intestinal parasitosis”. In: *Inform. Med. Unlocked* 13 (2018), pp. 101–111. doi: 10.1016/j.imu.2019.100238.

[80] A. Z. Peixinho, S. B. Martins, J. E. Vargas, A. X. Falcao, J. F. Gomes, and C. T. Suzuki. “Diagnosis of human intestinal parasites by deep learning”. In: *Computational Vision and Medical Image Processing V: Proceedings of the 5th Eccomas Thematic Conference on Computational Vision and Medical Image Processing (VipIMAGE 2015)*. Tenerife, Spain, 2015, p. 107. doi: 10.1201/b19241-19.

[81] X. Du, L. Liu, X. Wang, G. Ni, J. Zhang, R. Hao, J. Liu, and Y. Liu. “Automatic classification of cells in microscopic fecal images using convolutional neural networks”. In: *Biosci. Rep.* 39.4 (2019). doi: 10.1042/BSR20182100.

[82] Q. Li, S. Li, X. Liu, Z. He, T. Wang, Y. Xu, H. Guan, R. Chen, S. Qi, and F. Wang. “FecalNet: Automated detection of visible components in human feces using deep learning”. In: *Med. Phys.* 47.9 (2020), pp. 4212–4222. doi: 10.1002/mp.14352.

[83] A. Kitvimonrat, N. Hongcharoen, S. Marukatat, and S. Watcharabutsarakham. “Automatic Detection and Characterization of Parasite Eggs using Deep Learning Methods”. In: *2020 17th International Conference on Electrical Engineering/Electronics, Computer, Telecommunications and Information Technology (ECTI-CON)*. 2020, pp. 153–156.

[84] M. O. K. Hassan and K. M. Al-Hity. “Computer-aided diagnosis of schistosomiasis: automated schistosoma egg detection”. In: *Journal of Clinical Engineering* 37.1 (2012), pp. 29–34. doi: 10.1097/JCE.0b013e31823fda36.

[85] P. Oyibo, B. Meulah, M. Bengtson, L. van Lieshout, W. Oyibo, J. C. Diehl, G. Vdovine, and T. Agbana. “Two-stage automated diagnosis framework for urogenital schistosomiasis in microscopy images from low-resource settings”. In: *Journal of Medical Imaging* 10.4 (2023), pp. 044005–044005. doi: 10.1117/1.JMI.10.4.044005.

[86] A. Alva, C. Cangalaya, M. Quiliano, C. Krebs, R. H. Gilman, P. Sheen, and M. Zimic. “Mathematical algorithm for the automatic recognition of intestinal parasites”. In: *PLoS ONE* 12.4 (2017), e0175646. doi: 10.1371/journal.pone.0175646.

[87] N. Q. Viet, D. T. ThanhTuyen, and T. H. Hoang. “Parasite worm egg automatic detection in microscopy stool image based on Faster R-CNN”. In: *Proceedings of the 3rd International Conference on Machine Learning and Soft Computing*. New York, NY, USA: Association for Computing Machinery, 2019, pp. 197–202. isbn: 978-1-4503-6612-0. doi: 10.1145/3310986.3311014.

[88] A. Yang, N. Bakhtari, L. Langdon-Embry, E. Redwood, S. G. Lapierre, P. Rakotomanga, A. Rafalimanantsoa, J. D. D. Santos, I. Vigan-Womas, A. M. Knoblauch, and L. A. Marcos. “Kankanet: An artificial neural network-based object detection smartphone application and mobile microscope as a point-of-care diagnostic aid for soil-transmitted helminthiases”. In: *PLoS neglected tropical diseases* 13.8 (2019), e0007577. doi: 10.1371/journal.pntd.0007577.

[89] K. E. delas Peñas, E. A. Villacorte, P. T. Rivera, and P. C. Naval. “Automated Detection of Helminth Eggs in Stool Samples Using Convolutional Neural Networks”. In: *2020 IEEE REGION 10 CONFERENCE (TENCON)*. Osaka, Japan, 2020, pp. 750–755. doi: 10.1109/TENCON50793.2020.9293746.

[90] M. Roder, L. A. Passos, L. C. F. Ribeiro, B. C. Benato, A. X. Falcão, and J. P. Papa. “Intestinal Parasites Classification Using Deep Belief Networks”. In: *International Conference on Artificial Intelligence and Soft Computing*. Vol. 12415. Springer. Zakopane, Poland, 2020, pp. 242–251. doi: 10.1007/978-3-030-61401-0_23.

[91] Y. Huo, J. Zhang, X. Du, X. Wang, J. Liu, and L. Liu. “Recognition of parasite eggs in microscopic medical images based on YOLOv5”. In: *2021 5th Asian Conference on Artificial Intelligence Technology (ACAIT)*. Haikou, China, 2021, pp. 123–127. doi: 10.1109/ACAIT53529.2021.9731120.

[92] R. Nakasi, E. R. Aliija, and J. Nakatumba. “A Poster on Intestinal Parasite Detection in Stool Sample Using AlexNet and GoogleNet Architectures”. In: *Proceedings of the 4th ACM SIGCAS Conference on Computing and Sustainable Societies*. COMPASS ’21. New York, NY, USA: Association for Computing Machinery, 2021, pp. 389–395. isbn: 978-1-4503-8453-7. doi: 10.1145/3460112.3472309.

[93] C. C. Lim, N. A. A. Khairudin, S. W. Loke, A. S. A. Nasir, Y. F. Chong, and Z. Mohamed. “Comparison of Human Intestinal Parasite Ova Segmentation Using Machine Learning and Deep Learning Techniques”. In: *Applied Sciences* 12.15 (2022), p. 7542. doi: 10.3390/app12157542.

[94] N. A. A. Khairudin, C. C. Lim, A. S. A. Nasir, and Z. Mohamed. “Efficient Classification Techniques in Classifying Human Intestinal Parasite Ova”. In: *Journal of Telecommunication, Electronic and Computer Engineering (JTEC)* 14.3 (2022), pp. 17–23. doi: 10.54554/jtec.2022.14.03.003.

[95] C.-C. Lee, P.-J. Huang, Y.-M. Yeh, P.-H. Li, C.-H. Chiu, W.-H. Cheng, and P. Tang. “Helminth egg analysis platform (HEAP): An opened platform for microscopic helminth egg identification and quantification based on the integration of deep learning architectures”. In: *Journal of Microbiology, Immunology and Infection* 55.3 (2022), pp. 395–404. doi: 10.1016/j.jmii.2021.07.014.

[96] I. O. Libouga, L. Bitjoka, D. L. L. Gwet, O. Boukar, and A. M. N. Nlôga. “A supervised U-Net based color image semantic segmentation for detection & classification of human intestinal parasites”. In: *e-Prime - Advances in Electrical Engineering, Electronics and Energy* 2 (2022), p. 100069. doi: 10.1016/j.prime.2022.100069.

[97] K. M. Naing, S. Boonsang, S. Chuwongin, V. Kittichai, T. Tongloy, S. Prommongkol, P. Dekumyoy, and D. Watthanakulpanich. “Automatic recognition of parasitic products in stool examination using object detection approach”. In: *PeerJ Computer Science* 8 (2022), e1065. doi: 10.7717/peerj-cs.1065.

[98] B. A. S. Oliveira, J. M. P. Moreira, P. R. S. Coelho, D. A. Negrão-Corrêa, S. M. Geiger, and F. G. Guimarães. “Automated diagnosis of schistosomiasis by using faster R-CNN for egg detection in microscopy images prepared by the Kato–Katz technique”. In: *Neural Computing and Applications* 34.11 (2022), pp. 9025–9042. doi: 10.1007/s00521-022-06924-z.

[99] D. D. Acula, C. P. L. Buico, G. U. Cruzada, M. K. C. Encelan, and C. Y. G. Rivera. “Soil transmitted helminth egg detection and classification in fecal smear images using faster region-based convolutional neural network with residual network-50”. In: *International Conference on Green Energy, Computing and Intelligent Technology (GEn-CITy 2023)*. Vol. 2023. 2023, pp. 284–291. doi: 10.1049/icp.2023.1793.

[100] A. Caetano, C. Santana, and R. A. de Lima. “Diagnostic support of parasitic infections with an AI-powered microscope”. In: *Research on Biomedical Engineering* 39.3 (2023), pp. 561–572. doi: 10.1007/s42600-023-00288-6.

[101] S. Jaya Sundar Rajasekar, G. Jaswal, V. Perumal, S. Ravi, and V. Dutt. “Parasite.ai – An Automated Parasitic Egg Detection Model from Microscopic Images of Fecal Smears using Deep Learning Techniques”. In: *2023 International Conference on Advances in Computing, Communication and Applied Informatics (ACCAI)*. Chennai, India, 2023, pp. 1–9. doi: 10.1109/ACCAI58221.2023.10200869.

[102] J. Lundin, A. Suutala, O. Holmström, S. Henriksson, S. Valkamo, H. Kaingu, F. Kinyua, M. Muinde, M. Lundin, and V. Diwan. “Diagnosis of soil-transmitted helminth infections with digital mobile microscopy and artificial intelligence in a resource-limited setting”. In: *PLOS Neglected Tropical Diseases* 18.4 (2024), e0012041. doi: 10.1371/journal.pntd.0012041.

3

SCHISTOSCOPE: SMARTPHONE VS RASPBERRY PI DESIGN

Schistoscope: Smartphone versus Raspberry Pi based low-cost diagnostic device for urinary Schistosomiasis

Jan Carel Diehl, Prosper Oyibo, Temitope Agbana, Satyajith Jujjavarapu, G-Young Van, Gleb Vdovin, Wellington Oyibo

PUBLICATION REPORT

- **Conference Date:** 29 October - 01 November 2020
- **Proceedings:** 2020 IEEE Global Humanitarian Technology Conference (GHTC)
- **Publisher:** IEEE
- **DOI:** 10.1109/GHTC46280.2020.9342871

ABSTRACT

Schistosomiasis is a neglected tropical disease of Public Health importance affecting over 252 million people worldwide with Nigeria having a very high number of cases. It is caused by blood flukes of the genus Schistosoma and transmitted by freshwater snails. To achieve the current global elimination objectives, low-cost and easy-to-use diagnostic tools are critically needed. Recent innovations in optical and computer technologies have made handheld digital and smartphone-based microscopes a viable diagnostic approach. Development, validation and deployment of these diagnostic devices for field use, however, require the optimisation of its optical train for the registration of high-resolution images and the realisation of a robust system design that can be locally produced in low-income countries. Field research conducted in Nigeria with active involvement of key stakeholders in research and development (R&D) led to the design of an initial prototype device for the diagnosis of urinary schistosomiasis, called Schistoscope 1.0. In this paper, we present further development of the Schistoscope 1.0 along two parallel design trajectories: a Raspberry Pi and a Smartphone-based Schistoscope. Specifically, we focused on the optimization of the optics, embodiment design and the electronics systems of the devices so as to produce a robust design with potential for local production.

3.1. INTRODUCTION

3.1.1. SCHISTOSOMIASIS

Schistosomiasis is endemic in 76 countries and territories around the world [1] with an estimated 779 million people at risk of infection, and approximately 252 million people are currently infected [2]. It presents substantial public health and economic burden as it is a disease of poverty. Schistosomiasis is caused by blood flukes of the genus *Schistosoma (S.)*, and it is transmitted by vectors (freshwater snails) living in streams from where the parasites are contracted when humans come in contact with water while carrying-out their daily activities such as washing, bathing, and kids playing or swimming and wading through to the next community due to absence of bridges.

Both intestinal schistosomiasis (*S. mansoni*) and urinary schistosomiasis (*S. haematobium*) are endemic in Africa [3–6] with Nigeria having the highest burden of the disease. Current global to national strategies are aimed at eliminating this preventable disease by employing interventional measures that include the use of mass drug administration (MDA) with approved medicines alongside vector control and hygiene programmes. In the drive for attaining elimination targets, diagnosis for adequate monitoring of interventions and surveillance is critical. Microscopy examination of urine samples, prepared by filtration, sedimentation or centrifugation, is currently the WHO reference standard for the diagnosis of urinary schistosomiasis [7]. However, the laborious nature, time-consuming, high cost, the bulkiness of equipment, shortage of required expertise and lack of required maintenance skills, replaceable parts and associated human errors/subjectivity has limited its availability in remote rural communities [7, 8]. Hence, a field adaptable, rapid and easy-to-use diagnosis is critical for the prompt detection of cases, mapping communities and monitoring trends or progress of interventions toward the attainment of the elimination targets. This paper reports on the accomplishments of the first phase of our INSPIRED (INclusive diagnoStics for Poverty RElated parasitic Diseases) project which brings together a multidisciplinary team composed of biomedical scientists, engineers, public health specialists and product designers from universities in The Netherlands, Nigeria and Gabon. Here, we discussed and compared results from two parallel design trajectories, based on the Raspberry Pi and Smartphone, for an automated diagnostic device for urinary schistosomiasis.

3.1.2. TECHNOLOGICAL DEVELOPMENTS, CHALLENGES AND OPPORTUNITIES

Rapid progress in optical and computer technologies has made smartphone- and Raspberry Pi-based microscopes promising alternatives for field diagnosis of schistosomiasis [9]. Their availability and portability

make them suitable for use outside of a typical lab setting [7, 10, 11]. Also, with integrated data-driven algorithms for automated detection and quantification of *S. haematobium* eggs in filtered urine samples, the lack of experienced microscope operators at the point-of-care and the challenge of data storage can be compensated for. Based on the performance of the algorithm, diagnosis can be achieved with sufficient performance and operational utility. Aside from automated sample analysis, detection, and infection load estimation, the imaging platform could also enable seamless data sharing for disease mapping toward effective control and elimination. This provides an additional utility over conventional manual microscopy where data will be manually generated, recorded and archived.

Despite a wealth of technological innovation in this field which meets many technical and medical criteria, there are still challenges in implementing handheld-microscopy devices in resource-constrained environments [12]. Smartphone-based microscope provides relatively poor image quality due to the inherent aberration of the optics and the limitation posed by the numerical aperture [13]. Furthermore, the limited field of view (FoV), results in the need for multiple measurements of the sample, which reduces the performance of the diagnostic device [14]. An optical setup which consists of a smartphone optical train aligned with a smartphone micro-objective lens (positioned in a reverse format as shown in fig. 3.1) has shown promising results. This optical configuration provides a relatively larger FoV (the entire sensor plane), and a resolution limited mostly by the pixel size of the camera sensor [15].

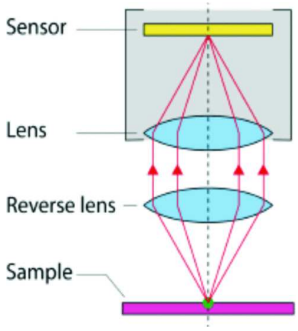

Figure 3.1: Reverse lens setup.

Due to an enormous logistics effort required, Currently available diagnostic devices produced in the West are expensive, scarce, and difficult to maintain (due to lack of spare parts and required technical skills) at the point of need in sub-Saharan Africa [13]. Mass production of components for the consumer electronics market in

recent years, enabled the fabrication of low-cost, effective and portable digital imaging devices [7]. Manufacturing these devices by using locally sourced materials could also reduce costs as well as improve maintenance due to the availability of spare parts in the target areas. Integrating this with innovative manufacturing pathways (i.e. local distributed production) [12], we could overcome import dependency and unnecessary long distribution value chains, that comes with additional costs. Accessible manufacturing technologies like 3D-printing and Laser-cutting offer new opportunities of setting up local production facilities that can produce and supply the devices and spares for local use [13].

Once these challenges are addressed, portable digital microscopy could provide and create access to high-quality schistosomiasis diagnostics. Consequently, timely information on the distribution of the disease, which will reinforce the control and elimination efforts could also be made readily available for use by interested organisations and the National Programme [13]. The design goals and challenges for the Schistoscope development are discussed in the next section.

3.2. DESIGN SETUP

3.2.1. GAPS, CHALLENGES AND OPPORTUNITIES FOR SCHISTOSCOPE 1.0 IMPROVEMENT

A prototype of a diagnostic device for urinary schistosomiasis called the Schistoscope 1.0 was developed in [13] through an iterative design process with implementation research conducted in Nigeria and involving key stakeholders in the research and development process (see fig. 3.2). After several design iterations, the main body of the Schistoscope 1.0 was fabricated in a local workshop. This makes the device easier to repair and maintain locally. The authors further reported on the design of a simple 3-D printed sample holder used with widely available filter material for urine filtration. The device was tested with real urine samples at the University of Lagos and at peri-urban settings in Lagos Nigeria for simulating the diagnostic test in practice.

From the implementation and development research, a range of practical design issues, which needed further consideration in the next design iteration, were identified and hereby proposed. The recommendations listed below, therefore, formed the basis of the next design iteration contained in this paper.

1. **Local manufacturing:** The use of plastic as an alternative to sheet metal for the embodiment design considering the context. To enable more detailed and easy-to-clean embodiment, 3D-printing seems to be the most promising option for manufacturing the Schistoscopes as Makerspaces and small businesses which provide

Figure 3.2: Schistoscope 1.0 (left) and filter process (right).

3D printing services and resources are available in Nigeria and other Low and Middle-Income Countries.

2. **Mobile phone:** A smartphone has the advantage of being locally repairable. However, this severely limits the possibilities of the technical design. The use of a Raspberry Pi or a similar computer could be an interesting alternative in terms of the ease of implementation of the control and artificial intelligence algorithms because it has a large open-source community. Adopting a Raspberry Pi will also enable the modular design and make it more efficient in terms of physical embodiment and battery capacity. Adapting to a new component or expanding the functionality would be relatively easier. Nevertheless, using a smartphone still has many benefits such as its ease of use, availability and familiar interface.

3. **Urine filtration:** The syringe was not well secured in the holder, which caused spillage of the urine samples. Due to the small surface area of the cloth filter and amount of volume injected through it, the pressure on the mesh was high, and since the sample holder does not have a handle, easy spillage of content was observed. The recommendation was to use either established WHO protocol, or at least to use standard filters.

Based on this feedback from the field, the design process for the next design iteration was initiated. The project was carried out between February and July 2019.

3.2.2. DESIGN GOALS FOR SCHISTOSCOPE 1.0 IMPROVEMENT

To develop a digital microscope which offers an integrated diagnostics solution (sample preparation and diagnosis) with the support of a smart algorithm (for detection and quantification of the *S. haematobium* eggs) which can be produced and maintained in sub-Saharan Africa (with the use of locally available components and 3D-printing).

For the specific development goals, product scope is defined, which relates to the primary function of the product, namely diagnosis of urinary schistosomiasis, and its sub-functions and components. The three main component groups are the embodiment of the product, the optics, and electronics. These three components overlap, interact with each other and are responsible for the successful execution of the diagnosis of schistosomiasis. Hence, we initiated two parallel Schistoscope designs trajectories, one based on the Raspberry Pi (Schistoscope RP) and the other based on the smartphone (Schistoscope SP). Also, the Schistoscope has to be culturally accepted and trusted, while keeping costs low.

The four main drivers were chosen to guide the development focus are as follows:

1. **Robustness:** The product needs to withstand the harsh tropical environment in Nigerian, such as humidity and heat. Also, to aid reparability, the product should be built with locally accessible parts in the years following the deployment of the device.
2. **Potential for Local Production:** The product should be locally producible, using largely standard off-the-shelf components in combination with local available distributed production methods.
3. **Intuitiveness:** In order for the product to be accepted and used, operational considerations such as the ease-of-use should be given priority with supporting use cues. Furthermore, the choice of materials and the appearance should contribute to better product appreciation and acceptance.
4. **Hygiene:** Aseptic considerations in the handling of the device, since it works with urine, are imperative to ensure that the product could be easily cleaned to prevent possible cross-contamination.

3.2.3. TECHNICAL DESIGN CHALLENGES FOR SCHISTOSCOPE RP & SP

The three main technical design challenges of the technology behind the product are:

1. Accurate alignment of the camera sensor, micro-objective lens and sample in order to reduce aberrations in the optical system.

2. Imaging the filtered sample in a single FoV, with optimal illumination and sufficient resolution for automated analysis.
3. Robust design and material selection of the casing taking into consideration 3D-printing and off-the-shelf components, in order to be resistant against the environment in rural Nigeria.

3.3. DESIGN RESULTS

3.3.1. SCHISTOSCOPE RP

The Schistoscope RP (see fig. 3.3) analyses *schistosoma* eggs by means of an algorithm running on a Raspberry Pi. The device was designed such that its casing and development board are modular. This will enable easy and quick part replacement in case of device failure at the point of need.

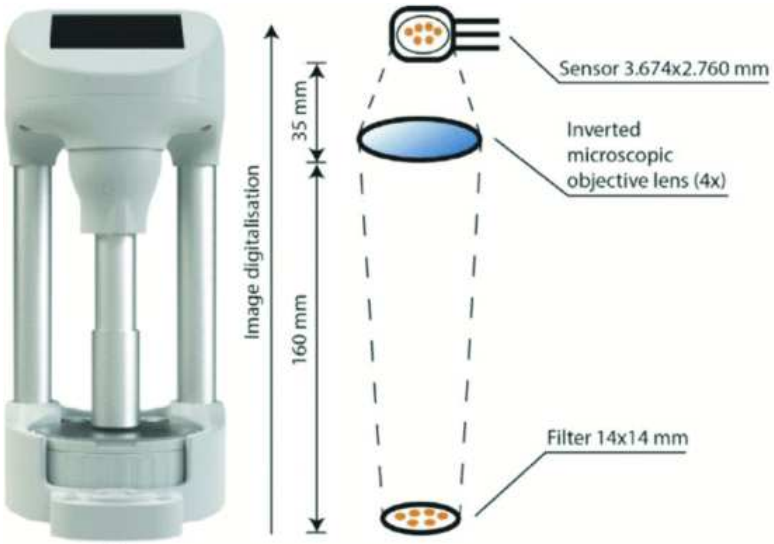

Figure 3.3: Schistoscope RP (left) with working principle of sensor and lens combination (right).

1. **Optics:** The Schistoscope RP made use of a Raspberry Pi Camera Module V2.1, which has a relatively large sensor size (3.674 x 2.760 mm) and offers extensive control over its settings. In order to image the entire standard 13 mm (urine) filter, an inverted microscope objective lens (4x) was placed at a distance of 16 cm between the sample and the lens, and 3.5 cm between the lens and camera as shown in fig. 3.3. A microscope condenser lens was used to focus the light in such a way that all the light that

passes through the sample continues through the objective lens. Achieving this illumination will result in the maximum contrast. Additionally, providing an illumination source with high intensity positioned beneath the sample will reduce the effect of stray light, which can result in image noise. A manual focusing mechanism consisting of a 3D printed rotating knob with a thread pitch of 3 mm and 3 revolutions was developed to accurately adjust the camera to the appropriate focal plane to mitigate the effect of the defocus aberration in the registered image.

2. **Electronics:** The internal electronic design of the Schistoscope RP consists of a variety of electronic components which include a Raspberry Pi 3B+ which use Python scripting for implementing all the software functionality. The Raspberry Pi 3B+ is used in combination with a HAT (Hardware on top) which makes it easier to place, on a smaller footprint, electronic components like the power management block, I2C breakout, Buzzer, EEPROM, screen connector, indicator light, LED controller, fan controller and a button connector. These design choices result in a modular system with components that are easy to repair and upgrade. However, one disadvantage is that the components may be less protected from dust and other contextual factors like humidity.

3. **Embodiment:** All parts of the Schistoscope RP casing were designed based on three main drivers: robustness, hygiene and the potential for local production. They consist of the upper cover (contains the display and closes the upper frame), upper frame (contains the lens holder, camera sensor, Raspberry Pi), structural beams (gives structure to the device and helps position the optics at appropriate distance from the sample), base (contains the LED, fan, input buttons, USB protocol) and base plate (closes the base). The design of the casing was optimized for mechanical strength and robustness in terms of stiffness, material use and printability by performing static Solidworks load simulations, using Finite Element Method (FEM). This minimises deflection of the structural connection between the lens/ sensor and the sample stage which can result in a noticeable shift in the field of view.

   User inputs are with the help of five buttons which are a ‘power’ button, an ‘OK’ button, a ‘back’ button and two ‘directional’ buttons used for navigating menus and zooming the sample images. The Schistoscope RP’s feedback to the user includes the diagnosis of the patient, the amount of eggs found in the sample by the algorithm and whether the sample is in focus or not, are provided via a 3.5 inch thin-film transistor (TFT) display with a resolution of 320 x 480 pixels.

4. **Production and maintenance:** Most components of the Schistoscope RP such as the electronic components, fasteners and structural aluminium pipes are available off-the-shelf and can be easily ordered from China via Aliexpress or similar online stores. The parts that are custom designed include the casing of the Schistoscope - which is 3D printed - and the printed circuit board. The cost of manufacturing one Schistoscope RP is estimated at 125 Euro excluding VAT, shipping cost of off-the-shelf components.

   Certain parts of the Schistoscope RP, such as the glass staging area, need to be cleaned after every sample analysis or every day to remove any cross-contamination by infected urine. Other parts need to be cleaned after a certain period of time to remove any dust or mold that has found its way into the device. It might also be necessary to perform corrective maintenance in cases of device overheating or the failure of electronic components. Software updates to add new features and performance improvements of the device can be automatically installed when the device is powered on and connected to the internet via a WiFi network.

3.3.2. SCHISTOSCOPE SP

The Schistoscope SP (See fig. 3.4) is a smartphone-based design that was developed with the main goal of creating a high-resolution image of the sample. A combination of the optics, focusing system and the sample arm is necessary for realizing the desired high resolution image.

1. **Optics:** The Schistoscope SP optics system consists of a smartphone camera and a reversed lens mounted between the phone lens and the internal framework as shown in fig. 3.4. The light sources and a frosted clear acrylic diffuser, positioned 10 mm above the source form the illumination system. This combination allows even distribution of light across the specimen. The resolution of the optical system depends on the numerical aperture of the micro-objective lenses. Higher numerical aperture equals higher resolution. Also, the FoV strongly influenced the design of the sample preparation. The complementary metal-oxide-semiconductor (CMOS) sensor size is 4.8 x 6.4 mm but creates an effective image of 4 x 6 mm as a result of the image edge being blurred because of a reduction in the lens' resolution around its edge. Hence the sample membrane is designed to be smaller than the effective FoV.

   The smartphone camera has a glass layer over it for protection, thus creating a distance of 3.68 mm between it and the reverse lens. This distance reduces the possible distance between the reverse lens and the sample to 0.5 mm which restricts the range

Figure 3.4: Schistoscope SP (up) with working principle of sensor and lens combination (down).

of movement and steps of the focus mechanism, and also the placement of samples. The focus mechanism performs the high precision task of moving the sample slide along the axis of the reversed lens. It consists of 3 main parts: a knob, a thread and a movement part. The thread is the leading component of this system as it enables movement of the sample in the vertical direction. The knob houses the female part of the thread. The movement part moves it over a distance of 2 mm. It is hollow, so it houses the light and holds the diffuser on top. The sample holder, which is a U-shaped track, functions as an insertion system and holds the sample slide in position from where it is moved by the focus mechanism.

2. **Electronics:** After patient diagnosis, relevant diagnostic data are uploaded to a cloud database via the smartphone using 4G network. This data can influence the future treatment and prevention of the disease. Other electronics of the Schistoscope SP include a circuit, control for the smartphone, sample illumination LED and a 20,000 mAh Xiaomi power bank which can power the smartphone and the LED for three days in rural areas without electricity supply.

3. **Embodiment:** The internal framework of the Schistoscope SP consists of a uniform top part with a hollow axis which aligns all holes, from the lens of the phone to the movement part in the

knob, and the bottom part which secures the knob. A phone holder in the top part of the framework fixates the phone together with its charging cable and earphone jack. A cone shape underneath the phone holder which ends in a cylinder is designed to guide the movement parts. The clamping of the knob is done by fixating the second internal framework part to the first, using bolts in nuts.

The Schistoscope SP has three buttons: the power, light and home screen buttons. The power and the light buttons are connected with a wired switch to the power bank. The home screen button works as an extension of the original home screen button of the phone. The designed Schistoscope SP uses the screen of the phone as the main form of visual feedback to its user.

4. **Production and maintenance:** Almost all the manufactured parts of the Schistoscope SP (internal framework, movement part, buttons) are 3D printed. The male and female thread and the sample holder were produced on a lathe machine from stainless steel because they need to withstand high forces and wear. Polyester Velcro, which is suitable in context of moisture and light, is used to secure the power bank to the housing. The cost per device without the cost of the sample slide and the sample preparation device is estimated at 480 euro. The initial tooling and service costs for running the tools not taken into account.

   There are three levels of the product system that are likely to be contaminated, which should be sanitized and disinfected regularly. These include the outer surface of the device, the sample holder and the filtration system which consists of a membrane, sample slide, snap ring, sample preparation device and syringes. The Schistoscope SP is designed for easy repair which can be done alone by one craftsman, using only standard screwdrivers, in a limited amount of time. The products' three levels of reparability (Level 1: opening the house, Level 2: removing the framework, Level 3: Disassembling the focus mechanism) make its maintenance time- and cost-efficient.

5. **Sample Preparation Device:** The sample preparation device (see fig. 3.5) design focuses on hygienic usage and being leak proof, fulfilling the optics requirements of a relatively small 3.5 mm FoV compared to the Schistoscope RP with a 15 mm FoV. In addition, it keeps the membrane surface flat and improves handling while also reducing human error for the healthcare worker. It consists of three main components: The sample slide which is reusable after cleaning according to WHO guidelines and allows for easy insertion into the Schistoscope. A spout on top indicates where to put the syringe and for support when filtering the urine. The urine exits the sample preparation device through a hole at the bottom. It has a

soft silicone rubber channel that helps press the membrane to the side of the sample preparation device. This creates a leak proof design which ensures the urine and eggs are contained in the 3.5 mm channel during the filtration process. It also aids in lifting the membrane as close to the optics system as possible to fulfil the 0.5 mm focal length requirement. The snap fit ring helps to hold the filter membrane tightly to the sample slide making it as flat as possible so as to reduce warping of the image. A rubber part is added to the top of the sample slide to prevent spillage during filtering.

Figure 3.5: Sample preparation device.

3.4. DISCUSSION

In both the Schistoscope designs, all three product subsystems; embodiment, optics and electronics were thoroughly developed (as described in section 3.3), and the devices were built to implement the four main drivers: robustness, potential for local production, intuitiveness and hygiene. The performance of the two prototypes based on these drivers is summarized in table 3.1.

The first objective of this project was to create a single FoV optics system with optimal illumination and sufficient resolution. The Schistoscope RP didn't fully satisfy this criterion, as a single field of view (15 mm) image was obtained in which *S. haematobium* eggs could be identified, but some of the terminal spines, which is the distinctive characteristic of these eggs were not visible. This issue can be resolved by using a high-end setup with an infinity corrected 4x objective and 200 mm tube and tube lens which would bring the cost of the device to above 500 Euros. A more affordable alternative is to increase the numerical aperture by using two Raspberry Pi Camera V2.1 lenses of which one is inverted. However, the image from the Schistoscope SP had a high enough quality to detect the spine of the *S. haematobium* egg (see fig. 3.6). The second objective was the accurate alignment of

Table 3.1: Performance of Schistoscope Prototypes in Design Main Drivers

Main Drivers	Schistoscope RP	Schistoscope SP
Robustness	The embodiment consists of structural tubes which provides a stable design and protects the electronics components. Also, a fan with an air filter located in the product base plate, dissipates heat from the electrical components, resulting in a dust proof product.	The internal framework, housing and its ribs, enhance strength and stiffness. The sample holder was produced with steel to withstand wear and tear caused by abrasive cleaners. A large power capacity that can withstand 3 days diagnostic without recharging is implemented in the design.
Potential for Local Production	The parts are either locally produced by 3D printing or bought off the shelf. Hence the product can be easily manufactured at a cost of Euro 125 per unit and damaged parts can be reprinted or replaced locally.	Local manufacturing and off-the-shelf parts were used in the design and the cost per unit of the device is Euro 480. The product level assemble makes device maintenance cost and time efficient.
Intuitiveness	The device is designed with multiple use cues such as: • A specific circle at the bottom of the sample stage to aid correct placement on the focus knob • A circle of light projected on the glass stage to which serves as cue on where to place the sample for correct alignment • Icons on the buttons for user guidance	The device has use cues that suggest the user holds the device with two hands in different ways to secure stability. Also, the two sliding buttons in the housing have a coloured bed indicating whether they are switched on or off and icons to indicate functionality. A slight blue colour ring is added around the rounded sample insertion hole to indicate the placement to the user.
Hygiene	Components which come in contact with the urine sample are easily removable and cleaned separately. Components are also designed to be rounded and smoothed for easy cleaning.	White is colour giving the product a hygienic feeling. Due to the design of the sample holder and the hole in the embodiment, samples can be inserted easily without touching any other parts.
Data	Enables data transfer to the cloud via WiFi technology.	Real time data can be uploaded to the cloud database via the smart phone through 4G network.

the camera sensor, lens and sample in order for the product to function, which was met by both designs of the Schistoscope. However, there was clogging of the filter by urine sediment due to the small surface area of the filter used for the filtration process. This problem can be solved by using the standard filters with larger surface area but the designed optical system cannot image the entire standard filter in a one FoVs.

Therefore, moving the sample along the X and Y axes to obtain multiple FoVs will be a preferred solution.

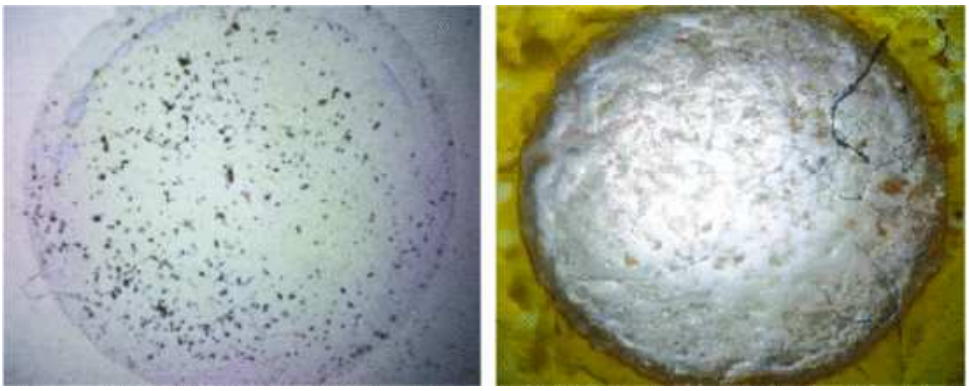

Figure 3.6: Image of sample with eggs in one field of view obtained from Schistoscope RP (left) and Schistoscope SP (right).

Finally, both products had a robust design made of materials that are resistant against the environment in rural Nigeria. The final design of the Schistoscopes consisted of materials that are 3D printed as well as purchased off-the-shelf. However, it took about 40 hours to 3D-print the various components of each device. Using a Laser-cut model would greatly reduce this delay. Also, the production cost per unit for the Schistoscope RP and the Schistoscope SP were Euro 125 and Euro 480 respectively. The Schistoscope SP is therefore thrice the price of the Schistoscope RP. Hence, the Schistoscope RP, if developed further will be a more suitable low-cost diagnostic device for urinary schistosomiasis.

3.5. CONCLUSION

The goal of the project was to develop a digital microscope which offers an integrated diagnostics solution (sample preparation and diagnosis) with the support of a smart algorithm (for detection and quantification of the *S. haematobium* eggs) which can be produced and maintained in sub Saharan Africa (with the use of locally available components and 3D-printing). This was achieved by the further development of the Schistoscope 1.0 along two parallel design trajectories: a Raspberry Pi and a Smartphone-based Schistoscope. The three main component groups of the design were the embodiment, optics and electronics systems as prime focus. Both Schistoscopes were able to capture single FoV images of filtered *schistosoma* eggs (see fig. 3.6), with optical alignment of camera, sensor and lens. Most of the materials used in the production were 3D printed while others were accessible off-the-shelf,

hence easily replaced when damaged.

In our next design trajectory, the Raspberry pi design will be further developed because of its cheaper production cost. The standard filter with a larger surface area will be adopted along with a multiple FoVs optical system. To reduce the production, Laser-cutting would be explored for the embodiment design of the device. Also we will automate the process of imaging and analysing the prepared samples so validation with laboratory microscopy using a large sample size can be realized. After the validation in the lab, we will begin testing with communities in Nigeria based on standard ethical approval.

ACKNOWLEDGEMENT

We want to acknowledge the design teams. Schistoscope RP Team; Resy Aarts, Dione Leeger, Sam Kernan Freire, Bente Vermaat, Indy Vester, Jerry de Vos; and the Schistocope SP Team; Maite Gieskes, Tina Ekhtiar, Talitha Brenninkmeyer, Chenye Xu, Mingmei Yang, Jard Van Lent. We further want to thank Design coaches Stefan Persaud and Gerard Nijenhuis for their critical design thinking input This research has been partly funded by the NWO-WOTRO SDG programme grant INSPiRED (W7.30318.009).

REFERENCES

[1] B. Bruun and J. Aagaard-Hansen. *The social context of schistosomiasis and its control: an introduction and annotated bibliography*. World Health Organization, 2008. isbn: 9789241597180.

[2] V. Silva-Moraes, L. M. Shollenberger, L. M. V. Siqueira, W. Castro-Borges, D. A. Harn, R. F. Q. E. Grenfell, A. L. T. Rabello, and P. M. Z. Coelho. "Diagnosis of Schistosoma mansoni infections: what are the choices in Brazilian low-endemic areas?" In: *Mem. Inst. Oswaldo Cruz* 114 (2019), e180478. doi: 10.1590/0074-02760180478.

[3] B. Gryseels, K. Polman, J. Clerinx, and L. Kestens. "Human schistosomiasis". In: *The Lancet* 368.9541 (2006), pp. 1106–1118. doi: 10.1016/S0140-6736(06)69440-3.

[4] P. Steinmann, J. Keiser, R. Bos, M. Tanner, and J. Utzinger. "Schistosomiasis and water resources development: systematic review, meta-analysis, and estimates of people at risk". In: *The Lancet infectious diseases* 6.7 (2006), pp. 411–425. doi: 10.1016/S1473-3099(06)70521-7.

[5] J. Utzinger, G. Raso, S. Brooker, D. De Savigny, M. Tanner, N. Ornbjerg, B. H. Singer, and E. K. N'goran. "Schistosomiasis and neglected tropical diseases: towards integrated and sustainable control and a word of caution". In: *Parasitology* 136.13 (2009), pp. 1859–1874. doi: 10.1017/S0031182009991600.

[6] M. J. van der Werf, S. J. de Vlas, S. Brooker, C. W. Looman, N. J. Nagelkerke, J. D. Habbema, and D. Engels. "Quantification of clinical morbidity associated with schistosome infection in sub-Saharan Africa". In: *Acta Tropica* 86.2-3 (2003), pp. 125–139. doi: 10.1016/s0001-706x(03)00029-9.

[7] O. Holmström, N. Linder, B. Ngasala, A. Mårtensson, E. Linder, M. Lundin, H. Moilanen, A. Suutala, V. Diwan, and J. Lundin. "Point-of-care mobile digital microscopy and deep learning for the detection of soil-transmitted helminths and *Schistosoma haematobium*". en. In: *Global Health Action* 10.sup3 (June 2017), p. 1337325. doi: 10.1080/16549716.2017.1337325.

[8] M. D. French, D. Evans, F. M. Fleming, W. E. Secor, N. Biritwum, B. S. J., A. Bustinduy, A. Gouvras, N. Kabatereine, C. H. King, M. Rebollo Polo, J. Reinhard-Rupp, D. Rollinson, L. A. Tchuem Tchuenté, J. Utzinger, J. Waltz, and Y. Zhang. "Schistosomiasis in Africa: Improving strategies for long-term and sustainable morbidity control". In: *PLoS neglected tropical diseases* 12.6 (2018). doi: 10.1371/journal.pntd.0006484.

[9] J. Balsam, M. Ossandon, H. A. Bruck, I. Lubensky, and A. Rasooly. "Low-cost technologies for medical diagnostics in low-resource settings". In: *Expert opinion on medical diagnostics* 7.3 (2013), pp. 243–255. doi: 10.1517/17530059.2013.767796.

[10] I. I. Bogoch, J. T. Coulibaly, J. R. Andrews, B. Speich, J. Keiser, J. R. Stothard, E. K. N'goran, and J. Utzinger. "Evaluation of portable microscopic devices for the diagnosis of Schistosoma and soil-transmitted helminth infection". In: *Parasitology* 141.14 (2014), pp. 1811–1818. doi: 10.1017/S0031182014000432.

[11] H. C. Koydemir, J. T. Coulibaly, D. Tseng, I. I. Bogoch, and A. Ozcan. "Design and validation of a wide-field mobile phone microscope for the diagnosis of schistosomiasis". In: *Travel medicine and infectious disease* 30 (2019), pp. 128–129. doi: 10.1016/j.tmaid.2018.12.001.

[12] J. Rajchgot, J. T. Coulibaly, J. Keiser, J. Utzinger, N. C. Lo, M. K. Mondry, J. R. Andrews, and I. I. Bogoch. "Mobile-phone and handheld microscopy for neglected tropical diseases". In: *PLoS Neglected Tropical Diseases* 11.7 (2017), e0005550. doi: 10.1371/journal.pntd.0005550.

[13] T. Agbana, G. Y. Van, O. Oladepo, G. Vdovin, W. Oyibo, and J. C. Diehl. "Schistoscope: Towards a locally producible smart diagnostic device for Schistosomiasis in Nigeria". In: *2019 IEEE Global Humanitarian Technology Conference (GHTC)*. Seattle, WA, USA, 2019, pp. 1–8. doi: 10.1109/GHTC46095.2019.9033049.

[14] N. A. Switz, M. V. D'Ambrosio, and D. A. Fletcher. "Low-cost mobile phone microscopy with a reversed mobile phone camera lens". In: *PLoS ONE* 9.5 (2014), e95330. doi: 10.1371/journal.pone.0095330.

[15] S. Jujjavarapu. "Automating the Diagnosis and Quantification of Urinary Schistosomiasis". MA thesis. Delft, The Netherlands: Delft University of Technology, 2020.

4

SCHISTOSCOPE 5.0 DESIGN

Schistoscope: An Automated Microscope with Artificial Intelligence for detection of *Schistosoma haematobium* eggs in Resource-limited Settings

Prosper Oyibo, Satyajith Jujjavarapu, Brice Meulah, Tope Agbana, Ingeborg Braakman, Angela van Diepen, Michel Bengtson, Lisette van Lieshout, Wellington Oyibo, Gleb Vdovine, Jan-Carel Diehl

PUBLICATION REPORT

- **Publication Date:** 19 April 2022
- **Journal:** Micromachines
- **Publisher:** MDPI
- **DOI:** 10.3390/mi13050643

ABSTRACT

For many parasitic diseases, the microscopic examination of clinical samples such as urine and stool still serves as the diagnostic reference standard, primarily because microscopes are accessible and cost-effective. However, conventional microscopy is laborious, requires highly skilled personnel, and is highly subjective. Requirements for skilled operators, coupled with the cost and maintenance needs of the microscopes, which is hardly done in endemic countries, presents grossly limited access to the diagnosis of parasitic diseases in resource-limited settings. The urgent requirement for the management of tropical diseases such as schistosomiasis, which is now focused on elimination, has underscored the critical need for the creation of access to easy-to-use diagnosis for case detection, community mapping, and surveillance. In this paper, we present a low-cost automated digital microscope—the Schistoscope—which is capable of automatic focusing and scanning regions of interest in prepared microscope slides, and automatic detection of Schistosoma haematobium eggs in captured images. The device was developed using widely accessible distributed manufacturing methods and off-the-shelf components to enable local manufacturability and ease of maintenance. For proof of principle, we created a Schistosoma haematobium egg dataset of over 5000 images captured from spiked and clinical urine samples from field settings and demonstrated the automatic detection of Schistosoma haematobium eggs using a trained deep neural network model. The experiments and results presented in this paper collectively illustrate the robustness, stability, and optical performance of the device, making it suitable for use in the monitoring and evaluation of schistosomiasis control programs in endemic settings.

4.1. INTRODUCTION

Bright-field microscopy is still the dominant method for imaging in numerous engineering and scientific domains as a result of its accessibility. Of particular interest to this work is the medical discipline of diagnostics, in which it is still the reference standard procedure for diagnosis and load estimation for many infectious diseases, particularly those caused by parasites [1].

Schistosomiasis is a neglected tropical disease (NTD) [2] caused by the parasitic flatworm called *Schistosoma*. Approximately 700 million people living in 80 countries are at risk of infection, of which around 90% live in Africa [2–4]. Several *Schistosoma (S)* species can infect humans, with *S. haematobium* being one of the most prevalent species in Africa and the cause of urogenital schistosomiasis [5]. The reference standard procedure for the diagnosis of *S. haematobium* infection is the detection of eggs in urine via microscopic examination, while counting the number of eggs in a specified volume of urine (quantitative analysis) is used for epidemiological surveillance [3–7]. One of the major limitations of this procedure is that it is operator-dependent, meaning it is prone to discrepancies in performance since expertise and skills can vary across individuals [8, 9]. Furthermore, since infections are predominantly found in rural settings in poor-resource regions, the availability of functioning microscopes can be a challenge [10]. Additionally, the employment of skilled microscope operators is costly and requires investment in ongoing training [8, 9]. Furthermore, the diagnostic performance of this procedure is inversely related to the number of worms present, meaning that light infections with low egg excretion will be easily missed, while these individuals can still contribute to the transmission of the disease [10]. Finally, the current World Health Organisation's (WHO) agenda to eliminate neglected tropical diseases (including schistosomiasis) [11], requires the precision mapping of communities and conventional microscopy, which is mostly used in resource-constrained settings where schistosomiasis is endemic, may not be able to accelerate this elimination agenda. The critical need for periodic monitoring of interventions in communities at the ward level will require devices with automation and self-diagnostic capacities that human operators alone may not be able to readily provide.

For these reasons, there is a need for inexpensive and smart portable devices capable of slide-scanning and performing digital microscopic examination. Such a device will ensure better and consistent performance across diagnosis, speed up sample scanning, compensate for the lack of trained microscope operators in some countries, and assist in diagnosis using artificial intelligence algorithms where needed. When used with an onboard computer, regional epidemiological data can potentially be uploaded to a database, therefore allowing stakeholders involved in epidemiological surveillance to plan and authorize control

and elimination schemes. Moreover, such devices will ease the workload on microscopists in epidemiological surveys or impact assessment programs, where there are a lot of samples to be analyzed, thus minimizing errors in diagnosis.

In recent years, accessibility of manufacturing methods such as 3D printing and laser-cutting has increased. Furthermore, the availability of smartphones, which have an in-built camera, and miniature computers such as Raspberry Pi have also increased. This growth has led to the development of computerized instruments.

Studies on smartphone-based microscopes have been reported [12–16] with optical setup with numerical aperture (NA) and magnification equivalent to or higher than some microscope objectives. However, these microscopes do not have mechanical stages, making it challenging to maintain focus while manually changing the field of view (FoV). On the other hand, the scientific literature also includes studies that has developed open-source microscope designs, automated movement of the XYZ sample stages and microscope objectives [17–20]. One notable design is the open-source OpenFlexure device by Collins *et al.* [21], which uses a 100× microscope objective and was applied to clearly resolve malaria parasites in thin blood smears. Li *et al.* [22] developed a highly configurable instrument at a variable cost of USD 250–500 (depending on the configuration) that is capable of quantifying malaria parasites by scanning 1.5 million red blood cells per minute. There have also been studies on automatic *S. haematobium* egg detection which focus mainly on identifying eggs in images pre-captured by professional clinical operators mostly with isolated and non-overlapping eggs in an FoV [23–25]. Essentially, captured images of urine samples prepared in field settings often contain a lot of artifacts such as crystals, glass debris, air bubbles, fabric fibers and human hair. Thus, an automatic *S. haematobium* egg detection system applicable in field settings remains unexplored.

In this work we demonstrate the potential for a low-cost yet high-quality instrument, called the Schistoscope, that can function as a reliable digital microscope, slide scanner and an automatic diagnostic tool for use in point-of-need diagnostics. We build on our earlier efforts [26–28] with a focus on the detection of *S. haematobium* eggs in urine. The Schistoscope performs autofocusing, automated filter membrane scanning (creating an image grid of the sample) and automatic *S. haematobium* egg detection and count estimation. The four main drivers in the design of the Schistoscope are focused on: (i) the robustness of the device in its ability to withstand the harsh tropical working environment in sub-Saharan Africa, such as humidity, dust and heat; (ii) potential for local production mainly using standard off-the-shelf components in combination with locally available distributed production methods to bring the cost of the device to approximately USD 700 and

enable local maintenance and repair; (iii) operational considerations such as the intuitiveness and ease of use; (iv) hygiene considerations in the handling of the device to ensure that the product could be easily cleaned to prevent possible cross-contamination between samples.

With these factors in mind, our design of the Schistoscope has undergone five design iterations [27, 28] with implementation research conducted in the field, involving key stakeholders in the research and development process, where the device will potentially be used. For further proof of principle, we also demonstrate the detection of *S. mansoni* and hookworm eggs in fecal samples prepared using Kato–Katz technique.

4.2. MATERIALS AND METHODS

4.2.1. OPTICAL SYSTEM

We designed the Schistoscope optical system using the working principle of a conventional light microscope (fig. 4.1a,b). The illumination system is positioned below the sample stage. Light rays that have passed through the sample are transmitted through the microscope objective lens, which sits just above the specimen, and the image is recorded on the image sensor which is further away from the sample. We employed two convex lenses in the illumination system: the collector lens and the condenser lens. It is designed to provide bright and even illumination on the sample plane and the image plane where the image produced from the objective is recorded by the sensor. This is important because it eliminates glare in the captured image since backlight illumination floods the object with light from behind.

The Schistoscope optical train is similar to that of a standard microscope, except in our design the eyepiece is replaced by a camera sensor, focus adjustment knobs are replaced by an automated Z-axis movement system and software-based autofocus, while the mechanical stage is replaced by automated XY-axis movement systems. With the open-source philosophy in mind, we use an easily accessible and community supported camera module for the Schistoscope—Raspberry Pi High-Quality Camera Module V2.1, equipped with a Sony IMX477R stacked, back-illuminated sensor, 12.3 megapixel resolution, 7.9 mm sensor diagonal and 1.55 μm $\times$ 1.55 μm sensor pixel size. We aligned the camera module with a basic achromatic microscope objective using the Thorlabs Extra-Long 6 inches (152.4 mm) extension tube. To visualise *Schistosoma* eggs, we used a 4$\times$ magnification objective (with 0.10 numerical aperture, corresponding to a focal length of 40 mm); however, the device is designed such that the objective is easily interchangeable with a microscope objective up to 20$\times$ magnification. Higher magnifications cannot be used due to limited resolution of the Z-axis slider in our design. The illumination system consists of

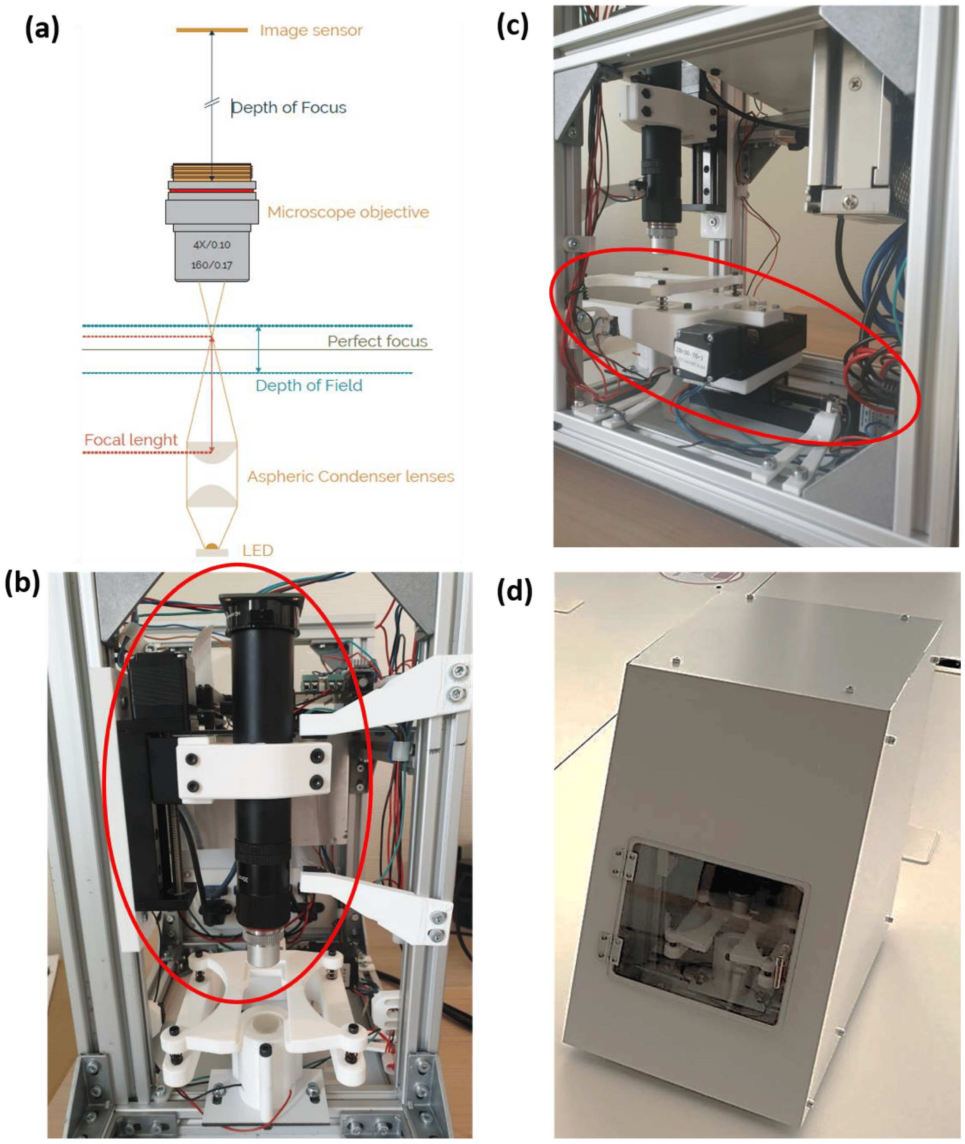

Figure 4.1: (a) Schematic diagram of the Schistoscope optical train (b) Region of interest showing the Z-axis consisting of a mechanical slider and optical setup (c) Region of interest showing the sample stage mounted on the X and Y slider mechanism (d) Exterior of the Schistoscope device (embodiment).

high-power white LED chips welded on a printed circuit board (PCB) and a 25 mm diameter, 20.1 mm focal length Thorlabs aspheric condenser with diffuser. The tube lens is connected to a motorized slider mechanism for effective movement of the optical train along the Z-axis to obtain accurate focus on the sample. In the design of the sample stage, it is important to ensure consistency when moving from one FoV to another in the sample plane to prevent errors during the automatic slide-scanning procedure. Hence, we designed the sample stage as a simplified cantilever beam system, in which the sample holder is mounted on top of an XY stage consisting of two motorized slider mechanisms (similar to the one on the Z-axis) with their individual stepper motors. The Y-axis slider mechanism is fixed, and it translates the X-axis slider mechanism on which the sample holder is directly mounted as shown in fig. 4.1c.

4.2.2. ELECTRONICS SYSTEM

The Schistoscope makes use of the Raspberry Pi 4 computer board, which provides a high-bandwidth interface to connect the Raspberry Pi camera module. The Raspberry Pi board is also connected to an Arduino Nano board with sufficient general-purpose input–output (GPIO) pins to communicate with other electronic components such as six limit switches positioned at both ends of the X-, Y- and Z-axis, 3 NEMA 11 stepper motors along with their respective controllers for movement along each axis. A custom-made PCB that acts as a shield connects the Arduino board to the various components. We adopted a 60W AC–DC double output switching power supply to power the onboard computer and various device's electrical components.

4.2.3. SUPPORTING STRUCTURES AND ENCLOSURE

We adopted aluminum profiles for designing the supporting system to ensure robustness and stability of the device [29]. This will prevent the need for frequent optical system re-calibration and highly trained personnel for system maintenance which is generally unavailable in low-resource settings. Aluminum profiles are widely used for 3D printers, CNC machinery, and research test set-ups. These profiles allow for easy attachment of other systems, and the corner joint allows for quick adaptations in design. The frame is constructed by attaching the profiles with metal corner joints, thus creating rectangle constructions. The frame uses several multiple profiles to allow for change and attachment of an enclosure. The setup creates multiple rectangles to increase rigidness. The bottom profiles prevent the device from tilting forwards, the upper profiles prevent the vertical profiles from leaning, and the middle profiles allow for the mounting of an electronics panel. To prevent the internal system from adverse exposure to external factors such as

dust, dampness, or accidental interference by humans, we designed an enclosure system using a material called 'Alubond', a lightweight, maintenance-free material. A very low expansion coefficient makes it suitable for temperatures in sub-Saharan Africa. The material allows for production with laser-cutting, CNC-milling, sawing and drilling. The enclosure system is robust and attaches easily to the supporting system. The surface is easy to clean, and the white color resembles a medical device.

4.2.4. SAMPLE PREPARATION

For this study, *S. haematobium* eggs were obtained from gut tissue of hamsters infected with *S. haematobium* at the Leiden University Medical Center (LUMC) following a standardized protocol approved by the Dutch Central Authority for Scientific Procedures on Animal (CCD) as described previously [30]. Briefly, five weeks after infection with *S. haematobium*, hamsters were sacrificed, and eggs were obtained following gut tissue digestion with collagenase B and extensive tissue washing. Eggs were concentrated in normal saline (5000 eggs per mL) to prevent hatching and stored appropriately for future use. The gut tissue derived eggs are morphologically identical to that seen in human-infected samples. Ten milliliters of urine samples provided by voluntary donors after oral consent were spiked with 0.1, 0.2, 0.3, 0.4, 0.5, 0.6, 0.7, 0.8, 0.9, 1 mL of the concentrated stock (5000 eggs per mL) to make 10 dilutions. In addition to the artificially spiked samples, clinical urine and stool samples were obtained during a field study in Federal Capital Territory (FCT), Abuja, Nigeria, in collaboration with the University of Lagos, Nigeria. Ethical approval for this study was obtained from the Federal Capital Territory Health Research Ethics Committee (FCT-HREC) Nigeria (reference No., FHREC/2019/01/73/18-07-19). After receiving informed consent, a total of 33 urine samples were collected in 20 mL sterile universal containers from school-age children who had observed the presence of blood in their urine or had been to the infected community river in the past six weeks. This screening increased the chances of having positive samples for our dataset. The spiked and clinical urine samples were processed using the standard urine filtration procedure [31]. With a syringe, 10 mL of urine was passed through a 13 mm diameter filter membrane with a pore size of 0.2 μm. After filtration, the membrane was placed on a microscopy glass slide, and covered with a coverslip to increase the flatness of the membrane for image capture using the Schistoscope. The fecal samples were processed using the standard Kato–Katz procedure with a 41.7 milligram template [32]. The prepared microscopic slides were imaged using the Schistoscope device.

4.2.5. AUTOFOCUS AND AUTO-SCANNING SYSTEM

Microscopic imaging of filter membranes for the detection of *S. haematobium* eggs usually encounters challenges such as uneven filter membranes, presence of artifacts, and deviations of slide angle and stage position. All these factors can result in loss of focus when capturing images across different FoVs, thus reducing the readability of the image by both humans and automatic object detection algorithms. Therefore, there is a need for an autofocusing system to ensure that the images captured are always in focus. We designed the autofocusing algorithm using the following steps [21, 22]: first, the microscope objective is moved sequentially through a set of positions along the Z-axis, and at each position an image is captured and converted to greyscale. Next, a sharpness metric is calculated from the edge image derived by applying a 2D Laplacian filter to the grayscale image. The image with the maximum sharpness metric is selected as the image with the best focus. Due to the high resolution of the system, only a limited FoV (1078 μm $\times$ 1470 μm) can be imaged at one time point. Therefore, a 13 $\times$ 9 grid of images is required to image an entire 13 mm filter membrane for accurate diagnosis. We reduced the risk of focusing on the slides by defining the top curvature of the membrane as a starting position for the auto-scanning procedure. The Schistoscope performs auto-scanning in a row-wise traversal order beginning from the upper-left position of the grid using the X and Y slider mechanism. An example grid of a filter membrane captured using the Schistoscope is shown in fig. 4.2.

4.2.6. AUTOMATIC *S. haematobium* EGG DETECTION

To automatically detect *S. haematobium* eggs, we first created a large-scale image dataset (SH dataset) of Schistoscope-captured microscopic images of filter membranes prepared from spiked and clinical samples. The corresponding ground-truth images were created by manually annotating *S. haematobium* eggs in the captured images. Expert parasitologists carried out this task using the coco annotator tool [33]. For the creation of the ground-truth images, we applied the following principles:

1. Annotation of the exact boundary pixels of the *S. haematobium* eggs was not strictly enforced due to the limitation posed by the size of the eggs.

2. The pixel values of the background and artifacts in the ground-truth image were labelled as ‘0’ and the eggs as ‘1’.

3. There were few *S. mansoni* eggs found in the images of the clinical urine samples and their pixel values were labelled as ‘1’.

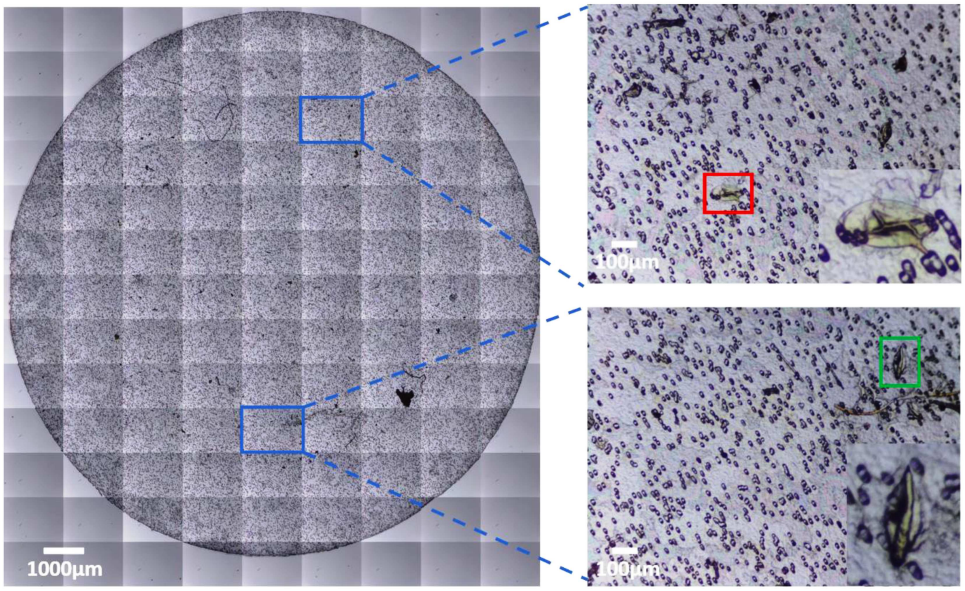

Figure 4.2: Automated image grid acquisition of *Schistosoma eggs* from a urine filter membrane. Blue region of interest shows individual sub-images, red and green regions of interest are *S. mansoni* and *S. haematobium eggs*, respectively, present in the urine sample. Enlarged areas show the eggs at 300% digital zoom.

4. Pixels of partially cut eggs at the edges of the images were labelled as '1'.

5. The region of the eggs covered by artifacts was labelled as '0'.

A deep neural network (DNN) based on a UNET architecture [34] was trained for the segmentation of *S. haematobium* egg pixels using the SH dataset. The SH dataset was split into 70%, 15% and 15% to train, validate and test the automated system, respectively, and the deep neural network was trained for 16 epochs using Google Colaboratory's Tesla P100-based servers. During the training stage, the image was resized to 512 $\times$ 512 pixels and the Adam solver was applied with a learning rate of 1×10^{-5}. The momentum and the decay coefficient were set to 0.9 and 1×10^{-8}, respectively. All the weights were initialized from a Gaussian distribution with a mean of 0 and a standard deviation of 0.02. The batch size was initialized to 8. After training, the test set was applied to the trained model and the segmentation performance was compared to the ground truth using the dice similarity coefficient [35] as metric. We developed a linear regression model for

egg count estimation using the pixel area of each connected component and its corresponding actual egg count in the ground-truth image. The derived model was applied estimating the egg counts per image in the segmented mask images of the test set. We compared the results with the actual egg count per image using mean absolute error (MAE) and root mean squared error (RMSE) as metrics.

4.3. RESULTS AND DISCUSSION

4.3.1. SAMPLE STAGE XY POSITION REPEATABILITY

We performed a sample stage XY position repeatability test [19, 20] to quantitatively measure the positioning repeatability of the sample stage in the X- and Y-axis. We imaged *S. haematobium* eggs spread out across three adjacent FoVs and measured the accuracy with which we could repeatedly center the microscope objective over these different FoVs. We selected eggs located approximately 2000 μm to 3000 μm apart and programmed the auto-scanning system to repeatedly cycle between them 50 times and capture a single 1520 $\times$ 2028 pixels image upon arriving at each FoV. We then estimated the positioning error across the 50 cycles by calculating the number of pixels (and hence microns) by which subsequent frames are displaced from the first frame. A displacement of zero would indicate that the stage returned exactly to the starting position. The path taken by the sample stage is shown in fig. 4.3a, where the three vertices are the locations of the eggs in each FoV. fig. 4.3b–d show XY positioning errors for each egg. The color scale corresponds to the motion cycle number, indicating the order in which the data were acquired. The first data point is yellow and the last is brown. The colors are not distributed randomly, which indicates that there is a systematic drift. The estimated drift after 50 motion cycles of the three eggs from their initial positions were 11.17 μm, 13.68 μm and 11.75 μm, respectively, which is small relative to the size of the FoV.

4.3.2. IMAGING PERFORMANCE

We evaluated the quantitative imaging performance of the Schistoscope by obtaining the resolution limit of the optical setup. Additionally, a qualitative comparison was performed between images taken by our device and images of the same FoV taken by a conventional microscope (BRESSER Science Infinity Microscope) equipped with a plan-achromatic objective (10$\times$ magnification and 0.25 numerical aperture). We adopted the ISO 12233 slanted-edge technique [36], which provides a fast and efficient way of estimation and Modulation transfer function (MTF). First, we registered a slanted-edge image (derived from a standard USAF 1951 resolution target) using the Schistoscope. Next, we selected a rectangular region of interest (ROI) in the image with a step edge

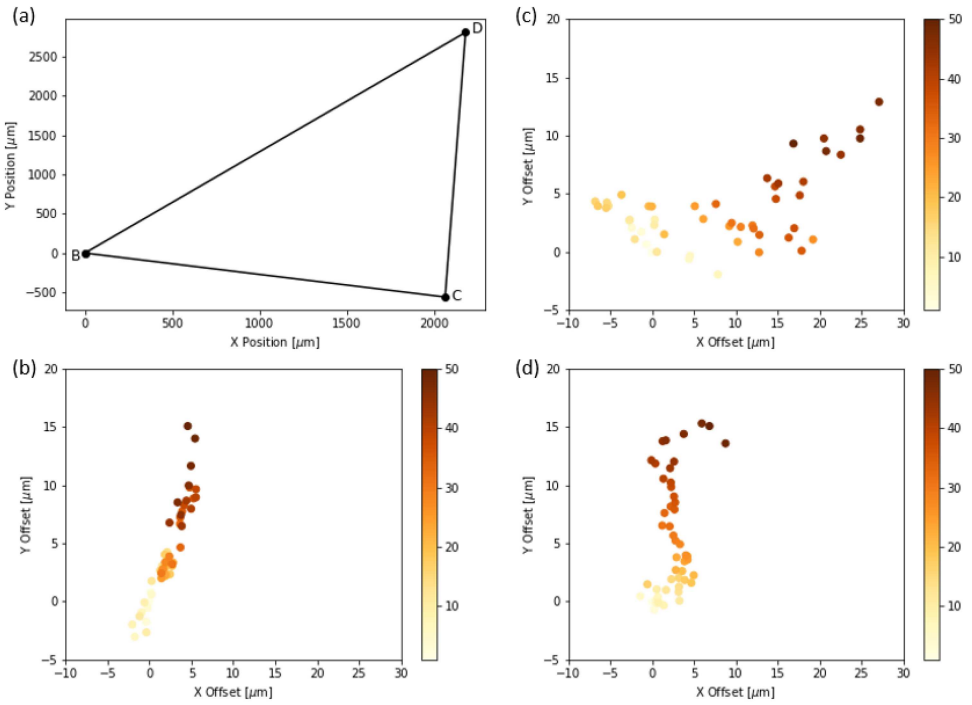

Figure 4.3: XY positioning accuracy. (a) the path taken by the sample stage. (b–d) the displacement of three eggs in the respective FoV from their initial positions in the captured frame from the first cycle.

(fig. 4.4a). The device's edge spread function (ESF) was then calculated by taking the response of the line perpendicular to the edge. Then we obtained the derivative of the ESF which is the line spread function (LSF). The MTF was derived by performing a one-dimensional Fourier transform of the LSF. The ESF, LSF and MTF curves are shown in fig. 4.4b–d. It was observed from the MTF curve that the limiting resolution (MTF10) of the device is 307 lp/mm (3.26 microns), which is in reasonable agreement with the Rayleigh theoretical value of 3.35 microns (assuming NA 0.1 and center wavelength 550 nm). Thus, the optical setup is more than sufficient to image the *Schistosoma* eggs with sizes within the bounds of $110-170 \times 40-70\,\mu$m.

In the qualitative comparison between the Schistoscope and a conventional microscope, we captured the same FoV on a sample slide containing *S. haematobium* eggs using both systems (fig. 4.5a,b). Despite the markedly superior optical characteristics of the conventional microscope, the overall FoV, field flatness, and visual perception of the two systems are not so different. A magnified region of interest

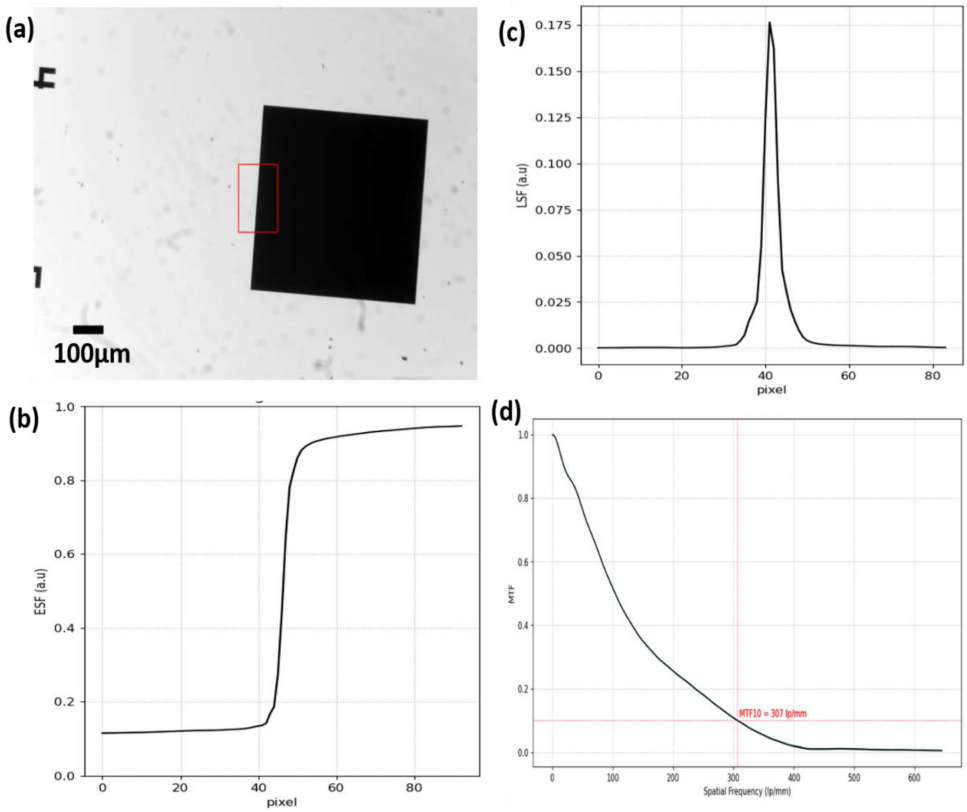

Figure 4.4: Resolution limit of the Schistoscope. (a) Slanted-edge image with selected rectangular region of interest (b) Edge spread function curve (c) Line spread function curve (d) Modulation transfer function curve with a resolution limit of 307 lp/mm.

is also presented for detailed comparison. Although the conventional microscope has an improved depth of focus and higher contrast, the quality of the Schistoscope image is acceptable as the terminal spine of the *S. haematobium* eggs and the lateral spine of the *S. mansoni* eggs (fig. 4.2) could be easily identified by a human reader. To further demonstrate the ability of the Schistoscope to aid in the diagnosis of intestinal parasites effectively, we used the device to image fecal smear containing eggs of *S. mansoni* and hookworm eggs. As can be clearly seen in fig. 4.6a,b, the Schistoscope device also can optically resolve the eggs of these intestinal parasites.

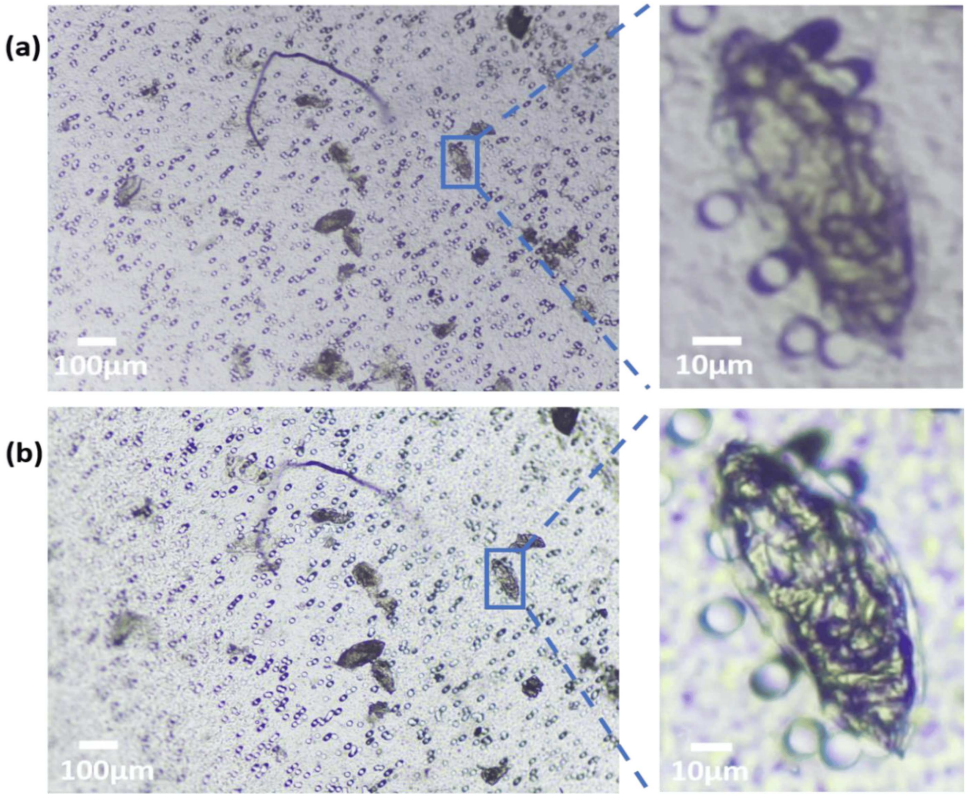

Figure 4.5: Optical performance of the Schistoscope. (a) Schistoscope (NA 0.1) and (b) conventional microscope (NA 0.25) images of fecal smear containing *Schistosoma haematobium* eggs. Enlarged ROIs show similar optical qualities.

4.3.3. PERFORMANCE EVALUATION OF S. haematobium EGG DETECTION ALGORITHM

We created an SH image dataset consisting of 5198 microscopic images of urine filter membranes (986 and 4212 images from spiked and clinical urine samples, respectively), along with their respective ground-truth images with 6437 annotated *S. haematobium* eggs (4776 and 1661 eggs in spiked and clinical urine samples images, respectively). Although images from the clinical samples had fewer or in some cases no eggs present compared to images of the spiked samples, they still contained artifacts such as crystals, glass debris, air bubbles, fabric fibers and human hair (selected images shown in fig. 4.7c,f), thus increasing the robustness of the dataset and the difficulty of the automatic egg detection task.

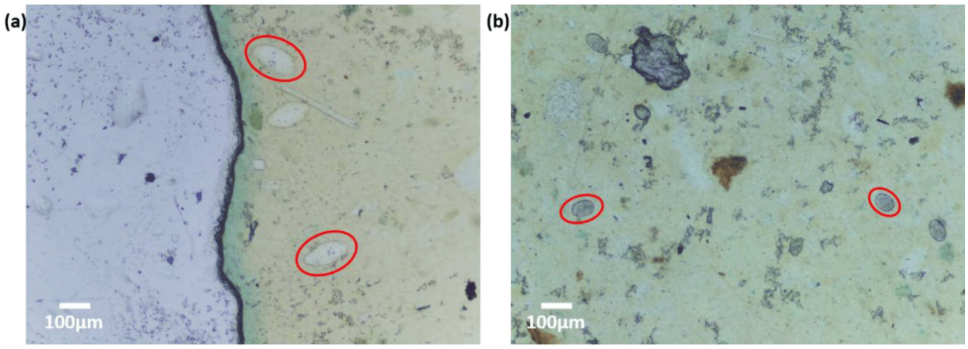

Figure 4.6: Captured images of intestinal parasites using the Schistoscope. Fecal smears of (a) region of interest showing *Schistosoma mansoni* eggs. (b) region of interest showing hookworm eggs.

To address this challenge, we applied the trained UNET model for the semantic segmentation of *S. haematobium* eggs present in images of the test dataset. In the qualitative segmentation results of images in the test dataset (fig. 4.7), we observed that the deep-learning model performed better in the segmentation of eggs in images from the spiked urine samples (fig. 4.7a,b) than in clinical samples (fig. 4.7c–f). Probable reasons for this difference may be that a higher percentage of eggs in the SH dataset were from the spiked samples, and the high presence of artifacts in the images captured from the clinical samples could have caused segmentation errors. An example of such an error can be seen in fig. 4.7f, where many uric acid crystals are present in the image. The similarity between morphological features of the crystals and the *S. haematobium* eggs causes the deep-learning model to falsely identify the crystals as eggs. In the quantitative results, we obtained a dice similarity coefficient of 0.44. The observed low dice similarity coefficient in the test data could be due to the following assumptions: (i) the non-strict-enforcement of exact boundary conditions in the annotation of the *S. haematobium* eggs in the ground-truth images; and (ii) poor segmentation performance of the UNET in the difficult clinical images with egg-like artifacts (uric acid crystals). We also estimated the egg count per captured FoV image using a linear prediction model with the area of the segmented egg pixels as the independent variable. We obtained a MAE and RMSE of 1.21 and 4.08, respectively. A box plot shows a visual summary of the estimated egg counts in test images with 0–10 actual egg count (98% of the test images) (fig. 4.8a). An increased number of outliers above the maximum whisker of the box plot is observed in the set of images with 0 or 1 actual egg count, which are predominantly images with artifacts from clinical urine samples.

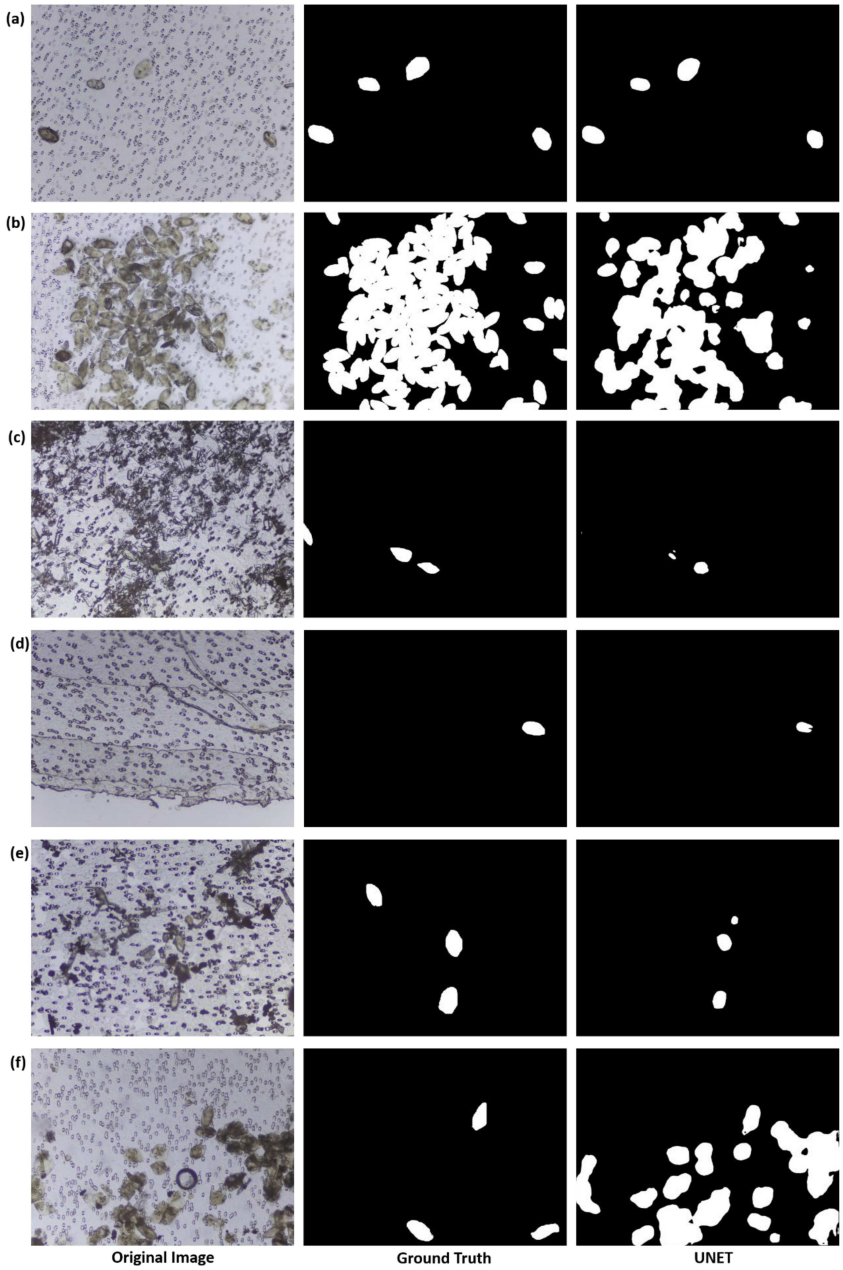

Figure 4.7: Visual comparison of semantic segmentation of images in test dataset (a,b) sample images from spiked urine samples (c–f) sample images from clinical urine samples.

From this result, we infer that the automated detection model could satisfy to the 80% sensitivity diagnostic requirement specified in the WHO Target Product requirement for the diagnosis of schistosomiasis [37].

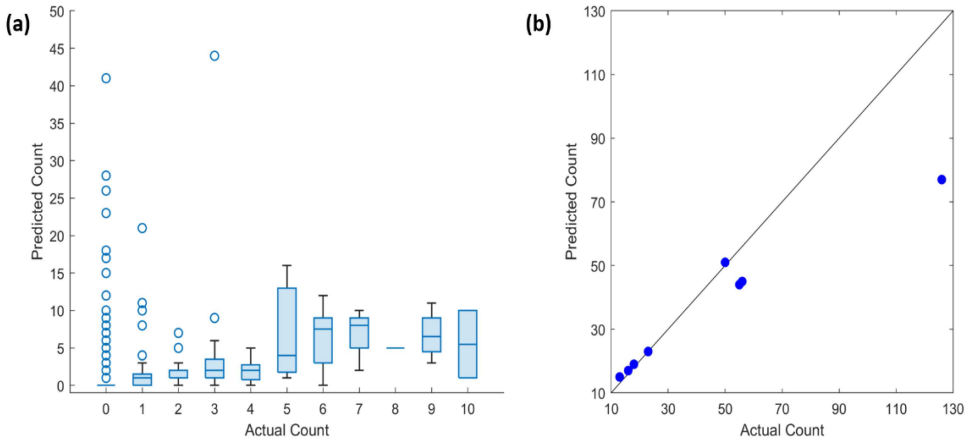

Figure 4.8: Quantitative result of the predicted egg counts per captured FoV image (a) visual summary of the egg counts in test images with 0–10 actual egg count (98% of the test images) (b) Scatter plot of test images with actual egg counts greater than 10.

Furthermore, there is a small difference between the average predicted egg count in each box and actual egg count, which is evident in the MAE value of the test dataset. fig. 4.8b shows the scatter plot of test images with actual egg count greater than 10. It is observed that the deviation from the line of perfect agreement (black line) increases with higher number of actual egg count per image. This is a result of the increasing occurrence of overlapping eggs with an increasing number of actual egg count per image. Thus, we believe a logarithmic model or an egg counting algorithm that explores the eggs' morphological properties (e.g., egg size and shape) might be a suitable solution to this problem.

4.4. CONCLUSIONS

We developed an optical diagnostic device called the Schistoscope, which incorporates an automated Z-axis movement for autofocusing a sample based on a Laplacian sharpness metric, as well as an automated XY movement of the sample stage for automated grid scanning. Our experiments showed that the optical system has comparable performance with conventional microscopes. We demonstrated the

automatic detection of *S. haematobium* eggs by creating a robust *S. haematobium* egg image dataset containing over 5000 FoV images of filtered spiked and clinical urine samples from field settings. We trained a deep neural network model for the semantic segmentation of the *S. haematobium* eggs prior to egg count estimation using a linear model based on the area of the segmented pixels. Although urine artifacts present in the images from the clinical sample posed a challenge, the algorithm clearly identified the eggs in the image, demonstrating that the quality of the images is suitable for automatic detection of *Schistosoma* eggs in line with the current diagnostic reference standard. High-quality microscopy images of *S. haematobium*, *S. mansoni* and hookworm eggs were captured using the device, and the eggs were clearly identified in captured digital images by microscopists. Therefore, it is evident that combining automated image acquisition with a suitable artificial intelligence algorithm in the device for diagnosis will significantly increase its potential as a diagnostic tool in resource-limited settings. Manuscripts describing the outcome of a population-based survey, and validating the diagnostic performance of the Schistoscope for the detection of *S. haematobium* eggs in urine samples in a low-resource field setting, are currently in progress. In conclusion, the Schistoscope was presented to the national technical working committee on the eradication of schistosomiasis in Nigeria. Possible potential benefits of the Schistoscope discussed include point-of-need diagnosis and drug efficacy monitoring, which could mitigate waste of human, material and financial resources. Ongoing discussions with local private and public partners aim to explore ways to integrate the Schistoscope into active schistosomiasis elimination and control programs in Nigeria.

AUTHOR CONTRIBUTIONS

Conceptualization, P.O., T.A. and J.-C.D.; methodology, P.O., S.J., B.M. and I.B.; software, S.J. and P.O.; resources, A.v.D. and W.O.; data curation, P.O. and B.M.; writing—original draft preparation, P.O. and S.J.; writing—review and editing, I.B., B.M., A.v.D., M.B., T.A., L.v.L., J.-C.D., W.O. and G.V.; visualisation, P.O.; supervision, W.O., G.V. and J.-C.D.; project administration, L.v.L. and J.-C.D.; funding acquisition, J.-C.D. and L.v.L. All authors have read and agreed to the published version of the manuscript.

FUNDING

This research was funded by NWO-WOTRO Science for Global Development program, Grant Number W 07.30318.009 (INSPiRED—INclusive diagnoStics for Poverty RElated parasitic Diseases in Nigeria and Gabon).

INSTITUTIONAL REVIEW BOARD STATEMENT

The study was conducted in accordance with the Declaration of Helsinki, and approved by the Federal Capital Territory Health Research Ethics Committee (FCT-HREC) in Abuja, Nigeria (reference no., FHREC/2019/01/73/18-07-19).

INFORMED CONSENT STATEMENT

Informed consent was obtained from all subjects involved in the study.

DATA AVAILABILITY STATEMENT

Schistosoma haematobium image dataset is available from the Zenodo Repository 10.5281/zenodo.6467268.

ACKNOWLEDGMENTS

We thank the Neglected Tropical Disease team from the Federal Ministry of Health Abuja and Federal Capital Territory Authority Public Health Laboratory Abuja. We also acknowledge researchers and staff of ANDI Center of Excellence for Malaria Diagnosis, College of Medicine, University of Lagos and TU Delft Global Initiative for their support towards this study.

CONFLICTS OF INTEREST

The authors declare no conflict of interest.

REFERENCES

[1] H. Zhu, S. O. Isikman, O. Mudanyali, A. Greenbaum, and A. Ozcan. “Optical imaging techniques for point-of-care diagnostics”. In: *Lab on a Chip* 13.1 (2013), pp. 51–67. doi: 10.1039/c2lc40864c.

[2] S. A. L. Thétiot-Laurent, J. Boissier, A. Robert, and B. Meunier. “Schistosomiasis Chemotherapy”. In: *Angewandte Chemie International Edition* 52.31 (2013), pp. 7936–7956. doi: 10.1002/anie.201208390.

[3] Centers for Disease Control and Prevention. *CDC-Schistosomiasis*. 2022. url: https://www.cdc.gov/parasites/schistosomiasis/index.html (visited on 02/12/2022).

[4] World Health Organization. “Schistosomiasis and soil-transmitted helminthiases: progress report, 2021”. In: *Weekly Epidemiological Record* 97.48 (2022), pp. 621–632. url: https://www.who.int/publications/i/item/who-wer9748-621-632.

[5] D. G. Colley, A. L. Bustinduy, W. E. Secor, and C. H. King. “Human schistosomiasis”. In: *The Lancet* 383.9936 (2014), pp. 2253–2264. doi: 10.1016/S0140-6736(13)61949-2.

[6] L. Le and M. H. Hsieh. “Diagnosing urogenital schistosomiasis: Dealing with diminishing returns”. In: *Trends in Parasitology* 33.5 (2017), pp. 378–387. doi: 10.1016/j.pt.2016.12.009.

[7] P. Hagemann. “Manual of Basic Techniques for a Health Laboratory”. In: *Clinical Chemistry* 49 (2003), pp. 1712–1713.

[8] A. D. Long. *Malaria: Obstacles and Opportunities*. Washington, DC, USA: Agency for International Development, 1991.

[9] W. P. O’Meara, M. Barcus, C. Wongsrichanalai, S. Muth, J. D. Maguire, R. G. Jordan, W. R. Prescott, and F. E. McKenzie. “Reader technique as a source of variability in determining malaria parasite density by microscopy”. In: *Malaria Journal* 5 (2006), pp. 1–7. doi: 10.1186/1475-2875-5-118.

[10] S. Jujjavarapu. “Automating the Diagnosis and Quantification of Urinary Schistosomiasis”. MA thesis. Delft, The Netherlands: Delft University of Technology, 2020.

[11] World Health Organization. *Ending the Neglect to Attain the Sustainable Development Goals: A Global Strategy on Water, Sanitation and Hygiene to Combat Neglected Tropical Diseases, 2021–2030*. World Health Organization, 2021. isbn: 9789240022782. url: https://iris.who.int/handle/10665/340240.

[12] I. I. Bogoch, J. R. Andrews, B. Speich, J. Utzinger, S. M. Ame, S. M. Ali, and J. Keiser. "Mobile phone microscopy for the diagnosis of soil-transmitted helminth infections: A proof-of-concept study". In: *The American Journal of Tropical Medicine and Hygiene* 88.4 (2013), pp. 626–629. doi: 10.4269/ajtmh.12-0742.

[13] N. A. Switz, M. V. D'Ambrosio, and D. A. Fletcher. "Low-cost mobile phone microscopy with a reversed mobile phone camera lens". In: *PLoS ONE* 9.5 (2014), e95330. doi: 10.1371/journal.pone.0095330.

[14] J. S. Cybulski, J. Clements, and M. Prakash. "Foldscope: Origami-based paper microscope". In: *PLoS ONE* 9 (2014), e98781. doi: 10.1371/journal.pone.0098781.

[15] S. J. Sowerby, J. A. Crump, M. C. Johnstone, K. L. Krause, and P. C. Hill. "Smartphone microscopy of parasite eggs accumulated into a single field of view". In: *The American Journal of Tropical Medicine and Hygiene* 94.1 (2016), pp. 227–230. doi: 10.4269/ajtmh.15-0427.

[16] J. T. Coulibaly, M. Ouattara, M. V. D'Ambrosio, D. A. Fletcher, J. Keiser, J. Utzinger, E. K. N'Goran, J. R. Andrews, and I. I. Bogoch. "Accuracy of mobile phone and handheld light microscopy for the diagnosis of schistosomiasis and intestinal protozoa infections in Côte d'Ivoire". In: *PLoS Neglected Tropical Diseases* 10.6 (2016), e0004768. doi: 10.1371/journal.pntd.0004768.

[17] A. M. Chagas, L. L. Prieto-Godino, A. B. Arrenberg, and T. Baden. "The €100 Lab: A 3D-Printable Open-Source Platform for Fluorescence Microscopy, Optogenetics, and Accurate Temperature Control during Behaviour of Zebrafish, Drosophila, and Caenorhabditis Elegans". In: *PLoS Biology* 15.7 (2017), e2002702. doi: 10.1371/journal.pbio.2002702.

[18] T. Aidukas, R. Eckert, A. R. Harvey, L. Waller, and P. C. Konda. "Low-cost, sub-micron resolution, wide-field computational microscopy using opensource hardware". In: *Scientific Reports* 9 (2019), p. 7457. doi: 10.1038/s41598-019-43845-9.

[19] R. A. Campbell, R. W. Eifert, and G. C. Turner. "Openstage: A low-cost motorized microscope stage with sub-micron positioning accuracy". In: *PLoS ONE* 9.2 (2014), e88977. doi: 10.1371/journal.pone.0088977.

[20] Z. Grier, M. F. Soddu, N. Kenyatta, S. A. Odame, J. Sanders, L. Wright, and F. Anselmi. “A low-cost do-it-yourself microscope kit for hands-on science education”. In: *Proceedings of the Optics Education and Outreach V*. Vol. 10741. International Society for Optics and Photonics. San Diego, California, United States, 2018, 107410K. doi: 10.1117/12.2320655.

[21] J. T. Collins, J. Knapper, J. Stirling, J. Mduda, C. Mkindi, V. Mayagaya, G. A. Mwakajinga, P. T. Nyakyi, V. L. Sanga, D. Carbery, L. White, S. Dale, Z. J. Lim, J. J. Baumberg, P. Cicuta, S. McDermott, B. Vodenicharski, and R. Bowman. “Robotic microscopy for everyone: the OpenFlexure microscope”. In: *Biomed. Opt. Express* 11.5 (May 2020), pp. 2447–2460. doi: 10.1364/BOE.385729.

[22] H. Li, H. Soto-Montoya, M. Voisin, L. Valenzuela, and M. Prakash. *Octopi: Open configurable high-throughput imaging platform for infectious disease diagnosis in the field*. preprint. 2019. doi: 10.1101/684423. BioRxiv: 684423.

[23] D. Avci and A. Varol. “An expert diagnosis system for classification of human parasite eggs based on multi-class SVM”. In: *Expert Systems with Applications* 36.1 (2009), pp. 43–48. doi: 10.1016/j.eswa.2007.09.012.

[24] G. Sengul. “Classification of parasite egg cells using gray level cooccurence matrix and kNN”. In: *Biomedical Research* 27.3 (2016), pp. 829–834.

[25] C.-C. Lee, P.-J. Huang, Y.-M. Yeh, P.-H. Li, C.-H. Chiu, W.-H. Cheng, and P. Tang. “Helminth egg analysis platform (HEAP): An opened platform for microscopic helminth egg identification and quantification based on the integration of deep learning architectures”. In: *Journal of Microbiology, Immunology and Infection* 55.3 (2022), pp. 395–404. doi: 10.1016/j.jmii.2021.07.014.

[26] T. E. Agbana, J. C. Diehl, F. van Pul, S. M. Khan, V. Patlan, M. Verhaegen, and G. Vdovin. “Imaging & Identification of Malaria Parasites Using Cellphone Microscope with a Ball Lens”. In: *PLoS ONE* 13 (2018), e0205020. doi: 10.1371/journal.pone.0205020.

[27] T. Agbana, G. Y. Van, O. Oladepo, G. Vdovin, W. Oyibo, and J. C. Diehl. “Schistoscope: Towards a locally producible smart diagnostic device for Schistosomiasis in Nigeria”. In: *2019 IEEE Global Humanitarian Technology Conference (GHTC)*. Seattle, WA, USA, 2019, pp. 1–8. doi: 10.1109/GHTC46095.2019.9033049.

[28] J. C. Diehl, P. Oyibo, T. Agbana, S. Jujjavarapu, G. Van, G. Vdovin, and W. Oyibo. “Schistoscope: Smartphone versus Raspberry Pi based low-cost diagnostic device for urinary Schistosomiasis”. In: *Proceedings of the 2020 IEEE Global Humanitarian Technology Conference (GHTC)*. Seattle, WA, USA, 2020, pp. 1–8. doi: 10.1109/GHTC46280.2020.9342871.

[29] I. Braakman. “Improving an Optical Diagnostics Device for Schistosomiasis”. MA thesis. Delft, The Netherlands: Delft University of Technology, 2021.

[30] T. Agbana, P. Nijman, M. Hoeber, D. van Grootheest, A. van Diepen, L. van Lieshout, J. C. Diehl, M. Verhaegen, and G. Vdovine. “Detection of Schistosoma haematobium using lensless imaging and flow cytometry, a proof of principle study”. In: *Proceedings of the Optical Diagnostics and Sensing XX: Toward Point-of-Care Diagnostics*. Vol. 11247. 2020, 112470F. doi: 10.1117/12.2545220.

[31] K. C. Kosinski, K. M. Bosompem, M. J. Stadecker, A. D. Wagner, J. Plummer, J. L. Durant, and D. M. Gute. “Diagnostic accuracy of urine filtration and dipstick tests for Schistosoma haematobium infection in a lightly infected population of Ghanaian school children”. In: *Acta Tropica* 118.2 (2011), pp. 123–127. doi: 10.1016/j.actatropica.2011.02.006.

[32] F. Bosch, M. S. Palmeirim, S. M. Ali, S. M. Ame, J. Hattendorf, and J. Keiser. “Diagnosis of soil-transmitted helminths using the Kato-Katz technique: What is the influence of stirring, storage time and storage temperature on stool sample egg counts?” In: *PLoS Neglected Tropical Diseases* 15.1 (2021), e0009032. doi: 10.1371/journal.pntd.0009032.

[33] J. Brooks. *COCO Annotator*. GitHub repository. 2019. url: https://github.com/jsbroks/coco-annotator/ (visited on 12/18/2021).

[34] O. Ronneberger, P. Fischer, and T. Brox. “U-net: convolutional networks for biomedical image segmentation”. In: *Medical Image Computing and Computer-Assisted Intervention – MICCAI 2015*. Vol. 9351. Munich, Germany, 2015, pp. 234–241. doi: 10.1007/978-3-319-24574-4_28.

[35] Y. H. Nai, B. W. Teo, N. L. Tan, S. O’Doherty, M. C. Stephenson, Y. L. Thian, E. Chiong, and A. Reilhac. “Comparison of metrics for the evaluation of medical segmentations using prostate MRI dataset”. In: *Computers in Biology and Medicine* 134 (2021), p. 104497. doi: 10.1016/j.compbiomed.2021.104497.

[36] International Organization for Standardization. *ISO 12233:2017*. 2017. url: https://www.iso.org/cms/render/live/en/sites/isoorg/contents/data/standard/07/16/71696.html (visited on 03/03/2022).

[37] World Health Organization. *Diagnostic target product profiles for monitoring, evaluation and surveillance of schistosomiasis control programmes*. World Health Organization, 2021. isbn: 9789240031104. url: https://iris.who.int/handle/10665/344813.

5

USABILITY AND USER-ACCEPTANCE STUDY

A usability study of an innovative optical device for the diagnosis of schistosomiasis in Nigeria

Michel Bengtson, Adeola Onasanya, Prosper Oyibo, Brice Meulah, Karl Tondo Samenjo, Ingeborg Braakman, Wellington Oyibo, J.C. Diehl

PUBLICATION REPORT

- **Conference Date:** 8 - 11 September 2022
- **Proceedings:** 2022 IEEE Global Humanitarian Technology Conference (GHTC)
- **Publisher:** IEEE
- **DOI:** 10.1109/GHTC55712.2022.9911019

ABSTRACT

Schistosomiasis is a neglected tropical disease that is predominantly diagnosed by conventional microscopy in SubSaharan Africa. However, effective diagnosis by conventional microscopy is limited by multiple technical and logistic barriers. Alternative diagnostic techniques are needed. The Schistoscope is a digital optical device that has been designed to support microscopists for the detection of schistosomiasis in endemic resource-limited settings. Aim: A user-centered design approach was used to assess the usability and user-acceptance of the Schistoscope compared to conventional microscopy in the Federal Capital Territory, Abuja, Nigeria. In this study, usability and acceptance are defined as being easy-to-use, efficient, and suitable in the daily workflow by end-users. Methods: Using a qualitative conventional context analysis approach, a mixed-methods questionnaire was used to elucidate themes related to the usability and user-acceptance of the device. Participants included trained microscopists and university students (n=17). Results: Participants answered both ranked and open questions. Overall the device's use was considered to be easy and acceptable in the routine workflow of a microscopist. The auto-scan feature was considered to have added value. Critical feedback regarding aesthetics of the device, particularly related to size, was noted by the participants. Conclusion: The usability approach used in this study elucidated valuable insights of end-users. The Schistoscope was very well perceived by both medical students and trained microscopists. Critical feedback will be used to further improve the next iterative design of the device.

5.1. INTRODUCTION

5.1.1. EPIDEMIOLOGY OF SCHISTOSOMIASIS

Schistosomiasis is a neglected tropical disease caused by infection with parasitic worms called schistosomes (trematode flatworms of the *Schistosoma (S)* genus), affecting more than 250 million people worldwide [1]. The majority of infected people live in Sub-Saharan Africa (SSA), especially in poor communities that lack access to clean water and adequate sanitation [2]. Populations in endemic regions are further affected by limited access to adequate diagnostics and general healthcare services. Schistosomiasis is spread through contact with larvae-infected fresh water [1]. The main human infective species in SSA are *S. haematobium* causing urinary schistosomiasis, and *S. mansoni* causing intestinal schistosomiasis. Symptoms of acute schistosomiasis are fever, diarrhea, fatigue, anemia and generally depleted nutritional status, myalgia, and malaise. Long term health consequences include organ failure, and for infected children growth stunting and cognitive impairment. The high socio-economic burden of this disease is exacerbated by indirect effects, including school absenteeism and reduced productivity in adults. Schistosomiasis can be treated with an anthelmintic drug called praziquantel which is safe and effective against all infective species [1, 2].

5.1.2. CURRENT DIAGNOSTIC APPROACHES AND CHALLENGES IN RESOURCE-LIMITED SETTINGS

Conventional microscopy is recommended by the World Health Organisation as the reference standard technique for the diagnosis of schistosomiasis [2]. For urinary schistosomiasis, *S. haematobium* eggs are excreted in urine. To increase sensitivity, urine samples are concentrated by filtration, sedimentation, or centrifugation (provided a centrifuge and electricity are available). Eggs are then detected by examining either the filter-membrane or the urine sediment under a conventional microscope (manual examination) [3].

Although conventional microscopy is highly specific and quantitative, it has several limitations. Egg excretions are variable. Therefore, eggs are often missed in low-intensity infections or due to inter- and intra-variation in egg distribution, collectively resulting in reduced sensitivity [1]. Although the limitation of uneven egg distribution is not unique to microscopy, even highly trained microscopists can miss eggs and report inconsistent results. Microscopy is time-consuming and highly operator-dependent and therefore error-prone, particularly as user-fatigue develops after many hours of analyzing samples (field observations). It is also difficult to standardize microscopy as a readout. The use of conventional microscopy in (remote) endemic regions is further hindered by logistic constraints [4]. The availability

of microscopes is limited by high costs, lack of both spare parts and required skills for repairs and maintenance, and erratic power supplies [4]. The use of alternative diagnostic tests, e.g. that detect adult worm-associated circulating antigens [3], is currently not feasible for routine use due to logistic and financial constraints.

5.1.3. PROPOSED DIAGNOSTIC SOLUTION: DIGITAL OPTICAL DEVICES

To address these diagnostic challenges, digital optical devices, some supported by artificial intelligence (AI), are being developed by various international research groups. They range from stand-alone devices to auxiliary components that are added to conventional microscopes [5], with or without the option of offline data analysis. All developments aim to achieve (semi-) automated detection and quantification of parasites in clinical samples. In line with these goals, the INSPiRED project aims to improve the diagnosis of parasitic diseases by developing and validating expert-independent, easy-to-use, and cost effective automated optical diagnostic devices for use in resource-limited settings. We have developed a digital optical device called the Schistoscope [6] (figs. 5.1 and 5.2). The development and validation processes involve multiple steps: (1) prototype development (i.e. system hardware design that includes optics; electrical components and embodiment, and currently costs approximately USD 700, and the interaction design); (2) data collection for the development of AI algorithms (i.e. training data set for system software) that are programmed to automatically identify specific pathogen features in a data set e.g. eggs (manuscript in preparation); (3) diagnostic performance evaluation, with and without AI, with respect to conventional microscopy as the reference standard (manuscript in preparation); and (4) usability and user-acceptance in the local context.

5.1.4. BEYOND TECHNICAL DEVELOPMENTS: USABILITY AND USER ACCEPTANCE IN THE LOCAL CONTEXT

User-centered design (UCD) is an iterative design process in which designers focus on the users and their needs in each phase of the design process, from product conception to the final product [7]. A UCD approach involves four distinct phases: contextual inquiry, user specification, prototyping, and user experience [7]. Co-creation is the foundation of UCD during the research and development phase, and it facilitates researchers to elucidate product specifications [8]. While designing the Schistoscope, we understood the context of the users [8] and opportunities for this device [9]. We also identified and specified the user's requirements by developing a target product profile [10]. We are currently evaluating the diagnostic performance of the device, and assessing how the product fits into the end-user's work environment in

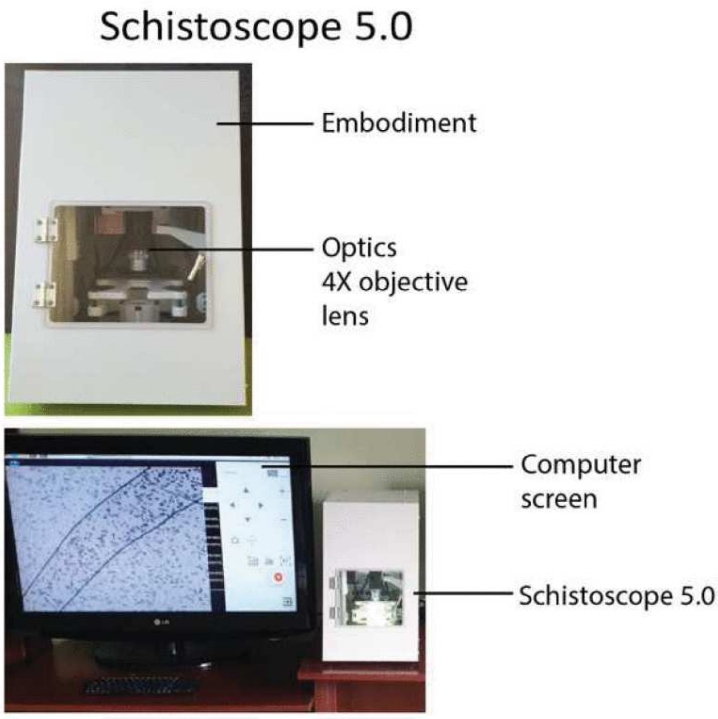

Figure 5.1: Schistoscope 5.0 (top) connected to a computer screen (bottom).

SSA by conducting a usability and acceptability study. This close user involvement will enhance the probability of meeting their expectations, and consequently increase uptake of the device in their daily practice [8]. The usability and user-acceptance study of the Schistoscope (version 5.0) was conducted in the Federal Capital Territory (FTC), Abuja, Nigeria, by health workers and medical students who are likely to use the device in their daily work activities. The aim of this paper is to describe the findings of the usability study.

5.2. METHODS

5.2.1. STUDY DESIGN AND SETTING

Governed by a UCD approach, a mixed-model questionnaire was formulated by industrial designers of the INSPiRED project who also developed the prototype. The questionnaire consisted of several ranked questions using a 5point Likert scale, and open questions to assess the usability of the device compared to conventional microscopy. This study

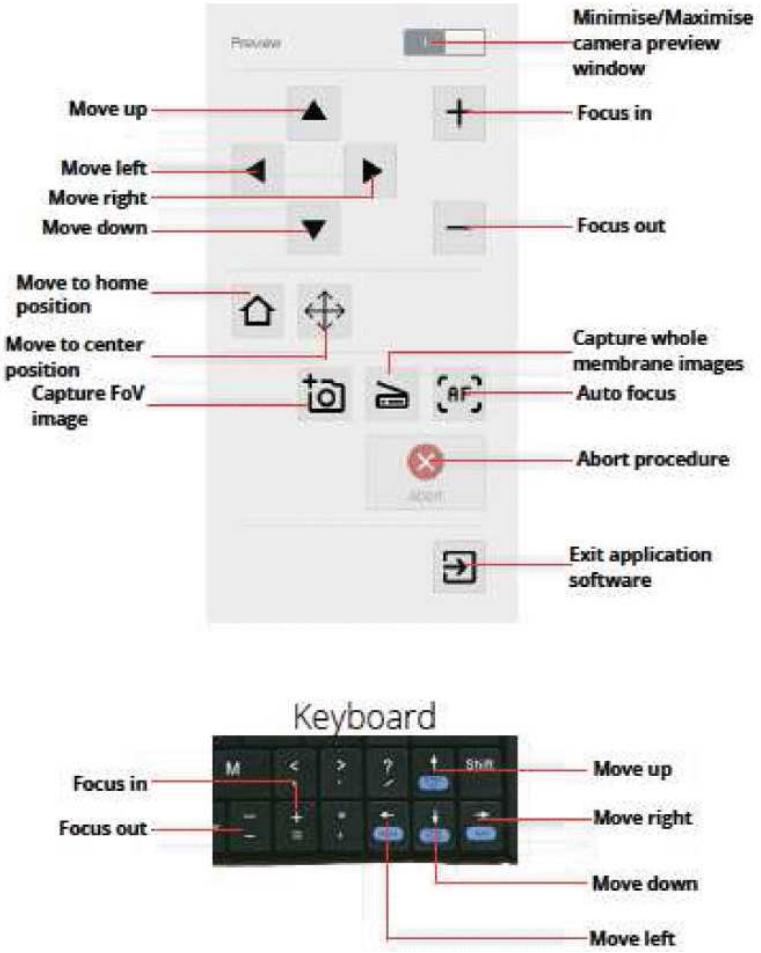

Figure 5.2: The graphical user interface of the Schistoscope 5.0.

was embedded within a larger epidemiology study that was conducted in the FTC (Abuja, Nigeria) in two area councils based on schistosomiasis prevalence and control with praziquantel treatment.

5.2.2. ETHICAL CONSIDERATIONS

The study protocol to obtain urine samples was approved by the College of Medicine University of Lagos, Health Research Ethics Committee (CMUL/HREC/07/16/017) and the Federal Capital Territory's Health Research Ethics Committee (FHREC/2019/01/73/18-07-19). Community members who were asked to provide a urine sample for the epidemiology study, as well as participants of the usability study were informed that

participation was voluntary and that they were free to withdraw from the study at any time.

5.2.3. ELIGIBILITY CRITERIA AND SAMPLE SIZE

Participants that met the following criteria were considered to be eligible: aged 18 and older, able to speak, read, and write English, have experience with conventional microscopy, and live and work in an endemic region. A purposive sampling method was employed where maximum variation selection was used in an effort to produce a study sample that varied in terms of age, sex, and duration of microscopy experience (years). Thereafter, a snowballing sample method was employed which facilitated recruitment of 7 students at the College of Medicine, University of Lagos (table 5.1). These participants represented the intended end-users as they had experience using conventional microscopy for the detection of schistosomiasis. The initial sample size was 18 end-users. Upon analyzing the data, one user was excluded from further analyses as the participant clearly did not understand the phrasing of the questions, as reflected in contradicting ranked responses. Data saturation can usually be reached with a sample size of 5-7 participants [11]. The final sample size included in this study was 17 end-users.

Table 5.1: Performance of Schistoscope Prototypes in Design Main Drivers

Characteristics	**n**	**Average (range)**
Age (years)	14	27.5 (20-41)
Sex (total)	15	-
Female	10	67%*
Male	5	33%*
Time active as a microscopist	8	5.6 (1-11)

*presented as a percentage

5.2.4. PROCEDURE

Five samples were prepared by the investigators by passing 10 mL urine through a filter membrane (13 mm diameter; 0.2μm pore size), and placing the filter membrane onto a glass slide. The purpose of the prepared slides was only to facilitate the use of the device, and participants were not required to prepare or formally analyze the filter membrane on the slides (fig. 5.3).

Two investigators provided a brief introduction (study aim and their backgrounds) to the participants and remained present for the duration

of the study. A printed user manual for the device of 5 pages (fig. 5.4) and accompanying questionnaire were given to each participant. Participants were not given a time-limit to complete the questionnaire, nor were they required to provide an answer for each question. Hardcopies of the questionnaires were collected at the end of the day.

The device was placed in its OFF-state by the investigators. Participants were asked to turn on the device and start the desktop application (fig. 5.3). Next, a slide containing a filter membrane was given to the participant to perform the following tasks according to the user manual: (1) using the directional control buttons on the user-interface or a keyboard (fig. 5.2), move the stage to a position such that the microscope objective is directly above the filter membrane on the slide; (2) focus on the filter membrane by using the autofocus feature; (3) capture an image of the filter membrane; (4) initialize the automatic slide scanning operation; (5) save the captured images to a USB and shut-down the device. On completion of the tasks the participants filled-in the questionnaire. The ranked statements in the questionnaire were formulated to understand the users' experience during different steps in the procedure. The 5-point Likert scale ranged from -2 to 2 in response to each statement. A "-2" score denotes that participants strongly disagreed with the statement, and a "2" score denotes strong agreement (table 5.2).

5.2.5. DATA ANALYSIS

Confidentiality of information retrieved and anonymity of results was ensured by assigning unique codes to the questionnaires before data analysis. The data were digitized by two investigators. Thereafter all data were analyzed descriptively using Microsoft Excel software by one investigator. Ranked responses were analyzed quantitatively (Mann-Whitney statistics; Prism 9), and open-questions were used to support the ranked responses in a descriptive manner. A conventional qualitative content analysis approach was used to code the data [12]. User impressions were considered as 'codes', which were then grouped into meaningful categories based on the relationship between the codes. Categories were generated until all the data were considered, and then grouped into a central usability theme (operational performance). The co-authors discussed the codes that emerged from the descriptive analysis. No discrepancies occurred (fig. 5.5).

5.3. RESULTS AND DISCUSSION

The aim of this study was to elucidate the perceptions of end-users as they document their experiences with the device. The following codes were identified: ease of use; size; efficiency (time); acceptability

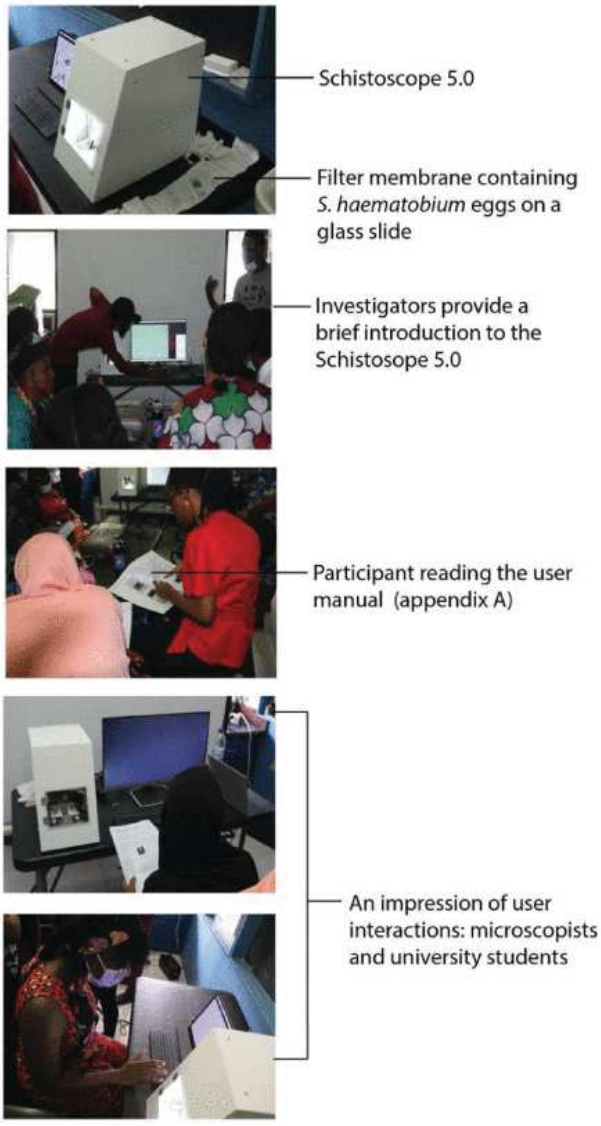

Figure 5.3: The study setting at the University of Lagos. From top to bottom: the investigators set-up the Schistoscope device and a computer screen. Slides containing a filter membrane were prepared by the investigators. After a brief introduction from the investigators, participants read the user manual. Thereafter, they began the user-interaction.

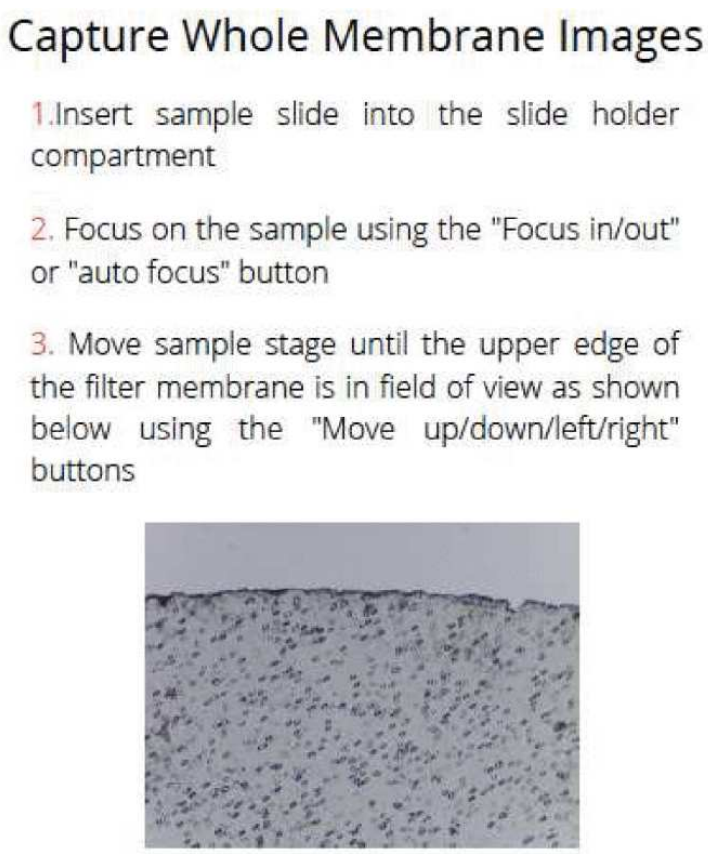

Figure 5.4: Sample page of the user manual.

compared to microscopy (workflow in daily routine); reliability of outcomes, and general aesthetic impressions (fig. 5.5). Participants were also asked 8 open questions to document their overall experience when using the Schistoscope compared to conventional microscopy. Their responses were stratified into the codes, and the average score in response to each statement are discussed here:

5.3.1. EASE OF USE

The participants agreed that it was easy to start the device (average score -1.8), and that this task was not time consuming (-0.6). They perceived this task as different compared to microscopy (0.6). The participants agreed that it was easy to place a sample into the Schistoscope (-1.7), however, placing a sample in a conventional

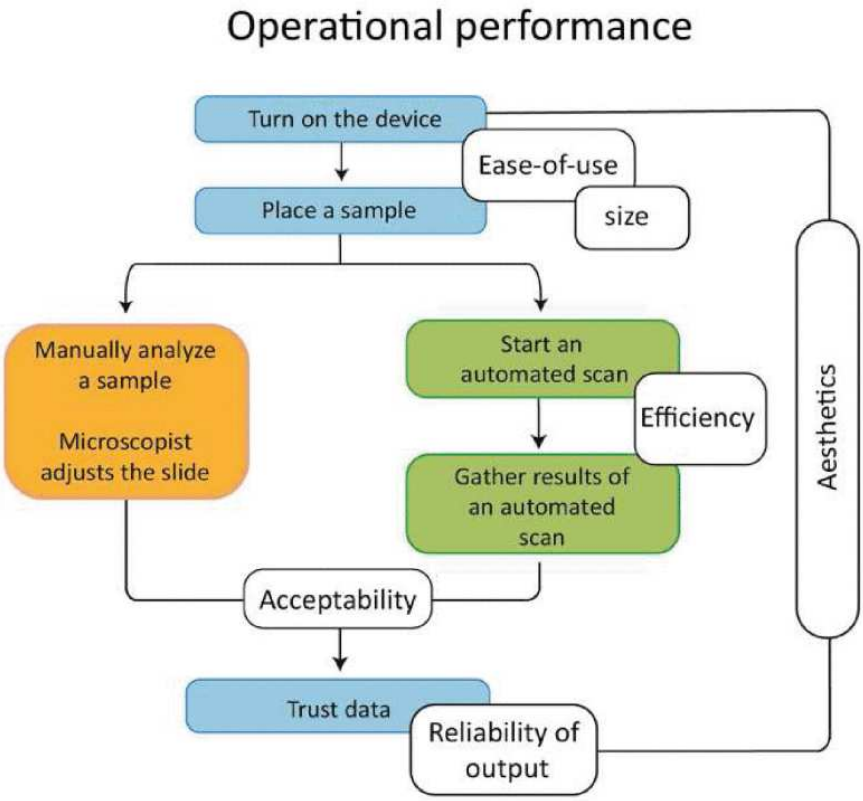

Figure 5.5: Graphical summary of the manual and automated procedure (orange and green blocks, respectively), and codes identified in this study (white blocks) that collectively relate to the operational performance of the device. The manual detection workflow is analogous to conventional microscopy (orange). The automated scan is unique to the Schistoscope 5.0 (green).

microscope was considered to be easier (-1.5). Although participants reported a neutral response to the time taken to place a sample in the device (0), this task was perceived as different compared to microscopy (0.7). These responses to starting a new device and placing a sample in the device are inherently perceived as different. In the open questions, all the participants reported that the Schistoscope was easy to use from sample placement to capturing a digital image. The use of a computer screen (fig. 5.1) was well-perceived, and multiple participants stated that it was impressive to see the parasitic eggs projected clearly on the screen.

Table 5.2: Participant Responses Related To Use of the Schistoscope 5.0 In Comparison To Conventional Microscopy Using A 5-Point Likert Scale (N=17, Unless Stated Otherwise).

Statement	Likert scale					
	disagree			agree		Average ± std dev
	-2	-1	0	1	2	
Turn on the device						
Executing this task was difficult	14	3	-	-	-	-1.8 ± 0.4
The task is easier on the Schistoscope than on a standard microscope	14	3	-	-	-	-1.8 ± 0.4
I spend more time on this task than I expected	10	1	-	2	4	-0.6 ± 1.8
With standard microscopy, this task is different	2	2	3	3	7	0.6 ± 1.5
Place a sample						
Executing this task was difficult	12	5	-	-	-	-1.7 ± 0.5
The task is easier on the Schistoscope than on a standard microscope	12	3	1	-	1	-1.5 ± 1
I spend more time on this task than I expected	2	6	3	2	4	0 ± 1.5
With standard microscopy, this task is different	0	3	5	3	6	0.7 ± 1
Manually analyze a sample						
Executing this task was difficult	9	8	-	-	-	-1.5 ± 0.5
The task is easier on the Schistoscope than on a standard microscope	9	7	-	1	-	-1.4 ± 0.8
I spend more time on this task than I expected	2	3	4	2	6	0.4 ± 1.5
With standard microscopy, this task is different	-	1	1	6	9	1.4 ± 0.9
Start an automated scan						
Executing this task was difficult	10	6	1	-	-	-1.5 ± 0.6
I spend more time on this task than I expected (n=16)	2	3	2	1	8	0.6 ± 1.6
Gather results of the automated scan						
Executing this task was difficult	7	6	2	1	-	-1 ± 1.1
I spend more time on this task than I expected	2	2	2	3	8	0.8 ± 1.5
Trust (n=16)	-	-	-	6	10	1.6 ± 0.5

Key to the 5-Point Likert scale

-2	Strongly disagree with the statement
-1	Disagree with the statement
0	Neutral
1	Agree with the statement
2	Strongly agree with the statement

> *"I was impressed that I could see the eggs projected on the screen with ease."*
> – microscopist with 10 years' work experience

Other comments included the added value of the digital display on the screen which circumvented the need to look directly into the eyepiece for a magnified view of the slide, as would be required when using a conventional microscope. Interestingly, a student reported that the Schistoscope was easy to use without formal training, which is in line with the WHO recommendation of one-day training for diagnostic devices [4]. The use of the Schistoscope as both a manual and automated device was positively reported. In addition to one participant that stated that the manual operation of the device was easy, multiple participants noted that the automatic focus and scanning features of the Schistoscope were value added features.

> *"The simplicity of the device in focusing samples was amazing, the auto-focus button was one of the best features, it saves time and energy."*
> – microscopist with 3 years' work experience

Although the Schistoscope prototype tested in this study had an auto-focus feature, the analysis of the sample was performed manually, meaning that the end-user (microscopists and students) manually counted the number of *S. haematobium* eggs identified, analogous to conventional microscopy. Numerous participants noted that automatic analysis would be an added value feature, where AI software could quantify the number of eggs. Such 'sample-in-answer-out' capabilities were noted as desirable features by the participants. Other display features that were suggested include a digital indication of which part of the slide is scanned during the auto-scan process as the field of view is changed in real-time, and the magnification status.

5.3.2. SUITABILITY IN THE WORKFLOW AND ACCEPTABILITY

The participants agreed that it was easy to manually analyze a sample (-1.5), however, this task was considered to be easier and less time consuming when using a conventional microscope (-1.4 and 0.4, respectively). Manually analyzing a sample on the Schistoscope was perceived as different compared to microscopy, as expected (1.4). To enhance the suitability and desirability of the device in the workflow in the field, an integrated sample storage unit was noted as an additional feature to store samples safely. Conventional microscopes contain 4 objective lenses (4X; 10X; 40X; and 100X). The Schistoscope 5.0 prototype had a single 4X objective lens which was sufficient to identify *Schistosoma* eggs, however, one participant noted that it would

be advantageous to incorporate additional objective lenses. Another suggestion included the possibility to detect other pathogens, however, the scope of this particular prototype was focused on the detection of Schistosoma eggs. Finally, large data storage capabilities were noted by participants as desirable.

5.3.3. EFFICIENCY

The participants agreed that it was easy to start an automated scan (-1.5), and to save the results of the scan (-1). They noted that it did not take more time than expected to start an automated scan or save results (0.6 and 0.8, respectively). Although participants were encouraged to provide their insights to each open question, this was not a requirement. Only two participants provided elaborate responses related to efficiency of use. In terms of the amount of time that it takes the end-user to scan a slide when using the auto-scan function, one participant reported that there should be a time limit on the device for this function. This participant noted that the use of the Schistoscope takes more time to perform a scan compared to a microscopist using a conventional microscope (approximately 15 minutes for the Schistoscope, and less than 10 minutes for a conventional microscope; personal observations in the field). In agreement with this observation, another participant also noted that the auto-scan time should ideally take less than 10 minutes. It is well acknowledged that scan time and accuracy is a common trade-off i.e. a faster scan time could reduce accuracy, however, further improvements in scan-time can be explored in the next design iteration.

5.3.4. RELIABILITY OF DATA GENERATED BY THE SCHISTOSCOPE

Given that captured images are displayed on a screen, the majority of the participants noted that the data generated would be considered reliable. Interestingly, one participant noted that digital microscopy, like conventional microscopy, is only reliable provided that the microscopist can identify the eggs, and this relies on the expertise of the microscopist. However, a challenge remains when dealing with a negative sample.

> *"Yes, it is reliable if I can see a positive result, but not reliable if negative. Quality control is needed."*
> – microscopist with 10 years' experience

5.3.5. AESTHETICS

Responses related to the size of the device demonstrate that it was generally perceived as too big. Suggestions were to reduce the size of the device to increase portability; and also reduce the amount of space that would be occupied on a laboratory bench or a table in the field.

However, a device that is too small can also be easily misplaced. Other responses included the size of the door handle used to place a sample in the device was too small, undesirability of visible wires, and added value of a small screen fitted to the device to enhance portability by replacing the computer screen.

For each step in the process, no statistically significant differences in responses were identified between microscopists and students, indicating the ease-of-use for both groups.

5.4. CONCLUSION

The aim of this study was to elucidate the perception(s) of end-users related to the use of the Schistoscope in a representative context. The mixed-model questionnaire consisted of several ranked and open questions to assess the usability of the device compared to conventional microscopy, and user-acceptance in terms of overall experience (interaction with the device), reliability of data generated, and aesthetics (size and general appearance). One user was excluded from the study due to contradicting responses. Therefore, negatively-worded questions are a limitation of the questionnaire design and can be rephrased as positively-worded (agreeable statements) in future usability studies.

The Schistoscope is a digital microscope, designed to support the daily work of a microscopist, that can be used manually, analogous to a conventional microscope except with a digital interface, or automated. Sample preparation is the same for both detection methods, so use of Schistoscope does not disrupt the workflow of the microscopist or other technicians in the laboratory or at field sites. It is therefore not surprising that the Schistoscope was perceived as easy to use by both students and trained microscopists with very little training or explanation for operation. Summing up, it is expected that the use of this device can be implemented with minimal capacity building.

ACKNOWLEDGEMENT

We thank the field team who conducted the epidemiology study in Abuja, Nigeria, and the team from the University of Lagos who facilitated this usability study. We also thank Lisette van Lieshout, Angela van Diepen, Tope Agbana, Satyajith Jujjavarapu, Jo van Engelen, and the industrial design engineering students at the Delft University of Technology and parasitologists at the Leiden University Medical Centre who contributed to the development and validation of the Schistoscope. Finally, we thank NWO-WOTRO for funding this research (GRANT_NUMBER: W 07.30318.009).

REFERENCES

[1] D. P. McManus, D. W. Dunne, M. Sacko, J. Utzinger, B. J. Vennervald, and X. N. Zhou. “Schistosomiasis”. In: *Nature Reviews Disease Primers* 4.1 (2018), p. 13. doi: 10.1038/s41572-018-0013-8.

[2] World Health Organisation. *Schistosomiasis*. 2024. url: https://www.who.int/news-room/fact-sheets/detail/schistosomiasis (visited on 09/26/2024).

[3] P. T. Hoekstra, G. J. van Dam, and L. van Lieshout. “Context-specific procedures for the diagnosis of human schistosomiasis – a mini review”. In: *Frontiers in Tropical Diseases* 2 (2021), p. 722438. doi: 10.3389/fitd.2021.722438.

[4] World Health Organization. *Diagnostic target product profiles for monitoring, evaluation and surveillance of schistosomiasis control programmes*. World Health Organization, 2021. isbn: 9789240031104. url: https://iris.who.int/handle/10665/344813.

[5] E. Dacal, D. Bermejo-Peláez, L. Lin, E. Álamo, D. Cuadrado, Á. Martínez, A. Mousa, M. Postigo, A. Soto, E. Sukosd, A. Vladimirov, C. Mwandawiro, P. Gichuki, N. A. Williams, J. Muñoz, S. Kepha, and M. Luengo-Oroz. “Mobile microscopy and telemedicine platform assisted by deep learning for the quantification of Trichuris trichiura infection”. In: *PLoS neglected tropical diseases* 15.9 (2021). doi: 10.1371/journal.pntd.0009677.

[6] T. Agbana, G. Y. Van, O. Oladepo, G. Vdovin, W. Oyibo, and J. C. Diehl. “Schistoscope: Towards a locally producible smart diagnostic device for Schistosomiasis in Nigeria”. In: *2019 IEEE Global Humanitarian Technology Conference (GHTC)*. Seattle, WA, USA, 2019, pp. 1–8. doi: 10.1109/GHTC46095.2019.9033049.

[7] A. R. Dopp, K. E. Parisi, S. A. Munson, and A. R. Lyon. “A glossary of user-centered design strategies for implementation experts”. In: *Translational Behavioral Medicine* 9.6 (Nov. 2019), pp. 1057–1064. doi: 10.1093/tbm/iby119.

[8] A. Onasanya, M. Keshinro, O. Oladepo, J. V. Engelen, and J. C. Diehl. “A Stakeholder Analysis of Schistosomiasis Diagnostic Landscape in South-West Nigeria: Insights for Diagnostics Co-creation”. In: *Frontiers in Public Health* 8 (2020). doi: 10.3389/fpubh.2020.564381.

[9] G. Y. Van, A. Onasanya, J. van Engelen, O. Oladepo, and J. C. Diehl. “Improving Access to Diagnostics for Schistosomiasis Case Management in Oyo State Nigeria: Barriers and Opportunities”. In: *Diagnostics* 10.5 (2020), p. 328. doi: 10.3390/diagnostics10050328.

[10] M. Sluiter, A. Onasanya, O. Oladepo, J. van Engelen, M. Keshinro, and T. Agbana. “Target product profiles for devices to diagnose urinary schistosomiasis in Nigeria”. In: *2020 IEEE Global Humanitarian Technology Conference (GHTC)*. Seattle, WA, USA, 2020, pp. 1–8. doi: 10.1109/GHTC46280.2020.9342953.

[11] A. W. Kushniruk and V. L. Patel. “Cognitive and usability engineering methods for the evaluation of clinical information systems”. In: *Journal of Biomedical Informatics* 37.1 (2004), pp. 56–76. doi: 10.1016/j.jbi.2004.01.003.

[12] V. Renjith, R. Yesodharan, J. A. Noronha, E. Ladd, and A. George. “Qualitative Methods in Health Care Research”. In: *International Journal of Preventive Medicine* 12 (Feb. 2021), p. 20. doi: 10.4103/ijpvm.IJPVM_321_19.

6

NIGERIA FIELD VALIDATION STUDY

Performance Evaluation of the Schistoscope 5.0 for (Semi-)automated Digital Detection and Quantification of *Schistosoma haematobium* Eggs in Urine: A Field-based Study in Nigeria

Brice Meulah, Prosper Oyibo, Michel Bengtson, Temitope Agbana, Roméo Aimé Laclong Lontchi, Ayola Akim Adegnika, Wellington Oyibo, Cornelis Hendrik Hokke, Jan Carel Diehl, Lisette van Lieshout

PUBLICATION REPORT

- **Publication Date:** 17 October 2022
- **Journal:** The American Journal of Tropical Medicine and Hygiene (AJTMH)
- **Publisher:** ASTMH
- **DOI:** 10.4269/ajtmh.22-0276

ABSTRACT

Conventional microscopy is the standard procedure for the diagnosis of schistosomiasis, despite its limited sensitivity, reliance on skilled personnel, and the fact that it is error prone. Here, we report the performance of the innovative (semi-)automated Schistoscope 5.0 for optical digital detection and quantification of Schistosoma haematobium eggs in urine, using conventional microscopy as the reference standard. At baseline, 487 participants in a rural setting in Nigeria were assessed, of which 166 (34.1%) tested S. haematobium positive by conventional microscopy. Captured images from the Schistoscope 5.0 were analyzed manually (semiautomation) and by an artificial intelligence (AI) algorithm (full automation). Semi- and fully automated digital microscopy showed comparable sensitivities of 80.1% (95% confidence interval [CI]: 73.2-86.0) and 87.3% (95% CI: 81.3-92.0), but a significant difference in specificity of 95.3% (95% CI: 92.4-97.4) and 48.9% (95% CI: 43.3-55.0), respectively. Overall, estimated egg counts of semi- and fully automated digital microscopy correlated significantly with the egg counts of conventional microscopy ($r = 0.90$ and $r = 0.80$, respectively, $P < 0.001$), although the fully automated procedure generally underestimated the higher egg counts. In 38 egg positive cases, an additional urine sample was examined 10 days after praziquantel treatment, showing a similar cure rate and egg reduction rate when comparing conventional microscopy with semiautomated digital microscopy. In this first extensive field evaluation, we found the semiautomated Schistoscope 5.0 to be a promising tool for the detection and monitoring of S. haematobium infection, although further improvement of the AI algorithm for full automation is required.

6.1. INTRODUCTION

Schistosomiasis is a neglected tropical disease affecting approximately 250 million people, and more than 700 million people are at risk of infection [1]. Sub-Saharan Africa shares the greatest burden of this disease [2], and preschool and school-age children are the most affected. It is a parasitic worm infection of poverty, leading to chronic disease and significant disability-adjusted life years lost [3]. Several *Schistosoma* species are known to affect humans. Urogenital schistosomiasis is caused by *S. haematobium*, and *S. mansoni* is the major species causing intestinal disease. *S. haematobium* infections are most prevalent in Africa, affecting the urogenital system with hematuria, bladder and kidney failure as the main complications and genital schistosomiasis presentations such as vaginal discharge and postcoital bleeding in women and hematospermia in men [3, 4]. Chronic infections can lead to miscarriage and infertility and may facilitate infection with sexually transmitted diseases, including HIV [4].

The prevailing strategy to control and eliminate this disease is a comprehensive integrated program of mass drug administration (MDA) with praziquantel, water, sanitation, and hygiene (WASH); snail vector control; and a multisectoral approach to diagnostic monitoring and evaluation [5]. The diagnosis of *S. haematobium* infection typically involves the detection of eggs in urine by conventional light microscopy. Counting the number of eggs seen per 10 mL of urine is commonly done to indicate the intensity of infection in a target population [3, 5], which is relevant for the purpose of monitoring and evaluation. However, the need for expert laboratory personnel, basic laboratory infrastructure, and a permanent power supply limits the use of conventional light microscopy in endemic resource-limited settings. In addition, in areas where laboratory infrastructure is inadequate, the ratio of trained personnel to sample analysis is often very low, resulting in a high workload per technician and above threshold eye exposure to the microscopy light source, causing visual health complications [6, 7]. Therefore, there is a need for innovative, and preferably easy-to-use, diagnostics that will suit endemic resource-limited settings to diagnose infections and complement control and elimination efforts.

During the past decade innovative optical diagnostic devices, with or without artificial intelligence (AI), have been developed for the detection of *S. haematobium* eggs [8–15]. Although several of these devices scan through samples and save digitalized images for manual identification of *Schistosoma spp* [8–12], only a few have an integrated AI program for automated detection [13–15]. To our knowledge, only four of these devices have been field validated using samples from a *Schistosoma*-exposed population [9–12], and only the Newton Nm1 microscope has been marketed commercially as a portable field microscope, although without a fully automated AI application [12]. This limited validation

highlights the technical challenges that are faced to transition working prototypes to commercialized and field applicable devices. Also, most studies have used only a small, often nonrandomly selected, number of clinical samples to validate the diagnostic devices. Hence, there is a clear need for more extensive field-based studies.

The Schistoscope device (version 5.0) is a low-cost digital microscope (fig. 6.1A and B) that has gone through five design iterations in an ongoing process of co-creation including different potential stakeholders. In its current form, it can function either as a semiautomated or AI integrated fully automated digital microscope to detect and quantify *S. haematobium* eggs [16, 17]. In a recent proof-of-principle study, the device and its AI algorithms were trained successfully with phosphate buffer saline and urine samples that were spiked with *S. haematobium* eggs obtained from a laboratory maintained parasite life cycle and a limited number of clinical samples [18]. This led to the conclusion that the Schistoscope was ready for further validation. The aim of the current study is to evaluate the performance of the Schistoscope 5.0 as a semi- and fully automated digital microscope for the detection and quantification of *S. haematobium* eggs in a prospective study design under field conditions. For this purpose, urine samples were collected in a rural area in Nigeria and filtered, and each membrane filter was independently examined locally by conventional microscopy and the Schistoscope 5.0.

6.2. METHODS

6.2.1. ETHICAL CONSIDERATIONS

This study was done in collaboration with the Schistosomiasis Program of the Neglected Tropical Diseases Department, Federal Ministry of Health, Abuja, and embedded in an ongoing, cross-sectional community-based survey in collaboration with the Public Health Department in charge of the MDA of praziquantel in the Federal Capital Territory (FCT), Nigeria. The ethical approval for this study was obtained from the FCT Health Research Ethics Committee in Abuja, Nigeria (reference no. FHREC/2019/01/73/18-07-19). Written consent from adults and from parents or legal guardians of children and teenagers was obtained before sample collection from persons willing to participate through their signatures or thumbprints. Confidentiality and anonymity of results were ensured by assigning unique codes to samples. According to the local standard operational procedures, all participants with detectable hematuria (discussed subsequently) were considered *S. haematobium* positive and therefore treated with praziquantel (40 mg/kg of body weight). The local health authorities have been informed of the outcome of the study, and all participants have been offered (re)treatment where appropriate.

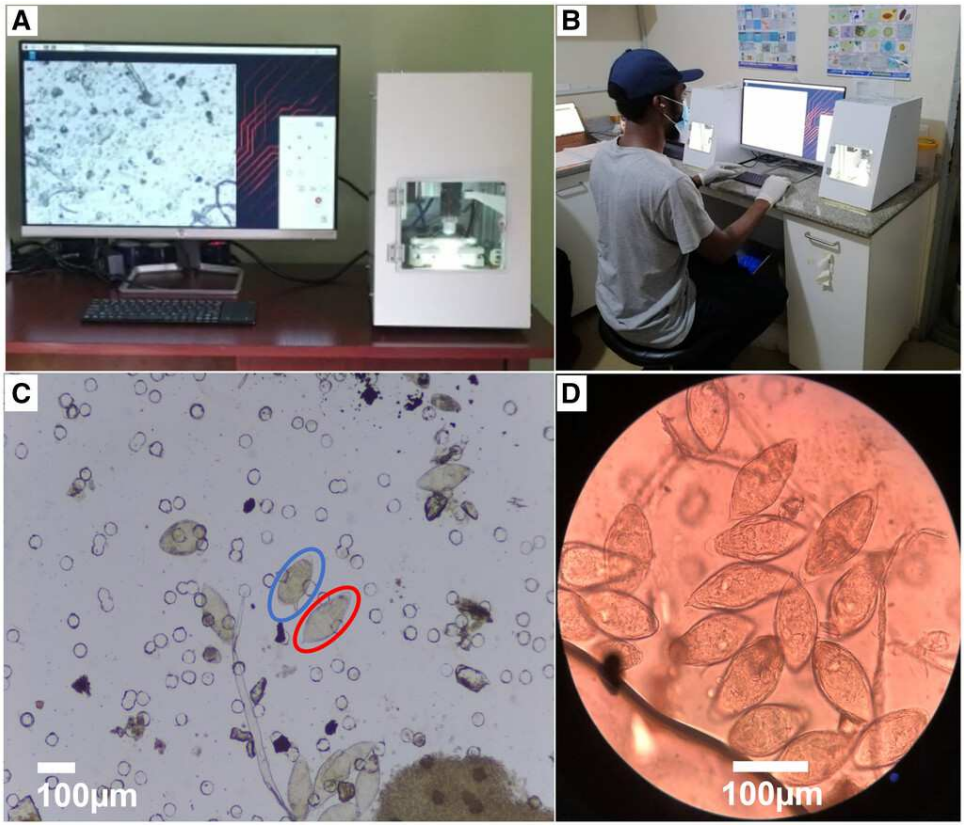

Figure 6.1: (A) Schistoscope 5.0 device (right) connected to a computer monitor (left), showing an image of a digitally screened sample. (B) Schistoscope 5.0 operated by a laboratory technician in the field. (C) Digital image of a urine filtered membrane showing several *Schistosoma* eggs captured with the Schistoscope 5.0 (4× objective). The red circle indicates a *S. haematobium* egg, the blue circle indicates a *S. mansoni* egg. (D) Image of a urine filtered membrane with several *S. haematobium* eggs captured by a camera attached to a conventional microscope (10× objective).

6.2.2. STUDY DESIGN AND POPULATION

This cross-sectional and longitudinal study was carried out in August–September 2021 in two area councils in FCT, Abuja, Nigeria (geographic coordinates: 9.0618° N latitude, 7.4221° E longitude and 8.950833° N latitude, 7.076737° E longitude). The FCT is the third highest endemic state for schistosomiasis in Nigeria [19]. In total, 14 communities from these two area councils were visited, where

preschool, school-age children and adults were allowed to participate. Strategic advocacy and engagement with community leaders in the study area preceded the sample collection at the communities studied.

6.2.3. SAMPLE COLLECTION AND PROCESSING

fig. 6.2 depicts the flowchart of sample collection. Briefly, a sterile 20 mL universal container with a unique identification code was given to those who consented to participate with the request to collect a urine sample between 11:00 am and 13:00 pm. Dipstick (Combur 10-Test M Roche Mannheim, Germany) urinalysis was performed on site according to the manufacturer's instructions. Of those who were confirmed as positive by conventional urine microscopy, 50 were randomly selected and asked to provide an additional sample 10 days after baseline screening. This small-scale posttreatment evaluation was done to examine whether drug treatment could influence the performance of the Schistoscope 5.0, possibly via praziquantel-induced changes in egg morphology [20, 21].

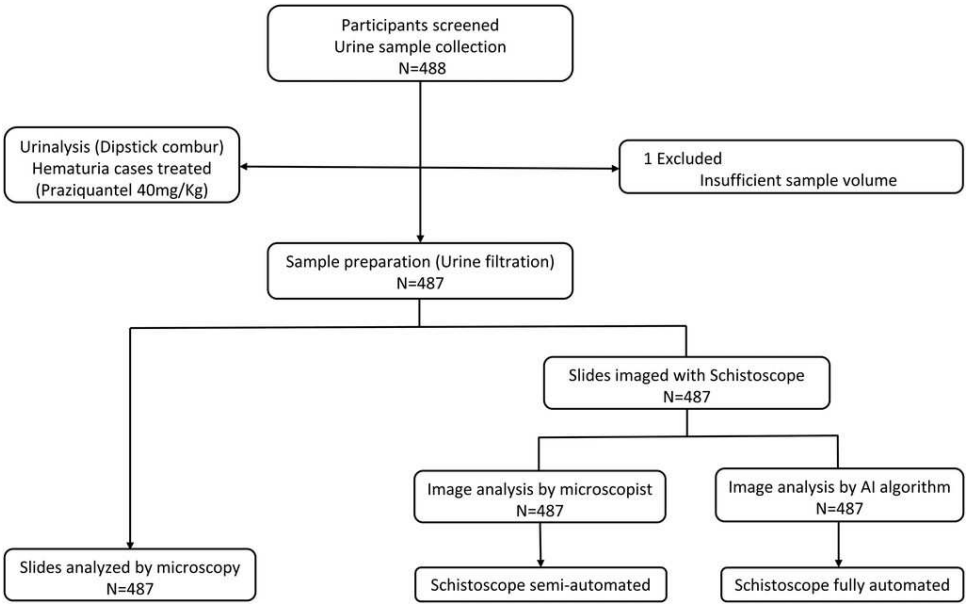

Figure 6.2: Flow chart of urine sample collection and analysis comparing conventional microscopy with semiautomated and fully automated digital microscopy.

All urine samples were transported to the laboratory of the Department of Public Health, Abuja, FTC, within 2 hours of sample collection and prepared for microscopy by urine filtration [22]. Urine samples were homogenized, and 10 mL of urine was obtained with a syringe and

pressed through a filter membrane (diameter 13 mm; pore size 30 μm; Whatman International Ltd., Maidenstone, UK). The filter membrane was then placed on a standard microscope glass slide, and a cover slip was placed over the membrane to keep the filter moist. Each slide was viewed under a standard microscope and the Schistoscope.

6.2.4. DESCRIPTION OF THE SCHISTOSCOPE 5.0

The Schistoscope 5.0 (fig. 6.1) is a low-cost automated slide-scanner digital microscope that can be supported with AI algorithms for image processing [18]. The system is composed of custom-designed optical bright-field illumination, three-axis movement (X, Y, Z), and electronic and computing modules. The illumination module comprises a bright white light-emitting diode and condenser lenses to generate uniform illumination. The custom three-axis motorized stage provides a step resolution of 2.5 μm on all three axes. A custom printed circuit board is used to control all three motors and the illumination. The on-board computer is a Raspberry Pi 4B connected to a Raspberry Pi HQ camera that has a pixel size of 1.55 μm and an image resolution of 2028 × 1520 pixels. The current study used a 4× microscope objective that provides an experimental resolution limit of 3.26 μm [18], which is sufficient to resolve *S. haematobium* eggs (fig. 6.1C). The device runs on mains electricity and does not have a built-in battery. Dedicated software with a graphical user interface was developed and installed on the device's onboard computer for easy user interaction and control of the device. The software comprises a simple autofocus procedure and an algorithm to scan the complete filter membrane and capture each field of view as an image. It takes 12 minutes to scan and capture 117 images of an entire 13-mm filter membrane. Additional analysis of the captured images, including counting the number of eggs, takes approximately 5 minutes on average per filter when done either manually or by AI. Captured images are stored in folders by their sample identification code. Semiautomated analysis can be done via a connected computer monitor, or automated analysis can be done on an external computer. Further development is ongoing to enable automated processing and analysis on the device itself.

6.2.5. DETECTION OF *S. haematobium* EGGS BY MICROSCOPY AND THE SCHISTOSCOPE

Slides were examined immediately after preparation. The order of examination was randomized, resulting in approximately half of the slides being first analyzed by conventional microscopy and then imaged with the Schistoscope 5.0 and the other half analyzed in the opposite sequence.

For conventional light microscopy, slides were analyzed using a 10× objective on an Olympus (Tokyo, Japan) CX22RFS1 microscope (fig. 6.1D). Two microscopists independently examined each slide for the detection and quantification of *S. haematobium* eggs with results blinded from each other. The average of egg counts from both microscopists was computed as the final result. Discrepancies of more than 20% between both microscopy readings were resolved by a third independent microscopy reading, of which an average between two closest among the three readings was considered.

The imaging procedure of the Schistoscope included manual counting of the eggs seen on the images, which was done in the field by a fourth microscopist who was blinded from the results of the conventional light microscopy. The images were also uploaded to a cloud server (Google Colaboratory; https://colab.research.google.com) for remote access and AI analysis. For quality control of the manual analysis of the captured images, 10% of the images were randomly selected and reexamined by an independent senior microscopist, but because this showed no significant differences from the original manual readings, these data are not further considered. Data from the two independent microscopists, the manual reading, and the AI analysis were independently entered in an Excel spreadsheet and only shared with the results collation officer after finalizing.

6.2.6. POWER CALCULATIONS AND STATISTICAL ANALYSES

For the cross-sectional evaluation of the Schistoscope, the number of positive cases needed to achieve an assumed sensitivity and specificity of 80% and 90% using conventional microscopy as the reference was calculated to be 107 [23]. The power of this calculation was set to 80%, and a 5% degree of error was considered to be able to detect a difference of at most 10% from the assumed sensitivity and specificity. With a schistosomiasis prevalence of 25% in the FCT region [19], a total of 450 samples was needed to meet our target case number. Microscopy and Schistoscope data were merged and double-checked by the collation officer. Descriptive statistics for the data were obtained using IBM Statistical Package for Social Sciences version 25 (SPSS Inc., Chicago, IL). For the baseline sample subset, sensitivity, specificity, positive predictive value (PPV), and negative predictive value (NPV) of the semi- and fully automated digital microscope were calculated for *S. haematobium* detection using conventional light microscopy as the reference standard. Qualitative agreement between the Schistoscope and conventional microscopy was assessed using the adjusted Cohen's kappa, considering true positives and true negatives, as well as false positives and false negatives [24]. Egg counts were categorized as low-intensity infection ($\leq$ 50 eggs/10 mL urine) or high-intensity infection

(> 50 eggs/10 mL urine). Because of the non-Gaussian nature and wide range of the egg count estimates for all three methods, the data set was log transformed before analysis was performed. The linear association in terms of egg counts (eggs/10 mL) between the different optical procedures was estimated using the Pearson's correlation coefficient (r), excluding the negative data points. Bland–Altman analysis was performed for quantitative assessment of the agreement between semi- and fully automated digital microscopy and conventional microscopy using GraphPad Prism version 9.0.1 for windows (GraphPad Software, San Diego, CA; http://www.graphpad.com). Cure rate (CR), defined as the percentage of follow-up samples with no detectable eggs, and egg reduction rate (ERR), defined as the percentage reduction in the geometric mean (GM; formula: GM (egg count +1) - 1) egg counts pre- and post-treatment, were estimated for each of the microscopy procedures.

6.3. RESULTS

6.3.1. PERFORMANCE EVALUATION OF THE SCHISTOSCOPE AND ESTIMATION OF EGG COUNTS

To evaluate the capacity of the Schistoscope to detect and count *S. haematobium* eggs, each of the 487 prepared slides was examined by conventional microscopy and by both semi- and fully automated digital microscopy. No differences resulting from the order in which the filters were examined were noted (e.g., first by conventional microscopy, followed by image capturing by the Schistoscope or vice versa). The three detection methods (i.e., conventional and semiautomated and fully automated digital microscopy) independently identified 166 (34.1%), 148 (30.4%), and 309 (63.4%) of the slides as positive for *S. haematobium*, respectively (table 6.1). Egg count estimates per 10 mL of urine ranged from 1 to 4,386 eggs/10 mL for conventional microscopy, 1 to 2,059 eggs/10 mL for semiautomated digital microscopy, and 1 to 573 eggs/10 mL for fully automated digital microscopy, with a median of 12, 12, and 2 eggs/10 mL, respectively. Compared with conventional microscopy, semi- and fully automated digital microscopy showed an overall accuracy of 90.1% and 62.0%, respectively (table 6.1).

Conventional microscopy classified 129 (78%) as low-intensity infection and 37 (22%) as high-intensity infection, whereas semi- and fully automated microscopy classified 111 (75%) and 294 (95%) as low-intensity infection and 37 (25%) and 15 (5%) as high-intensity infection, respectively. The sensitivities of semi- and fully automated digital microscopy for low-intensity infections were 75.2% (95% CI: 67.0–82.3%) and 83.7% (95% CI: 76.1–90.0%), which increased for high-intensity infections (table 6.2). The adjusted Cohen's kappa

Table 6.1: Cross tabulation of the detection of *Schistosoma haematobium* eggs by the Schistoscope 5.0 and conventional microscopy performed on 487 urines collected at baseline screening

		Conventional microscopy		
Schistoscope 5.0		Positive (n = 166)	Negative (n = 321)	Total (N = 487)
Semi-automated digital microscope	Positive	133	15	148
	Negative	33	306	339
Fully automated digital microscope	Positive	145	164	309
	Negative	21	157	178

Table 6.2: Diagnostic performance of the Schistoscope 5.0 for the detection of *Schistosoma* eggs performed on 487 urines collected at baseline screening

Conventional microscopy	Schistoscope 5.0							
	Semiautomated digital microscopy				**Automated digital microscopy**			
	Sen (95% CI)	Spec (95% CI)	PPV (95% CI)	NPP (95% CI)	Sen (95% CI)	Spec (95% CI)	PPV (95% CI)	NPV (95% CI)
All samples with *S. haematobium* infection (N = 166)	80.1 (73.2 – 86.0)	95.3 (92.4 – 97.4)	89.8 (84.0 – 94.2)	90.3 (87.0 – 93.2)	87.3 (81.3 – 92.0)	48.9 (43.3 – 55.0)	46.9 (41.2 – 53.0)	88.2 (83.0 – 93.0)
Low-intensity infection* (n = 129)	75.2 (67.0 – 82.3)	-	-	-	83.7 (76.1 - 90.0)	-	-	-
High-intensity infection† (n = 37)	97.3 (86.0 – 100.0)	-	-	-	100	-	-	-

CI = confidence interval; NPV = negative predictive value; PPV = positive predictive value; Sen = sensitivity; Spec = specificity.
* ≤ 50 eggs/10 mL urine.
† > 50 eggs/10 mL urine.

demonstrated a fair (0.34) and a slight (0.2) qualitative agreement between conventional microscopy and semi- and fully automated digital microscopy, respectively.

In terms of *S. haematobium* egg count estimates, conventional microscopy correlated strongly to semiautomated digital microscopy (N=133, r=0.90, P < 0.001) and fully automated digital microscopy (N=145, r=0.80, P < 0.001) (fig. 6.3). To demonstrate reliability of conventional microscopy, Bland–Altman analysis showed a strong agreement between the first and second microscopy readings across the range of mean egg counts for both readings (bias=0.13, 95% limits of agreement from –0.66 to 0.94). Further Bland–Altman analysis demonstrated a strong agreement between conventional microscopy and semiautomated digital microscopy across the range of mean egg counts for both methods (bias=0.08, 95% limits of agreement from –0.69 to 0.85) (fig. 6.4). Conventional microscopy and fully automated

digital microscopy revealed a strong agreement at low mean egg counts of both methods. However, an underestimation of egg counts by fully automated digital microscopy was observed at egg counts greater than 100 eggs/10 mL (bias=0.47, 95% limits of agreement from –0.69 to 1.63).

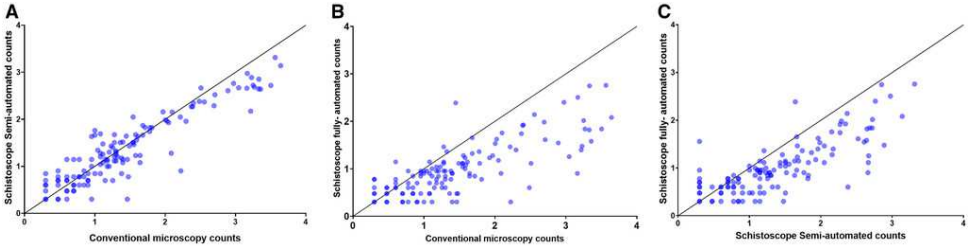

Figure 6.3: Correlation in *Schistosoma haematobium* egg counts per 10 mL of urine on a Log10 scale on samples collected at baseline screening. Negative data points are excluded. (A) Semiautomated digital microscopy versus conventional microscopy (n = 133, r = 0.90, P < 0.001). (B) Fully automated digital microscopy versus conventional microscopy (n = 145, r = 0.80, P < 0.001). (C) Semiautomated versus fully automated digital microscopy (n = 137, r = 0.80, P < 0.001). The depicted solid line indicates y = x.

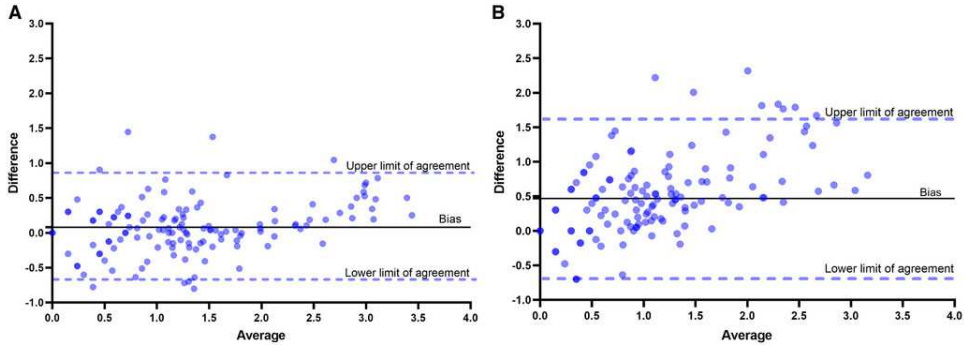

Figure 6.4: Bland–Altman plots showing the level of agreement between (A) conventional microscopy and semiautomated digital microscopy counts and (B) conventional microscopy and fully automated digital microscopy counts.

6.3.2. FOLLOW-UP AFTER PRAZIQUANTEL TREATMENT

Conventional microscopy and the semiautomated Schistoscope procedure were also compared on 38 urine samples collected 10 days post-praziquantel treatment from participants with a confirmed infection at baseline. Thirty (79%) and 27 (71%) samples still had detectable *S. haematobium* eggs by conventional microscopy and semiautomated digital microscopy, resulting in a CR of 21% (95% CI: 10–37) and 29% (95% CI: 15–46), respectively. In four follow-up samples, eggs were only seen by conventional microscopy, and only one sample was positive by semiautomated digital microscopy. The ERR of conventional microscopy (80%; 95% CI: 64–90) and semiautomated digital microscopy (77%; 95% CI: 60–91) were similar.

6.4. DISCUSSION

In this study, the performance of the Schistoscope 5.0 was evaluated as a semiautomated digital microscope and as an AI-based fully automated digital microscope for the detection and quantification of *S. haematobium* eggs in a field setting. The diagnostic parameters that were assessed include sensitivity, specificity, PPV, NPV, and infection intensity. At baseline screening, the sensitivity of the semiautomated digital microscope (80.1%) was lower than that of the fully automated digital microscope (87.3%); however, this difference was not statistically significant. As expected, the sensitivity of the Schistoscope increased with increasing egg excretion. On the other hand, the Schistoscope detected additional cases as positive, which might have been true cases missed by conventional microscopy. Conventional microscopy was used as the standard reference, and this resulted in a reduced specificity of the Schistoscope. The specificity was significantly lower for the fully automated digital microscope (48.9%) than for the semiautomated digital microscope (95.3%).

A probable reason for the low specificity recorded by the fully automated digital microscope is the limited datasets used to train the AI algorithm to detect *S. haematobium* eggs. The AI algorithm was developed using two training datasets consisting of images obtained from egg-spiking experiments resulting in relatively clean samples and a limited number of field samples that did not contain many egg-like artifacts (e.g., uric crystals). Therefore, the AI algorithm seemed insufficiently trained to separate egg-like artifacts from *S. haematobium* eggs. Another reason could be limitations in the deep learning model used by the AI algorithm that was optimized for enhanced sensitivity at a trade-off of specificity. Additional iterations to enhance specificity are therefore needed and are currently in progress.

Several other studies have also field evaluated digital optical devices, with or without AI, for the detection and/or quantification of *S.*

haematobium eggs [9, 11, 12]. The sensitivities and specificities obtained for the various devices in these studies, with conventional microscopy as a reference, range from 35.6% to 81.1% and 91.0% to 100%, respectively. The sensitivities of the semi- and fully automated digital microscope reported in the current study were generally higher compared with previous reports, except for results reported by Coulibaly *et al.* [12], for the Newton Nm1 microscope, which is considered comparable in sensitivity. However, the study by Coulibaly *et al.* [12] had a slightly lower power than our study, with 266 samples examined, of which 90 were egg positive.

For egg count estimates, a strong correlation was observed between semiautomated digital microscopy and conventional microscopy, whereas for fully automated digital microscopy, a clear underestimation of the intensity of infection was observed for samples with more than 100 eggs/10 mL urine. A possible explanation is that overlapping eggs were recognized as a single egg by the deep learning model, leading to an underestimation of egg counts. In addition, hematuria might have also caused interference. Although not systematically recorded, our impression was that samples with more than 100 eggs/10 mL of urine were often strongly positive for hematuria, with an abundance of blood cells compared with samples with lower egg counts. This could have resulted in shading the eggs on the filter membrane and subsequently limiting the detection by the AI algorithm.

Although only performed in a small subset of cases and at one time point, no substantial differences were noticed before and after treatment when comparing the semiautomated digital microscope with the conventional microscopy, suggesting that the Schistoscope could also be used for monitoring treatment. More extensive posttreatment follow-up studies are needed to demonstrate how well the Schistoscope can differentiate viable *S. haematobium* eggs from dead eggs, which can be excreted up to many weeks after receiving praziquantel (personal observation).

The Schistoscope 5.0 captured high-resolution images that clearly show the specific features of *S. haematobium* and *S. mansoni* eggs (i.e., the terminal and lateral spines; fig. 6.1C). In terms of potential use-cases, this supports the application of the semiautomated microscope as a diagnostic tool to assist microscopists in field laboratory settings. The use of (semi-)automated digital microscopy could reduce visual health complications caused by high eye exposure to a conventional microscope light source. Upon further development to improve the AI, the fully automated microscope would be useful for nonexpert microscopists as well (e.g., community health workers and laboratory technicians). In both cases, task shifting could be gained because personnel could focus on other activities while the device analyzes samples. The added value of task shifting could compensate for the

current time difference between conventional microscopy that requires less than 10 minutes to scan a urine filter and the Schistoscope 5.0, which can take on average 17 minutes to complete scanning and analysis.

Limitations of this study include the choice of conventional light microscopy on a single 10 mL urine sample as the reference test, which is known for its limited sensitivity, especially in cases with low infection intensity. Further evaluation studies should be conducted to field validate the Schistoscope 5.0 for the detection of *S. haematobium* eggs compared with more sensitive reference tests such as the detection of adult worm-associated circulating anodic antigens or the detection of parasite specific DNA [25]. The Schistoscope 5.0 currently does not meet the target product profile set by the WHO for new diagnostics needed for monitoring and evaluating schistosomiasis control programs [26]. For example, it does not have an onboard display and is connected to a computer monitor for visual control of the device, thus making transportation impractical. Furthermore, the device lacks a backup power supply. Additional functionalities such as an onboard computer with a graphical processing unit for higher image processing capabilities and internet access would also be beneficial. These functionalities would create the capacity to generate results in real time for patient management, store and share digital images with other experts, and facilitate mapping of schistosomiasis [27], thereby making (semi-)automated digital devices an attractive tool for future use in epidemiology and public health settings. Here we evaluated the Schistoscope 5.0 for the first time in a rural field setting, demonstrating its potential as a digital diagnostic tool for the detection and quantification of *S. haematobium* eggs, as well as for monitoring the effect of schistosomiasis treatment in settings with limited resources.

ACKNOWLEDGEMENTS

We acknowledge the staff of the FCT Public Health Department and Neglected Tropical Diseases (NTD) Department of the Federal Ministry of Health Abuja; the Area Council authorities/NTD coordinators and focal persons; and the community leaders and community members in the FCT Area Councils who were assessed in the study.

REFERENCES

[1] World Health Organization. “Schistosomiasis and soil-transmitted helminthiases: progress report, 2021”. In: *Weekly Epidemiological Record* 97.48 (2022), pp. 621–632. url: https://www.who.int/publications/i/item/who-wer9748-621-632.

[2] O. P. Aula, D. P. McManus, M. K. Jones, and C. A. Gordon. “Schistosomiasis with a focus on Africa”. In: *Tropical Medicine and Infectious Disease* 6.3 (2021), p. 109. doi: 10.3390/tropicalmed6030109.

[3] D. P. McManus, D. W. Dunne, M. Sacko, J. Utzinger, B. J. Vennervald, and X. N. Zhou. “Schistosomiasis”. In: *Nature Reviews Disease Primers* 4.1 (2018), p. 13. doi: 10.1038/s41572-018-0013-8.

[4] A. L. Bustinduy, B. Randriansolo, A. S. Sturt, S. A. Kayuni, P. D. C. Leustcher, B. L. Webster, L. V. Lieshout, J. R. Stothard, H. Feldmeier, and M. Gyapong. “An update on female and male genital schistosomiasis and a call to integrate efforts to escalate diagnosis, treatment and awareness in endemic and non-endemic settings: the time is now”. In: *Advances in Parasitology* 115 (2022), pp. 1–44. doi: 10.1016/bs.apar.2021.12.003.

[5] World Health Organization. *Ending the Neglect to Attain the Sustainable Development Goals—A Road Map for Neglected Tropical Diseases 2021–2030*. World Health Organization, 2020. isbn: 9789240010352. url: https://iris.who.int/handle/10665/338565.

[6] R. Ngakhushi, R. Kaiti, S. Bhattarai, and G. Shrestha. “Prevalence of myopia and binocular vision dysfunctions in microscopists”. In: *International Eye Science* 18 (2018), pp. 1180–1183. doi: 10.3980/j.issn.1672-5123.2018.7.03.

[7] I. Söderberg, B. Calissendorff, S. Elofsson, B. Knave, and K. G. Nyman. “Investigation of visual strain experienced by microscope operators at an electronics plant”. In: *Applied Ergonomics* 14.4 (1983), pp. 297–305. doi: 10.1016/0003-6870(83)90010-8.

[8] H. C. Koydemir, J. T. Coulibaly, D. Tseng, I. I. Bogoch, and A. Ozcan. “Design and validation of a wide-field mobile phone microscope for the diagnosis of schistosomiasis”. In: *Travel medicine and infectious disease* 30 (2019), pp. 128–129. doi: 10.1016/j.tmaid.2018.12.001.

[9] I. I. Bogoch, J. T. Coulibaly, J. R. Andrews, B. Speich, J. Keiser, J. R. Stothard, E. K. N’goran, and J. Utzinger. “Evaluation of portable microscopic devices for the diagnosis of Schistosoma and soil-transmitted helminth infection”. In: *Parasitology* 141.14 (2014), pp. 1811–1818. doi: 10.1017/S0031182014000432.

[10] I. I. Bogoch, H. C. Koydemir, D. Tseng, R. K. D. Ephraim, E. Duah, J. Tee, J. R. Andrews, and A. Ozcan. “Evaluation of a mobile phone-based microscope for screening of Schistosoma haematobium infection in rural Ghana”. In: *American Journal of Tropical Medicine and Hygiene* 96.6 (2017), pp. 1468–1471. doi: 10.4269/ajtmh.16-0912.

[11] R. K. D. Ephraim, E. Duah, J. S. Cybulski, M. Prakash, M. V. D’Ambrosio, D. A. Fletcher, J. Keiser, J. R. Andrews, and I. I. Bogoch. “Diagnosis of Schistosoma haematobium infection with a mobile phone-mounted Foldscope and a reversed-lens CellScope in Ghana”. In: *American Journal of Tropical Medicine and Hygiene* 92.6 (2015), pp. 1253–1256. doi: 10.4269/ajtmh.14-0741.

[12] J. T. Coulibaly, M. Ouattara, M. V. D’Ambrosio, D. A. Fletcher, J. Keiser, J. Utzinger, E. K. N’Goran, J. R. Andrews, and I. I. Bogoch. “Accuracy of mobile phone and handheld light microscopy for the diagnosis of schistosomiasis and intestinal protozoa infections in Côte d’Ivoire”. In: *PLoS Neglected Tropical Diseases* 10.6 (2016), e0004768. doi: 10.1371/journal.pntd.0004768.

[13] O. Holmström, N. Linder, B. Ngasala, A. Mårtensson, E. Linder, M. Lundin, H. Moilanen, A. Suutala, V. Diwan, and J. Lundin. “Point-of-care mobile digital microscopy and deep learning for the detection of soil-transmitted helminths and *Schistosoma haematobium*”. en. In: *Global Health Action* 10.sup3 (June 2017), p. 1337325. doi: 10.1080/16549716.2017.1337325.

[14] T. Agbana, P. Nijman, M. Hoeber, D. van Grootheest, A. van Diepen, L. van Lieshout, J. C. Diehl, M. Verhaegen, and G. Vdovine. “Detection of Schistosoma haematobium using lensless imaging and flow cytometry, a proof of principle study”. In: *Proceedings of the Optical Diagnostics and Sensing XX: Toward Point-of-Care Diagnostics*. Vol. 11247. 2020, 112470F. doi: 10.1117/12.2545220.

[15] E. Linder, A. Grote, S. Varjo, N. Linder, M. Lebbad, M. Lundin, V. Diwan, J. Hannuksela, and J. Lundin. “On-chip imaging of Schistosoma haematobium eggs in urine for diagnosis by computer vision”. In: *PLoS Neglected Tropical Diseases* 7.12 (2013), e2547. doi: 10.1371/journal.pntd.0002547.

[16] T. Agbana, G. Y. Van, O. Oladepo, G. Vdovin, W. Oyibo, and J. C. Diehl. “Schistoscope: Towards a locally producible smart diagnostic device for Schistosomiasis in Nigeria”. In: *2019 IEEE Global Humanitarian Technology Conference (GHTC)*. Seattle, WA, USA, 2019, pp. 1–8. doi: 10.1109/GHTC46095.2019.9033049.

[17] J. C. Diehl, P. Oyibo, T. Agbana, S. Jujjavarapu, G. Van, G. Vdovin, and W. Oyibo. “Schistoscope: Smartphone versus Raspberry Pi based low-cost diagnostic device for urinary Schistosomiasis”. In: *Proceedings of the 2020 IEEE Global Humanitarian Technology Conference (GHTC)*. Seattle, WA, USA, 2020, pp. 1–8. doi: 10.1109/GHTC46280.2020.9342871.

[18] P. Oyibo, S. Jujjavarapu, B. Meulah, T. Agbana, I. Braakman, A. van Diepen, M. Bengtson, L. van Lieshout, W. Oyibo, G. Vdovine, and J. C. Diehl. “Schistoscope: An Automated Microscope with Artificial Intelligence for Detection of Schistosoma haematobium Eggs in Resource-Limited Settings”. In: *Micromachines* 13.5 (2022), p. 643. doi: 10.3390/mi13050643.

[19] G. A. Amuga, O. J. Nebe, F. O. Nduka, N. N., D. A. Dakul, S. Isiyaku, E. Ngige, S. Jibrin, S. M. Jacob, I. A. Nwoye, U. Nwankwo, R. Urude, S. M. Aliyu, A. Garba, W. Adamani, C. O. Nwosu, I. A. Anagbogu, R. Dixon, A. clark, and G. O. Adeoye. “Schistosomiasis: epidemiological factors enhancing transmission in Nigeria”. In: *Global Research Journal of Public Health and Epidemiology* 8.7 (2020), pp. 023–032.

[20] A. Pinto-Almeida, T. Mendes, R. N. de Oliveira, S. A. P. Corrêa, S. M. Allegretti, S. Belo, A. Tomás, F. F. Anibal, E. Carrilho, and A. Afonso. “Morphological characteristics of Schistosoma mansoni PZQ-resistant and -susceptible strains are different in presence of Praziquantel”. In: *Frontiers in Microbiology* 7 (2016), p. 00594. doi: 10.3389/fmicb.2016.00594.

[21] F. Richards Jr, J. Sullivan, E. Ruiz-Tiben, M. Eberhard, and H. Bishop. “Effect of praziquantel on the eggs of Schistosoma mansoni, with a note on the implications for managing central nervous system schistosomiasis”. In: *Annals of Tropical Medicine and Parasitology* 83.5 (1989), pp. 465–472. doi: 10.1080/00034983.1989.11812373.

[22] K. C. Kosinski, K. M. Bosompem, M. J. Stadecker, A. D. Wagner, J. Plummer, J. L. Durant, and D. M. Gute. “Diagnostic accuracy of urine filtration and dipstick tests for Schistosoma haematobium infection in a lightly infected population of Ghanaian school children”. In: *Acta Tropica* 118.2 (2011), pp. 123–127. doi: 10.1016/j.actatropica.2011.02.006.

[23] S. R. Jones, S. Carley, and M. Harrison. “An introduction to power and sample size estimation”. In: *Emergency Medicine Journal* 20.5 (2003), pp. 453–458. doi: 10.1136/emj.20.5.453.

[24] M. L. McHugh. “Interrater reliability: the kappa statistic”. In: *Biochemia Medica (Zagreb)* 22.3 (2012), pp. 276–282.

[25] P. T. Hoekstra, G. J. van Dam, and L. van Lieshout. “Context-specific procedures for the diagnosis of human schistosomiasis – a mini review”. In: *Frontiers in Tropical Diseases* 2 (2021), p. 722438. doi: 10.3389/fitd.2021.722438.

[26] World Health Organization. *Public consultation: Target Product Profiles for diagnostic tests to meet Schistosomiasis and soil-transmitted Helminth programme needs*. 2021. url: https://www.who.int/news-room/articles-detail/public-consultation-target-product-profiles-for-diagnostic-tests-to-meet-schistosomi and-soil-transmitted-helminth-programme-needs (visited on 03/17/2022).

[27] I. I. Bogoch, J. Lundin, N. C. Lo, and J. R. Andrews. “Mobile phone and handheld microscopes for public health applications”. In: *The Lancet Public Health* 2.8 (2017), e355. doi: 10.1016/S2468-2667(17)30120-2.

7

AUTOMATED UROGENITAL SCHISTOSOMIASIS DIAGNOSIS

Two-stage automated diagnosis framework for urogenital schistosomiasis in microscopy images from low-resource settings

Prosper Oyibo. Brice Meulah, Michel Bengtson, Lisette van Lieshout, Wellington Oyibo, Jan-Carel Diehl, Gleb Vdovine, Tope Agbanaa

PUBLICATION REPORT

- **Publication Date:** 7 August 2023
- **Journal:** Journal of Medical Imaging
- **Publisher:** SPIE
- **DOI:** 10.1117/1.JMI.10.4.044005

ABSTRACT

PURPOSE

Automated diagnosis of urogenital schistosomiasis using digital microscopy images of urine slides is an essential step toward the elimination of schistosomiasis as a disease of public health concern in Sub-Saharan African countries. We create a robust image dataset of urine samples obtained from field settings and develop a two-stage diagnosis framework for urogenital schistosomiasis.

APPROACH

Urine samples obtained from field settings were captured using the Schistoscope device, and S. haematobium eggs present in the images were manually annotated by experts to create the SH dataset. Next, we develop a two-stage diagnosis framework, which consists of semantic segmentation of S. haematobium eggs using the DeepLabv3-MobileNetV3 deep convolutional neural network and a refined segmentation step using ellipse fitting approach to approximate the eggs with an automatically determined number of ellipses. We defined two linear inequality constraints as a function of the overlap coefficient and area of a fitted ellipses. False positive diagnosis resulting from over-segmentation was further minimized using these constraints. We evaluated the performance of our framework on 7605 images from 65 independent urine samples collected from field settings in Nigeria, by deploying our algorithm on an Edge AI system consisting of Raspberry Pi + Coral USB accelerator.

RESULT

The SH dataset contains 12,051 images from 103 independent urine samples and the developed urogenital schistosomiasis diagnosis framework achieved clinical sensitivity, specificity, and precision of 93.8%, 93.9%, and 93.8%, respectively, using results from an experienced microscopist as reference.

CONCLUSION

Our detection framework is a promising tool for the diagnosis of urogenital schistosomiasis as our results meet the World Health Organisation target product profile requirements for monitoring and evaluation of schistosomiasis control programs.

7.1. INTRODUCTION

Schistosomiasis is endemic in 76 countries worldwide with approximately 252 million people infected and an estimated 779 million people at risk of infection [1]. Schistosomiasis is caused by blood flukes of the genus *Schistosoma* (S); both *S. mansoni* (intestinal schistosomiasis) and *S. haematobium* (urogenital schistosomiasis) are endemic in Africa [2]. Schistosomiasis presents a substantial public health and economic burden as it is a disease of poverty. In the drive to attain the World Health Organisation (WHO) control and elimination targets, diagnosis for adequate monitoring of interventions and surveillance is critical [2, 3]. Recently, the WHO published the diagnostic target product profiles (TPP) for monitoring, evaluation, and surveillance of schistosomiasis control programs [4], which identifies development of diagnostic tests for *S. haematobium* detection as a high-risk requirement due to lack of its availability. The TPP suggests a semi-quantitative analysis, capable of providing some degree of information regarding intensity of infection, as ideal for a diagnostic test for schistosomiasis to support monitoring and evaluation [4]. Currently, microscopy is the WHO reference standard for the diagnosis of schistosomiasis in resource-limited settings. For the detection of *S. haematobium* infection, urine samples, after filtration, sedimentation, or centrifugation, are microscopically examined for the presence of eggs [3]. This method is operator dependent, costly, laborious, and time-consuming. Furthermore, it requires expertise, which means microscopy skills need to be gained and maintained, which can be an economic challenge, particularly in remote rural communities [3]. There is also the risk of visual health complications among microscopists resulting from excessive workload due to the low ratio of trained microscopists to samples for analysis in endemic regions [5]. Hence, a field adaptable, rapid, and easy-to-use automated diagnosis is relevant for the prompt detection of cases, which will facilitate mapping and monitoring of interventions [4]. Recent advances in opto-mechanics and opto-electronics have rapidly transformed the field of biomedical optics. Optical imaging technologies, such as conventional light microscopes, are being redesigned to integrate and miniaturize portable light microscopes for use at the point of care [6–10]. Although these technologies are readily available in high-income countries, unfortunately, nearly all schistosomiasis cases are seen in low-resource regions of low-income countries, significantly justifying the need for cost-effective and easy-to-use smart diagnostic technologies. In this work, we address these challenges by first increasing the size of the *S. haematobium* (SH) dataset in our previous work [10] from 5198 to 12,051 images of clinical samples [11]. We carry out detection and counting of *S. haematobium* eggs present in each image by proposing a two-stage framework consisting of a DeepLabv3 with MobilenetV3 backbone deep convolutional neural network [12] trained on the SH

dataset using a transfer learning approach. The second stage of our proposed framework is a refined segmentation and egg counting procedure, which adapts the region-based fitting of overlapping ellipses [13] to efficiently separate the boundaries of overlapping eggs in the image. Finally, the detected isolated eggs are screened for the presence of an egg, which meets the defined boundary condition before the sample can be determined as positive/negative diagnosis. We further demonstrate the robustness and applicability of the proposed framework for field diagnoses of urogenital schistosomiasis by implementing our framework on an Edge AI system (Raspberry Pi + Coral USB accelerator) and testing 65 clinical urine samples obtained in a field settings in Nigeria. The main contributions of this work can be summarized as follows.

1. A large-scale *S. haematobium* egg dataset of 12,051 images captured in field settings is created with respective manually annotated mask images. The dataset contains images with artifacts, such as crystals, glass debris, air bubbles, and fibres.

2. A *S. haematobium* egg detection framework consisting of the DeepLabv3 with MobileNetV3 backbone deep convolutional neural network, trained using transfer learning approach for semantic segmentation of the eggs. This effectively segments transparent eggs in noisy images taken in the field. The framework also separates overlapping eggs using a refined segmentation algorithm resulting in a more accurate egg count.

3. The implementation and testing of the *S. haematobium* egg on an Edge AI system to demonstrate its field applicability for the diagnosis of schistosomiasis in low-resource settings.

7.2. RELATED WORK

A pioneering study on the identification and classification of human helminth eggs based on computer vision algorithms was carried out by Yang *et al.* [14]. However, their focus was on helminth eggs found in microscopic faecal samples. Subsequent works [15–18] included the detection of *S. haematobium* eggs found in urine but only in images pre-captured by professional clinical operators mostly with isolated and non-overlapping eggs in the field of view (FoV) images. Regarding the detection of *S. haematobium* eggs in microscopy images of urine from field settings, these images contain many artifacts with morphological and textural similarity to eggs, such as crystals, glass debris, air bubbles, fabric fibres, and human hair. This makes it difficult to achieve high accuracy using traditional AI methods, which detect objects in the images based on some threshold value or discontinuous local features

of an image. The *S. haematobium* eggs are oval-shaped structures (110-170 μm long and 40-70 μm wide) with a thick transparent capsule and a sword-shaped protrusion known as the terminal spine located at the narrow end of the egg. Detecting an egg is challenging due to its similar appearance to its surroundings. Automated detection of an isolated *S. haematobium* egg by thresholding the cross-correlation coefficient of two sets of invariant moments for both a reference and sample image was performed by Hassan and Al-Hity [19]. However, this method had poor performance in noisy images and hence cannot be used for *S. haematobium* eggs detection in field settings.

Recently, deep learning algorithms were used by Armstrong *et al.* [20] to solve the challenges of *S. haematobium* egg detection in images captured in field settings. Using transfer learning, they compared RetinaNet [21], MobileNet [22], and EfficientDet [23] architectures pre-trained on the COCO 2017 dataset [24]. They retained the feature extraction layers and fine-tuned the dense layers of these models to detect *S. haematobium* eggs as a single class. The RetinaNet architecture had improved egg detection performance with egg counts closely related to manual egg counts obtained by a trained user. It was also able to detect isolated eggs and reject other debris from a crowded FoV. However, air bubbles were incorrectly classified as eggs, and the automated detection of eggs aggregated in large clumps with other eggs or debris remained a challenge. In our previous work, we developed a low-cost automated digital microscope (Schistoscope V5.0) with AI for the detection *S. haematobium* eggs [10], and we reported the results from a field validation study in Nigeria [11]. A U-Net model [25] trained with the *S. haematobium* dataset consisting of 5198 images captured from both clinical and spiked urine samples was used for automated egg detection. Although we achieved a high diagnostic sensitivity of 87.3%, the diagnostic specificity was low (48.9%). This was due to the high number of false positives by the U-Net architecture and the inability of the segmented pixel area-based linear model to filter out incorrectly segmented eggs while counting.

All these studies show that deep learning is a promising approach for the automated diagnosis of urogenital schistosomiasis. However, developing a model that is field applicable requires a robust dataset of images with varying degrees of urine artifacts from field settings. Also the separation of overlapping eggs for improved estimation of infection intensity has remained a challenge. This paper proposes a two-stage framework to solve these challenges.

7.3. METHODS

To meet the WHO TPP requirements for a diagnostic test for schistosomiasis, the proposed urogenital schistosomiasis diagnostic framework

consists of two stages (fig. 7.1). The first stage involves the semantic segmentation of candidate *S. haematobium* eggs in captured images. The segmentation results are further refined in the second stage by ellipse fitting and morphological filtering of the segmented regions. The two-stage framework minimizes false positive detection that enables a high diagnostic specificity, which is a requirement for diagnostic tools for monitoring and evaluation of schistosomiasis control programs and determining transmission interruption.

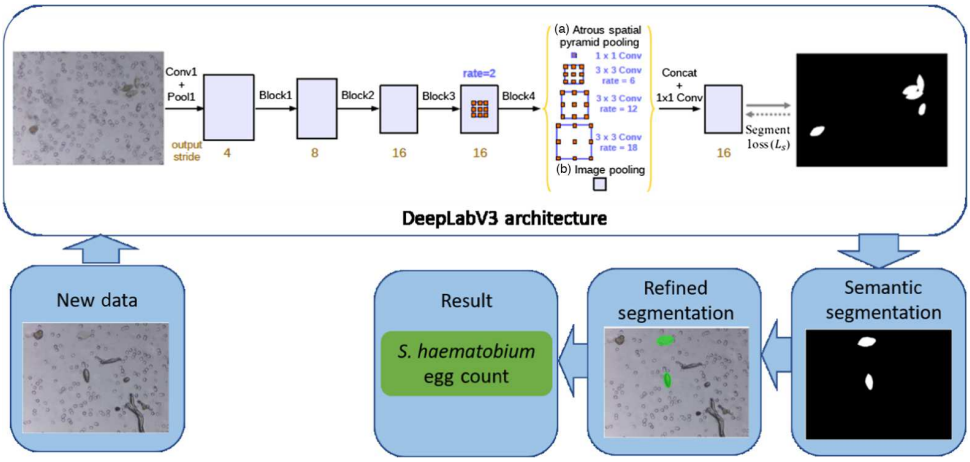

Figure 7.1: Schematics of the proposed two-stage diagnosis framework urogenital schistosomiasis with DeepLabV3-MobileNetV3 deep learning architecture for semantic segmentation of eggs and refined segmentation for overlapping eggs separation and count.

7.3.1. SAMPLE IMAGE CAPTURE AND *S. haematobium* EGG ANNOTATION

The details of the Schistoscope's mechanical precision and optical quality are described in our previous work [10]. The Schistoscope optical system consists of a 4× magnification microscope objective and a Raspberry Pi High-Quality Camera Module V2.1 equipped with a Sony IMX477R camera sensor. The camera sensor has a pixel-pitch of 1.55 µm and registers an image size of 2028 × 1520 pixels. The device consists of an autofocusing and an automated slide scanning system. For urine filtration, we made use of a 13 mm filter membrane, which results in 117 image grid segments per sample when scanned by the device. The *S. haematobium* eggs in the captured images used for training and development testing were manually annotated by an

expert parasitologist using the coco annotator tool [26]. The annotation process is highlighted as follows.

1. Annotation of the exact boundary pixels of the *S. haematobium* eggs was not strictly enforced due to the limitation posed by the size of the eggs.

2. The pixel values of the filter membrane and artifacts in the ground-truth image were labeled as “0” (background) and the eggs as “1” (foreground).

3. There were few *S. mansoni* eggs found in the images of the clinical urine samples and their pixel values were labeled as “1” (foreground).

4. Pixels of partially cut eggs at the edges of the images were labeled as “1” (foreground).

5. The region of the eggs covered by artifacts was labeled as “0” (background).

7.3.2. Stage 1: Semantic segmentation of S. haematobium eggs

Transfer learning using DeepLabv3-MobileNetv3

In transfer learning, a model trained on one task is repurposed to another related task, usually by some adaptation toward the new task. This approach is mainly useful for tasks where enough training samples are not available to train a model from scratch, such as medical image classification for neglected tropical diseases or emerging diseases [27]. To overcome the limited data sizes, transfer learning was used to retrain the DeepLabv3-MobileNetV3[12] model for semantic segmentation of candidate *S. haematobium* eggs using the SH dataset. DeepLabv3 is a semantic segmentation architecture that was developed to handle the problem of segmenting objects at multiple scales. Modules are designed, which employ atrous convolution in cascade or in parallel to capture multi-scale context by adopting multiple atrous rates. We initialize the model with weights obtained from the pre-trained model on a subset of COCO train2017, on the 20 categories that are present in the Pascal VOC dataset [28]. Since our case consists of two output classes (background and foreground), we replace the 21-output channel convolutional layer with a single output-channel convolutional layer. The weights of all layers of the model are then updated during the training stage.

LOSS FUNCTION

The model was trained using the Dice similarity coefficient (DSC) loss function [29], which is widely used in medical image segmentation tasks to address the data imbalance problem between foreground and background:

$$L_{DSC} = \frac{2\sum_{x,y}(S_{i,x,y} \times G_{i,x,y})}{\sum_{x,y} S_{i,x,y}^2 + \sum_{x,y} G_{i,x,y}^2} \tag{7.1}$$

Where $S_{i,x,y}$ and $G_{i,x,y}$ refer to the value of pixel (x, y) in the segmentation result S_i and ground truth G_i respectively.

7.3.3. STAGE 2: REFINED SEGMENTATION OF S. haematobium EGGS

To solve the challenge of obtaining accurate egg counts in the occurrence of false positives or overlapping and clustered eggs, we adopted a refined segmentation procedure, which involves fitting ellipses over the region of interest in the binary output image of the semantic segmentation. The refined segmentation algorithm as shown in algorithm 1 operates in a number of steps, which can be summarized as follows.

Algorithm 1: The Refined Segmentation Algorithm

Input: Binary segmentation mask image I
Output: Set of Ellipse E_I^*, Egg Count N_I^*
$N_I^* = 0$
$E_I^* = \emptyset$
for each region image $R \in I$ **do**
  $N_R^* = 0$
  $E_R^* = \emptyset$
  $AIC_R^* = \infty$
  $N_{lb}, N_{ub} = ComputeBoundary(A_R)$
  $N_R = N_{lb}$
  repeat
    $E_R = FitEllipse(R, N_R)$
    $AIC_R = ComputeAIC(R, U_E)$
    if $AIC_R < AIC_R^*$ **then**
      $N_R^* = N_R$
      $AIC_R^* = AIC_R$
      $E_R^* = E_R$
    $N_R = N_R + 1$
  until $N_R = N_{ub}$
  $E_I^* = union(E_I^*, E_R^*)$
  $N_I^* = N_I^* + N_R^*$
end
return N_I^*, E_I^*

Legend
I: Binary segmentation mask image
E_I^*: Optimal set of ellipses for I
N_I^*: Optimal number of ellipses for I
R: Segmented egg region image
N_R^*: Optimal number of ellipses for R
E_R^*: Optimal set of ellipses for R
AIC_R^*: Optimal Akaike Information Criterion for R
N_{lb}: Lower boundary for N
N_{ub}: Upper boundary for N

OPTIMIZATION PROBLEM FORMULATION

We assume a binary image I that represents the segmentation mask output of the DeepLabV3-MobileNetV3 deep neural network model. The binary image may contain one or more sliced binary region image R which has the same size as the bounding box. This region image R represents a segmented isolated or overlapping eggs. A pixel p of R belongs to either the foreground FG ($R(p) = 1$) or the background BG ($R(p) = 0$). The area A_R of the segmented egg is given by:

$$A_R = \sum_{p \in FG} R(p) \tag{7.2}$$

We also assume a set E_R of N_R ellipses are fitted over the region image R. The binary image U_E is defined such that $U_E(p) = 1$ at point p that is inside any of the ellipse $E_{R,i}$; otherwise $U_E(p) = 0$. Also, we define the coverage $\alpha(E_r)$ of the segmented eggs by the given set of ellipses E_R as:

$$\alpha(E_r) = \frac{1}{A_R} \sum_{p \in FG} R(p) U_E(p) \tag{7.3}$$

Essentially $\alpha(E_r)$ is the percentage of the segmented eggs that are under some of the ellipse in E_R. Let the sum of the areas of all the ellipses be denoted by $|E_R| = \sum_(i = 1)|E_{R,i}|$ and let $C(E_R)$ denote the coverage area by all the ellipses:

$$C(E_R) = \sum_{p \in R} U_E(p) \tag{7.4}$$

It should be stressed that $C(E_R) < |E_R|$, with the equality holding in the case that all ellipses are pairwise disjoint. This is because in case of two overlapping ellipses, $|E_R|$ counts the area of their intersection two times, while $C(E_R)$ does not. Similar to the work of Panagiotakis and Argyros [13], we want to maximize the shape coverage $\alpha(E_R^*)$ with a set of ellipses E_R^* whose covered area by all ellipses $C(E_R^*)$ is as close as possible to A_R:

$$E_R^* = \arg\max_{E_R} \alpha(E_r) \quad s.t. \quad C(E_R) = A_R \tag{7.5}$$

We defined a model complexity measure the ratio of the area A_R of the segmented region to experimentally observed average area of segmented isolated egg A_R^*.

$$C = \frac{A_R}{A_R^*} \tag{7.6}$$

To estimate the optimal number N_R^* of ellipses in a segmented egg region image R, a trade-off between the egg coverage $\alpha(E_r)$ and the model complexity C, is optimised by employing the Akaike Information Criterion (AIC) [30]. The AIC-based model selection criterion amounts to the minimization of the quantity [13]:

$$AIC_R = C \ln(1 - \alpha(E_r)) + 2N_R \tag{7.7}$$

This minimises the error in egg count as intuitively the complexity is proportional to the area of the segmented eggs.

EXTRACTING SEGMENTED EGG REGIONS

First, connected components in the binary segmentation mask image are extracted and binary region image R which has the same size as bounding box of the connected component is created. If area A_R of the region image (i.e. the number of pixels in the segmented egg region) is less than the defined area threshold A_th, then the detected region is classified as noise; otherwise we solve for the optimal number of ellipses as described in the next section.

INITIALIZING ELLIPSES SOLUTIONS

For defined number N_R of ellipses in a segmented egg region image R, we initialise the ellipse hypotheses using k-means clustering this defines a set E_R of clusters which are circular in shape with hard cut-off borders where each pixel is strictly allocated to one cluster. The cluster centres are the mean vector of the points belonging to the respective cluster, while the diameters are the maximum Euclidian distances of the cluster members from their respective cluster centres.

OPTIMIZING ELLIPSES SOLUTIONS

To obtain a more complex, ellipsoid shapes with soft cut-off borders (i.e., overlapping ellipses) which closely describes the shape of *S. haematobium* eggs, the ellipse hypotheses is evolved using the Gaussian Mixture Model Expectation Maximization (GMM-EM) algorithm to finetune the parameters of the initialised set E_R of clusters with the best coverage $\alpha(E_r)$ of the given segmented egg region. This is achieved by Expectation-Step and the Maximisation-Step iteratively of the GMM-EM algorithm. The log likelihood function is maximized until the GMM-EM algorithm converges. A detailed explanation of the GMM-EM algorithm can be found in the works of Bishop [31] and Mitchell [32].

SOLVING FOR THE OPTIMAL NUMBER OF ELLIPSES

Different models (i.e., solutions involving different numbers N_R of ellipses) for a segmented egg image region are evaluated based on the AIC criterion [defined in equation (7.7)] that balances the trade-off between model complexity and approximation error. To minimize AIC_R, the refined segmentation algorithm increments the number of candidate ellipses, N_R, starting from a lower boundary, $N_lb = 0.6ceil(C)$,with a step size of 1. At each value of N_R, the set E_R of clusters is first initialised by k-means clustering (described in section 7.3.3) and then evolved using the GMM-EM algorithm (described in section 7.3.3). This process continues until N_R is equal to the upper boundary, $N_ub = 1.1ceil(C)$. In each iteration, the AIC_R criterion is computed. The lower and

upper boundaries of the number of ellipses are formulated using the complexity measure C, derived from prior knowledge about the average pixel area of the *S haematobium* eggs. This helps to reduce the search space for the optimal number of ellipses. From all possible models (involving from N_lb to N_ub), the refined segmentation algorithm reports as the optimal solution as the set of ellipses E_R^* with the minimum AIC_R.

MORPHOLOGICAL FILTERING OF DETECTED ISOLATED EGGS

To reduce these false positives diagnosis caused by pixels of artifacts such as crystals wrongly segmented as isolated egg, we introduced two linear inequality constraints which are functions of the area of the detected ellipse $|E_R|$ and Overlap coefficient $OC(R, U_E)$ defined by the following ratio:

$$OC(R, U_E) = \frac{R \cap U_E}{\min(R, U_E)} \tag{7.8}$$

These inequality constraints are derived experimentally and only applied to segmented regions with a single fitted ellipse for determination of diagnosis result. This improves the specificity of the algorithm by accepting only regions that fall within an experimentally defined boundary region as candidate *S. haematobium* eggs while discarding the others as a false positive prediction.

7

7.4. DATASET AND IMPLEMENTATION DETAILS

7.4.1. DATASET DESCRIPTION

A total of 103 captured urine samples were used for the creation of the SH dataset. The SH dataset was used for training and development testing of the DeepLabV3-MobileNetV3 deep neural network model, while a separate set of 65 captured urine samples referred to as diagnosis test dataset was used for testing the developed framework for urogenital schistosomiasis diagnosis. The images were captured from urine samples collected in a rural area in central Nigeria with the Schistoscope V5.0 [11]. The size of the captured images are 1520× 2028 pixels. The details of the sample collection and preparation process are described in our previous works [10, 11]. The procedure followed in capturing and annotation of the *S. haematobium* eggs in images is described in section 7.3.1. A summary of the SH image dataset is shown in table 7.1. It consists of 12,051 images of clinical urine samples and their respective mask images. There are 17,799 annotated *S. haematobium* eggs in 2,997 captured FoV images., The dataset consists of images that are easy to identify eggs (fig. 7.2) without the presence of artifacts in the background, as well as images that are difficult to analyse (fig. 7.3) with backgrounds containing artifacts such as crystals,

glass debris, air bubbles, fabric fibres and human hair which makes egg identification difficult. The SH dataset is split into 80% (9641 images) and 20% (2410 images) for training and development testing respectively. To our best knowledge, this SH dataset is the largest robust dataset focused on *S. haematobium* egg images captured in a field setting.

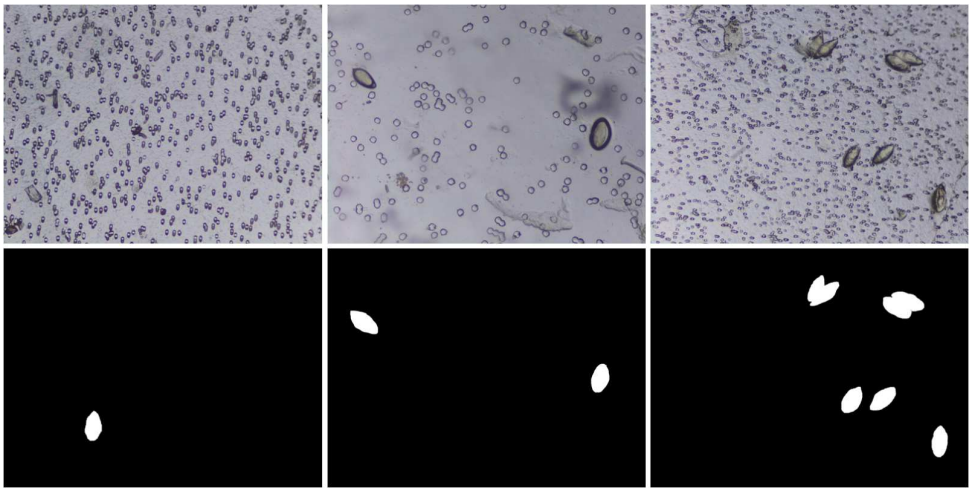

Figure 7.2: Example of sample images that are easy-to-identify eggs having glass slides and filter membranes as background and their respective ground truth images.

7.4.2. IMPLEMENTATION DETAILS

The training of the DeepLabv3-MobileNetV3 model was performed using the Pytorch framework [33] on NVIDIA A100-SXM4-40GB GPU. All images were pre-processed by centring and normalizing the pixel density per channel. We fine-tuned the model for 100 epochs. The batch size is set to 8, and ADAM optimizer is used to optimize the Dice loss function, with an initial learning rate of $1e-4$. We employ a "poly" learning rate policy [12] where the initial learning rate is multiplied by $(1-iter/(max_iter))^{power}$ with $power = 0.9$. All images were down sampled to 507×676 before being fed to the neural network.

To demonstrate the field applicability of the two-stage framework in low-resource settings, we performed the development testing and diagnosis testing on a Raspberry Pi 4 model B using a Coral USB accelerator. To perform semantic segmentation on the Edge AI system, we converted the DeepLabv3-MobileNetV3 model from Pytorch to tensorflow lite [34]. This was done by first exporting the Pytorch model in Open Neural Network Exchange (ONNX) Format. The ONNX

Table 7.1: Number of images per category in the SH dataset

Split	Positive Images	Negative images	Total
Training Set (80%)	2,420	7,221	9,641
Test Set (20%)	577	1,833	2,410
Total	2,997	9,054	12,051

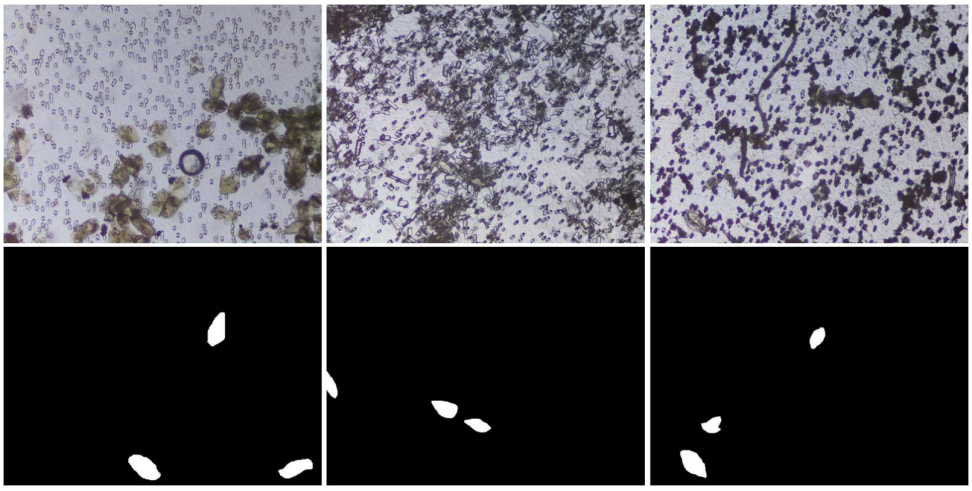

Figure 7.3: Example of sample images that are difficult-to-identify eggs with artifacts, such as crystals, glass debris, air bubbles, and fabric fibers in the background, and their respective ground truth images.

model is then converted to Tensorflow before the final conversion from Tensorflow to Tensorflow Lite. The refined segmentation algorithm was implemented on the Raspberry Pi.

7.4.3. EVALUATION METRICS

We evaluated the performance of semantic segmentation of *S. haematobium* egg by comparing the deepLabV3-MobileNetV3 Segmentation (DS) which are the prediction results with a ground truth (GT) that was manually annotated by a trained parasitologist using the Pixel Accuracy (PA):

$$PA = \frac{1}{n}\sum_{i=0}^{n} 1_{(GT_i = DS_i)} \tag{7.9}$$

We also compared the semantic segmentation performance using Dice Similarity Coefficient (DSC) and Jaccard Similarity Coefficient (JAC), which are widely used in evaluating medical segmentation algorithms.

$$DSC = 2\frac{|GT \cap DS|}{|GT| + |DS|} \tag{7.10}$$

$$JAC = \frac{|GT \cap DS|}{|GT \cup DS|} \tag{7.11}$$

While the diagnostic performance of our two-stage diagnosis framework was evaluated by employing three metrics, precision, sensitivity and specificity, which are commonly used for evaluating diagnostic devices.

$$Precision = \frac{TP}{TP + FP} \tag{7.12}$$

$$Sensitivity = \frac{TP}{(TP + FN)} \tag{7.13}$$

$$Specificity = \frac{TN}{(TN + FP)} \tag{7.14}$$

Where TP, FP, TN and FN are True Positive, False Positive, True Negative and False Negative samples respectively.

7.5. EXPERIMENTS AND RESULTS

7.5.1. DEEPLABV3-MOBILENETV3 S. haematobium EGG SEMANTIC SEGMENTATION

The determine the applicability of the framework on Edge AI system in low resource settings with no internet connectivity, we implemented and evaluated its performance on a Raspberry Pi 4B with Coral USB accelerator. We evaluate the DeepLabV3-MobileNetV3 deep learning model for the semantic segmentation of *S. haematobium* eggs using the development test dataset. As shown in table 7.2., the deep learning model achieved a segmentation accuracy of 99.69%. It is however important to note the existence of a very high imbalance between the foreground and background pixels in the images which could hamper the segmentation accuracy. While using, the Jaccard and dice coefficient as performance metric, the model obtained 85.30% and 87.20% respectively. However, the average inference time per image was 7.13s with a model size of 7.13mb. We considered the inference time too high given the need to process 117 images per sample diagnosis. In order to reduce the processing time on the Edge AI system, we optimised the DeepLabV3-MobileNetV3 deep learning model

using post-training quantisation on Tensorflow. The optimised model was applied to the development test dataset. We observed a significant reduction in inference time and model size (2x and 4x respectively) with little effect (about 1% reduction) in the Jaccard and Dice coefficient metric. However, the segmentation accuracy remained the same. All further experiments in the work were carried out using the optimised model.

The visual performance of the segmentation model is shown in fig. 7.4(c). We observed that the model detected eggs in images heavily cluttered with artefacts such as crystals and other particles (sample image 3). It also detected highly transparent *S. haematobium* eggs (sample image 1) present in the captured images. Partially cut eggs on the edge of the images and overlapping eggs were also detected as observed in sample image 2. However, the boundaries in the overlapping eggs are not clearly segmented.

7.5.2. Refined Segmentation and Egg Count

In the second stage of our framework, we applied a refined segmentation algorithm on the output segmentation mask image of the DeepLabV3-MobileNetV3 deep learning model as described in section 7.3.2 From fig. 7.4(d), we observed that the refined segmentation steps fills-in eggs pixels missed in the deep learning semantic segmentation stage. This improves the visual perceptibility of the eggs in the segmentation mask image especially in regions with overlapping eggs as seen in sample image 2. fig. 7.5 shows example regions with overlapping eggs in the deep learning segmentation mask image. We observed that the correct number of eggs in fig. 7.5(a) and (c) are equivalent to the optimal AIC criterion values in fig. 7.5(b) and (d) respectively. The refined segmentation stage is able to separate overlapping eggs thus improving the accuracy of determining the infection intensity of the sample.

fig. 7.6 shows the scatter log-scale plots of the automated egg counts versus the manual egg count (i.e., egg count by an experienced microscopist) of samples in the diagnosis test dataset. Although we observed that the predicted egg counts were mostly under the 1:1 line. This signifies under-prediction especially in samples with high egg counts. However, the manual and automated egg count are highly correlated in samples with both low and high egg counts which indicates the applicability for the developed framework in determining infection intensity of a sample.

7.5.3. Urogenital Schistosomiasis Diagnosis

A 10mL urine sample consists of 117 FoV images when filtered with a 13mm membrane and captured by the Schistoscope. For a sample to be determined as true negative diagnosis, the 117 FoV images

Table 7.2: Performance of DeepLabV3-MobileNetV3 for Semantic segmentation of *S. haematobium* eggs.

	PA	JAC	DSC	Model size (mb)	Inference time (S)
Base Model	99.69	85.30	87.20	42.1	7.13
Optimised Model	99.69	84.64	86.55	11.1	4.39

must contain no false positives. We experimentally defined boundary conditions for the detected isolated eggs using inequality functions, defined by the overlap and area of the fitted ellipse as shown in fig. 7.7. The boundary conditions are defined by $OC \geq -4.75e^{-4}|E_R| + 1.15$ and $OC \leq 3.25e^{-4}|E_R| + 0.74$ where OC is the overlap and $|E_R|$ is the area of fitted ellipse The experiment was carried out using images from the development test dataset [fig. 7.7(a)] and boundaries were found to hold also in images from the diagnosis test dataset [fig. 7.7(b)]. A sample was determined as positive diagnosis if an isolated egg is detected in the set of 117 FoV images which satisfies the defined boundary conditions (an egg is detected in the green region of fig. 7.7). Otherwise, the sample is determined as negative diagnosis. We observed that most of the false negatives in fig. 7.7 (grey markers) were broken or partly captured eggs found at the edges of the image, while the false positives (yellow markers) are artefacts that are very similar in appearance to a *S. haematobium* egg.

The diagnostic performance of the developed framework is shown in table 7.3. We observed a significant improvement in diagnosis specificity (from 72.73% to 93.94%) and precision (from 77.50% to 93.75%) when the boundary conditions are applied in determining the sample diagnosis. However, a reduction in the diagnosis sensitivity is observed. This is due to some samples with very low infection intensities (eggs per 10mL of urine ≤ 2) not having any detected eggs which meet the boundary constraint represented by the green region of fig. 7.7(b). McNemar's test returned a $p-value$ of 0.008, which indicates a statistically significant difference between both methods ($p-value < 0.05$). Also, we achieved a 7.39% and 92.11% performance improvement in diagnosis sensitivity and specificity respectively, compared to our previously published work [11].

7.5.4. COMPUTATIONAL TIME

In order to evaluate the computational performance of the developed framework, we measured the computational time of both stages of the proposed method as function of infection intensity. *S. haematobium* infection intensity has consistently been characterized by the number of schistosome eggs per 10 mL of urine with 1 to 49 eggs per 10 mL

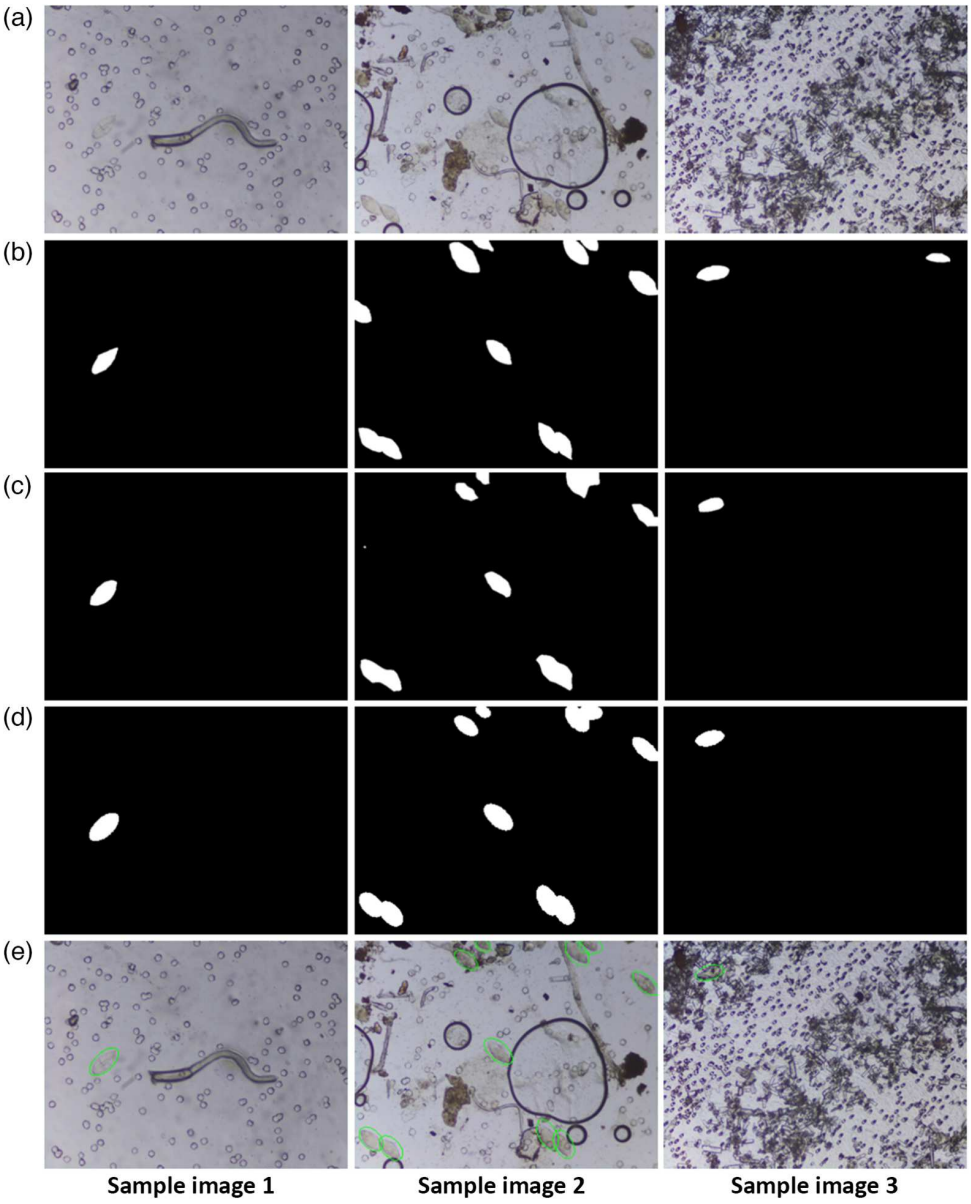

Figure 7.4: Visual performance of developed framework on sample images from the dataset. Schistoscope (a) captured and (b) ground truth images. The output mask images of (c) DeepLabV3-MobileNetV3 segmentation and (d) refined segmentation. (e) The result image with detected eggs.

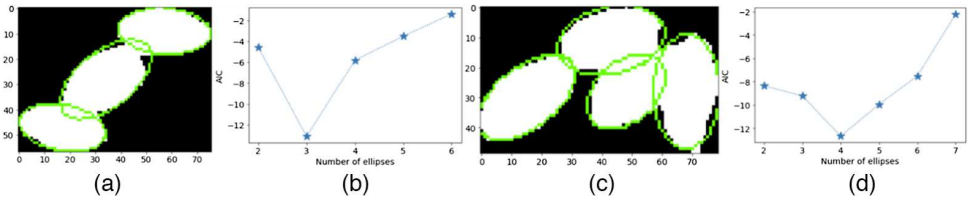

Figure 7.5: (b) and (d) shows estimated AIC criteria values for different number of ellipses fitted on the region images (a) and (c) respectively with optimal ellipses are highlighted in green.

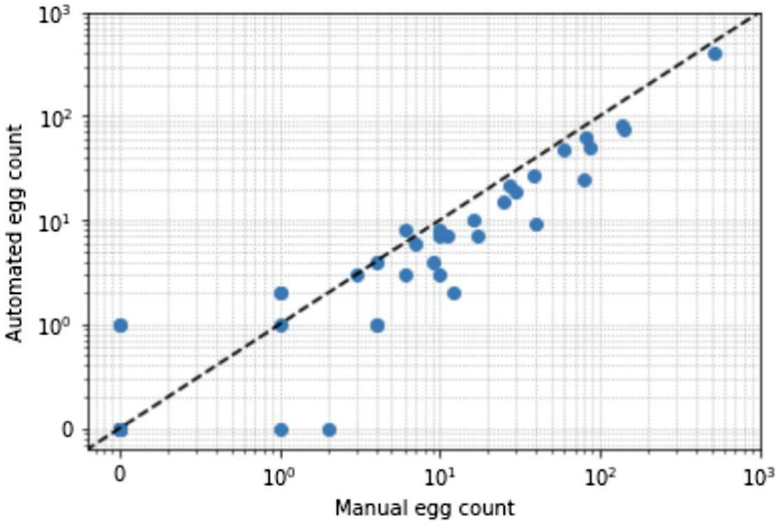

Figure 7.6: Logarithmic scale scatter plot of infection intensity per 10 mL urine sample. The manual egg count obtained by a microscopist manually counting the eggs in the diagnosis test image dataset, is used as a reference while the automated egg count is obtained using the developed framework.

Table 7.3: Diagnostic performance of developed framework on the diagnosis test dataset.

	Sensitivity	**Specificity**	**Precision**
Without boundary conditions	96.88	72.73	77.50
With boundary conditions	93.75	93.94	93.75

of urine defining a light infection and more than 50 eggs per 10 mL

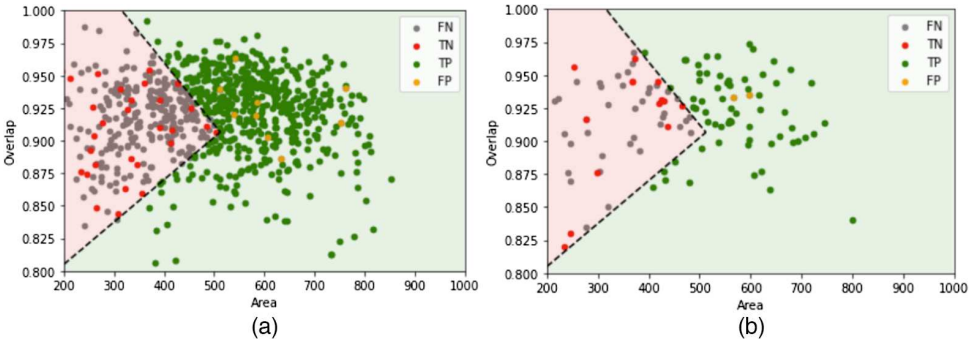

Figure 7.7: Boundary conditions to determine a sample as positive or negative diagnosis applied to images from (a) the development test dataset and (b) diagnosis test dataset; A samples is determined as positive if an egg in any of the 177 FoV images is detected in the green region.

of urine indicating a heavy infection [35]. We performed the running time experiments on a Raspberry PI 4B with Coral USB accelerator to study how the infection intensity affects the computational time. The algorithm was applied on images from the diagnosis test image dataset. fig. 7.8 shows the average computational time from the application of the first (DeeplabV3-MobileNetV3 semantic segmentation) and the second (refined segmentation and separation of overlapping eggs) stages of the developed framework to the diagnosis test image dataset as a function of the infection intensity. From fig. 7.8, it can be seen that there is little difference between the computational time of negative and light intensity samples (620 and 628 s respectively). However, processing samples with heavy infection intensity is more time consuming with an average computational time of 748 s.

7.6. DISCUSSION

7.6.1. IMPACT ON SCHISTOSOMIASIS CONTROL AND ELIMINATION

Schistosomiasis affects about 252 million people globally [2] with approximately 90% of infections and the vast majority of morbidity occurring in Sub-Saharan Africa. Chronic urogenital schistosomiasis infection can result in bladder fibrosis as well as female and male genital schistosomiasis, which is associated with greater risk of HIV transmission [36]. Also, the bulk of the more than 1.6 million disability-adjusted life years [37] caused by schistosomiasis worldwide affect children, who have the highest prevalence and intensity of infections. Morbidity in children include anaemia, delays in physical and cognitive development, and reduced tolerance to exercise [38]. The main strategy for control

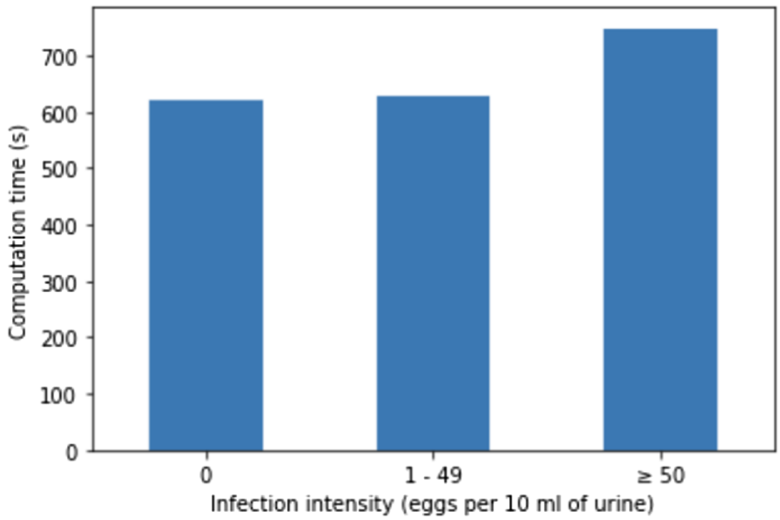

Figure 7.8: Average computational time in seconds from the application of framework on the diagnosis test image dataset.

of schistosomiasis focuses on mass drug administration (MDA) of praziquantel in priority to primary school-aged children because it is more cost-effective to treat all school-aged children in a community above a certain prevalence threshold than to test and treat each individual [4]. On a population level, higher intensities of infection are associated with higher levels of morbidity, but these relationships are poorly defined, as most control programmes monitor only prevalence of infection and not intensity [39]. Microscopic examination of urine samples is often a cheap and simple procedure recommended by WHO for the diagnosis of urogenital schistosomiasis. However, it has some critical shortcomings which include access to microscopes and trained personnel as well as poor sensitivity and reproducibility, and an error-prone manual read-out [40]. This led to the recent formation of the WHO Diagnostic Technical Advisory Group with the mandate to identify and prioritise diagnostic needs, and to subsequently develop TPPs for future diagnostics [4, 41, 42]. The TPP requires new diagnostic tools to have high specificity so as reliably measure when prevalence is above or below a cut-off of 10% in school-aged children. This informs decision on the frequency of the MDA. A diagnostic tool with high specificity is also needed to track changes of prevalence, ensuring that MDA is reducing overall prevalence; and to determine if transmission has been interrupted. In this work, we developed a two-stage diagnostic framework which is a suitable candidate for estimating infection intensity and diagnostic prevalence in urogenital schistosomiasis monitoring and control.

7.6.2. LIMITATIONS

- Image auto-focusing: Some of the images in the dataset captured by the Schistoscope were blurry due to sub-optimal autofocusing. Although this had no effect on the diagnostic performance, it did have an effect on the automated egg counts of a few samples in the diagnosis test dataset. This problem has been solved by a more accurate auto-focusing algorithm in subsequent version of the Schistoscope.
- Annotation problem: Annotating the exact boundaries of the eggs was difficult due to their small sizes. This may contribute to the difficulty of the model to segment the exact egg boundaries, especially in overlapping eggs.
- Diagnostic prevalence: The determining diagnosis of a sample with eggs that are either broken or are at the edges of the images are mostly not considered by the developed framework as they don't meet the boundary requirements. This increases the chances of a false negative diagnosis especially in samples with very low egg counts.
- Computational time: On a Raspberry Pi with Coral USB accelerator, the developed framework processes 117 images of the 13mm urine filter membrane in approximately 11 minutes. Therefore, an estimated processing time of 35 minutes required to process a 25mm filter membrane with 372 captured FoV images. However, the processing time can halved by the use of 2 Coral USB accelerators for computation through multi-threading.

7.7. CONCLUSION

We created a robust dataset of manually annotated *S. haematobium* eggs in microscopy images of urine samples collected from an endemic population, captured by the Schistoscope V5.0 device. We then developed a two-stage diagnosis framework for urogenital schistosomiasis using the SH dataset. The framework consists of two main stages, the first step involves the semantic segmentation of the eggs using the DeepLabV3 deep learning architecture with a MobileNetV3 backbone. The model effectively segmented the transparent eggs having low contrast with the background, and it also differentiated between eggs and other urine artifacts such as crystals that have egg-like structures. In the next stage, a refined segmentation algorithm was applied to detect and count the eggs present. The refined segmentation algorithm separates overlapping eggs by fitting the region image with an optimal number of ellipses determined by optimising the AIC criterion. For improved diagnostic

performance, we determine a sample as positive only if there is a detected egg present in the sample images which meet a defined boundary requirement which is a function of the overlap and area of the fitted ellipse. We implemented the developed framework on an Edge AI system consisting of a Raspberry Pi 4B with Coral USB accelerator and applied it to a diagnosis test dataset of 65 samples using results obtained by an expert microscopist as reference. We obtained 93.75%, 93.94% and 93.75% sensitivity, specificity and precision, respectively. The automated egg count was also highly correlated with the manual count of the microscopist. The framework also provides causality for its estimated egg counts which is relevant for diagnosis. From our results, it is evident that our automated framework for urogenital diagnosis combined with the Schistoscope device is a promising diagnostic tool for schistosomiasis. In a future study, the proposed multilayer framework, combined with the Schistoscope, will be validated for the diagnosis of urogenital schistosomiasis by comparing its performance with conventional microscopy, as well as more accurate diagnostic methods such as schistosome circulating antigen detection and DNA-based methods such as polymerase chain reaction assays [43].

INSTITUTIONAL REVIEW BOARD STATEMENT

The study was conducted in accordance with the Declaration of Helsinki, and approved by the Federal Capital Territory Health Research Ethics Committee (FCTHREC) in Abuja, Nigeria (reference no., FHREC/2019/01/73/18-07-19).

INFORMED CONSENT STATEMENT

Informed consent was obtained from all subjects involved in the study.

DATA AVAILABILITY STATEMENT

Schistosoma haematobium image dataset is available from the Zenodo Repository 10.5281/zenodo.6467268.

ACKNOWLEDGMENTS/FUNDING SOURCES

This work was funded by the NWO-WOTRO Science for Global Development program, Grant Number W 07.30318.009 (INSPiRED - INclusive diagnoStics for Poverty RElated parasitic Diseases in Nigeria and Gabon). We acknowledge the Neglected Tropical Disease team from the Federal Ministry of Health Abuja and Federal Capital Territory

Authority Public Health Laboratory Abuja, Nigeria and Delft University of Technology Global Initiative for their support towards this study.

CONFLICT OF INTEREST

The authors declare that they have no known competing financial interests or personal relationships that could have appeared to influence the work reported in this paper.

REFERENCES

[1] World Health Organisation. *Schistosomiasis*. 2024. url: https://www.who.int/news-room/fact-sheets/detail/schistosomiasis (visited on 09/26/2024).

[2] O. P. Aula, D. P. McManus, M. K. Jones, and C. A. Gordon. “Schistosomiasis with a focus on Africa”. In: *Tropical Medicine and Infectious Disease* 6.3 (2021), p. 109. doi: 10.3390/tropicalmed6030109.

[3] J. Utzinger, S. L. Becker, L. Van Lieshout, G. J. Van Dam, and S. Knopp. “New diagnostic tools in schistosomiasis”. In: *Clinical microbiology and infection* 21.6 (2015), pp. 529–542. doi: 10.1016/j.cmi.2015.03.014.

[4] World Health Organization. *Diagnostic target product profiles for monitoring, evaluation and surveillance of schistosomiasis control programmes*. World Health Organization, 2021. isbn: 9789240031104. url: https://iris.who.int/handle/10665/344813.

[5] N. Rajeshwori, K. Raju, B. Sanjeev, and S. B. Gulshan. “Prevalence of myopia and binocular vision dysfunctions in microscopists”. In: *International Eye Science* 18.7 (2018), pp. 1180–1183. doi: 10.3980/j.issn.1672-5123.2018.7.03.

[6] J. Rajchgot, J. T. Coulibaly, J. Keiser, J. Utzinger, N. C. Lo, M. K. Mondry, J. R. Andrews, and I. I. Bogoch. “Mobile-phone and handheld microscopy for neglected tropical diseases”. In: *PLoS Neglected Tropical Diseases* 11.7 (2017), e0005550. doi: 10.1371/journal.pntd.0005550.

[7] M. A. Saeed and A. Jabbar. “Smart diagnosis of parasitic diseases by use of smartphones”. In: *Journal of Clinical Microbiology* 56.1 (2018), e01469–17. doi: 10.1128/JCM.01469-17.

[8] A. Vasiman, J. R. Stothard, and I. I. Bogoch. “Mobile phone devices and handheld microscopes as diagnostic platforms for malaria and neglected tropical diseases (NTDs) in low-resource settings: a systematic review, historical perspective and future outlook”. In: *Advances in Parasitology* 103 (2019), pp. 151–173. doi: 10.1016/bs.apar.2018.09.001.

[9] H. Zhu, S. O. Isikman, O. Mudanyali, A. Greenbaum, and A. Ozcan. “Optical imaging techniques for point-of-care diagnostics”. In: *Lab on a Chip* 13.1 (2013), pp. 51–67. doi: 10.1039/c2lc40864c.

[10] P. Oyibo, S. Jujjavarapu, B. Meulah, T. Agbana, I. Braakman, A. van Diepen, M. Bengtson, L. van Lieshout, W. Oyibo, G. Vdovine, and J. C. Diehl. “Schistoscope: An Automated Microscope with Artificial Intelligence for Detection of Schistosoma haematobium Eggs in Resource-Limited Settings”. In: *Micromachines* 13.5 (2022), p. 643. doi: 10.3390/mi13050643.

[11] B. Meulah, P. Oyibo, M. Bengtson, T. Agbana, R. A. L. Lontchi, A. A. Adegnika, W. Oyibo, C. H. Hokke, J. C. Diehl, and L. v. Lieshout. “Performance Evaluation of the Schistoscope 5.0 for (Semi-)automated Digital Detection and Quantification of Schistosoma haematobium Eggs in Urine: A Field-based Study in Nigeria”. In: *The American Journal of Tropical Medicine and Hygiene* 107.5 (2022). doi: 10.4269/ajtmh.22-0276.

[12] L.-C. Chen, G. Papandreou, F. Schroff, and H. Adam. *Rethinking atrous convolution for semantic image segmentation*. preprint. 2017. doi: 10.48550/arXiv.1706.05587. arXiv: 1706.05587.

[13] C. Panagiotakis and A. Argyros. “Region-based fitting of overlapping ellipses and its application to cells segmentation”. In: *Image and Vision Computing* 93 (2020), p. 103810. doi: 10.1016/j.imavis.2019.09.001.

[14] Y. S. Yang, D. K. Park, H. C. Kim, M. H. Choi, and J. Y. Chai. “Automatic identification of human helminth eggs on microscopic fecal specimens using digital image processing and an artificial neural network”. In: *IEEE Transactions on Biomedical Engineering* 48.6 (2001), pp. 718–730. doi: 10.1109/10.923789.

[15] D. Avci and A. Varol. “An expert diagnosis system for classification of human parasite eggs based on multi-class SVM”. In: *Expert Systems with Applications* 36.1 (2009), pp. 43–48. doi: 10.1016/j.eswa.2007.09.012.

[16] C.-C. Lee, P.-J. Huang, Y.-M. Yeh, P.-H. Li, C.-H. Chiu, W.-H. Cheng, and P. Tang. “Helminth egg analysis platform (HEAP): An opened platform for microscopic helminth egg identification and quantification based on the integration of deep learning architectures”. In: *Journal of Microbiology, Immunology and Infection* 55.3 (2022), pp. 395–404. doi: 10.1016/j.jmii.2021.07.014.

[17] K. M. Naing, S. Boonsang, S. Chuwongin, V. Kittichai, T. Tongloy, S. Prommongkol, P. Dekumyoy, and D. Watthanakulpanich. “Automatic recognition of parasitic products in stool examination using object detection approach”. In: *PeerJ Computer Science* 8 (2022), e1065. doi: 10.7717/peerj-cs.1065.

[18] G. Sengul. “Classification of parasite egg cells using gray level cooccurence matrix and kNN”. In: *Biomedical Research* 27.3 (2016), pp. 829–834.

[19] M. O. K. Hassan and K. M. Al-Hity. “Computer-aided diagnosis of schistosomiasis: automated schistosoma egg detection”. In: *Journal of Clinical Engineering* 37.1 (2012), pp. 29–34. doi: 10.1097/JCE.0b013e31823fda36.

[20] M. Armstrong, A. R. Harris, M. V. D’Ambrosio, J. T. Coulibaly, S. Essien-Baidoo, R. K. D. Ephraim, J. R. Andrews, I. I. Bogoch, and D. A. Fletcher. “Point-of-care sample preparation and automated quantitative detection of schistosoma haematobium using mobile phone microscopy”. In: *American Journal of Tropical Medicine and Hygiene* 106.5 (2022), pp. 1442–1449. doi: 10.4269/ajtmh.21-1071.

[21] T.-Y. Lin, P. Goyal, R. Girshick, K. He, and P. Dollár. “Focal Loss for Dense Object Detection”. In: *2017 IEEE International Conference on Computer Vision (ICCV)*. Venice, Italy, 2017, pp. 2999–3007. doi: 10.1109/ICCV.2017.324.

[22] A. G. Howard, M. Zhu, B. Chen, D. Kalenichenko, W. Wang, T. Weyand, M. Andreetto, and H. Adam. *MobileNets: efficient convolutional neural networks for mobile vision applications*. preprint. 2017. doi: 10.48550/arXiv.1704.04861. arXiv: 1704.04861.

[23] M. Tan, R. Pang, and Q. V. Le. “EfficientDet: Scalable and Efficient Object Detection”. In: *Proceedings of the IEEE/CVF Conference on Computer Vision and Pattern Recognition (CVPR)*. Seattle, WA, USA, 2020, pp. 10781–10790. doi: 10.1109/CVPR42600.2020.01079.

[24] T.-Y. Lin, M. Maire, S. Belongie, J. Hays, P. Perona, D. Ramanan, P. Dollár, and C. L. Zitnick. “Microsoft COCO: Common Objects in Context”. In: *Computer Vision – ECCV 2014*. Vol. 8693. Zurich, Switzerland: Springer International Publishing, 2014, pp. 740–755. isbn: 978-3-319-10601-4 978-3-319-10602-1. doi: 10.1007/978-3-319-10602-1_48.

[25] O. Ronneberger, P. Fischer, and T. Brox. “U-net: convolutional networks for biomedical image segmentation”. In: *Medical Image Computing and Computer-Assisted Intervention – MICCAI*

2015. Vol. 9351. Munich, Germany, 2015, pp. 234–241. doi: 10.1007/978-3-319-24574-4_28.

[26] J. Brooks. *COCO Annotator*. GitHub repository. 2019. url: https://github.com/jsbroks/coco-annotator/ (visited on 12/18/2021).

[27] S. Minaee, R. Kafieh, M. Sonka, S. Yazdani, and G. J. Soufi. "Deep-COVID: predicting COVID-19 from chest X-ray images using deep transfer learning". In: *Medical Image Analysis* 65 (2020), p. 101794. doi: 10.1016/j.media.2020.101794.

[28] M. Everingham, L. Van Gool, C. K. I. Williams, J. Winn, and A. Zisserman. "The Pascal visual object classes (VOC) challenge". In: *International Journal of Computer Vision* 88.2 (2010), pp. 303–338. doi: 10.1007/s11263-009-0275-4.

[29] E. Xie, W. Wang, W. Wang, M. Ding, C. Shen, and P. Luo. "Segmenting transparent objects in the wild". In: *Computer Vision – ECCV 2020*. Vol. 12358. Glasgow, United Kingdom, 2020, pp. 696–711. doi: 10.1007/978-3-030-58601-0_41.

[30] H. Akaike. "A new look at the statistical model identification". In: *IEEE Transactions on Automatic Control* 19.6 (1974), pp. 716–723. doi: 10.1109/TAC.1974.1100705.

[31] C. M. Bishop. *Pattern Recognition and Machine Learning*. Springer, 2006. isbn: 978-0-387-31073-2.

[32] T. M. Mitchell. *Machine Learning*. New York: McGraw-Hill, 1997.

[33] A. Paszke, S. Gross, F. Massa, A. Lerer, J. Bradbury, G. Chanan, T. Killeen, Z. Lin, N. Gimelshein, L. Antiga, A. Desmaison, A. Köpf, E. Yang, Z. DeVito, M. Raison, A. Tejani, S. Chilamkurthy, B. Steiner, L. Fang, J. Bai, and S. Chintala. "Pytorch: an imperative style, high-performance deep learning library". In: *Proceedings of the 33rd International Conference on Neural Information Processing Systems*. Vol. 32. Vancouver, Canada: Curran Associates Inc., 2019, pp. 8026–803.

[34] Sithu3. *PyTorch-ONNX-TFLite*. GitHub repository. 2021. url: https://github.com/sithu31296/PyTorch-ONNX-TFLite (visited on 08/04/2023).

[35] R. E. Wiegand, W. E. Secor, F. M. Fleming, M. D. French, C. H. King, A. K. Deol, S. P. Montgomery, D. Evans, J. Utzinger, P. Vounatsou, and S. J. de Vlas. "Associations between infection intensity categories and morbidity prevalence in school-age children are much stronger for Schistosoma haematobium than for S. mansoni". In: *PLoS Neglected Tropical Diseases* 15.5 (2021), e0009444. doi: 10.1371/journal.pntd.0009444.

[36] UNAIDS. *No more neglect—female genital schistosomiasis and HIV—integrating sexual and reproductive health interventions to improve women's lives*. 2019. url: https://www.unaids.org/en/resources/documents/2019/female_genital_schistosomiasis_and_hiv (visited on 10/11/2023).

[37] World Health Organization. *Global health estimates: leading causes of death*. 2020. url: https://www.who.int/data/gho/data/themes/mortality-and-global-health-estimates/ghe-leading-causes-of-death (visited on 10/11/2023).

[38] D. G. Colley, A. L. Bustinduy, W. E. Secor, and C. H. King. "Human schistosomiasis". In: *The Lancet* 383.9936 (2014), pp. 2253–2264. doi: 10.1016/S0140-6736(13)61949-2.

[39] R. E. Wiegand, W. E. Secor, F. M. Fleming, M. D. French, C. H. King, S. P. Montgomery, D. Evans, J. Utzinger, P. Vounatsou, and S. J. de Vlas. "Control and elimination of schistosomiasis as a public health problem: thresholds fail to differentiate schistosomiasis morbidity prevalence in children". In: *Open Forum Infectious Diseases* 8.7 (2021), ofab179. doi: 10.1093/ofid/ofab179.

[40] L. J. Stuyver and B. Levecke. "The role of diagnostic technologies to measure progress toward WHO 2030 targets for soil-transmitted helminth control programs". In: *PLoS Neglected Tropical Diseases* 15.6 (2021). doi: 10.1371/journal.pntd.0009422.

[41] World Health Organization. *Report of the first meeting of the WHO Diagnostic Technical Advisory Group for Neglected Tropical Diseases Geneva, 30-31 October 2019*. World Health Organization, 2020. isbn: 9789240003590. url: https://iris.who.int/handle/10665/331954.

[42] A. A. Souza, C. Ducker, D. Argaw, J. D. King, A. W. Solomon, M. A. Biamonte, R. N. Coler, I. Cruz, V. Lejon, B. Levecke, F. K. Marchini, M. Marks, P. Millet, S. M. Njenga, R. Noordin, R. Paulussen, E. Sreekumar, and P. J. Lammie. "Diagnostics and the neglected tropical diseases roadmap: setting the agenda for 2030". In: *Transactions of the Royal Society of Tropical Medicine and Hygiene* 115.2 (2021), pp. 129–135. doi: 10.1093/trstmh/traa118.

[43] P. T. Hoekstra, G. J. van Dam, and L. van Lieshout. "Context-specific procedures for the diagnosis of human schistosomiasis – a mini review". In: *Frontiers in Tropical Diseases* 2 (2021), p. 722438. doi: 10.3389/fitd.2021.722438.

8

AUTOFOCUSING AND WHOLE SLIDE IMAGING

An automated slide scanning system for membrane filter imaging in diagnosis of urogenital schistosomiasis

Prosper Oyibo, Tope Agbana, Lisette van Lieshout, Wellington Oyibo, Jan-Carel Diehl, Gleb Vdovine

PUBLICATION REPORT

- **Publication Date:** 30 January 2024
- **Journal:** Journal of Microscopy
- **Publisher:** Wiley
- **DOI:** 10.1111/jmi.13269

ABSTRACT

Traditionally, automated slide scanning involves capturing a rectangular grid of field-of-view (FoV) images which can be stitched together to create whole slide images, while the autofocusing algorithm captures a focal stack of images to determine the best in-focus image. However, these methods can be time-consuming due to the need for X-, Y- and Z-axis movements of the digital microscope while capturing multiple FoV images. In this paper, we propose a solution to minimise these redundancies by presenting an optimal procedure for automated slide scanning of circular membrane filters on a glass slide. We achieve this by following an optimal path in the sample plane, ensuring that only FoVs overlapping the filter membrane are captured. To capture the best in-focus FoV image, we utilise a hill-climbing approach that tracks the peak of the mean of Gaussian gradient of the captured FoVs images along the Z-axis. We implemented this procedure to optimise the efficiency of the Schistoscope, an automated digital microscope developed to diagnose urogenital schistosomiasis by imaging Schistosoma haematobium eggs on 13 or 25 mm membrane filters. Our improved method reduces the automated slide scanning time by 63.18% and 72.52% for the respective filter sizes. This advancement greatly supports the practicality of the Schistoscope in large-scale schistosomiasis monitoring and evaluation programs in endemic regions. This will save time, resources and also accelerate generation of data that is critical in achieving the targets for schistosomiasis elimination.

8.1. INTRODUCTION

Sub-Saharan Africa is highly endemic for parasitic diseases such as malaria, schistosomiasis, lymphatic filariasis, trypanosomiasis and soil transmitted helminth infections [1–5]. These diseases have a profound impact on public health, affecting millions of individuals and leading to significant morbidity and mortality rates, particularly among vulnerable populations. Accurate and timely diagnosis is critical for prompt precision mapping, effective case management and periodic assessment of interventions overtime. In sub-Saharan Africa, microscopy has long been considered the gold standard for diagnosing parasitic diseases. It enables the visualisation of parasites and their morphological characteristics, facilitating accurate identification and quantification. Microscopic examination of filtered urine samples, stained blood smears, stool smears, and tissue biopsies has played a pivotal role in guiding treatment decisions and controlling the spread of parasitic diseases. Despite its utility, conventional microscopy techniques face several challenges, particularly in sub-Saharan Africa. Limited access to trained personnel and high-quality microscopes in remote and resource-limited areas can hinder timely and accurate diagnosis. The lack of skilled technicians often results in delays and increased diagnostic errors. Additionally, interobserver variability in expertise may lead to discrepancies in parasite detection and misdiagnosis, further impacting patient outcomes [6].

Advancements in digital optics and artificial intelligence have revolutionised the field of microscopy [7–9]. Digital microscopes equipped with high-resolution cameras and sophisticated imaging software can capture whole-slide images of specimens. These images can be analysed using artificial intelligence algorithms, enabling automated detection and classification of parasites. The integration of digital optics and artificial intelligence improves diagnostic accuracy, reduces human error and enhances efficiency.

Automated slide scanning systems with artificial intelligence capabilities have the potential to significantly improve and accelerate access to the optical diagnosis of parasitic diseases by overcoming challenges associated with conventional microscopy, such as limited access to skilled technicians and interobserver variability. It captures high-resolution images of entire glass slides, creating a digital representation of the specimen. By leveraging on innovation through advancements in digital optics and artificial intelligence, these technologies offer efficient and accurate parasite detection, facilitating timely interventions, effective disease management and large-scale precision diagnosis during disease mapping and periodic assessment. A fundamental challenge with automated slide scanning systems has been the ability to acquire high-quality, in-focus images at high speed [10]. Several studies have implicated poor focus as the main culprit for poor image quality in these

systems [11–13], and addressing this challenge is crucial to ensure the successful implementation and widespread adoption.

The autofocusing system, which involves moving a microscope optical train or sample stage along a Z-axis (optical axis) to find an optimal focus position, is a critical feature of automated digital microscopes, ensuring that the image remains sharp and in focus. However, autofocusing algorithms can encounter difficulties, particularly due to the topography of the biological sample and the glass slide underneath having depth variations [14]. Reflections, artefacts, and the presence of debris can also hinder accurate autofocusing, potentially impacting the quality of the captured images. Thus, the automated microscope needs to be continuously focused as it moves from one field-of-view to another.

Autofocusing systems can be broadly divided into three categories [10] – focus map surveying, real-time reflection based and real-time image based. Many automated slide scanning systems create a focus map before scanning by acquiring a Z-stack for each point on the map. This method is time-consuming and requires high-precision mechanical systems, increasing the overall system cost. In real-time reflection-based technique, a constant distance between the objective lens and a reference plane is maintained by repeatedly finding the axial location of the reference plane. However, it is less effective when the sample's location varies due to tissue topography variations [15–18]. Real-time image-based autofocusing offers several approaches, including dual sensor scanning [19], beam splitter arrays [20], tilted sensors [21], phase detection [22–24], deep learning [25–30] and dual-LED illumination [31–35]. These methods do not require a pregenerated focus map and can handle samples with varying topography. However, they come with their own challenges, such as the need for additional optical hardware, alignment issues and cost considerations. In the case of dual-LED illumination-based autofocusing, it allows real-time single-frame autofocusing, continuous sample motion and cost-effective design. Nonetheless, it may still require an extra camera and optical hardware and may not work well with transparent samples. Although time-consuming, focus map surveying is the most adopted autofocusing method in commercially available whole slide imaging systems. Manufacturers favour this approach because it requires no additional optical hardware, proves to be robust for different types of samples and reduces or eliminates potential intellectual property issues.

In the focus map surveying approach, multiple images are captured along the Z-axis. Then, a figure of merit (FoM) is calculated to evaluate the quality of focus for each image. The image with the highest FoM value is considered the in-focus image [14, 23]. One major challenge of this method is its time-consuming nature. Additionally, skipping tiles can reduce the focus map surveying time but comes at the expense of accuracy in the resulting focus map [19]. Various FoM measures have

been used in the literature, initially introduced by Brenner *et al.* [36]. Commonly used figure of merit (FoM) measures include the derivative of Gaussian, variance of Laplacian, norm of Sobel operator and norm of Boddeke's operator, among others. Nevertheless, the convolution with the derivative of a Gaussian smoothing function has been demonstrated to effectively mitigate the impact of noise on the FoM curve in various optical microscopy techniques, including fluorescence, bright-field and phase contrast microscopy, in both fixed and living cells, as well as in fixed tissue [37]. This approach was assessed in tuberculosis microscopy [38, 39], as well as in both bright-field microscopy of stained[40] and unstained cells [41]. Autofocusing systems commonly utilise search methods designed to pinpoint the peak of the FoM curve. However, the presence of mechanical backlash complicates the positioning system of the digital microscope, since positions are never fully reproducible [42]. Furthermore, in some cases, the FoM curve can have multiple peaks, which may not necessarily correspond to the best focus [43]. Thus, FoM-based peak finding may lead to capturing out-of-focus images.

In this paper, we present an automated slide scanning procedure aimed at reducing the imaging time required to capture circular membrane filters in the diagnosis of urogenital schistosomiasis. Our method optimises the scanning path within the sample plane, ensuring that only field-of-views (FoVs) overlapping the filter membrane are captured. Furthermore, we developed an autofocusing algorithm based on hill-climbing to detect the peak of the figure of merit (FoM) curve along the focal plane of the membrane filter. To achieve this, we utilise the mean Gaussian gradient of the FoV image as the FoM due to its unimodal nature when imaging the membrane filter.

8.2. PERTURB AND OBSERVE AUTOFOCUSING ALGORITHM

Microscopic imaging of filter membranes for the detection of *Schistosoma haematobium* eggs in urine usually encounters challenges such as uneven filter membranes, presence of artefacts and deviations in slide angle and stage position [44]. All these factors can result in loss of focus when capturing images across different FoVs, thus reducing the readability of the image by both humans and automatic object detection algorithms. Therefore, there is a need for an autofocusing system to ensure that the images captured are always in focus. We present an optimal autofocusing algorithm using a hill-climbing approach called perturb and observe. Perturb and observe algorithm is the most commonly used method in maximum power point tracking of photovoltaic (PV) solar systems due to its ease of implementation and top-level efficiency [45, 46]. We adapted the perturb and observe algorithm for detecting the best focus plane by including a perturbation in the position of the Z-axis and observing the change the FoM. Here we

adopted the mean of Gaussian gradient of the captured FoV image as the FoM due to its unimodal nature when imaging the membrane filter. The curve has its peak when the Z-axis position is at the optimal focal plane. fig. 8.1 shows an example FoM curve of a filter membrane FoV when the Z-axis moved for the start to end position.

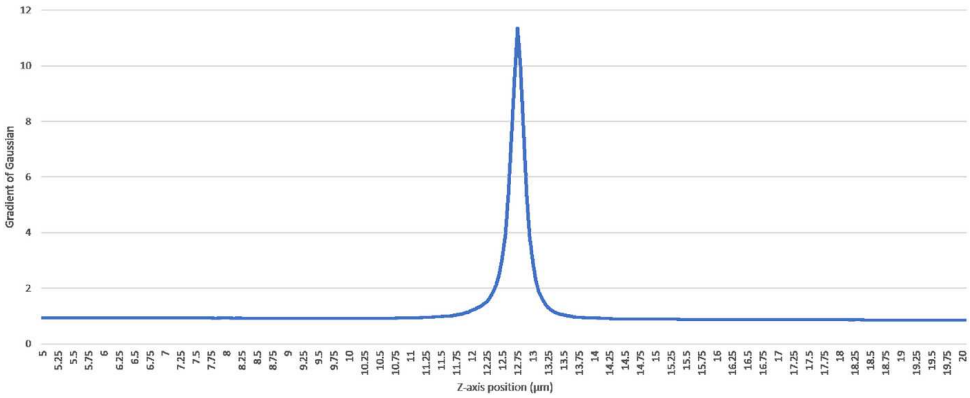

Figure 8.1: Plot of mean Gaussian gradient of captured FoV image of the membrane filter against Schistoscope's Z-axis position.

In our technique, incrementing the Z-axis position cause the FoM value to increase if the operation is on the left side of the FoM curve, and decreases the FoM value when the Z-axis position is on the right side of the FoM curve. We established an upper and lower boundary values for the Z-axis position which ensures a search space that encompasses the likely optimal Z-axis position based on the optical configuration of the Schistoscope. The autofocusing routine can be initiated either automatically within the membrane filter scanning procedure or manually by the Schistoscope operator from the device user interface. The perturb and observe autofocusing algorithm starts at the midpoint of the search space in the case of the former and at the current Z-axis position in the latter thus improving convergence speed.

First, we record the initial position (z) of the Z-axis and acquire the FoV image with dimension $r \times c$. Next, the recorded image is converted to greyscale and a figure of merit (F) is estimated as the mean of gradient magnitude of the convolution of a greyscale image (I) and a Gaussian derivatives filter (G) with standard deviation σ, as shown in equation (8.1).

$$F = \sum_{i=1}^{r} \sum_{j=1}^{c} I(i,j) * G(i,j,\sigma) \tag{8.1}$$

Subsequently, the Z-axis is incrementally adjusted to a new position, denoted as $z(n)$, and the figure of merit (FoM), $F(z(n))$, is calculated

using equation (8.1). We then employ equation (8.2) to determine the change in FoM (ΔF) for the captured image, representing an approximation of the gradient of F. A positive ΔF indicates that $z(n)$ is on the left side of the peak, leading to an increase in the Z-axis position by a step size. Conversely, a negative ΔF indicates that $z(n)$ is on the right side of the peak, resulting in a decrease in the Z-axis position by a step size.

$$\Delta F = F(\max\{z(n), z(n-1)\}) - F(\min\{z(n), z(n-1)\}) \tag{8.2}$$

The above procedure is repeated until the stopping criteria shown in equation (8.3) is achieved.

$$sign(\Delta F(z(n))) \neq sign(\Delta F(z(n-1))) \tag{8.3}$$

The stopping criteria indicates there is a change in the sign of ΔF between the current and previous Z-axis position. This translates to reaching the peak of the FoM curve where the recorded image of the FoV is at the best focus.

8.3. OPTIMAL CIRCULAR MEMBRANE FILTER IMAGING

In traditional automated slide scanning systems, grids of FoV images are captured by moving the optical axis or sample stage sequentially along the width and length of the glass slide. This procedure consumes a high amount of time and some of the FoV images may just be images of the glass slide without sample specimen present especially when the specimen is not rectangular in shape. This is, more evident in automated diagnosis of urogenital schistosomiasis in which a circular membrane filter is scanned in a rectangular grid resulting in a large number of the FoV images captured in which the membrane filter is not present. Eliminating these images by adopting an optimal membrane filter scanning procedure would lead to a significant savings in the total sample processing time of an automated slide scanning system. We propose a membrane filter scanning procedure, which optimises the scanning time by intelligently skipping FoVs which do not overlap the circular membrane filter. To further explain our approach, we make use of the illustration shown in fig. 8.2. Where the shaded circle represents a membrane filter and the rectangular grid cells represents FoVs. Our algorithm utilises the principle of circle geometry to estimate the positions of the grid cells that overlap with the filter membrane in each grid row.

From the illustration in fig. 8.2, let h_{fov} and w_{fov} be the height and width of the FoV obtained by optical system of the digital microscope which is represented by the grid cell. Therefore, the minimum number of grid rows n_{rows} and grid columns n_{cols} for a square grid required to

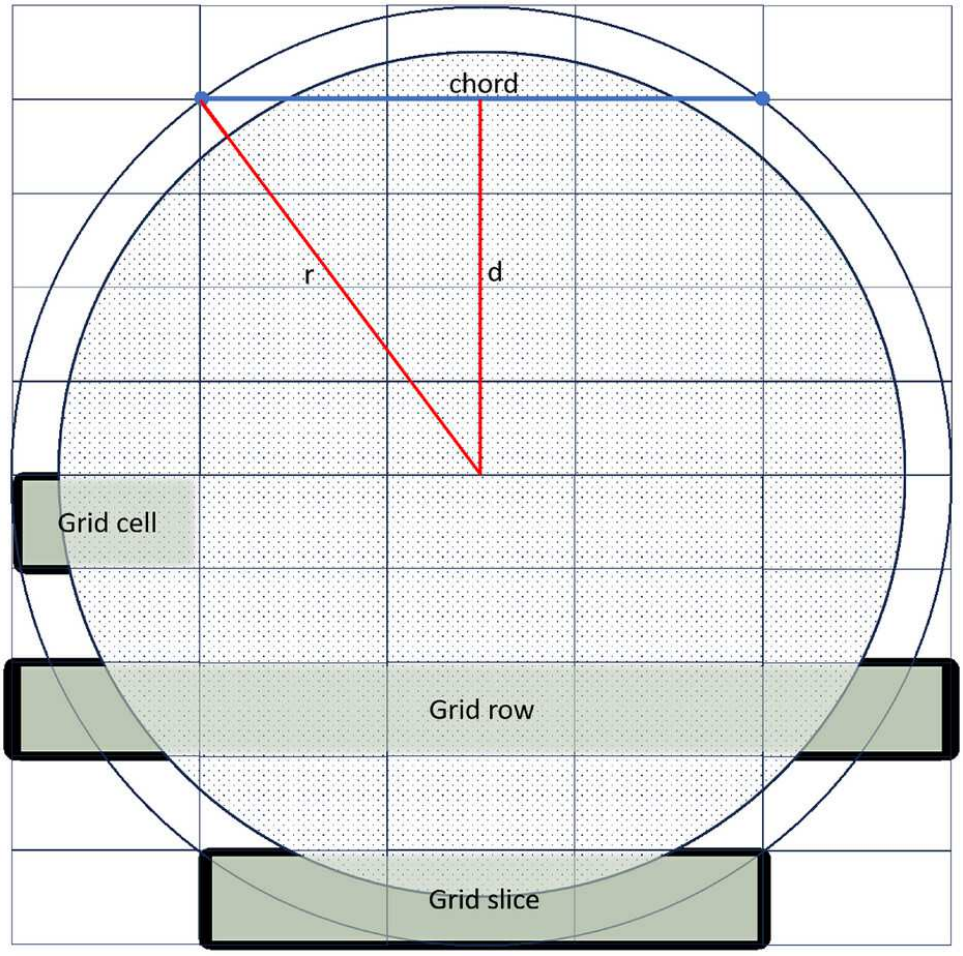

Figure 8.2: An example 10 x 5 grid illustration of a circular membrane filter.

capture circular membrane filter of diameter d_{mem}, with the membrane centred in the grid, can be obtained using equations (8.4) and (8.5):

$$n_{rows} = ceil\left(\frac{d_{mem}}{h_{fov}}\right) \tag{8.4}$$

$$n_{cols} = ceil\left(\frac{d_{mem}}{w_{fov}}\right) \tag{8.5}$$

Each grid row contains a grid slice with minimum number grid cells such that there is a complete overlap with the membrane filter. To

obtain the slice we assume a circle inscribed in the square grid as illustrated in fig. 8.2.

The length of chord l spans the grid cells in a grid slice can thus be estimated as follows:

$$l = 2\sqrt{(r^2 - d^2)} \tag{8.6}$$

where r is the radius of the inscribed circle defined as:

$$r = n_{rows} \times \frac{h_{fov}}{2} \tag{8.7}$$

And d is the distance between the chord and centre of the inscribed circle defined as:

$$d = abs\left(\frac{n_{row}}{2} - i_{row}\right) \times h_{fov} \tag{8.8}$$

We then estimate the number of grid cells n_{cells} overlapping the membrane filter in a grid row using equation (8.9):

$$\begin{cases} n_{cells} = round\_to\_nearest\_odd\left(\frac{l}{w_{fov}}\right) & \text{if } n_{col} \text{ is odd} \\ n_{cells} = round\_to\_nearest\_even\left(\frac{l}{w_{fov}}\right) & \text{otherwise} \end{cases} \tag{8.9}$$

It is observed that an odd number of grid cells is required for a grid with odd number of grid columns and vice versa. Also, the grid slice is always centred in the grid row. Therefore, the start column index and end column index of the grid slice is obtained using equations (8.10) and (8.11), respectively.

$$s_{col} = \frac{n_{cols} - n_{cells}}{2} + 1 \tag{8.10}$$

$$t_{col} = s_{col} + n_{cells} - 1 \tag{8.11}$$

The optimal membrane filter scanning is performed by sequentially moving the sample stage along a path defined by the optimal grid slices in each grid row beginning from the topmost row in the grid. The scan is performed from left to right in grid slices belonging to odd rows and in the reverse direction in grid slices of even rows. Autofocusing is performed at each grid cell position and the FoV image with the best focus is recorded before moving to the next grid cell. The algorithm is terminated after the FoV image of the last grid cell of the grid slice from the last grid row has been recorded.

8.4. THE SCHISTOSCOPE IMPLEMENTATION

The standard sample preparation procedure in diagnosing urogenital schistosomiasis involves filtering 10 mL of the patient's urine through a circular membrane filter with a mesh size small enough to retain the parasite eggs. The membrane is then placed on a glass slide and processed by the Schistoscope to for automated detection of *Schistosoma haematobium* eggs [44]. The Schistoscope is equipped with a graphical user interface through which the operator selects from two common sizes of membrane filters that are used in urogenetal schistosmiasis diagnosis, measuring 13 and 25 mm in diameter. The Schistocope captures FoV images of the membrane filter using the developed automated scanning procedure with perturb and observe autofocusing algorithm, implemented on the device using Python programming language. The size of the image captured for estimating the FoM in the autofocusing algorithm is 320 $\times$ 240 pixels and this covers a FoV of size 1.47 mm $\times$ 1.08 mm. The Z-axis step size was set to 0.25 μm.

8.5. RESULT AND DISCUSSION

We performed experiments to assess the impact of the presence of dirt, *S. haematobium* eggs, or the glass slide in the FoV, on the shape of the FoM curve and performance of the perturb and observe autofocusing algorithm. We examined four representative in-focus FoV images of a filter membrane captured using the perturb and observe autofocusing algorithm: two FoVs with a filter membrane containing dirt and *S. haematobium* eggs (fig. 8.3A and B), a FoV with a portion of the glass slide and a portion of the filter membrane (fig. 8.3C) and a FoV with a filter membrane without dirt and *S. haematobium* eggs (fig. 8.3D). The corresponding normalised figure of merit (FoM) curve obtained by analysing the mean Gaussian gradient of the captured stack of images along the Z-axis for the respective FoVs are displayed in fig. 8.3E. We obtained a unimodal FoM curve for all four cases. Notably, the optimal focus plane identified by the perturb and observe autofocusing algorithm (circle markers in fig. 8.3E) aligns with the peak in the FoM curves of images a, c and d. However, in the FoM curve of FoV image b, a Z-axis position error of 0.02 μm is observed in the perturb and observe autofocusing algorithm. This position error primarily stems from mechanical backlash in the positioning system and can be mitigated by reducing the step size of the Z-axis motor. Nevertheless, decreasing the step size would prolong the convergence time of the autofocusing algorithm without yielding significant improvements to the best focus image, as the device's microscope objective has a depth of view of 55.5 μm. Furthermore, the observed shifts in the FoM curves, despite the representative FoV images being from the same slide, arise

from variations in tissue composition and slide depth variation. The slide depth variation is attributed to the imperfectly flat sample bed, especially in a low-cost device like the Schistoscope, which involves manual assembly and utilises 3D-printed parts.

To demonstrate the practical feasibility of the optimal automated slide scanning procedure with the perturb and observe autofocusing algorithm, we implemented the algorithms on the Schistoscope and performed 10 experimental trials of scanning both the 13 and 25 mm membrane filters. In table 8.1, we present the mean and standard deviation of the time taken to scan both membrane filters using the proposed procedures.

Table 8.1: Performance in automated slide scanning of 13 mm and 25 mm membrane filter.

Procedure	**Scanning time (s)**		**Percentage improvement (%)***	
	13 mm	**25 mm**	**13 mm**	**25 mm**
Traditional grid scanning with focus map surveying	$1,812.31 \pm 18.66$	$5,335.75 \pm 64.50$	-	-
Traditional grid scanning with perturb and observe	768.47 ± 13.07	$1,774.00 \pm 24.92$	57.60	66.70
Optimal membrane scanning with perturb and observe	667.07 ± 11.21	$1,518.78 \pm 31.96$	63.18	71.52

*Percentage improvement compared to traditional grid scanning with focus map surveying.

We achieved a 57.60% and 66.70% improvement in scanning time for the 13 and 25 mm filter membranes, respectively, when employing the perturb and observe autofocusing with the traditional grid scanning procedure, compared to the base case of traditional grid scanning with focal mapping autofocusing approach. This improvement can be attributed to requiring a lesser number of steps for Z-axis movement (maximum of 4 steps) compared to the focal mapping autofocusing, which necessitates a minimum of 10 steps to acquire an in-focus image for every grid cell. The traditional grid scanning approach requires a 9 13 grid (117 images) and 18 24 grid (432 images) to capture the entire 13 and 25 mm membrane filters, respectively. By applying the developed optimal membrane scanning procedure in combination with the perturb and observe auto focusing algorithm, we achieved an additional improvement in scanning times of 13.15% and 14.43% for the 13 mm and 25 mm membrane filters respectively, compared to traditional grid scanning approach with perturb and observe autofocusing algorithm. Thus, we obtained an overall improvement in scanning time of 63.18% and 71.52% for the 13 and 25 mm membrane filters, respectively, compared to the base case of traditional grid scanning with focus map surveying autofocusing approach. This improvement was achieved by

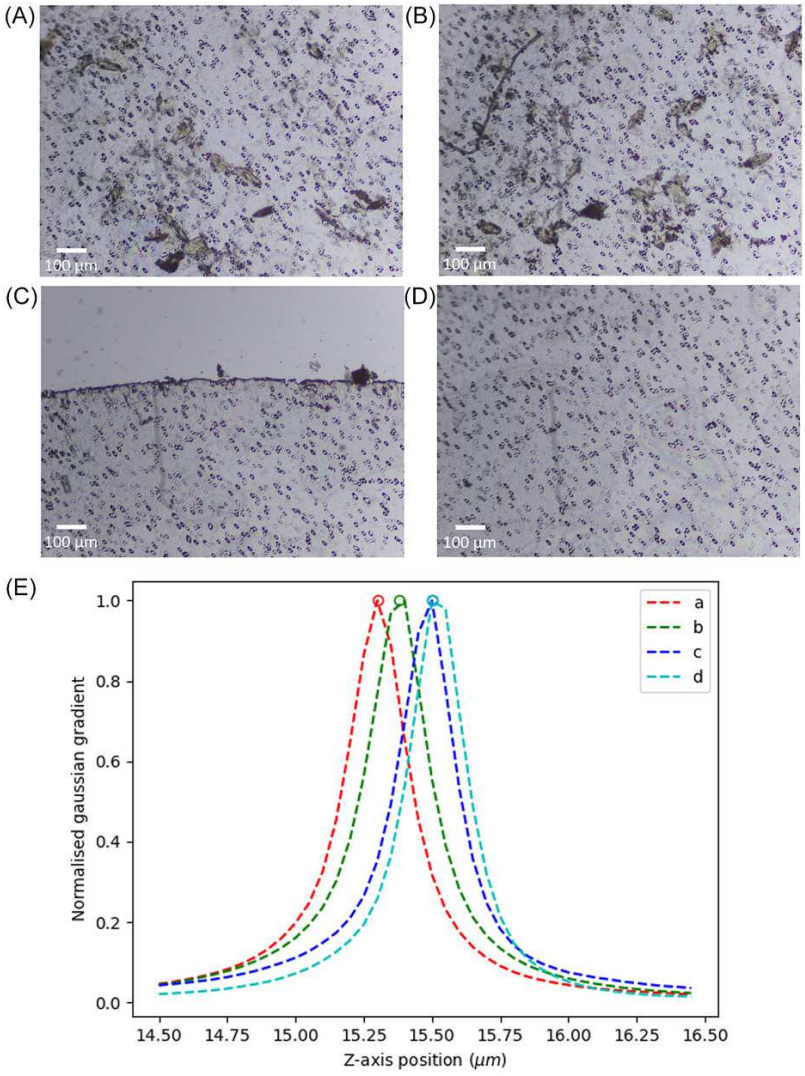

Figure 8.3: Representative in-focus FoV images from the same sample slide obtained using the perturb and observe autofocusing algorithm. (A, B) The FoV with a filter membrane containing dirt and *S. haematobium* eggs. (C) A FoV with a portion of the glass slide and a portion of the filter membrane. (D) A FoV with a filter membrane without dirt and *S. haematobium* eggs. (E) The normalised FoM curve corresponding to the respective images, with the detected peak indicated by the perturb and observe autofocusing algorithm.

the optimal scanning procedure consequently skipping 12 grid cells without membrane filter while scanning the 13 mm membrane and 76 grid cells when scanning the 25 mm membrane. Hence, only 105 and 356 images are to capture the 13 and 25 mm membrane filters, respectively, as illustrated in fig. 8.4.

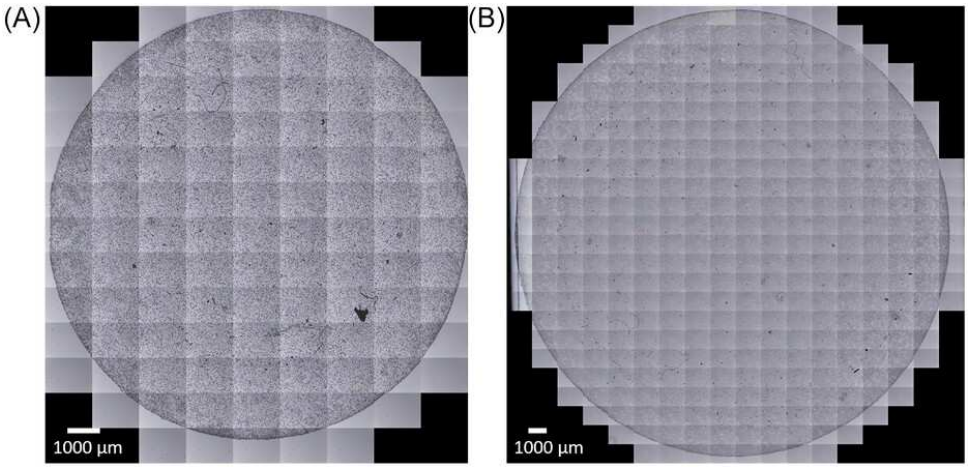

Figure 8.4: Capture of the (A) 13 mm and (B) 25 mm membrane filters using the optimal automated slide scanning procedure with skipped grid cells highlighted in black.

The efficiency gains become particularly crucial in resource-constrained settings with a significant disease burden, where microscopic examination of urine samples is recommended by the WHO for the diagnosis of urogenital schistosomiasis. Considering that conventional microscopy typically takes around 5 min per sample, the further reduction in scanning time for the 25 mm membrane filter from 30 to 25 min per sample, achieved through our optimised membrane scanning procedure, significantly enhances the practicality of deploying the Schistoscope for large-scale schistosomiasis monitoring and evaluation programs, especially in regions with a high disease burden. To further enhance the computational efficiency of the Schistoscope, we acknowledge the potential benefits of implementing the algorithm in a more efficient language like C++. Additionally, exploring low-cost options for hardware acceleration, such as GPUs and TPUs, could provide further improvements.

8.6. CONCLUSION

This paper introduces a novel procedure for automated slide scanning of membrane filters in the diagnosis of urogenital schistosomiasis.

The procedure focuses on estimating and capturing field-of-view (FoV) images only in grid cells where the membrane filter is present, optimising efficiency. Additionally, we have developed a perturb and observe autofocusing algorithm that employs a hill-climbing approach, utilising the mean of the Gaussian gradient of the FoV image as a figure of merit to determine the optimal focus plane. To evaluate the performance of our developed procedure, we implemented it on the Schistoscope and experimentally assessed of its scanning capabilities using the commonly used 13 and 25 mm membrane filters for diagnosing urogenital schistosomiasis. Our results obtained 63% and 72% s improvements in scanning times for the 13 and 25 mm membrane filters respectively compared to the traditional grid scanning procedure with the focus map surveying autofocusing algorithm.

The significant reduction in scanning time greatly enhances the applicability of the Schistoscope for large-scale schistosomiasis monitoring and evaluation programs in regions where the disease is prevalent. Moreover, the optimised scanning procedure can be adapted to minimise scanning time in whole slide imaging of other biological tissue smears with shapes closely resembling that of a circle (e.g., stool and thick blood smears in the diagnosis of soil transmitted helminth and malaria parasite infections respectively). Moving forward, our future work, we plan to conduct a large-scale validation study to evaluate the performance of the Schistoscope with artificial intelligence for diagnosis of urinogenital schistosomiasis in field settings.

ACKNOWLEDGEMENTS

We acknowledge the Neglected Tropical Disease team from the Federal Ministry of Health Abuja and Federal Capital Territory Authority Public Health Laboratory Abuja, Nigeria and Delft University of Technology Global Initiative for their support towards this study. This work was funded by the Nederlandse Organisatie voor Wetenschappelijk Onderzoek (NWO), WOTRO Science for Global Development program, Grant Number W 07.30318.009 (INSPiRED – INclusive diagnoStics for Poverty RELated parasitic Diseases in Nigeria and Gabon).

CONFLICT OF INTEREST STATEMENT

The authors declare no potential conflict of interests.

REFERENCES

[1] A. F. Adenowo, B. E. Oyinloye, B. I. Ogunyinka, and A. P. Kappo. “Impact of human schistosomiasis in sub-Saharan Africa”. In: *Brazilian Journal of Infectious Diseases* 19.2 (2015), pp. 196–205. doi: j.bjid.2014.11.004.

[2] S. Aksoy, P. Buscher, M. Lehane, P. Solano, and J. Van Den Abbeele. “Human African trypanosomiasis control: Achievements and challenges”. In: *PLoS Neglected Tropical Diseases* 11.4 (2017), e0005454. doi: 10.1371/journal.pntd.0005454.

[3] W. P. O’Meara, J. N. Mangeni, R. Steketee, and B. Greenwood. “Changes in the burden of malaria in sub-Saharan Africa”. In: *The Lancet Infectious Diseases* 10.8 (2010), pp. 545–555. doi: 10.1016/S1473-3099(10)70096-7.

[4] A. Silumbwe, J. M. Zulu, H. Halwindi, C. Jacobs, J. Zgambo, R. Dambe, M. Chola, G. Chongwe, and C. Michelo. “A systematic review of factors that shape implementation of mass drug administration for lymphatic filariasis in sub-Saharan Africa”. In: *BMC Public Health* 17.1 (2017), p. 484. doi: 10.1186/s12889-017-4414-5.

[5] M. O. Afolabi, A. Adebiyi, J. Cano, B. Sartorius, B. Greenwood, O. Johnson, and O. Wariri. “Prevalence and distribution pattern of malaria and soil-transmitted helminth co-endemicity in sub-Saharan Africa, 2000–2018: A geospatial analysis”. In: *PLoS Neglected Tropical Diseases* 16.9 (2022), e0010321. doi: 10.1371/journal.pntd.0010321.

[6] B. Meulah, P. Oyibo, M. Bengtson, T. Agbana, R. A. L. Lontchi, A. A. Adegnika, W. Oyibo, C. H. Hokke, J. C. Diehl, and L. v. Lieshout. “Performance Evaluation of the Schistoscope 5.0 for (Semi-)automated Digital Detection and Quantification of Schistosoma haematobium Eggs in Urine: A Field-based Study in Nigeria”. In: *The American Journal of Tropical Medicine and Hygiene* 107.5 (2022). doi: 10.4269/ajtmh.22-0276.

[7] J. C. Diehl, P. Oyibo, T. Agbana, S. Jujjavarapu, G. Van, G. Vdovin, and W. Oyibo. “Schistoscope: Smartphone versus Raspberry Pi based low-cost diagnostic device for urinary Schistosomiasis”. In: *Proceedings of the 2020 IEEE Global Humanitarian Technology*

Conference (GHTC). Seattle, WA, USA, 2020, pp. 1–8. doi: 10.1109/GHTC46280.2020.9342871.

[8] P. Ward, P. Dahlberg, O. Lagatie, J. Larsson, A. Tynong, J. Vlaminck, M. Zumpe, S. Ame, M. Ayana, V. Khieu, Z. Mekonnen, M. Odiere, T. Yohannes, S. V. Hoecke, B. Levecke, and L. J. Stuyver. "Affordable artificial intelligence-based digital pathology for neglected tropical diseases: A proof-of-concept for the detection of soil-transmitted helminths and Schistosoma mansoni eggs in Kato-Katz stool thick smears". In: *PLoS neglected tropical diseases* 16.6 (2022), e0010500. doi: 10.1371/journal.pntd.0010500.

[9] A. Caetano, C. Santana, and R. A. de Lima. "Diagnostic support of parasitic infections with an AI-powered microscope". In: *Research on Biomedical Engineering* 39.3 (2023), pp. 561–572. doi: 10.1007/s42600-023-00288-6.

[10] Z. Bian, C. Guo, S. Jiang, J. Zhu, R. Wang, P. Song, Z. Zhang, K. Hoshino, and G. Zheng. "Autofocusing technologies for whole slide imaging and automated microscopy". In: *Journal of Biophotonics* 13.12 (2020), e202000227. doi: 10.1002/jbio.202000227.

[11] J. R. Gilbertson, J. Ho, L. Anthony, D. M. Jukic, Y. Yagi, and A. V. Parwani. "Primary histologic diagnosis using automated whole slide imaging: A validation study". In: *BMC Clinical Pathology* 6 (2006), pp. 1–19. doi: 10.1186/1472-6890-6-4.

[12] T. Kohlberger, Y. Liu, M. Moran, P. H. C. Chen, T. Brown, J. D. Hipp, C. H. Mermel, and M. C. Stumpe. "Whole-slide image focus quality: Automatic assessment and impact on AI cancer detection". In: *Journal of Pathology Informatics* 10.1 (2019), p. 39. doi: 10.4103/jpi.jpi_11_19.

[13] C. Massone, H. P. Soyer, G. P. Lozzi, A. Di Stefani, B. Leinweber, G. Gabler, M. Asgari, R. Boldrini, L. Bugatti, V. Canzonieri, G. Ferrara, K. Kodama, D. Mehregan, F. Rongioletti, S. A. Janjua, V. Mashayekhi, I. Vassilaki, B. Zelger, B. Žgavec, and H. Kerl. "Feasibility and diagnostic agreement in teledermatopathology using a virtual slide system". In: *Human Pathology* 38.4 (2007), pp. 546–554. doi: 10.1016/j.humpath.2006.10.006.

[14] T. R. Dastidar and R. Ethirajan. "Whole slide imaging system using deep learning-based automated focusing". In: *Biomedical Optics Express* 11.1 (2020), pp. 480–491. doi: 10.1364/BOE.379780.

[15] Y. Liron, Y. Paran, N. G. Zatorsky, B. Geiger, and Z. Kam. “Laser autofocusing system for high-resolution cell biological imaging”. In: *Journal of Microscopy* 221.2 (2006), pp. 145–151. doi: 10.1111/j.1365-2818.2006.01550.x.

[16] G. Reinheimer. “Arrangement for automatically focussing an optical instrument”. Pat. US3721827A. 1973.

[17] A. Cable, J. Wollenzin, R. Johnstone, K. Gossage, J. S. Brooker, J. Mills, J. Jiang, and D. Hillmann. “Microscopy system with auto-focus adjustment by low-coherence interferometry”. Pat. US9869852B2. 2018.

[18] J. S. Silfies, E. G. Lieser, S. A. Schwartz, and M. W. Davidson. *Nikon Perfect Focus System (PFS)*. 2024. url: https://www.microscopyu.com/tutorials/the-nikon-perfect-focus-system-pfs (visited on 08/04/2024).

[19] R. R. McKay, V. A. Baxi, and M. C. Montalto. “The accuracy of dynamic predictive autofocusing for whole slide imaging”. In: *Journal of Pathology Informatics* 2.1 (2011), p. 38. doi: 10.4103/2153-3539.84231.

[20] T. Virág, A. László, B. Molnár, A. Tagscherer, and V. S. Varga. “Focusing method for the high-speed digitalisation of microscope slides and slide displacing device, focusing optics, and optical rangefinder”. Pat. US7663078B2. 2010.

[21] R. T. Dong, U. Rashid, and J. Zeineh. “System and method for generating digital images of a microscope slide”. Pat. US20050089208A1. 2005.

[22] K. Guo, J. Liao, Z. Bian, X. Heng, and G. Zheng. “InstantScope: A low-cost whole slide imaging system with instant focal plane detection”. In: *Biomedical Optics Express* 6.9 (2015), pp. 3210–3216. doi: 10.1364/BOE.6.003210.

[23] J. Liao, X. Chen, G. Ding, P. Dong, H. Ye, H. Wang, Y. Zhang, and J. Yao. “Deep learning-based single-shot autofocus method for digital microscopy”. In: *Biomedical Optics Express* 13.1 (2022), pp. 314–327. doi: 10.1364/BOE.446928.

[24] L. Silvestri, M. C. Müllenbroich, I. Costantini, A. P. D. Giovanna, L. Sacconi, and F. S. Pavone. *RAPID: Real-time image-based autofocus for all wide-field optical microscopy systems*. preprint. 2017. doi: 10.1101/170555. bioRxiv: 170555.

[25] S. Jiang, J. Liao, Z. Bian, K. Guo, Y. Zhang, and G. Zheng. “Transform- and multi-domain deep learning for single-frame rapid autofocusing in whole slide imaging”. In: *Biomedical Optics Express* 9.4 (2018), pp. 1601–1612. doi: 10.1364/BOE.9.001601.

[26] Y. Rivenson, Z. Göröcs, H. Günaydin, Y. Zhang, H. Wang, and A. Ozcan. “Deep learning microscopy”. In: *Optica* 4.11 (2017), pp. 1437–1443. doi: 10.1364/OPTICA.4.001437.

[27] N. Dimitriou, O. Arandjelović, and P. D. Caie. “Deep learning for whole slide image analysis: An overview”. In: *Frontiers in Medicine* 6 (2019). doi: 10.3389/fmed.2019.00264.

[28] H. R. Tizhoosh and L. Pantanowitz. “Artificial intelligence and digital pathology: Challenges and opportunities”. In: *Journal of Pathology Informatics* 9.1 (2018), p. 38. doi: 10.4103/jpi.jpi_53_18.

[29] H. Pinkard, Z. Phillips, A. Babakhani, D. A. Fletcher, and L. Waller. “Deep learning for single-shot autofocus microscopy”. In: *Optica* 6.6 (2019), pp. 794–797. doi: 10.1364/OPTICA.6.000794.

[30] P. H. C. Chen, K. Gadepalli, R. MacDonald, Y. Liu, S. Kadowaki, K. Nagpal, T. Kohlberger, J. Dean, G. S. Corrado, J. D. Hipp, C. H. Mermel, and M. C. Stumpe. “An augmented reality microscope with real-time artificial intelligence integration for cancer diagnosis”. In: *Nature Medicine* 25.9 (2019), pp. 1453–1457. doi: 10.1038/s41591-019-0539-7.

[31] J. Liao, Z. Wang, Z. Zhang, Z. Bian, K. Guo, A. Nambiar, Y. Jiang, S. Jiang, J. Zhong, M. Choma, and G. Zheng. “Dual light-emitting diode-based multichannel microscopy for whole-slide multiplane, multispectral and phase imaging”. In: *Journal of Biophotonics* 11.2 (2017), e201700075. doi: 10.1002/jbio.201700075.

[32] S. Jiang, Z. Bian, X. Huang, P. Song, H. Zhang, Y. Zhang, and G. Zheng. “Rapid and robust whole slide imaging based on LED-array illumination and color-multiplexed single-shot autofocusing”. In: *Quantitative Imaging in Medicine and Surgery* 9.5 (2019), pp. 823–831. doi: 10.21037/qims.2019.05.04.

[33] J. Liao, S. Jiang, Z. Zhang, K. Guo, Z. Bian, Y. Jiang, J. Zhong, and G. Zheng. “Terapixel hyperspectral whole-slide imaging via slit-array detection and projection”. In: *Journal of Biomedical Optics* 23.6 (2018), p. 066503. doi: 10.1117/1.JBO.23.6.066503.

[34] J. Liao, Y. Jiang, Z. Bian, B. Mahrou, A. Nambiar, A. W. Magsam, K. Guo, S. Wang, Y. K. Cho, and G. Zheng. “Rapid focus map surveying for whole slide imaging with continuous sample motion”. In: *Optics Letters* 42.17 (2017), pp. 3379–3382. doi: 10.1364/OL.42.003379.

[35] C. Guo, Z. Bian, S. Jiang, M. Murphy, J. Zhu, R. Wang, P. Song, X. Shao, Y. Zhang, and G. Zheng. “OpenWSI: A low-cost, high-throughput whole slide imaging system via single-frame autofocusing and open-source hardware”. In: *Optics Letters* 45.1 (2019), pp. 260–263. doi: 10.1364/OL.45.000260.

[36] J. F. Brenner, B. S. Dew, J. B. Horton, T. King, P. W. Neurath, and W. D. Selles. “An automated microscope for cytologic research a preliminary evaluation”. In: *Journal of Histochemistry & Cytochemistry* 24.1 (1976), pp. 100–111. doi: 10.1177/24.1.1254907.

[37] J. M. Geusebroek, F. Cornelissen, A. W. Smeulders, and H. Geerts. “Robust autofocusing in microscopy”. In: *Cytometry* 39.1 (2000), pp. 1–9. doi: 10.1002/(SICI)1097-0320(20000101)39:1<1::AID-CYTO2>3.0.CO;2-J.

[38] M. J. Russell and T. S. Douglas. “Evaluation of autofocus algorithms for tuberculosis microscopy”. In: *29th Annual International Conference of the IEEE Engineering in Medicine and Biology Society*. Lyon, France, 2007, pp. 3489–3492. doi: 10.1109/IEMBS.2007.4353082.

[39] J. M. Mateos-Pérez, R. Redondo, R. Nava, J. C. Valdiviezo, G. Cristóbal, B. Escalante-Ramírez, M. J. Ruiz-Serrano, J. Pascau, and M. Desco. “Comparative evaluation of autofocus algorithms for a real-time system for automatic detection of Mycobacterium tuberculosis”. In: *Cytometry Part A* 81A.3 (2012), pp. 213–221. doi: 10.1002/cyto.a.22020.

[40] R. Redondo, G. Bueno, J. C. Valdiviezo, R. Nava, G. Cristóbal, O. Déniz, M. García-Rojo, J. Salido, M. d. M. Fernández, J. Vidal, and B. Escalante-Ramírez. “Autofocus evaluation for brightfield microscopy pathology”. In: *Journal of Biomedical Optics* 17.3 (2012), pp. 036008–036008. doi: 10.1117/1.JBO.17.3.036008.

[41] S. Y. Wu, N. Dugan, and B. M. Hennelly. “Investigation of autofocus algorithms for brightfield microscopy of unstained cells”. In: *Proceedings of SPIE – The International Society for Optical Engineering*. Vol. 9131. Brussels, Belgium, 2014, 91310T. doi: 10.1117/12.2051944.

[42] F. R. Boddeke, L. J. Van Vliet, and I. T. Young. “Calibration of the automated z-axis of a microscope using focus functions”. In: *Journal of Microscopy* 186.3 (1997), pp. 270–274. doi: 10.1046/j.1365-2818.1997.2060766.x.

[43] T. Rai Dastidar. “Automated focus distance estimation for digital microscopy using deep convolutional neural networks”. In: *2019 IEEE/CVF Conference on Computer Vision and Pattern Recognition Workshops (CVPRW)*. Long Beach, CA, USA, 2019, pp. 1049–1056. doi: 10.1109/CVPRW.2019.00137.

[44] P. Oyibo, S. Jujjavarapu, B. Meulah, T. Agbana, I. Braakman, A. van Diepen, M. Bengtson, L. van Lieshout, W. Oyibo, G. Vdovine, and J. C. Diehl. “Schistoscope: An Automated Microscope with Artificial Intelligence for Detection of Schistosoma haematobium Eggs in Resource-Limited Settings”. In: *Micromachines* 13.5 (2022), p. 643. doi: 10.3390/mi13050643.

[45] A. S. Mahdi, A. K. Mahamad, S. Saon, T. Tuwoso, H. Elmunsyah, and S. W. Mudjanarko. “Maximum power point tracking using perturb and observe, fuzzy logic and ANFIS”. In: *SN Applied Sciences* 2.1 (2019), p. 89. doi: 10.1007/s42452-019-1886-1.

[46] M. Kavya and S. Jayalalitha. “Developments in perturb and observe algorithm for maximum power point tracking in photo voltaic panel: A review”. In: *Archives of Computational Methods in Engineering* 28.4 (2021), pp. 2447–2457. doi: 10.1007/s11831-020-09461-x.

9

GABON FIELD VALIDATION STUDY

Validation of artificial intelligence-based digital microscopy for automated detection of *Schistosoma haematobium* eggs in urine in Gabon

Brice Meulah, Prosper Oyibo, Pytsje T. Hoekstra, Paul Alvyn Nguema Moure, Moustapha Nzamba Maloum, Romeo Aime Laclong-Lontchi, Yabo Josiane Honkpehedji, Michel Bengtson, Cornelis Hokke, Paul L. A. M. Corstjens, Temitope Agbana, Jan Carel Diehl, Ayola Akim Adegnika, Lisette van Lieshout

PUBLICATION REPORT

- **Publication Date:** 23 February 2024
- **Journal:** PLOS Neglected Tropical Diseases
- **Publisher:** PLOS
- **DOI:** 10.1371/journal.pntd.0011967

ABSTRACT

INTRODUCTION

Schistosomiasis is a significant public health concern, especially in Sub-Saharan Africa. Conventional microscopy is the standard diagnostic method in resource-limited settings, but with limitations, such as the need for expert microscopists. An automated digital microscope with artificial intelligence (Schistoscope), offers a potential solution. This field study aimed to validate the diagnostic performance of the Schistoscope for detecting and quantifying Schistosoma haematobium eggs in urine compared to conventional microscopy and to a composite reference standard (CRS) consisting of real-time PCR and the up-converting particle (UCP) lateral flow (LF) test for the detection of schistosome circulating anodic antigen (CAA).

METHODS

Based on a non-inferiority concept, the Schistoscope was evaluated in two parts: study A, consisting of 339 freshly collected urine samples and study B, consisting of 798 fresh urine samples that were also banked as slides for analysis with the Schistoscope. In both studies, the Schistoscope, conventional microscopy, real-time PCR and UCP-LF CAA were performed and samples with all the diagnostic test results were included in the analysis. All diagnostic procedures were performed in a laboratory located in a rural area of Gabon, endemic for S. haematobium.

RESULTS

In study A and B, the Schistoscope demonstrated a sensitivity of 83.1% and 96.3% compared to conventional microscopy, and 62.9% and 78.0% compared to the CRS. The sensitivity of conventional microscopy in study A and B compared to the CRS was 61.9% and 75.2%, respectively, comparable to the Schistoscope. The specificity of the Schistoscope in study A (78.8%) was significantly lower than that of conventional microscopy (96.4%) based on the CRS but comparable in study B (90.9% and 98.0%, respectively).

CONCLUSION

Overall, the performance of the Schistoscope was non-inferior to conventional microscopy with a comparable sensitivity, although the specificity varied. The Schistoscope shows promising diagnostic accuracy, particularly for samples with moderate to higher infection intensities as well as for banked sample slides, highlighting the potential for retrospective analysis in resource-limited settings.

9.1. INTRODUCTION

Schistosomiasis is a tropical parasitic disease of significant public health concern, with an estimated 700 million individuals at risk of infection in areas known for transmission. Out of approximately 250 million people requiring preventive chemotherapy worldwide, Sub-Saharan Africa, including the centrally located country of Gabon, bears the highest proportion [1–3]. In order to control the disease morbidity and work towards its elimination as a public health problem, the World Health Organisation (WHO) recommends annual preventive chemotherapy using a single dose of praziquantel for all individuals aged two years and above in communities where the prevalence of schistosomiasis is 10% or higher [4]. For communities with a prevalence below 10%, an optional test-and-treat strategy is recommended [4]. In both cases, reliable diagnostic tools are essential to support the monitoring and evaluation of these control strategies [5, 6].

Conventional microscopy is the standard diagnostic procedure for schistosomiasis. However, the need for expert microscopists limits its application in resource-limited settings. Real-time polymerase chain reaction (PCR) for amplification and detection of schistosome-specific nucleic acid sequences, as well as a lateral flow test (LF) for the detection of schistosome-specific circulating anodic antigen (CAA), offer higher sensitivity and specificity than conventional microscopy [7, 8]. Nevertheless, the requirement for specialized skills and advanced infrastructure currently limits their application in resource-limited settings.

Alternatively, automated digital microscopes have shown promising results in the diagnosis of schistosomiasis by detecting parasite eggs in stool or urine [9–12]. The application of artificial intelligence (AI) algorithms in the diagnosis and surveillance of infectious diseases has received significant attention [13–15]. Automated digital microscopes are designed to capture images of samples with simultaneous analysis by an AI algorithm trained to detect parasite components. Such innovative tools are relatively easy to use and can be customised for rural endemic settings. These tools also have propitious downstream applications including digital health [11, 16–18]. In particular for the detection of *S. haematobium* eggs in urine, multiple studies have validated the diagnostic accuracy of AI-based digital microscopes, demonstrating sensitivities ranging from 32% to 91% compared to conventional microscopy, as summarised in a recent review [11].

The Schistoscope is an automated digital microscope with an integrated AI algorithm to detect *S. haematobium* eggs in urine samples. It was developed for use at point-of-need and is relatively easy to operate requiring minimal training [19, 20]. The Schistoscope was first assessed in Nigeria for diagnosing urogenital schistosomiasis, revealing a high sensitivity but a rather low specificity compared to conventional

microscopy [12]. Based on these results, the AI model was re-designed, retrained and embedded onboard the Schistoscope, and then validated using a set of field sample images, yielding better sensitivity and specificity [21]. A limitation of the previous studies has been the small size of validation sample dataset and the lack of an accurate reference standard. To perform more in-depth validation of the diagnostic accuracy of the Schistoscope in detecting *S. haematobium* eggs, urine samples were collected and analysed in a laboratory setting in Lambaréné, Gabon. The diagnostic performance of the Schistoscope was compared to conventional microscopy as well as to a composite reference standard (CRS), consisting of real-time PCR and UCP-LF CAA.

9.2. METHODS

9.2.1. ETHICS STATEMENT

Ethical approval for the study was obtained from the Comité d'Éthique Institutionnel (CEI) du Centre de Recherches Médicales de Lambaréné in Lambaréné, Gabon (reference no. CEI-CERMEL 005/2020). Prior to sample collection, written consent was obtained from adults and from parents or legal guardians of children and teenagers who wished to participate, indicated by their signatures. To ensure confidentiality and anonymity of the results, unique codes were assigned to the samples. Participants with detectable *S. haematobium* eggs/10 mL of urine based on microscopy were treated with praziquantel (40 mg/Kg of body weight) following local guidelines. The study was registered at ClinicalTrials.gov (NCT04505046).

9.2.2. STUDY DESIGN

The validation study was conducted in Lambaréné and surrounding areas, located in the Moyen-Ogooué province in Gabon, a region known to be endemic for *S. haematobium* with a prevalence of about 30% [22]. It was carried out in two parts: study A and study B (fig. 9.1). Study A was an independent cross-sectional study focusing on school-age children and adults from whom urine samples were collected and analysed by the Schistoscope, conventional microscopy, real-time PCR and UCP-LF CAA (see details below). Study B was partly embedded in several ongoing studies at Centre de Recherches Médicales de Lambaréné (CERMEL) in Gabon, where urine samples were collected from different populations (school-age children, adults and pregnant women) and analysed with a range of diagnostic methods including conventional microscopy, real-time PCR and UCP-LF CAA (see details below). Microscopy slides were subsequently biobanked at 4°C for retrospective analysis with the Schistoscope (2 years later). All diagnostic procedures were conducted at CERMEL.

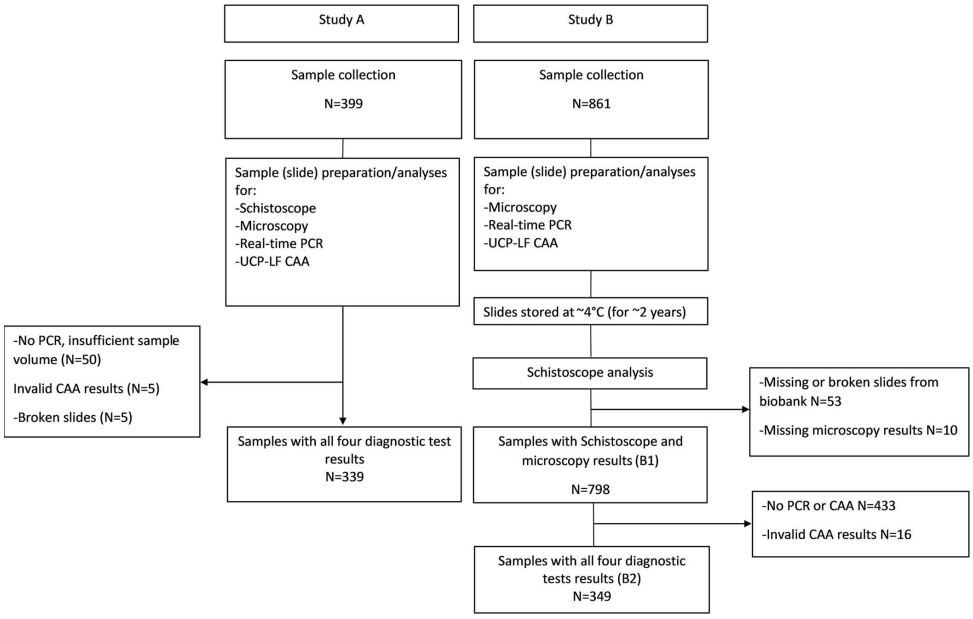

Figure 9.1: Comprehensive flow chart detailing the methodical sequence of urine sample collection, processing by the Schistoscope, conventional microscopy, real-time PCR and UCP-LF CAA and data analysis.

9.2.3. SAMPLE SIZE CALCULATIONS

The Schistoscope was assumed to have a sensitivity and specificity non-inferior to conventional microscopy, which were realistically assumed to be 80% and 90%, respectively based on field expert estimates using real-time PCR and UCP-LF CAA. The sample size for both study A and B were determined based on a 30% prevalence of schistosomiasis in Lambaréné and its surrounding areas using a two-sample matched paired design, resulting in a required sample size of 350 urine samples [23]. A power of 80% and a 5% degree of error was considered for the calculations.

9.2.4. SAMPLE COLLECTION AND PROCESSING

Collection of urine samples in study A was carried out starting in 2023 while the urine sample biobanking (study B) was initiated in 2020. Study participants were provided with sterile containers labelled with unique identifiers and instructed to provide urine samples between 11 am and 2 pm. The samples were transported to CERMEL within 2 hours of collection for analysis. Microscopy slides were prepared by pressing 10 mL of homogenised urine through a 25mm membrane (pore size

30 µm; Whatmann International Ltd) with the use of a syringe and a filter holder and transferred onto a glass slide. For study A, the slides were examined on the same day using conventional microscopy and the Schistoscope. For study B, the slides were examined using conventional microscopy and stored at 4°C for about 2 years awaiting analysis with the Schistoscope. For both studies, 1 mL of urine from each sample was used for UCP-LF CAA analysis and 10 mL of homogenised urine was centrifuged and the resulting 1mL pellet was used for DNA extraction and amplification before biobanking the sample slides for retrospective analysis with the Schistoscope.

9.2.5. DIAGNOSTIC METHODS

THE SCHISTOSCOPE

Five Schistoscopes were used in this study (fig. 9.2A and video S1). Analysis was done following the standard operating procedure (manual S1) of the Schistoscope. Briefly, the slide was placed on the slide holder of the Schistoscope such that its microscope objective aligned with the filter membrane of the slide. The device's autofocus algorithm positioned the microscope objective in the optimal focal plane. High resolution images of the sample were registered and analysed simultaneously by the integrated AI algorithm. The number of detected eggs (expressed in eggs/10 mL of urine) is displayed on a pop-up result window which also indicated the end of the sample analysis. Detected eggs are marked as shown in fig. 9.2B and C. The results from the Schistoscope were exported as an Excel-compatible file.

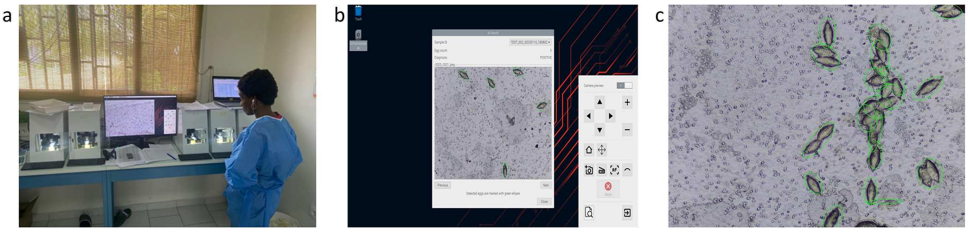

Figure 9.2: (a) Five Schistoscopes connected to a single display and in use for slide analysis by a laboratory technician. (b) Schistoscope display of result window after slide analysis is completed. (c) Schistoscope image showing some of the overlapping eggs counted as a single egg by the AI algorithm.

CONVENTIONAL MICROSCOPY

Slides from both studies were analysed immediately after urine filtration under 10x objective of a Leica microscope (model: DM1000 LED,

Microsystems CMS GmbH Ernt-Leitz-Str.17-37 Wetzlar, Germany). Each slide was examined by two independent microscopists and the mean egg count was calculated. In case of a >20% discrepancy in egg count, an additional reading by a third independent microscopist was required and the final egg count was determined by calculating the mean of the two closest egg counts obtained from the three readings. All egg counts were expressed as eggs/10 mL of urine. In addition, the storage conditions (4°C) and quality of the biobanked slides were monitored using conventional microscopy once every four months during the storage period. This was done by monitoring daily temperature of the fridge as well as by determining the egg counts of three known slides. Additionally, during the Schistoscope analysis the integrity of the biobank was quality controlled by re-examining a random selection of 10% of the slides by conventional microscopy and comparing the results to the outcomes before storage.

NUCLEIC ACID EXTRACTION AND REAL-TIME PCR

Genomic DNA extraction was carried out using the QIAamp Mini kit (cat: 51306; Qiagen) according to the manufacturer's instructions. Briefly, 195µL of each centrifuged urine pellet was mixed with 5µL of internal control DNA commercially available as a DNA Extraction Control (DEC) 670 kit (Cat: BIO-35028; Bioline). The DEC 670 kit is supplied as a vial of internal control DNA sequence (with no known homology to sequences of any organism) and a vial of control mix containing primers and probes complementary to the internal control DNA sequence. The final mixture was then processed as previously described [8].

Real-time PCR was performed as previously described [8, 24] using a set of primers (Ssp48F and Ssp124R) and probe (Ssp78T) complementary to the 77-bp internal transcribed spacer-2 (ITS2) sequence, with minor modifications on the internal control (see above) as well as on the reaction mixture and conditions used (see below).

Amplification reactions were performed in a 15µL reaction mixture containing 1x No-ROX master mix (Cat: BIO-86005; Bioline), 4.5pmol of each *Schistosoma*-specific primer, 1.5pmol *Schistosoma*-specific probe, 0.4µL of control mix, 1.2µL of nuclease free water and 2.5µL DNA extract. The PCR runs consisted of an initial step of 5 min at 95°C followed by 40 successive cycles of 10 sec at 95°C and 60 sec at 60°C. The reaction was run on a Light cycler 480 II real-time PCR system (Roche Diagnostics). *Schistosoma* DNA detection was expressed in threshold (Ct) cycles. For every run, a non-template control and a positive control (*S. haematobium* DNA, Ct-value 23–25) was included. A test was considered positive when the threshold was attained within 40 PCR cycles (Ct-value ≤ 40). Each sample was run in duplicate and was considered positive when at least one of the duplicates was positive. Amplification of the internal control at the expected Ct-value showed

success of nucleic acid extraction and no evidence of PCR inhibitors.

UCP-LF CAA

Urine CAA concentration was determined by the UCP-LF CAA assay using the UCAAhT417 format as previously described [7]. Briefly, 500µL of each urine sample was mixed with 100µL of 12% trichloroacetic acid, incubated and centrifuged. The clear supernatant obtained was concentrated to 20µL using an Amicon Ultra-4 concentration column (Millipore, Merck Chemicals B.V., Amsterdam, The Netherlands) and subsequently mixed with 50µL run buffer and added to 50 µL UCP solution. The resulting mixture was then used for the lateral flow assay. A set of CAA standards was used to validate the cut-off (2 pg/mL) as well as to reliably quantify the amount of CAA per sample up to 1000 pg/mL [7].

9.2.6. STATISTICAL ANALYSES

In study A, only samples with all four diagnostic test results available were included in the final analysis. For study B, samples with both the Schistoscope and conventional microscopy test results only were first analysed (B1). Additionally, a subset of samples (B2) which had outcomes of all four diagnostic tests was analysed separately (fig. 9.1). The percentage positive samples for a *Schistosoma* infection was determined for each diagnostic test. The sensitivity and specificity of the Schistoscope were assessed using conventional microscopy as the reference (study A, B1 and B2). Sensitivity and specificity of the Schistoscope and conventional microscopy were further evaluated using a combination of real-time PCR and/or UCP-LF CAA as a CRS (study A and B2). A sample was deemed positive by the CRS if it showed the presence of *Schistosoma* spp DNA and/or CAA. Conversely, a sample was considered negative if both diagnostic tests showed a negative outcome. A $\leq$ 10% difference in sensitivity and specificity between the Schistoscope and conventional microscopy based on the CRS was considered non-inferior. To determine the performance of the Schistoscope at different infection intensities, egg counts based on conventional microscopy were categorised into very low intensity infection (1–9 eggs/10 mL), low-intensity infection (10–49 eggs/10 mL) and high-intensity infection ($\geq$ 50 eggs/10 mL) [25, 26]. Cohen's Kappa (k) statistics was computed to assess the qualitative agreement between the Schistoscope and conventional microscopy, and the CRS. Spearman's correlation (r) was used to assess the strength of association between the Schistoscope and conventional microscopy, real-time PCR and UCP-LF CAA. Bland-Altman analysis was further used to assess the quantitative agreement between the Schistoscope and conventional microscopy. Wilcoxon sign rank test was used to compare the microscopy

egg count of the randomly selected banked slides before and after storage. Statistical analysis was performed using IBM Statistical Package for Social Sciences version 25 (SPSS Inc., Chicago, United States of America) and GraphPad Prism version 9.0.1 for Windows (GraphPad Software, San Diego, California USA, www.graphpad.com).

9.3. RESULTS

9.3.1. STUDY A: DIAGNOSTIC PERFORMANCE OF THE SCHISTOSCOPE ON FRESHLY PREPARED SAMPLES

A total of 339 samples had outcomes available for all four diagnostic tests and were included in the analysis. table 9.1 shows the proportion of positive results per diagnostic test. Real-time PCR found the highest proportion of positives (51.0%) followed by the UCP-LF CAA assay (46.6%). The proportion of positives detected by the Schistoscope (46.0%) was higher than that of conventional microscopy (38.3%). The median egg count of the Schistoscope (17 eggs/10mL) was lower than that of microscopy (31 eggs/10mL). The proportion of positives with egg count ≥ 50 eggs/10 mL by the Schistoscope and microscopy were comparable, 47 (30.1%) and 49 (37.7%), respectively (fig. S1A).

Table 9.1: Diagnostic outcomes of the Schistoscope in comparison to conventional microscopy, real-time PCR and UCP-LF CAA in study A and B.

Diagnostic test	**Study A (N = 339)**				**Study B1 (N = 798)**		**Study B2 (N = 349)**			
	Schisto-scope	**Micro-scopy**	**Real-time PCR**	**UCP-LF CAA**	**Schisto-scope**	**Micro-scopy**	**Schisto-scope**	**Micro-scopy**	**Real-time PCR**	**UCP-LF CAA**
Positive (%)	156 (46.0%)	130 (38.3%)	173 (51.0%)	158 (46.6%)	374 (46.9%)	307 (38.5%)	204 (58.5%)	190 (54.4%)	217 (62.2%)	225 (64.5%)
Range	1–1623 eggs/ 10mL	1–2516 eggs/ 10mL	20.2–37.0 Ct	2.6–1000.0 pg/ mL	1–2879 eggs/ 10mL	1–9350 eggs/ 10mL	1–1943 eggs/ 10mL	1–9350 eggs/ 10mL	19.1-38.7 Ct	2.1-1000.0 pg/mL
Median of the positives	17 eggs/ 10mL	31 eggs/ 10mL	29.0 Ct	65.0 pg/ mL	17 eggs/ 10mL	105 eggs/ 10mL	32 eggs/ 10mL	209 eggs/ 10mL	26.6 Ct	189.6 pg/mL
Mean of the positives	78 eggs/ 10mL	119 eggs/ 10mL	29.7 Ct	134.0 pg/ mL	136 eggs/ 10mL	464 eggs/ 10mL	160 eggs/ 10mL	565 eggs/ 10mL	27.8 Ct	310.5 pg/mL

Qualitatively, a moderate agreement between the Schistoscope and conventional microscopy was observed (K = 0.579, P<0.001). However, the agreement was only fair when compared to the CRS (K = 0.396, P<0.001) whereas a moderate agreement was observed between conventional microscopy and the CRS (K = 0.537, P<0.001) (table 9.2). The sensitivity and specificity of the Schistoscope were 83.1% and 77.0%, respectively, when conventional microscopy was used as reference.

In addition, when the Schistoscope and conventional microscopy were evaluated using the CRS, the sensitivity of the Schistoscope was 62.9% comparable to that of conventional microscopy, 61.9%. However, the specificity of the Schistoscope was significantly lower compared to the specificity of conventional microscopy. All samples with an egg count of *geq*50 eggs/10mL defined by conventional microscopy were detected by the Schistoscope (fig. S1A). Of the microscopy positive samples with 1–9 eggs/10mL and 10–49 eggs/10mL, the Schistoscope detected 52.6% and 90.7% respectively. Conversely, the Schistoscope found 48 additional cases (of which 40 had <50 eggs/10mL) which were not detected by conventional microscopy. Of these additional cases, 35.4% and 27.1% were confirmed by real-time PCR and the UCP-LF CAA assay, respectively.

Table 9.2: Diagnostic performance and pairwise level of agreement by Cohen's Kappa statistics between the Schistoscope and conventional microscopy and the composite reference for the detection of *S. haematobium* infection in study A and B.

Sample set	Diagnostic test	Reference test		Diagnostic test Sensitivity % (95% CI)	Diagnostic test Specificity % (95% CI)	Kappa	P value	Interpretation *
Study A (N=339)		Microscopy						
	Schistoscope	Positive	Negative	83.1 (75.5-89.1)	77.0 (70.7-82.5)	0.579	<0.001	Moderate
	Positive	108	48					
	Negative	22	161					
		Composite reference						
	Schistoscope	Positive	Negative	62.9 (55.8-69.6)	78.8 (71.0-85.3)	0.396	<0.001	Fair
	Positive	127	29					
	Negative	75	108					
		Composite reference						
	Schistoscope	Positive	Negative	61.9 (54.8-68.6)	96.4 (91.7-98.8)	0.537	<0.001	Moderate
	Positive	125	5					
	Negative	77	132					
Study B1 (N=798)		Microscopy						
	Schistoscope	Positive	Negative	93.2 (89.7-95.7)	82.1 (78.4-85.4)	0.723	<0.001	Substantial
	Positive	286	88					
	Negative	21	403					
Study B2 (N=349)		Microscopy						
	Schistoscope	Positive	Negative	96.3 (92.6-98.5)	86.8 (80.5-91.6)	0.837	<0.001	Almost perfect
	Positive	183	21					
	Negative	7	138					
		Composite reference						
	Schistoscope	Positive	Negative	78.0 (72.3-83.0)	90.9 (83.4-95.8)	0.604	<0.001	Moderate
	Positive	195	9					
	Negative	55	90					
		Composite reference						
	Schistoscope	Positive	Negative	75.2 (69.4-80.4)	98.0 (93.0-99.8)	0.619	<0.001	Substantial
	Positive	188	2					
	Negative	62	97					

A strong correlation was observed between egg counts estimated by the Schistoscope and conventional microscopy (r = 0.71, P<0.0001) (fig. 9.3A). A moderate correlation was observed between the Schistoscope egg counts and real-time PCR Ct-value (r = -0.58, P<0.0001), and CAA concentration (r = 0.58, P<0.0001) (fig. 9.3B and C, respectively). Bland-Altman analysis revealed that the Schistoscope tended to underscore egg counts compared to conventional microscopy, but approximately 95% of the difference in the egg count estimates between both methods fell within the limit of agreement (fig. 9.4A).

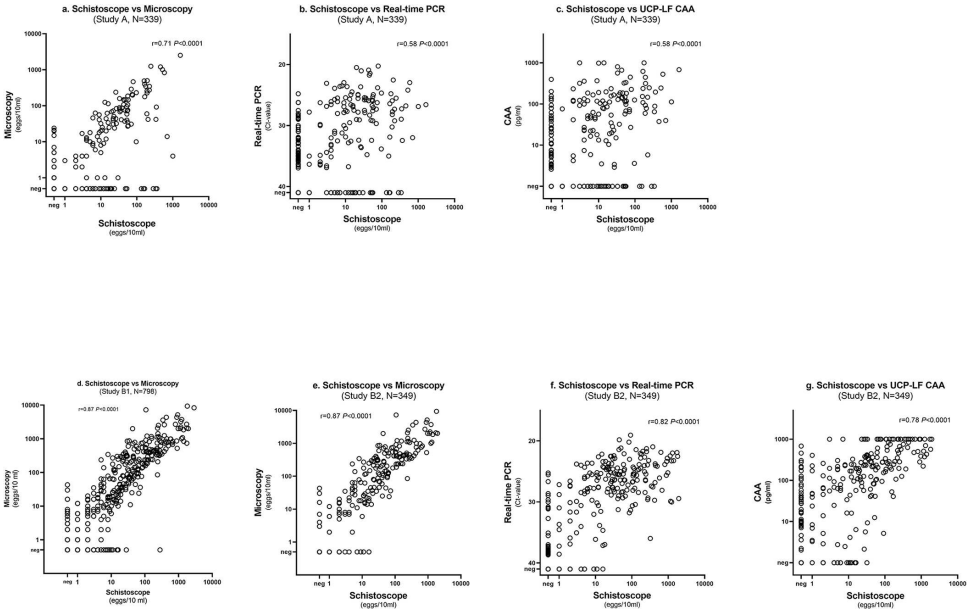

Figure 9.3: Correlation between *S. haematobium* egg counts measured by the Schistoscope and *S. haematobium* egg counts measured by conventional microscopy (a, d, e), Ct-values determined by real-time PCR (b, f) and urine CAA concentration measured by UCP-LF CAA (c, g) in study A and B.

9.3.2. STUDY B: DIAGNOSTIC PERFORMANCE OF THE SCHISTOSCOPE ON BANKED SAMPLES

A total of 798 samples, for which both Schistoscope and conventional microscopy results were available, were included in the analysis (Study B1). Quality control of the biobank revealed no significant difference in microscopy egg count before and after storage which confirmed the integrity of the biobank. The percentage of positive cases detected by the Schistoscope (46.9%) was higher than by conventional microscopy

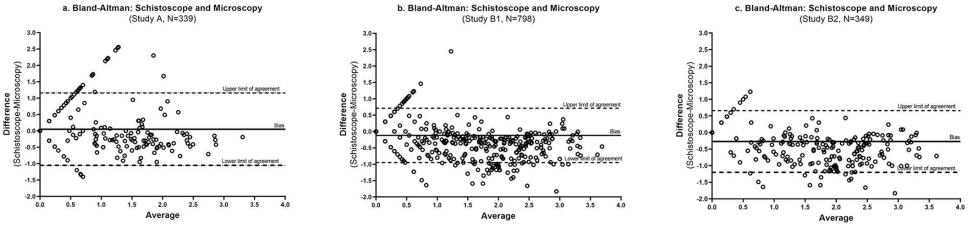

Figure 9.4: Bland-Altman analysis demonstrating the quantitative agreement between the Schistoscope and conventional microscopy in study A (a) and B (b, c).

(38.5%). The proportion of positives with an egg count of ≥ 50 eggs/10 mL was substantially lower by the Schistoscope (32.6%) than by conventional microscopy (59.3%) (fig. S1B and C).

A subset of 349 samples had test results available from all four diagnostic tests and were further analysed (Study B2). Based on real-time PCR and UCP-LF CAA a high percentage positive was observed, 62.2% and 64.5%, respectively. The percentage of positive cases detected by the Schistoscope and conventional microscopy were similar, 58.5% and 54.4% respectively, with a significantly different median egg count (table 9.1). All samples with high infection intensity were detected by the Schistoscope (fig. S1C). In addition, the Schistoscope detected 76.5% and 93.0% of samples with microscopy egg count 1–9 eggs/10mL and 10–49 eggs/10mL respectively. On the contrary, the Schistoscope found 21 additional cases with low infection intensity not detected by conventional microscopy. Of the 21 cases, 57.6% and 38.1% were confirmed by real-time PCR and UCP-LF CAA assay respectively.

A substantial to almost perfect qualitative agreement between the Schistoscope and conventional microscopy was observed in study B1 and B2 respectively (table 9.2). The agreement between the Schistoscope and the CRS was similar to the agreement between conventional microscopy and the CRS. The sensitivities and specificities of the Schistoscope in study B1 and B2 when conventional microscopy was used as a reference were comparable. Furthermore, a comparable sensitivity and specificity between the Schistoscope and conventional microscopy was observed when evaluating both methods against the CRS.

A very strong correlation between the egg counts of the Schistoscope and conventional microscopy was observed in study B1 ($r = 0.87$; $P<0.0001$, fig. 9.3D) and study B2 ($r = 0.93$, $P<0.0001$, fig. 9.3E). In study B2, a lower though significant correlation was observed between the Schistoscope egg counts and PCR Ct-values ($r = -0.82$, $P<0.0001$) and CAA concentration ($r = 0.78$, $P<0.0001$) (fig. 9.3F and G). Bland-Altman analysis further demonstrated a strong quantitative

agreement between the Schistoscope and conventional microscopy in both study B1 and B2 (fig. 9.4B and C) with a trend in the Schistoscope underestimating egg count.

9.4. DISCUSSION

For the first time, we demonstrate the sensitivity and specificity of the Schistoscope with an onboard integrated AI on fresh (study A) and stored (study B) sample sets in comparison to conventional microscopy as well as to a more sensitive CRS consisting of real-time PCR and UCP-LF CAA. Five Schistoscopes were successfully transported and implemented in the parasitology laboratory of CERMEL, a reference laboratory setting within a rural part of Gabon, which is a region endemic for *S. haematobium*. All other diagnostic tests were also performed at CERMEL. Overall, the performance of the Schistoscope was non-inferior to conventional microscopy with a comparable sensitivity and a slightly lower specificity. The Schistoscope is a promising tool for urogenital schistosomiasis screening in endemic settings and offers the advantage of data connectivity and the possibility of task shifting [27–29].

Qualitatively, a moderate to almost perfect agreement between the Schistoscope and conventional microscopy was found while a fair to moderate agreement was observed when compared to the CRS. This lower agreement can mainly be attributed to the fact that the two additional diagnostic tests included in the CRS (PCR and CAA) are more accurate, especially at low infection intensities, and these tend to be missed by the Schistoscope and/or conventional microscopy. The sensitivity of the Schistoscope was found to be non-inferior to conventional microscopy in both study A and B2. The specificity of the Schistoscope was however inferior to conventional microscopy in study A, but comparable in study B2. This is thought to be a consequence of the presence of relatively more artifacts in the freshly prepared slides (study A) compared to stored slides (study B), which the AI algorithm could not differentiate from eggs. Secondly, although samples in study A and B were obtained from the same geographical area in Gabon (Lambaréné and its surrounding villages), they were collected at different time points (2 years apart) as well as from different populations, i.e. community-based in study A versus specific populations including pregnant women in study B. Differences in urine composition due to differential seasonal concomitant bacterial infections was assumed to explain increase in egg-like crystals formation in urine that interfered with AI detection. Manual re-analysis of the images of a selection of samples that were positive by the Schistoscope but negative by conventional microscopy, revealed that indeed crystals were present in these slides, which the AI incorrectly identified as eggs (fig. S3).

Although the sensitivity of the Schistoscope in study A (83.1%) was

comparable to previously reported results from a field setting in Nigeria (87.3%) [12], the observed specificity was significantly higher (77.0% compared to 48.9% in Nigeria) as well as the correlation between egg counts by the Schistoscope and conventional microscopy, indicating the successful re-designing and re-training of the AI algorithm [21]. The slightly lower correlation observed between the Schistoscope egg count and real-time PCR Ct-values or CAA concentration could be because of the differences in diagnostic target; eggs, egg-DNA and circulating antigen, respectively. The correlation between conventional microscopy and real-time PCR or UCP-LF CAA resulted in a similar observation (fig. S2). The correlation observed between egg counts by conventional microscopy and Ct-values is comparable to previous findings [30]. Furthermore, although a better correlation would be expected between egg counts and Ct-values (egg-DNA), considering that they are both egg-based detection methods, it is important to note that, an egg does not have a fixed target DNA copy number. This variation is influenced by the egg developmental stage, which could account for the broad spectrum of Ct-values observed across varying infection intensities or egg count [31].

In study B overall, over 50% of the samples had only results for microscopy and the Schistoscope and rather than discarding this number of samples from our data set, it was analysed separately as B1. For both studies, all cases with high infection intensity based on conventional microscopy, known to correlate strongly with morbidity of the disease [32], were detected by the Schistoscope. Following Bland-Altman's analysis, a constant but clinically fair bias (absolute error) between Schistoscope and conventional microscopy egg counts was observed in both the fresh and stored sample sets, suggesting that the Schistoscope is slightly underestimating egg counts at a constant rate. This could be explained by the fact that with increasing infection intensity, eggs tend to overlap which could not be accurately counted by the AI algorithm (fig. 9.2C), as also observed previously [12]. Furthermore, the AI algorithm was designed and optimised for specificity at the expense of sensitivity, i.e. it was programmed to refrain from detecting truncated eggs located on boundaries of images so as to reduce the chances of detecting artifacts as well as eggs with lower morphological attributes. Such errors can be corrected by further optimisation of the AI algorithm in order to quantify the number of eggs more accurately. Also, in both the fresh and stored sample set, the majority of missed cases by the Schistoscope had a very low intensity of infection based on conventional microscopy ($\leq$ 5 eggs/10mL), highlighting another area of focus for the next generation of the Schistoscope.

Our results indicated a better sensitivity of the Schistoscope on banked sample slides compared to fresh samples. This could be due to the difference in the infection intensity observed in the two studies.

The median egg count, based on conventional microscopy, was lower in the fresh samples compared to the banked samples, which implies that the Schistoscope performs better on samples with a higher infection intensity, as also previously reported [12, 21]. Nevertheless, our results demonstrate a good performance of the Schistoscope on banked sample slides, indicating the possibility for retrospective analysis of banked sample slides in settings lacking direct access to microscopists.

In study A, the sensitivity of conventional microscopy estimated based on the CRS (62%) was lower than the sensitivity (80%) assumed for power calculations, in contrast to study B where the sensitivity (75.2%) observed was comparable. Retrospectively, the sample size calculation was limited in that it did not take into account the proportion of high-intensity infections but only incorporated prevalence, which could have had a significant impact on the sensitivity of conventional microscopy as it is known that the sensitivity of microscopy is limited in case of low intensity infections [33]. Overall, the proportion of high-intensity infections in study A was significantly lower compared to study B, resulting in a lower sensitivity of conventional microscopy as observed in study A. Despite the difference between the assumed and obtained sensitivity of conventional microscopy, we still believe our study had sufficient power to accurately determine the performance of the Schistoscope. So far, the performance of the Schistoscope has been evaluated in two endemic settings in urine samples producing promising outcomes. There is need for more performance evaluation in diverse schistosomiasis endemic settings (in urine and stool) with different climatic conditions, such as the northern part of Sahel region. Also, a cost effective analysis should be performed to support the integration of such a tool in large scale control programmes.

Limitations of this study include the time it took to analyse a slide by the Schistoscope, which on average was 25 mins. for samples with egg counts $\geq$ 200 egg/10mL even more time was needed. Furthermore, in this study a filter membrane of diameter 25mm was used (following the standard protocol of CERMEL), which also increased the time of analysis by 3-fold compared to the use of a 13mm filter membrane [12]. If a smaller filter membrane is used and the Schistoscope is programmed to stop counting when reaching 50 eggs/10mL–as this is classified as a high infection intensity and in such cases a detailed egg count is often not required [26]–the total reading time could be reduced to less than 10 mins. A tool as such would complement the existing POC-CCA urine test, which has been recommended by the WHO for *S. mansoni* infections, in settings co-endemic for *S. haematobium*. Although the Schistoscope has been fully automated, the aesthetics are currently unsatisfactory [20]. Furthermore, there is need to make the Schistoscope field-friendly and compatible to very rural settings, including the addition of a power source, improving the user interface and making it more compact and

portable.

To conclude, in this study a follow-up assessment of the Schistoscope was conducted in a rural laboratory setting in Gabon, further validating its potential as a digital diagnostic tool for the identification and quantification of *S. haematobium* eggs in freshly collected as well as banked urine sample slides. Although the specificity of the Schistoscope could still be improved, its overall performance was non-inferior to conventional microscopy hence, a promising tool for urogenital schistosomiasis screening in endemic settings.

SUPPORTING INFORMATION

CHECKLIST S1

STARD-2015-Checklist. https://doi.org/10.1371/journal.pntd.0011967.s001 (DOCX)

FIG. S1

Agreement between the Schistoscope and microscopy per category of infection intensity in study A and B. https://doi.org/10.1371/journal.pntd.0011967.s002 (TIF)

FIG. S2

Correlation between *S. haematobium* egg counts measured by the conventional microscopy and Ct-values determined by by real-time PCR (a, c) and urine CAA concentration. https://doi.org/10.1371/journal.pntd.0011967.s003 (TIF)

FIG. S3

Image showing crystal incorrectly detected as an egg by the Schistoscope. https://doi.org/10.1371/journal.pntd.0011967.s004 (TIF)

MANUAL S1

Schistoscope user manual. https://doi.org/10.1371/journal.pntd.0011967.s005 (PDF)

VIDEO S1

Video showing the Schistoscopes running in the laboratory. https://doi.org/10.1371/journal.pntd.0011967.s006 (MOV)

RAW DATASET S1

Overall raw dataset containing data for Schistoscope validation on fresh urine samples (study A), Banked slides (study B) and quality control of banked slides. https://doi.org/10.1371/journal.pntd.0011967.s007 (XLSX)

ACKNOWLEDGMENTS

We extend our appreciation to Mermoz Ndong-Essone Ondong, Danny Carrel Manfoumbi Mabicka, Moutsinga Dalia Coralline ep Lehoumbou, Elsy Myrna N'noh Dansou, Marguerite Nzame Ngome, and the coordination team, along with all the members of Immuno-Epi research group of CERMEL. We thank Bertrand Lell for IT support in the field. Our gratitude also goes to Jean-Aimé Massande Ndzokou's and the CERMEL field team for their valuable contributions to the advancement of this project.

REFERENCES

[1] A. F. Adenowo, B. E. Oyinloye, B. I. Ogunyinka, and A. P. Kappo. “Impact of human schistosomiasis in sub-Saharan Africa”. In: *Brazilian Journal of Infectious Diseases* 19.2 (2015), pp. 196–205. doi: j.bjid.2014.11.004.

[2] World Health Organization. “Schistosomiasis and soil-transmitted helminthiases: progress report, 2021”. In: *Weekly Epidemiological Record* 97.48 (2022), pp. 621–632. url: https://www.who.int/publications/i/item/who-wer9748-621-632.

[3] World Health Organisation. *Schistosomiasis*. 2024. url: https://www.who.int/news-room/fact-sheets/detail/schistosomiasis (visited on 09/26/2024).

[4] World Health Organization. *WHO guideline on control and elimination of human schistosomiasis*. World Health Organization, 2022. isbn: 9789240041608. url: https://iris.who.int/handle/10665/351856.

[5] World Health Organisation. *Strengthening diagnostic capacity*. 2023. url: https://www.eliminateschisto.org/news-events/news/world-health-assembly-resolution-on-strengthening-diagnostics-capacity (visited on 07/17/2023).

[6] World Health Organization. *Public consultation: Target Product Profiles for diagnostic tests to meet Schistosomiasis and soil-transmitted Helminth programme needs*. 2021. url: https://www.who.int/news-room/articles-detail/public-consultation-target-product-profiles-for-diagnostic-tests-to-meet-schistosomiasi and-soil-transmitted-helminth-programme-needs (visited on 03/17/2022).

[7] P. L. A. M. Corstjens, C. J. de Dood, S. Knopp, M. N. Clements, G. Ortu, I. Umulisa, E. Ruberanziza, U. Wittmann, T. Kariuki, P. LoVerde, W. E. Secor, L. Atkins, S. Kinung’hi, S. Binder, C. H. Campbell Jr., D. G. Colley, and G. J. van Dam. “Circulating Anodic Antigen (CAA): a highly sensitive diagnostic biomarker to detect active Schistosoma infections—improvement and use during SCORE”. In: *The American Journal of Tropical*

Medicine and Hygiene 103.1 Suppl (2020), pp. 50–57. doi: 10.4269/ajtmh.19-0819.

[8] B. B. Obeng, Y. A. Aryeetey, C. J. de Dood, A. S. Amoah, I. A. Larbi, A. M. Deelder, M. Yazdanbakhsh, F. C. Hartgers, D. A. Boakye, J. J. Verweij, G. J. van Dam, and L. van Lieshout. "Application of a circulating-cathodic-antigen (CCA) strip test and real-time PCR, in comparison with microscopy, for the detection of Schistosoma haematobium in urine samples from Ghana". In: *Annals of Tropical Medicine and Parasitology* 102.7 (2008), pp. 625–633. doi: 10.1179/136485908X337490.

[9] P. Ward, P. Dahlberg, O. Lagatie, J. Larsson, A. Tynong, J. Vlaminck, M. Zumpe, S. Ame, M. Ayana, V. Khieu, Z. Mekonnen, M. Odiere, T. Yohannes, S. V. Hoecke, B. Levecke, and L. J. Stuyver. "Affordable artificial intelligence-based digital pathology for neglected tropical diseases: A proof-of-concept for the detection of soil-transmitted helminths and Schistosoma mansoni eggs in Kato-Katz stool thick smears". In: *PLoS neglected tropical diseases* 16.6 (2022), e0010500. doi: 10.1371/journal.pntd.0010500.

[10] J. T. Coulibaly, K. D. Silue, M. Armstrong, M. Díaz de León Derby, M. V. D'Ambrosio, D. A. Fletcher, J. Keiser, K. Fisher, J. R. Andrews, and I. I. Bogoch. "High Sensitivity of Mobile Phone Microscopy Screening for Schistosoma haematobium in Azaguié, Côte d'Ivoire". In: *The American Journal of Tropical Medicine and Hygiene* 108.1 (2023), p. 41. doi: 10.4269/ajtmh.22-0527.

[11] B. Meulah, M. Bengtson, L. Van Lieshout, C. H. Hokke, A. Kreidenweiss, J. C. Diehl, A. A. Adegnika, and T. E. Agbana. "A Review on Innovative Optical Devices for the Diagnosis of Human Soil-Transmitted Helminthiasis and Schistosomiasis: From Research and Development to Commercialization". In: *Parasitology* 150.2 (2023), pp. 137–149. doi: 10.1017/S0031182022001664.

[12] B. Meulah, P. Oyibo, M. Bengtson, T. Agbana, R. A. L. Lontchi, A. A. Adegnika, W. Oyibo, C. H. Hokke, J. C. Diehl, and L. v. Lieshout. "Performance Evaluation of the Schistoscope 5.0 for (Semi-)automated Digital Detection and Quantification of Schistosoma haematobium Eggs in Urine: A Field-based Study in Nigeria". In: *The American Journal of Tropical Medicine and Hygiene* 107.5 (2022). doi: 10.4269/ajtmh.22-0276.

[13] S. Agrebi and A. Larbi. "Use of artificial intelligence in infectious diseases". In: *Artificial Intelligence in Precision Health*. Academic Press, 2020, pp. 415–438. isbn: 978-0-12-817133-2. doi: 10.1016/B978-0-12-817133-2.00018-5.

[14] J. S. Brownstein, B. Rader, C. M. Astley, and H. Tian. “Advances in Artificial Intelligence for infectious-disease surveillance”. In: *New England Journal of Medicine* 388.17 (2023), pp. 1597–1607. doi: 10.1056/NEJMra2107472.

[15] S. Shenoy, A. K. Rajan, M. Rashid, V. P. Chandran, P. G. Poojari, V. Kunhikatta, D. Acharya, S. Nair, M. Varma, and G. Thunga. “Artificial intelligence in differentiating tropical infections: A step ahead”. In: *PLoS Neglected Tropical Diseases* 16.6 (2022), e0010455. doi: 10.1371/journal.pntd.0010455.

[16] I. Prieto-Egido, A. González-Escalada, V. García-Giganto, and A. Martínez-Fernández. “Design of New Procedures for Diagnosing Prevalent Diseases Using a Low-Cost Telemicroscopy System”. In: *Telemedicine Journal and e-Health* 22.11 (2016), pp. 952–959. doi: 10.1089/tmj.2015.0239.

[17] E. Dacal, D. Bermejo-Peláez, L. Lin, E. Álamo, D. Cuadrado, Á. Martínez, A. Mousa, M. Postigo, A. Soto, E. Sukosd, A. Vladimirov, C. Mwandawiro, P. Gichuki, N. A. Williams, J. Muñoz, S. Kepha, and M. Luengo-Oroz. “Mobile microscopy and telemedicine platform assisted by deep learning for the quantification of Trichuris trichiura infection”. In: *PLoS neglected tropical diseases* 15.9 (2021). doi: 10.1371/journal.pntd.0009677.

[18] A. Onasanya, M. Bengtson, L. de Goeje, J. Van Engelen, J. C. Diehl, and L. van Lieshout. “Developing inclusive digital health diagnostic for schistosomiasis: a need for guidance via target product profiles”. In: *Frontiers in Parasitology* 2 (2023). doi: 10.3389/fpara.2023.1255848.

[19] P. Oyibo, S. Jujjavarapu, B. Meulah, T. Agbana, I. Braakman, A. van Diepen, M. Bengtson, L. van Lieshout, W. Oyibo, G. Vdovine, and J. C. Diehl. “Schistoscope: An Automated Microscope with Artificial Intelligence for Detection of Schistosoma haematobium Eggs in Resource-Limited Settings”. In: *Micromachines* 13.5 (2022), p. 643. doi: 10.3390/mi13050643.

[20] M. Bengtson, A. Onasanya, P. Oyibo, B. Meulah, K. T. Samenjo, I. Braakman, W. Oyibo, and J. C. Diehl. “A usability study of an innovative optical device for the diagnosis of schistosomiasis in Nigeria”. In: *2022 IEEE Global Humanitarian Technology Conference (GHTC)*. Santa Clara, CA, USA: IEEE, 2022, pp. 17–22. doi: 10.1109/GHTC55712.2022.9911019.

[21] P. Oyibo, B. Meulah, M. Bengtson, L. van Lieshout, W. Oyibo, J. C. Diehl, G. Vdovine, and T. Agbana. “Two-stage automated diagnosis framework for urogenital schistosomiasis in microscopy images from low-resource settings”. In: *Journal of Medical Imaging*

10.4 (2023), pp. 044005–044005. doi: 10.1117/1.JMI.10.4.044005.

[22] J. C. Dejon-Agobé, Y. J. Honkpehedji, J. F. Zinsou, J. R. Edoa, B. R. Adégbitè, A. Mangaboula, S. T. Agnandji, G. Mombo-Ngoma, M. Ramharter, P. G. Kremsner, B. Lell, M. P. Grobusch, and A. A. Adegnika. "Epidemiology of schistosomiasis and soil-transmitted helminth coinfections among schoolchildren living in Lambaréné, Gabon". In: *The American Journal of Tropical Medicine and Hygiene* 103.1 (2020), p. 325. doi: 10.4269/ajtmh.19-0835.

[23] D. Machin, M. J. Campbell, S. B. Tan, and S. H. Tan. *Sample size tables for clinical studies*. 3rd. John Wiley Sons, 2011. isbn: 9781444357967.

[24] H. M. Kenguele, A. A. Adegnika, A. M. Nkoma, U. Ateba-Ngoa, M. Mbong, J. Zinsou, B. Lell, and J. J. Verweij. "Impact of short-time urine freezing on the sensitivity of an established Schistosoma real-time PCR assay". In: *American Journal of Tropical Medicine and Hygiene* 90.6 (2014), pp. 1153–1155. doi: 10.4269/ajtmh.14-0005.

[25] R. E. Wiegand, W. E. Secor, F. M. Fleming, M. D. French, C. H. King, A. K. Deol, S. P. Montgomery, D. Evans, J. Utzinger, P. Vounatsou, and S. J. de Vlas. "Associations between infection intensity categories and morbidity prevalence in school-age children are much stronger for Schistosoma haematobium than for S. mansoni". In: *PLoS Neglected Tropical Diseases* 15.5 (2021), e0009444. doi: 10.1371/journal.pntd.0009444.

[26] World Health Organization. *Prevention and control of schistosomiasis and soil-transmitted helminthiasis: report of a WHO expert committee*. World Health Organization, 2002. isbn: 9241209127. url: https://iris.who.int/handle/10665/42588.

[27] B. Tilahun, K. D. Gashu, Z. A. Mekonnen, B. F. Endehabtu, and D. A. Angaw. "Mapping the role of digital health technologies in the case detection, management, and treatment outcomes of neglected tropical diseases: a scoping review". In: *Tropical Medicine and Health* 49 (2021), pp. 1–10. doi: 10.1186/s41182-020-00285-7.

[28] U. K. Mustafa, K. S. Kreppel, J. Brinkel, and E. Sauli. "Digital Technologies to Enhance Infectious Disease Surveillance in Tanzania: A Scoping Review". In: *Healthcare* 11.4 (2023), p. 470. doi: 10.3390/healthcare11040470.

[29] A. Onasanya, M. Bengtson, T. Agbana, O. Oladunni, J. van Engelen, O. Oladepo, and J. C. Diehl. “Towards Inclusive Diagnostics for Neglected Tropical Diseases: User Experience of a New Digital Diagnostic Device in Low-Income Settings”. In: *Tropical Medicine and Infectious Disease* 8.3 (2023), p. 176. doi: 10.3390/tropicalmed8030176.

[30] N. V. Vinkeles Melchers, G. J. van Dam, D. Shaproski, A. I. Kahama, E. A. Brienen, B. J. Vennervald, and L. van Lieshout. “Diagnostic performance of Schistosoma real-time PCR in urine samples from Kenyan children infected with Schistosoma haematobium: day-to-day variation and follow-up after praziquantel treatment”. In: *PLoS Neglected Tropical Diseases* 8.4 (2014), e2807. doi: 10.1371/journal.pntd.0002807.

[31] D. Keller, J. Rothen, J.-P. Dangy, C. Saner, C. Daubenberger, F. Allan, S. M. Ame, S. M. Ali, F. Kabole, J. Hattendorf, D. Rollinson, R. Seyfarth, and S. Knopp. “Performance of a real-time PCR approach for diagnosing Schistosoma haematobium infections of different intensity in urine samples from Zanzibar”. In: *Infectious Diseases of Poverty* 9.1 (Sept. 2020), p. 128. doi: 10.1186/s40249-020-00726-y.

[32] K. Kura, R. J. Hardwick, J. E. Truscott, J. Toor, T. D. Hollingsworth, and R. M. Anderson. “The impact of mass drug administration on Schistosoma haematobium infection: what is required to achieve morbidity control and elimination?” In: *Parasites & Vectors* 13.1 (2020), pp. 1–10. doi: 10.1186/s13071-020-04329-y.

[33] P. T. Hoekstra, G. J. van Dam, and L. van Lieshout. “Context-specific procedures for the diagnosis of human schistosomiasis – a mini review”. In: *Frontiers in Tropical Diseases* 2 (2021), p. 722438. doi: 10.3389/fitd.2021.722438.

10

AUTOMATED STH AND *S. mansoni* EGG DETECTION

Deep learning-based automated detection and multiclass classification of soil-transmitted helminths and *Schistosoma mansoni* eggs in fecal smear images

Prosper Oyibo, Brice Meulah, Tope Agbana, Lisette van Lieshout, Wellington Oyibo, Gleb Vdovin, Jan-Carel Diehl

PUBLICATION REPORT

- **Publication Date:** 1 July 2025
- **Journal:** Scientific Reports
- **Publisher:** Springer Nature
- **DOI:** 10.1038/s41598-025-02755-9

ABSTRACT

In this work, we developed an automated system for the detection and classification of soil-transmitted helminths (STH) and Schistosoma (S.) mansoni eggs in microscopic images of fecal smears. We assembled an STH and S. mansoni dataset comprising over 3,000 field-of-view (FoV) images containing parasite eggs, extracted from more than 300 fecal smear prepared using the Kato-Katz technique. These images were acquired using Schistoscope - a cost-effective automated digital microscope. After annotating the STH and S. mansoni eggs, we employed a transfer learning approach to train an EfficientDet deep learning model, using 70% of the dataset for training, 20% for validation, and 10% for testing. The developed model successfully identified STH and S. mansoni eggs in the FoV images, achieving weighted average scores of 95.9%(±1.1%) *Precision,* 92.1%(±3.5%) *Sensitivity,* 98.0%(±0.76%) *Specificity, and* 94.0%(±1.98%) *F-Score across four classes of helminths (A. lumbricoides, T. trichiura, hookworm, and S. mansoni). Our system highlights the potential of the Schistoscope, enhanced with artificial intelligence, for detecting STH and S. mansoni infections in remote, resource-limited settings and for supporting the monitoring and evaluation of neglected tropical disease (NTD) control programs.*

10.1. INTRODUCTION

Intestinal helminths are a group of parasitic worms that primarily reside in the intestines of their hosts, including humans. These infections are a significant public health concern, affecting a substantial portion of the global population, particularly in low- and middle-income countries. The most common intestinal helminth infections are caused by soil-transmitted helminths (STH) such as roundworm (*Ascaris lumbricoides*), whipworm (*Trichuris trichiura*), and hookworm (*Necator americanus* and *Ancylostoma duodenale*) [1]. Also, intestinal schistosomiasis caused primarily by *Schistosoma* (*S.*) *mansoni*, *S. japonicum* and *S. intercalatum*, similarly affect the intestines[2]. Over 1.5 billion people, equating to 24% of the global population, are infected with STH infections [3] while at least 251.4 million people required preventive treatment for schistosomiasis in 2021[4]. Together, STH infections and schistosomiasis account for over 5 million disability-adjusted life years annually [5]. The highest incidences of STH infections and schistosomiasis are reported in Sub-Saharan Africa, the Americas, China, and East Asia [6].

The WHO has published a roadmap for STH infections and schistosomiasis for the next decade (2020–2030), recognizing the importance of diagnostics in stool samples to achieve elimination targets for these diseases [7, 8]. Manual screening of a Kato-Katz (KK) thick stool smear by expert microscopists remains the current standard for monitoring the impact of large-scale deworming programs against STH infections and intestinal schistosomiasis [9]. However, this method requires specialized expertise that must be continually developed and maintained, posing an economic challenge, particularly in remote rural communities [10]. There is also a risk of diagnostic errors and visual health complications among microscopists due to excessive workloads resulting from the low ratio of trained microscopists to samples for analysis in endemic regions [11].

To address these diagnostic challenges, several low-cost automated digital microscopy devices have been developed and validated for the automated detection of STH infections and intestinal schistosomiasis [12, 13]. Among these devices is the Schistoscope[14], developed by our research group, which is capable of automatically focusing and scanning regions of interest on prepared microscopy slides [15], as well as performing edge artificial intelligence processing[16]. Validation studies have shown it to be a promising and cost-effective tool for the automatic detection of urogenital schistosomiasis in urine samples collected in field settings [17, 18]. Preliminary results also indicate the Schistoscope's potential for analyzing fecal samples, demonstrated by a human reader's ability to accurately identify *S. mansoni* and hookworm eggs on images of fecal smears captured using the device [14].

In this study, we aim to develop an artificial intelligence system that can run effectively on the Schistoscope's edge computing system for

the fully automated detection of STH and *S. mansoni* eggs in KK smear in low-resource settings. Specific contributions of this study include:

1. Development of a robust image dataset of KK smears with STH and *S. mansoni* eggs, along with their annotated ground truth.
2. Development of a deep learning based STH and *S. mansoni* egg detection system for low-resource settings.

10.2. RELATED WORK

Recent advancements in automating the detection of STH and *S. mansoni* eggs in human fecal smears have leveraged artificial intelligence techniques, with significant progress in accuracy and applicability. These efforts can be broadly categorized into traditional machine learning approaches, deep learning-based detection and segmentation, and dataset-driven challenges, each contributing to the field while facing distinct limitations.

Early work focused on traditional machine learning methods to identify parasite eggs based on handcrafted features. For instance, Alva *et al.* [19] employed a logistic regression model using geometric and brightness features but struggled to differentiate parasites with similar morphologies. Similarly, Khairudin *et al.* [20] explored k-NN, SVM, and Ensemble classifiers, incorporating feature extraction techniques like Hu's invariant moments and Gray Level Co-occurrence Matrix (GLCM). Caetano, Santana, and de Lima [21] advanced this direction by optimizing an AdaBoost classifier with swarm intelligence for detecting *S. mansoni* and other helminth eggs, though limited image datasets constrained their accuracy. These studies highlight the potential of traditional methods but underscore their reliance on robust feature engineering and sufficient data, prompting a shift toward deep learning for more generalized solutions.

Deep learning approaches, particularly convolutional neural networks (CNNs) and object detection frameworks, have significantly improved detection performance by learning complex patterns directly from images. Viet, ThanhTuyen, and Hoang [22] and Oliveira *et al.* [23] utilised Faster R-CNN to detect parasite eggs, achieving higher accuracy than traditional methods, though small datasets limited generalization. Huo *et al.* [24] and Naing *et al.* [25] adopted YOLO-based models (YOLOv5 and YOLOv4-Tiny, respectively), demonstrating improved speed and accuracy, particularly when high-magnification images captured distinct features. Jaya Sundar Rajasekar *et al.* [26] further advanced this trend, showing that YOLOv8 with an SGD optimizer outperformed models like Detectron2 and InceptionV3. For real-time applications, delas Peñas *et al.* [27] implemented a tiny YOLO framework, which showed promise for rapid processing but lower accuracy for STH eggs

compared to *S. mansoni*. Meanwhile, segmentation-focused studies, such as Libouga *et al.* [28] with a modified U-Net and Lim *et al.* [29] comparing VGG and ResNet to traditional fuzzy c-Mean clustering, demonstrated deep learning's superiority in delineating parasite eggs from complex backgrounds.

Innovative pipelines combining detection and classification have also emerged. Dacal *et al.* [30] proposed an SSD-MobileNet pipeline for remote analysis of *Trichuris trichiura* eggs in KK samples, while Lee *et al.* [31] integrated SSD, U-Net, and Faster R-CNN for comprehensive egg identification and quantification. Lundin *et al.* [32] employed sequential CNNs (YOLOv2 for detection and ResNet50 for classification) to identify STH eggs by species, though their system overestimated egg counts compared to manual microscopy, highlighting challenges in calibration. Mobile and resource-constrained settings have also been explored, with Yang *et al.* [33] developing Kankanet, an ANN-based smartphone application, and Lin *et al.* [34] applying MobileNetV2 for egg classification, both constrained by low-quality images or small datasets.

Despite these advancements, dataset limitations remain a critical challenge across studies. Roder *et al.* [35] achieved promising results with Deep Belief Networks on a small grayscale dataset, but scalability was limited. Ward *et al.* [36] created a large dataset of 7,780 KK smear images, yet uneven egg distribution (50% belonging to *A. lumbricoides*) and reliance on high-infection-intensity slides risked biasing their model. Acula *et al.* [37] and Nakasi, Aliija, and Nakatumba [38] also noted that insufficiently robust datasets hampered CNN performance, even with architectures like ResNet-50, AlexNet, and GoogleNet.

Collectively, these studies illustrate the field's progress toward accurate and scalable helminth egg detection while highlighting persistent challenges in dataset quality, image resolution, and model generalization. This work builds on these efforts by addressing dataset robustness and enhancing model accuracy, with a focus on practical deployment in low-resource settings where automated diagnostics are most needed.

10.3. METHODOLOGY

10.3.1. STH AND S. mansoni DATASET

Image acquisition was performed during field studies carried out in the Federal Capital Territory (FCT), Nigeria. Ethical approval for the research was granted by the FCT Health Research Ethics Committee under approval number FHREC/2022/01/102/05-07-22 and the research was performed in accordance with the relevant guidelines and regulations. The project was presented to the NTD Unit of the Public Health Department, FCT Abuja, which then informed the local NTD officer in the selected area councils. Following informed consent, fecal samples

Figure 10.1: Field laboratory setup, equipped with 6 Schistoscope devices.

were collected from school-age children in sterile 20 mL universal containers. The fecal samples were processed using the standard Kato–Katz technique with a 41.7 mg template [39]. To accelerate data acquisition, we established a field lab equipped with 6 Schistoscope devices (as shown in fig. 6.1) to image the processed slides.

The Schistoscope was configured with a 4X 0.10 NA objective. A total of 300 sample slides prepared using the KK stool thick smears technique were registered, resulting in 141,600 FoV images with a resolution of 2028 x 1520 pixels. The images were screened and manually annotated by expert microscopists, identifying 889 hookworm and 3,238 *S. mansoni* eggs present in 3,040 FoV images. To obtain a robust dataset for the development of the deep learning model, we combined our registered dataset with the dataset from Ward *et al.* [40], which contains FoV images, from over 300 KK freshly prepared stool thick smears, registered with a prototype slide scanner and annotated labels containing 8,600 *A. lumbricoides*, 4,083 *T. trichiura*, 3,623 hookworm, and 682 *S. mansoni*. The combined dataset consists of 10,820 FoV (71.9% adopted from Ward *et al.* [40] and 28.1% registered by the Schistoscope) images with a total of 8,600 *A. lumbricoides*, 4,082 *T. trichiura*, 4,512 hookworm, and 3,920 *S. mansoni* eggs as shown in Table table 10.1. FoV images were randomly shuffled and split into three datasets: a training set, a validation set, and a test set. We aimed for a desired split ratio of 70:20:10 for both our created dataset and the Ward *et al.* [40] dataset in the combined dataset as shown in Table table 10.2.

Table 10.1: Number of Intestinal helminth eggs in the datasets.

Dataset	**Scanned slides**	**FoV images**		**Verified intestinal helminth eggs**				
		Registered	With eggs	*A. lumbricoides*	*T. trichiura*	hookworm	*S. mansoni*	**Total**
Ward *et al.* [40]	272	1,386,186	7,780	8,600	4,083	3,623	682	16,990
Present work	300	141,600	3,040	0	0	889	3,238	4,127
Combined	572	1,527,786	10,820	8,600	4,083	4,512	3,920	21,117

Table 10.2: Train, validation and test dataset split.

Split set	**FoV images**	**Verified intestinal helminth eggs**				
		A. lumbricoides	*T. trichiura*	hookworm	*S. mansoni*	**Total**
Train (70% target)	7,953 (69.4%, 30.6%)	6,071	2,839	3,226	3,070	15,205
Validation (20% target)	1,808 (83.2%, 16.8%)	1,646	859	803	466	3,774
Test (10% target)	1,059 (71.0%, 29.0%)	883	385	483	384	2,135
Total	10,820 (71.9%, 28.1%)	8,600	4,083	4,512	3,920	21,117

10.3.2. DEEP LEARNING MODEL

EfficientDet[41] is a state-of-the-art deep learning architecture developed by Google brain team. It is designed to be both fast and accurate across a wide range of computing environments, from mobile devices to servers which makes it suitable for applications such as edge systems with limited computational resource. It builds on EfficientNet, a scalable neural network architecture, by incorporating a novel compound scaling method that simultaneously scales up the resolution, depth, and width of the model, as well as the feature network and the box/class prediction network. Our developed model for the Classification of the STH and *S. mansoni* eggs (i.e., *A. lumbricoides*, *T. trichiura*, hookworm and *S. mansoni*), is based on the EfficientDet-D0 architecture, which integrates a Single Shot Detector (SSD) framework with an EfficientNet-B0 backbone. The backbone, EfficientNet-B0, is augmented by a Bi-directional Feature Pyramid Network (BiFPN). The BiFPN is configured to operate across feature levels 3 to 7 with three iterations and 64 filters, enhancing the model's ability to fuse features from different resolutions. The model employs a weight-shared convolutional box predictor, which helps in reducing the number of parameters by sharing weights across different layers. This predictor has a depth of 64, utilises depthwise separable convolutions, and is optimized with SWISH activation and L2 regularization. For classification, the model uses a weighted sigmoid focal loss with parameters $\alpha = 0.25$ and $\gamma = 1.5$, which is particularly effective in dealing with class imbalance by down-weighting the loss assigned to well-classified examples. The localization loss is computed using a weighted smooth L1 loss, balancing the accuracy of bounding box pre-

dictions. Both classification and localization losses are normalized by the number of matches and code size to ensure stable training. Multiscale anchors are generated with scales ranging from level 3 to 7, an anchor scale of 4.0, and three aspect ratios (1.0, 2.0, 0.5). This allows the model to detect objects at multiple scales. The model uses an argmax matcher with a threshold of 0.5 for both matched and unmatched cases, ensuring that every ground truth box is assigned to the best-matching anchor. Input images are resized to maintain their aspect ratio within dimensions of 512x512 pixels, with padding added to fit the maximum dimension. The training process includes data augmentation techniques like random horizontal flips and random scaling, cropping, and padding, enhancing the model's robustness to various image transformations. The model is fine-tuned from a pre-trained EfficientDet-D0 checkpoint trained on the COCO dataset [42], specifically tailored for detection tasks. A momentum optimizer is used with a cosine decay learning rate schedule, starting at 0.0008 and gradually decreasing over 400,000 steps, with a warmup phase for the first 2,500 steps. The model was implemented using the Python TensorFlow library and trained on the Google Colab platform with an A100 GPU, using a batch size of 16.

10.3.3. PERFORMANCE MEASUREMENT

To evaluate the performance of the STH and *S. mansoni* egg classification task, we used precision, sensitivity, specificity, and F1-score. These metrics are mathematically defined as follows:

$$Precision = \frac{TP}{TP + FP} \tag{10.1}$$

$$Sensitivity = \frac{TP}{TP + FN} \tag{10.2}$$

$$Specificity = \frac{TN}{TN + FP} \tag{10.3}$$

$$F1\text{-}score = 2 \times \frac{Precision \times Sensitivity}{Precision + Sensitivity} \tag{10.4}$$

Where TP, FP, TN and FN are True Positive, False Positive, True Negative and False Negative samples respectively.

10.4. RESULTS

Figure 10.2 shows the results of images with presence of artifacts in the fecal material which complicates the identification of eggs. Images a), c), e), and g) originate from Ward *et al.* [40], while images b), d), f), and h) were acquired using the Schistoscope. The eggs detected

and classified by the developed deep learning model are enclosed in bounding boxes: red for *A. lumbricoides*, blue for *T. trichiura*, yellow for hookworm, and green for *S. mansoni*. Arrows indicate instances of missed or misclassified eggs using the same color scheme. Black arrows point to artifacts that were incorrectly identified as eggs by the model. The developed model failed to detect *Ascaris lumbricoides*, hookworm, *Trichuris trichiura*, and *Schistosoma mansoni* eggs in images a), b), c), and e), respectively, due to improperly cleared fecal smears. In image d), two *S. mansoni* eggs were obscured by artifacts and not detected. Artifacts in images f) and h) were misidentified as hookworm eggs, and a *T. trichiura* egg in image g) was incorrectly classified as a *S. mansoni* egg. Differences in egg sizes across the dataset result from varying optical device configurations used for image acquisition (Ward *et al.* [40]: 10× magnification, 0.25 NA; Schistoscope: 4× magnification, 0.1 NA). These variations in resolution, combined with artifacts and diverse background colors and textures in fecal samples, enhance the dataset's robustness and help mitigate overfitting.

The confusion matrix (shown in Table table 10.3) evaluates the model's performance in detecting the four classes of helminth eggs. The model exhibited high detection and classification accuracy (shown in Table table 10.4), with precision and sensitivity for *A. lumbricoides* at 0.968 and 0.949, and for *T. trichiura* at 0.943 and 0.951, respectively. hookworm had a precision of 0.949 and sensitivity of 0.878, while *S. mansoni* showed 0.968 precision and 0.878 sensitivity. Our deep learning model, based on EfficientDet-D0, achieves a weighted average precision of 95.9% (±1.1%), sensitivity of 92.1% (±3.5%), specificity of 98.0% (±0.76%), and F1-score of 94.0% (±1.98%) across the four helminth classes. These metrics confirm the model's accuracy and reliability in detecting and classifying STH and *S. mansoni* eggs, despite variations in image conditions.

Table 10.3: Confusion Matrix.

		AI predictions and performance				**False negatives (missed eggs)**
		A. lumbricoides	*T. trichiura*	hookworm	*S. mansoni*	
Verified ground truth	*A. lumbricoides*	790	1	0	0	42
	T. trichiura	1	364	0	0	19
	hookworm	0	0	424	0	59
	S. mansoni	0	0	0	337	47
False positives (background artefacts)		26	22	23	11	-

10.5. DISCUSSION

The World Health Organisation (WHO) has outlined Target Product Profiles (TPPs) for diagnostic tools to control STH infections and schistosomiasis,

Table 10.4: Performance Metrics

	A. lumbricoides	***T. trichiura***	**hookworm**	***S. mansoni***	**Weighted Average**	**Standard Deviation**
Precision	0.968	0.943	0.949	0.968	0.959	0.011
Sensitivity	0.949	0.951	0.878	0.878	0.921	0.035
Specificity	0.972	0.984	0.982	0.992	0.980	0.0076
F-Score	0.959	0.947	0.912	0.921	0.940	0.0198

emphasizing affordability, accessibility, and effectiveness in resource-limited settings [43, 44]. This study advances these goals through the Schistoscope, a cost-effective automated microscope enhanced with an artificial intelligence (AI) system for detecting and classifying STH and *S. mansoni* eggs. Unlike many prior efforts, our work uniquely integrates edge-computing capabilities, a robust and diverse dataset, and a focus on practical deployment, offering distinct advantages over existing approaches.

The Schistoscope's design prioritizes affordability and usability, leveraging off-the-shelf components for easy maintenance and scalability in low-resource settings. Its AI-driven system enables automatic focusing, scanning, and egg detection, reducing reliance on skilled microscopists—a critical bottleneck noted in manual KK diagnostics [10]. Compared to earlier automated microscopy systems, such as those by Holmström *et al.* [12], which required external computational resources, the Schistoscope's edge-computing capability allows real-time processing in remote areas without internet connectivity. This contrasts with studies like Dacal *et al.* [30], which relied on telemedicine pipelines, limiting their applicability in disconnected settings. Our prior work validated the Schistoscope's efficacy for *S. haematobium* egg detection [16, 18], and this study extends its utility to STH and *S. mansoni* eggs detection, demonstrating versatility across parasitic diseases.

A key contribution of this work is the development of a comprehensive STH and *S. mansoni* eggs Dataset, comprising 141,600 FoV images from 300 KK slides captured using the Schistoscope's 4X objective, with 3,040 FoVs containing 889 hookworm and 3,238 *S. mansoni* eggs. By augmenting this with the Ward *et al.* [40] dataset, we created a combined dataset of 10,820 FoVs with 21,117 eggs across four species (*Ascaris lumbricoides*, *Trichuris trichiura*, hookworm, *S. mansoni*). Unlike Ward et al.'s dataset, which suffered from class imbalance (50% *A. lumbricoides* eggs) and high-infection-intensity bias, our dataset improves balance for *S. mansoni* and incorporates diverse stool samples from over 200 individuals. This addresses limitations in prior datasets, such as those used by Roder *et al.* [35] and Nakasi, Aliija, and Nakatumba [38], which were constrained by small or grayscale images, enhancing model generalizability.

Our developed model's performance compares favorably to prior studies. For instance, Viet, ThanhTuyen, and Hoang [22] and Oliveira *et al.* [23] used Faster R-CNN but faced generalization issues due to small datasets, while Huo *et al.* [24] and Jaya Sundar Rajasekar *et al.* [26] achieved high accuracy with YOLO models but required high-magnification images impractical for low-cost devices. Our model's performance on lower-magnification (4X) images, combined with edge-computing efficiency, makes it more suitable for field deployment than resource-intensive models like ResNet-50 used by Lundin *et al.* [32], which overestimated egg counts. Additionally, unlike mobile-based solutions like Kankanet by Yang *et al.* [33], which were limited by image quality, the Schistoscope ensures consistent imaging, improving reliability.

Despite these strengths, a limitation of our dataset is the absence of *A. lumbricoides* and *T. trichiura* eggs captured with the Schistoscope, due to their non-prevalence at our study sites. This may bias the model toward hookworm and *S. mansoni* detection in Schistoscope images, a challenge also noted in studies with uneven class distributions [40]. Sensitivity for hookworm (0.878) and *S. mansoni* (0.878) is slightly lower than for other classes, likely due to variability in image sources, but precision (0.949–0.968) and specificity (0.921–0.992) remain high, with low standard deviations indicating robustness. Future work will expand the dataset to include more *A. lumbricoides* and *T. trichiura* eggs and refine annotations to boost sensitivity, explore other deep learning architectures to improve quantification building on insights from medical imaging studies.

This study's uniqueness lies in its end-to-end solution: a low-cost, AI-enhanced device with a robust dataset and high performance tailored for low-resource settings. While prior works advanced classification, they lacked scalable hardware integration. Our system aligns with WHO TPPs, offering a practical tool for monitoring deworming programs. Evaluating performance at the slide/patient level, as opposed to only image-level metrics, will further ensure clinical reliability.

10.6. CONCLUSION

In conclusion, the Schistoscope, combined with an AI-based detection system, demonstrates strong potential for accurately detecting STH and *S. mansoni* eggs, aligning with WHO's vision for affordable and accessible diagnostics in low-resource settings. Our model exhibited high precision, sensitivity, and specificity across all classes, with room for improvement in the detection of hookworm and *S. mansoni* eggs. Expanding the dataset and optimizing model parameters will further enhance performance and generalizability. Overall, the system holds promise for supporting large-scale monitoring and deworming efforts in

endemic regions. In future we would like to evaluate the diagnostic performance of the system in a resource limited settings.

ACKNOWLEDGEMENTS

We acknowledge the Neglected Tropical Disease team from the Federal Ministry of Health, Abuja, and the Federal Capital Territory Administration (FCTA) Public Health Department, Abuja, Nigeria, as well as the Delft University of Technology Global Initiative for their support of this study.

FUNDING

This work was funded by the NTD innovation prize and NWO-WOTRO Science for Global Development program, Grant Number W 07.30318.009 (INSPiRED - INclusive diagnoStics for Poverty RElated parasitic Diseases in Nigeria and Gabon).

DATA AVAILABILITY

The data used in this study is publicly available for research and development from the following sources: AI4NTD KK2.0 P1.5 STH & SCHm Dataset: https://www.kaggle.com/datasets/peterkward/ai4ntd-p1-5, Hookworm and Schistosoma mansoni Eggs Image Dataset: https://doi.org/10.5281/zenodo.13843815

AUTHOR CONTRIBUTIONS STATEMENT

P.O., T.A., and J.D. conceived and designed the study. P.O. and T.A. collected the data. P.O. analyzed the data and wrote the paper. B.M. contributed to data analysis. L.v.L., W.O., G.V., and J.D. supervised the research and reviewed the manuscript. All authors read and approved the final submitted version of the manuscript.

COMPETING INTERESTS

The authors declare no competing interests.

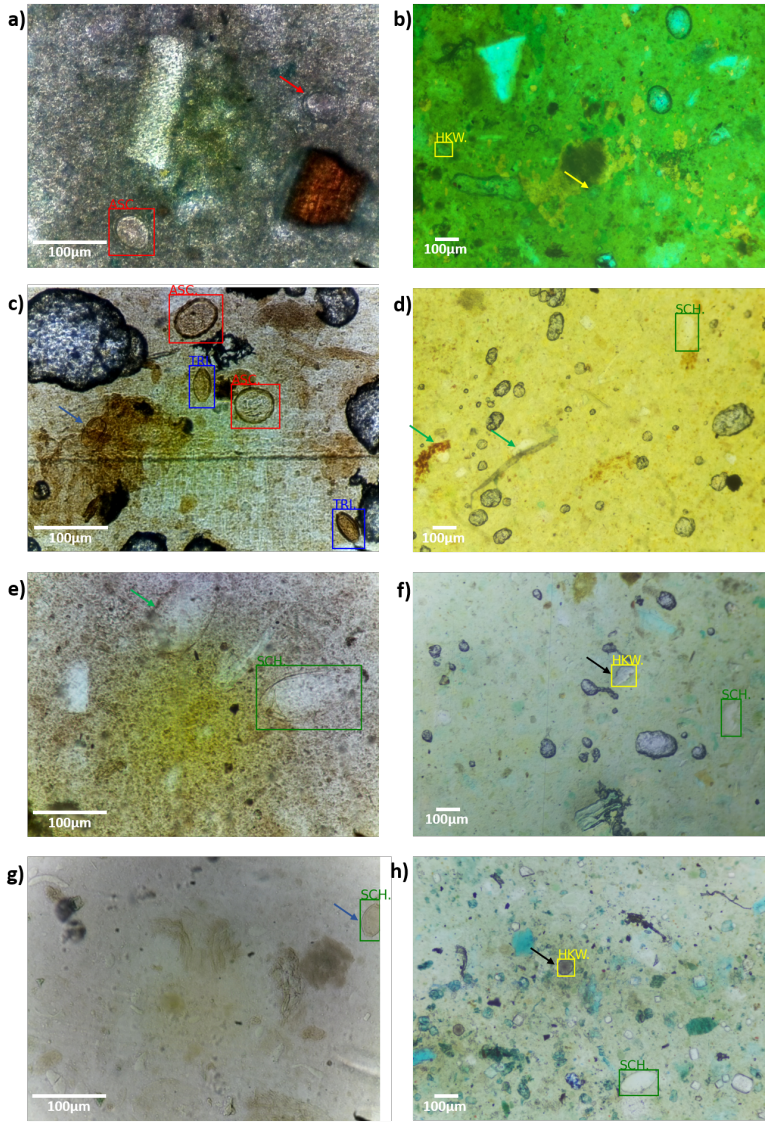

Figure 10.2: Example images from the combined test dataset. Images a), c), e), and g) are from Ward *et al.* [40], while images b), d), f), and h) were captured using the Schistoscope. Eggs detected and classified by the deep learning model are highlighted with red, blue, yellow, and green bounding boxes, corresponding to *Ascaris lumbricoides*, *Trichuris trichiura*, hookworm, and *Schistosoma mansoni*, respectively. Arrows indicate missed or misclassified eggs: red, blue, yellow, and green for *A. lumbricoides*, *T. trichiura*, hookworm, and *S. mansoni*, respectively; black arrows mark artifacts incorrectly classified as eggs.

REFERENCES

[1] P. M. Jourdan, P. H. L. Lamberton, A. Fenwick, and D. G. Addiss. “Soil-transmitted helminth infections”. In: *The Lancet* 391.10117 (2018), pp. 252–265. doi: 10.1016/S0140-6736(17)31930-X.

[2] P. T. LoVerde. “Schistosomiasis”. In: *Digenetic Trematodes*. Springer International Publishing, 2024, pp. 75–105. isbn: 978-3-031-60121-7. doi: 10.1007/978-3-031-60121-7_3.

[3] World Health Organization. *Soil-transmitted helminth infections*. Aug. 2023. url: https://www.who.int/news-room/fact-sheets/detail/soil-transmitted-helminth-infections (visited on 09/26/2024).

[4] World Health Organisation. *Schistosomiasis*. 2024. url: https://www.who.int/news-room/fact-sheets/detail/schistosomiasis (visited on 09/26/2024).

[5] T. Vos, S. S. Lim, C. Abbafati, K. M. Abbas, M. Abbasi, M. Abbasifard, M. Abbasi-Kangevari, H. Abbastabar, and F. Abd-Allah. “Global burden of 369 diseases and injuries in 204 countries and territories, 1990–2019: a systematic analysis for the Global Burden of Disease Study 2019”. In: *The Lancet* 396.10285 (2020), pp. 1204–1222. doi: 10.1016/S0140-6736(20)30925-9.

[6] World Health Organization. “Schistosomiasis and soil-transmitted helminthiases: progress report, 2021”. In: *Weekly Epidemiological Record* 97.48 (2022), pp. 621–632. url: https://www.who.int/publications/i/item/who-wer9748-621-632.

[7] A. A. Souza, C. Ducker, D. Argaw, J. D. King, A. W. Solomon, M. A. Biamonte, R. N. Coler, I. Cruz, V. Lejon, B. Levecke, F. K. Marchini, M. Marks, P. Millet, S. M. Njenga, R. Noordin, R. Paulussen, E. Sreekumar, and P. J. Lammie. “Diagnostics and the neglected tropical diseases roadmap: setting the agenda for 2030”. In: *Transactions of the Royal Society of Tropical Medicine and Hygiene* 115.2 (2021), pp. 129–135. doi: 10.1093/trstmh/traa118.

[8] A. Montresor, D. Mupfasoni, A. Mikhailov, P. Mwinzi, A. Lucianez, M. Jamsheed, E. Gasimov, S. Warusavithana, A. Yajima, Z. Bisoffi, D. Buonfrate, P. Steinmann, J. Utzinger, B. Levecke, J. Vlaminck, P. Cools, J. Vercruysse, G. Cringoli, L. Rinaldi, B. Blouin, and T. W. Gyorkos. "The global progress of soil-transmitted helminthiases control in 2020 and World Health Organization targets for 2030". In: *PLoS neglected tropical diseases* 14.8 (2020), e0008505. doi: 10.1371/journal.pntd.0008505.

[9] L. J. Stuyver and B. Levecke. "The role of diagnostic technologies to measure progress toward WHO 2030 targets for soil-transmitted helminth control programs". In: *PLoS Neglected Tropical Diseases* 15.6 (2021). doi: 10.1371/journal.pntd.0009422.

[10] J. Utzinger, S. L. Becker, L. Van Lieshout, G. J. Van Dam, and S. Knopp. "New diagnostic tools in schistosomiasis". In: *Clinical microbiology and infection* 21.6 (2015), pp. 529–542. doi: 10.1016/j.cmi.2015.03.014.

[11] N. Rajeshwori, K. Raju, B. Sanjeev, and S. B. Gulshan. "Prevalence of myopia and binocular vision dysfunctions in microscopists". In: *International Eye Science* 18.7 (2018), pp. 1180–1183. doi: 10.3980/j.issn.1672-5123.2018.7.03.

[12] O. Holmström, N. Linder, B. Ngasala, A. Mårtensson, E. Linder, M. Lundin, H. Moilanen, A. Suutala, V. Diwan, and J. Lundin. "Point-of-care mobile digital microscopy and deep learning for the detection of soil-transmitted helminths and *Schistosoma haematobium*". en. In: *Global Health Action* 10.sup3 (June 2017), p. 1337325. doi: 10.1080/16549716.2017.1337325.

[13] P. Ward, B. Levecke, and S. Ajjampur. "Harnessing artificial intelligence microscopy to improve diagnostics for soil-transmitted helminthiasis and schistosomiasis: a review of recent advances and future pathways". In: *Current Opinion in Infectious Diseases* 37.5 (2024), pp. 376–384. doi: 10.1097/QCO.0000000000001048.

[14] P. Oyibo, S. Jujjavarapu, B. Meulah, T. Agbana, I. Braakman, A. van Diepen, M. Bengtson, L. van Lieshout, W. Oyibo, G. Vdovine, and J. C. Diehl. "Schistoscope: An Automated Microscope with Artificial Intelligence for Detection of Schistosoma haematobium Eggs in Resource-Limited Settings". In: *Micromachines* 13.5 (2022), p. 643. doi: 10.3390/mi13050643.

[15] P. Oyibo, T. Agbana, L. van Lieshout, W. Oyibo, J. C. Diehl, and G. Vdovine. "An automated slide scanning system for membrane filter imaging in diagnosis of urogenital schistosomiasis". In:

Journal of Microscopy 294.1 (2024), pp. 52–61. doi: 10.1111/jmi.13269.

[16] P. Oyibo, B. Meulah, M. Bengtson, L. van Lieshout, W. Oyibo, J. C. Diehl, G. Vdovine, and T. Agbana. "Two-stage automated diagnosis framework for urogenital schistosomiasis in microscopy images from low-resource settings". In: *Journal of Medical Imaging* 10.4 (2023), pp. 044005–044005. doi: 10.1117/1.JMI.10.4.044005.

[17] B. Meulah, P. Oyibo, M. Bengtson, T. Agbana, R. A. L. Lontchi, A. A. Adegnika, W. Oyibo, C. H. Hokke, J. C. Diehl, and L. v. Lieshout. "Performance Evaluation of the Schistoscope 5.0 for (Semi-)automated Digital Detection and Quantification of Schistosoma haematobium Eggs in Urine: A Field-based Study in Nigeria". In: *The American Journal of Tropical Medicine and Hygiene* 107.5 (2022). doi: 10.4269/ajtmh.22-0276.

[18] B. Meulah, P. Oyibo, P. T. Hoekstra, P. A. N. Moure, M. N. Maloum, R. A. Laclong-Lontchi, Y. J. Honkpehedji, M. Bengtson, C. Hokke, P. L. A. M. Corstjens, T. Agbana, J. C. Diehl, A. A. Adegnika, and L. v. Lieshout. "Validation of artificial intelligence-based digital microscopy for automated detection of Schistosoma haematobium eggs in urine in Gabon". In: *PLoS neglected tropical diseases* 18.2 (2024). doi: 10.1371/journal.pntd.0011967.

[19] A. Alva, C. Cangalaya, M. Quiliano, C. Krebs, R. H. Gilman, P. Sheen, and M. Zimic. "Mathematical algorithm for the automatic recognition of intestinal parasites". In: *PLoS ONE* 12.4 (2017), e0175646. doi: 10.1371/journal.pone.0175646.

[20] N. A. A. Khairudin, C. C. Lim, A. S. A. Nasir, and Z. Mohamed. "Efficient Classification Techniques in Classifying Human Intestinal Parasite Ova". In: *Journal of Telecommunication, Electronic and Computer Engineering (JTEC)* 14.3 (2022), pp. 17–23. doi: 10.54554/jtec.2022.14.03.003.

[21] A. Caetano, C. Santana, and R. A. de Lima. "Diagnostic support of parasitic infections with an AI-powered microscope". In: *Research on Biomedical Engineering* 39.3 (2023), pp. 561–572. doi: 10.1007/s42600-023-00288-6.

[22] N. Q. Viet, D. T. ThanhTuyen, and T. H. Hoang. "Parasite worm egg automatic detection in microscopy stool image based on Faster R-CNN". In: *Proceedings of the 3rd International Conference on Machine Learning and Soft Computing*. New York, NY, USA: Association for Computing Machinery, 2019, pp. 197–202. isbn: 978-1-4503-6612-0. doi: 10.1145/3310986.3311014.

[23] B. A. S. Oliveira, J. M. P. Moreira, P. R. S. Coelho, D. A. Negrão-Corrêa, S. M. Geiger, and F. G. Guimarães. “Automated diagnosis of schistosomiasis by using faster R-CNN for egg detection in microscopy images prepared by the Kato–Katz technique”. In: *Neural Computing and Applications* 34.11 (2022), pp. 9025–9042. doi: 10.1007/s00521-022-06924-z.

[24] Y. Huo, J. Zhang, X. Du, X. Wang, J. Liu, and L. Liu. “Recognition of parasite eggs in microscopic medical images based on YOLOv5”. In: *2021 5th Asian Conference on Artificial Intelligence Technology (ACAIT)*. Haikou, China, 2021, pp. 123–127. doi: 10.1109/ACAIT53529.2021.9731120.

[25] K. M. Naing, S. Boonsang, S. Chuwongin, V. Kittichai, T. Tongloy, S. Prommongkol, P. Dekumyoy, and D. Watthanakulpanich. “Automatic recognition of parasitic products in stool examination using object detection approach”. In: *PeerJ Computer Science* 8 (2022), e1065. doi: 10.7717/peerj-cs.1065.

[26] S. Jaya Sundar Rajasekar, G. Jaswal, V. Perumal, S. Ravi, and V. Dutt. “Parasite.ai – An Automated Parasitic Egg Detection Model from Microscopic Images of Fecal Smears using Deep Learning Techniques”. In: *2023 International Conference on Advances in Computing, Communication and Applied Informatics (ACCAI)*. Chennai, India, 2023, pp. 1–9. doi: 10.1109/ACCAI58221.2023.10200869.

[27] K. E. delas Peñas, E. A. Villacorte, P. T. Rivera, and P. C. Naval. “Automated Detection of Helminth Eggs in Stool Samples Using Convolutional Neural Networks”. In: *2020 IEEE REGION 10 CONFERENCE (TENCON)*. Osaka, Japan, 2020, pp. 750–755. doi: 10.1109/TENCON50793.2020.9293746.

[28] I. O. Libouga, L. Bitjoka, D. L. L. Gwet, O. Boukar, and A. M. N. Nlôga. “A supervised U-Net based color image semantic segmentation for detection & classification of human intestinal parasites”. In: *e-Prime - Advances in Electrical Engineering, Electronics and Energy* 2 (2022), p. 100069. doi: 10.1016/j.prime.2022.100069.

[29] C. C. Lim, N. A. A. Khairudin, S. W. Loke, A. S. A. Nasir, Y. F. Chong, and Z. Mohamed. “Comparison of Human Intestinal Parasite Ova Segmentation Using Machine Learning and Deep Learning Techniques”. In: *Applied Sciences* 12.15 (2022), p. 7542. doi: 10.3390/app12157542.

[30] E. Dacal, D. Bermejo-Peláez, L. Lin, E. Álamo, D. Cuadrado, Á. Martínez, A. Mousa, M. Postigo, A. Soto, E. Sukosd, A. Vladimirov, C. Mwandawiro, P. Gichuki, N. A. Williams, J. Muñoz, S. Kepha, and M. Luengo-Oroz. “Mobile microscopy and telemedicine platform

assisted by deep learning for the quantification of Trichuris trichiura infection". In: *PLoS neglected tropical diseases* 15.9 (2021). doi: 10.1371/journal.pntd.0009677.

[31] C.-C. Lee, P.-J. Huang, Y.-M. Yeh, P.-H. Li, C.-H. Chiu, W.-H. Cheng, and P. Tang. "Helminth egg analysis platform (HEAP): An opened platform for microscopic helminth egg identification and quantification based on the integration of deep learning architectures". In: *Journal of Microbiology, Immunology and Infection* 55.3 (2022), pp. 395–404. doi: 10.1016/j.jmii.2021.07.014.

[32] J. Lundin, A. Suutala, O. Holmström, S. Henriksson, S. Valkamo, H. Kaingu, F. Kinyua, M. Muinde, M. Lundin, and V. Diwan. "Diagnosis of soil-transmitted helminth infections with digital mobile microscopy and artificial intelligence in a resource-limited setting". In: *PLOS Neglected Tropical Diseases* 18.4 (2024), e0012041. doi: 10.1371/journal.pntd.0012041.

[33] A. Yang, N. Bakhtari, L. Langdon-Embry, E. Redwood, S. G. Lapierre, P. Rakotomanga, A. Rafalimanantsoa, J. D. D. Santos, I. Vigan-Womas, A. M. Knoblauch, and L. A. Marcos. "Kankanet: An artificial neural network-based object detection smartphone application and mobile microscope as a point-of-care diagnostic aid for soil-transmitted helminthiases". In: *PLoS neglected tropical diseases* 13.8 (2019), e0007577. doi: 10.1371/journal.pntd.0007577.

[34] L. Lin, D. Bermejo-Peláez, D. Capellán-Martín, D. Cuadrado, C. Rodríguez, L. García, N. Díez, R. Tomé, M. Postigo, M. J. Ledesma-Carbayo, and M. Luengo-Oroz. "Combining collective and artificial intelligence for global health diseases diagnosis using crowdsourced annotated medical images". In: *2021 43rd Annual International Conference of the IEEE Engineering in Medicine & Biology Society (EMBC)*. Mexico, 2021, pp. 3344–3348. doi: 10.1109/EMBC46164.2021.9630868.

[35] M. Roder, L. A. Passos, L. C. F. Ribeiro, B. C. Benato, A. X. Falcão, and J. P. Papa. "Intestinal Parasites Classification Using Deep Belief Networks". In: *International Conference on Artificial Intelligence and Soft Computing*. Vol. 12415. Springer. Zakopane, Poland, 2020, pp. 242–251. doi: 10.1007/978-3-030-61401-0_23.

[36] P. Ward, P. Dahlberg, O. Lagatie, J. Larsson, A. Tynong, J. Vlaminck, M. Zumpe, S. Ame, M. Ayana, V. Khieu, Z. Mekonnen, M. Odiere, T. Yohannes, S. V. Hoecke, B. Levecke, and L. J. Stuyver. "Affordable artificial intelligence-based digital pathology for neglected tropical diseases: A proof-of-concept for the detection of soil-transmitted helminths and Schistosoma mansoni eggs

in Kato-Katz stool thick smears". In: *PLoS neglected tropical diseases* 16.6 (2022), e0010500. doi: 10.1371/journal.pntd.0010500.

[37] D. D. Acula, C. P. L. Buico, G. U. Cruzada, M. K. C. Encelan, and C. Y. G. Rivera. "Soil transmitted helminth egg detection and classification in fecal smear images using faster region-based convolutional neural network with residual network-50". In: *International Conference on Green Energy, Computing and Intelligent Technology (GEn-CITy 2023)*. Vol. 2023. 2023, pp. 284–291. doi: 10.1049/icp.2023.1793.

[38] R. Nakasi, E. R. Aliija, and J. Nakatumba. "A Poster on Intestinal Parasite Detection in Stool Sample Using AlexNet and GoogleNet Architectures". In: *Proceedings of the 4th ACM SIGCAS Conference on Computing and Sustainable Societies*. COMPASS '21. New York, NY, USA: Association for Computing Machinery, 2021, pp. 389–395. isbn: 978-1-4503-8453-7. doi: 10.1145/3460112.3472309.

[39] F. Bosch, M. S. Palmeirim, S. M. Ali, S. M. Ame, J. Hattendorf, and J. Keiser. "Diagnosis of soil-transmitted helminths using the Kato-Katz technique: What is the influence of stirring, storage time and storage temperature on stool sample egg counts?" In: *PLoS Neglected Tropical Diseases* 15.1 (2021), e0009032. doi: 10.1371/journal.pntd.0009032.

[40] P. Ward, T. Yohannes, M. Ayanna, G. Jonsson-Glans, O. Lagatie, M. Zumpe, A. Tynnong, P. Dahlberg, M. Odiere, V. Khieu, Z. Mekonnen, M. Odiere, T. Yohannes, S. V. Hoecke, B. Levecke, and L. J. Stuyver. *AI4NTD KK2.0 P1.5 STH & SCHm Dataset*. Kaggle repository. 2022. doi: 10.34740/KAGGLE/DS/1896823.

[41] M. Tan, R. Pang, and Q. V. Le. "EfficientDet: Scalable and Efficient Object Detection". In: *Proceedings of the IEEE/CVF Conference on Computer Vision and Pattern Recognition (CVPR)*. Seattle, WA, USA, 2020, pp. 10781–10790. doi: 10.1109/CVPR42600.2020.01079.

[42] T.-Y. Lin, M. Maire, S. Belongie, J. Hays, P. Perona, D. Ramanan, P. Dollár, and C. L. Zitnick. "Microsoft COCO: Common Objects in Context". In: *Computer Vision – ECCV 2014*. Vol. 8693. Zurich, Switzerland: Springer International Publishing, 2014, pp. 740–755. isbn: 978-3-319-10601-4 978-3-319-10602-1. doi: 10.1007/978-3-319-10602-1_48.

[43] World Health Organization. *Diagnostic target product profile for monitoring and evaluation of soil-transmitted helminth control programmes*. World Health Organization, 2021. isbn:

9789240031227. url: https://iris.who.int/handle/10665/342539.

[44] World Health Organization. *Diagnostic target product profiles for monitoring, evaluation and surveillance of schistosomiasis control programmes*. World Health Organization, 2021. isbn: 9789240031104. url: https://iris.who.int/handle/10665/344813.

11

CONCLUSION

This chapter offers a comprehensive overview of the development and impact of an automated digital microscope (the Schistoscope) to diagnose schistosomiasis and soil-transmitted helminth (STH) infections in resource-limited settings. It begins with a summary of Chapters 2 through 10, highlighting an in-depth review of quantitative diagnostic methods; the design and optimization of the Schistoscope's hardware, software, and AI components; usability and acceptability studies among healthcare workers; and field validation in Nigeria and Gabon evaluating the device's performance in real-world conditions. The chapter concludes with reflections on key findings and proposes key areas for future improvements, thereby rounding off the thesis.

11.1. SUMMARY

This thesis focused on developing an automated digital microscope, the Schistoscope, to improve both accessibility and accuracy of diagnosis of schistosomiasis and soil-transmitted Helminth (STH) infections. We optimized the whole slide imaging capabilities of the microscope for consistent performance in field conditions. We also compiled robust and large-scale image datasets of *Schistosoma (S.) haematobium* and intestinal helminth eggs, which were crucial for the development of automated helminth egg detection models. Furthermore, by integrating digital microscopy with Edge AI analysis, we have created a transformative point-of-care diagnostic tool for disease control with great potential to accelerate the achievement of elimination goals as enshrined in the WHO's NTD Road Map, 2021-2030 in resource-limited settings.

Quantitative diagnostic tools for schistosomiasis and STH: Chapter 2 offers an in-depth review of diagnostic methods for schistosomiasis and STH infections, focusing on sample preparation devices, portable digital microscopes, and AI-driven automated detection and identification methodologies. The World Health Organisation (WHO) recommends the urine filtration method to diagnose urogenital schistosomiasis, but it faces costs and availability problems in endemic regions. Using local materials can degrade image quality due to introduced artifacts. The Kato-Katz technique, also recommended by the WHO for intestinal helminth diagnosis, is affordable and standardized but less effective for detecting low-intensity infections. Other methods such as sedimentation and flotation enhance egg recovery but are hindered by long processing times and sensitivity to fixative types and solution density. Innovations such as FLOTAC, Mini-FLOTAC, and FECPAK systems improve data handling and egg recovery, but accessibility in resource-constrained areas remains a challenge. The shift to portable digital microscopes offers better accessibility for field use, allowing real-time imaging and field diagnostics, though challenges in manual sample manipulation and variable image quality in field conditions persist. Early AI models using Support Vector Machines (SVM) and Artificial Neural Networks (ANN) improved diagnostics, but were limited by complex samples with the presence of artifacts. Deep learning, especially through Convolutional Neural Networks (CNN), has revolutionized the field by handling high-variability images, although it requires diverse datasets to perform robustly.

The review underscores the need for cost-effective and user-friendly diagnostic tools that maintain accuracy in resource-limited settings. Automated digital microscopes powered by AI could significantly mitigate the lack of trained professionals in endemic regions by enabling field diagnostics. The performance of AI models is critically dependent

on the quality and diversity of training data, highlighting the need for expansive, varied datasets to handle real-world conditions and artifacts. Integrating portable digital microscopes with edge AI analysis presents a scalable solution for diagnostics, potentially revolutionizing disease monitoring and control in low-resource environments.

Raspberry Pi vs Smartphone based Schistoscope Designs: Chapter 3 explores two primary design pathways for an automated digital microscope (the Schistoscope): one utilising a Raspberry Pi (RP) and the other a smartphone (SP). The RP-based Schistoscope is cost-effective, with an estimated production cost of 125 euros, featuring modular components that can be locally manufactured, including 3D-printed casings and custom sample preparation setups. However, it suffers from a limited field-of-view (FoV) and less clear imaging. In contrast, the SP-based design offers higher-resolution imaging, crucial for identifying *S. haematobium* eggs, but at a higher cost. Both designs consider local repair and maintenance, vital for deployment in remote, resource-limited settings.

The development of both Schistoscopes underscores the potential of using consumer electronics in biomedical engineering to address diagnostic challenges in low-resource environments, particularly in sub-Saharan Africa, where schistosomiasis is prevalent. This approach not only reduces the dependency on expensive and complex infrastructure, but also aligns with the principles of sustainable and locally adaptable technology. The integration of community-specific needs in the device's design, including durability, modularity, and ease of repair, highlights a model for public health innovation that could be replicated for other diseases in similar settings.

Both Schistoscope designs face certain limitations. The RP version's constrained FoV and image clarity could potentially miss low-density infections. The SP version, while providing better resolution, increases the cost, which might limit its scalability in the most resource-poor areas. In addition, both devices require further development to ensure they can consistently perform under varied environmental conditions and with diverse sample qualities. These include enhancing the FoV through multi-field-of-view imaging approaches to allow for more comprehensive sample analysis, expanding on manufacturing techniques, such as incorporating laser cutting and using standardized WHO sample preparation procedures, in order to improve production efficiency and device consistency.

Schistoscope 5.0 Design: Chapter 4 delves into the next iteration of the automated digital microscope (Schistoscope 5.0). This iteration of the device enhances conventional bright field microscopy by incorporating

AI algorithms, automated stage movements, and on-board computing to tackle the challenges of operator dependency, the need for skilled personnel, and inconsistent imaging quality. The Schistoscope 5.0 features a high-resolution Raspberry Pi camera with automated XYZ movement for improved focus and field-of-view, along with structured autofocusing and auto-scanning functionalities to address common imaging issues such as artifacts and blurriness. A UNET deep learning model was trained on Schistoscope-captured images for *S. haematobium* egg detection, demonstrating sensitivity that meets WHO standards and shows potential for epidemiological monitoring through accurate estimation of the egg count.

The Schistoscope 5.0 has profound implications for public health, particularly in the context of supporting WHO's efforts to eliminate neglected tropical diseases. By offering a reliable, field-ready diagnostic tool, it improves the ability to monitor and control schistosomiasis in low-resource areas. Its design, which uses locally sourced materials for robustness and repairability, demonstrates how AI and automation can revolutionize diagnostics, making them more accessible and scalable. This approach not only aligns with sustainable health solutions, but also has the potential to influence diagnostic methodologies beyond parasitology, promoting health equity in underserved regions.

Despite its advancements, the Schistoscope 5.0 faces challenges with uneven sample surfaces, artifacts and overlapping eggs in field samples, which can impact diagnostic accuracy. In addition, the performance of the UNET model, while promising, needs further validation across a broader range of real-world conditions to ensure reliability. Additionally, the device's sample processing time, specifically in registering whole slide images of 25mm membrane filters and Kato-Katz smears, could be a barrier for its application in large-scale surveys.

Usability and User-acceptance: Chapter 5 presents a study of the usability and acceptability of Schistoscope 5.0 conducted in Nigeria with local healthcare workers and medical students. The study used questionnaire feedback and open discussions to assess the impact of the device on diagnostic workflows. Users found the Schistoscope to be easy to operate, especially praising the autofocus and image capture features to reduce operator fatigue. The modular design, allowing for semi- and fully automated use, was seen as advantageous in settings with varying access to trained microscopists. Feedback also included suggestions for greater portability and faster scanning capabilities, highlighting the current design's bulkiness as a limitation.

The potential of the Schistoscope to improve diagnostics in resource-limited environments is significant. By reducing the need for highly skilled personnel and overcoming infrastructure barriers, it could improve diagnostic accuracy and efficiency for schistosomiasis and potentially

other neglected tropical diseases. This could lead to scalable health interventions, making the Schistoscope a model for future low-cost, AI-assisted diagnostic devices.

Although the Schistoscope was well received, users also pointed out the need for quality control to avoid errors in negative sample identification. These practical limitations suggest that further refinement is necessary to ensure the device's effectiveness in real-world settings where diagnostic accuracy is crucial. They suggested that future development should focus on enhancing the portability of the Schistoscope through more compact designs and possibly adding more objective lenses to widen its diagnostic range. Integrating user feedback into a User-Centered Design (UCD) approach will be essential for future iterations, ensuring that the device not only meets technical standards but also fits seamlessly into the workflows of its users. Additional improvements might include features for sample storage and enhanced digital interfaces. Continuous engagement with users to refine the Schistoscope based on their practical experiences will be key. Expanding this model to other NTDs through similar user-engaged design processes could further amplify the impact of digital diagnostic tools on global health initiatives.

Nigeria Field Validation: Chapter 6 details a field study in Nigeria evaluating the Schistoscope 5.0's performance in detecting *S. haematobium* eggs. The device embedded with a UNET-based *S. haematobium* egg detection algorithm was compared with conventional microscopy in semi- and fully automated modes. The findings showed that while the sensitivity matched traditional methods, the specificity in the automated mode was lower. The AI algorithm faced challenges in distinguishing eggs from similar structures due to inadequate training data. There were also notable differences in egg counts at high infection levels, highlighting potential issues with the accuracy of the AI model.

The Schistoscope 5.0 offers a pathway to accessible diagnostics in areas affected by schistosomiasis, demonstrating the benefits of integrating technology into public health. Its potential to transform disease monitoring and control is evident, but the study also highlights the need for robust training of the AI model to improve diagnostic specificity. This could lead to better public health outcomes by ensuring accurate diagnosis, surveillance, and treatment monitoring in low-resource settings.

The primary limitation observed was that the UNET-based algorithm struggled with specificity, particularly in distinguishing between eggs and artifacts. This points to the need for a more comprehensive dataset for AI training, which would help reduce false positives. Furthermore, the discrepancies in egg counts in highly infected samples with a high occurrence of overlapping eggs suggest that the UNET-based deep

learning model might not fully capture the complexities of infection intensity. Hence, more work needs to be done to improve the AI algorithm through broader and more diverse training data. An additional post-processing step to refine the segmentation output of the deep learning model would also improve both sensitivity and specificity.

Autofocusing and Whole Membrane Imaging: Chapter 7 discusses significant enhancements to the Schistoscope 5.0 to diagnose parasitic diseases, particularly schistosomiasis, in field settings. Key developments include the implementation of an automated slide scanning system with a perturb and observe (P&O) autofocusing algorithm, which adjusts the position of the Z axis to optimize the focus of the registered FoV, thus addressing issues such as uneven sample surfaces and the presence of artifacts. This algorithm, borrowed from photovoltaic technology, optimizes scanning speed and accuracy. Furthermore, an optimized circular membrane filter scanning procedure was developed, which reduces the whole slide scanning time by up to 72% by focusing only on relevant FoVs, offering a significant benefit for high-throughput diagnostics in urogenital schistosomiasis.

These technological advances have substantial implications for public health, particularly in enabling large-scale schistosomiasis surveys. Automation reduces the need for skilled personnel, making diagnostics more scalable in remote areas. The P&O algorithm's efficiency is vital for implementing low-cost diagnostic devices, thus promoting wider adoption in areas with limited resources. This not only aids in disease monitoring, but also supports broader public health strategies aimed at reducing morbidity and enhancing productivity.

Despite advances, there are still challenges to overcome. Mechanical backlash and variability in image quality across different slides are issues that can affect diagnostic reliability. The effectiveness of the autofocus algorithm could be limited by these mechanical and environmental factors, which could lead to inconsistencies in diagnostic results. In addition, integration of low-cost GPUs or TPUs could enhance computational capabilities for real-time diagnostics. In addition, extensive field testing and validation is necessary to adapt and confirm the robustness of these systems in diverse and challenging environments. This will ensure that the technology can be scaled up effectively, transforming the landscape of parasitic disease diagnosis in resource-limited settings in sub-Saharan Africa and possibly around the world.

Automated Urogenital Schistosomiasis Diagnosis: Chapter 8 introduces a large scale *S. haematobium* egg dataset of field microscopy images and a two-stage diagnostic framework for detecting urogenital

schistosomiasis, employing semantic segmentation with a DeepLabV3-MobileNetV3 model. This approach uses deep neural networks for Stage 1, where it addresses the differentiation of eggs from artifacts in noisy images. Stage 2 applies region-based ellipse fitting to better identify overlapping eggs, enhancing the assessment of infection intensity. Validation in a significant dataset and implementation in an Edge AI system consisting, of Raspberry pi and Google coral TPU onboard computer, highlight the effectiveness of the framework, with diagnostic performance in 65 clinical samples showing sensitivity and specificity rates greater than 93%, meeting WHO diagnostic standards for schistosomiasis.

This framework significantly advances the diagnosis of urogenital schistosomiasis in low-resource settings by making sophisticated AI-based diagnostics more accessible. By adapting complex deep learning models to portable devices, it democratizes healthcare, allowing more accurate and timely diagnosis in areas where traditional diagnostics are challenged by a lack of resources or expertise. This innovation could pave the way for a broader application in the diagnosis of other parasitic diseases, aligning with global health goals to control and eliminate neglected tropical diseases.

The computational demands of running such models on Edge AI platforms could limit the framework's real-world performance in terms of speed and power consumption, crucial considerations in field settings where power and processing capabilities might be constrained. Validation studies in various field environments will be crucial in confirming the reliability of the Schistoscope under different conditions of infection intensity and environmental challenges.

Gabon Field Validation: Chapter 9 explores the diagnostic performance of the improved Schistoscope 5.0, with the two-stage detection algorithm, in Gabon for detecting and quantifying *S. haematobium* eggs in urine. The study was divided into two parts: Study A with freshly collected samples and Study B with fresh and banked samples. The Schistoscope showed sensitivities of 83.1% and 96.3% compared to conventional microscopy for studies A and B, respectively, with sensitivities against a composite reference standard (CRS) at 62.9% and 78%. The specificity varied between 78. 8% in Study A and 90.9% in Study B, indicating the variability of the performance according to the type of sample. The ability of the device to handle fresh and banked samples highlights its utility for retrospective analyses.

The Schistoscope emerges as a viable alternative to traditional microscopy, particularly suitable for high-infection-intensity cases and in resource-limited environments. Its ability for retrospective analysis could revolutionize the way schistosomiasis is monitored and controlled in regions where immediate diagnostic facilities are scarce. The correlation

with conventional microscopy in egg quantification (r=0.71 to 0.93) suggests the potential for accurate disease assessment, helping public health decisions for screening and treatment.

The study revealed that the specificity of the Schistoscope could be compromised by environmental artifacts, leading to false positives. This indicates a need for further refinement of the AI algorithm to improve accuracy, especially for low-intensity infections where diagnostic precision is critical. There is also an observed underestimation in high-intensity cases due to egg overlap, which needs further improvement for comprehensive diagnostics.

Automated Intestinal Helminths Egg Detection: Chapter 10 introduces an innovative approach to detecting intestinal helminth infections using the Schistoscope 5.0. Addresses the limitations of the traditional Kato-Katz (KK) method by automating egg detection for *Ascaris lumbricoides*, *Trichuris trichiura*, hookworm, and *S. mansoni*. An extensive dataset was developed, combining images from various sources, which was used to train an EfficientDet-D0 deep learning model. This model demonstrated high precision and sensitivity in the detection of helminth eggs from fecal samples, indicating its versatility for field diagnostics.

The implementation of the Schistoscope could significantly transform intestinal helminthiasis diagnostics in low-resource settings by reducing the dependence on skilled technicians and minimizing human error. This aligns with WHO's Target Product Profiles for diagnostics, supporting broad deworming and treatment initiatives. Automation not only promises more consistent results, but also addresses issues such as visual fatigue among microscopists, potentially improving the effectiveness of disease control programs in endemic areas.

Despite its promising performance, the model needs further improvement in sensitivity, especially for hookworm and *S. mansoni* egg detection. The current data set might still have biases or lack diversity, which could affect the generalization to all field conditions. Additionally, while individual egg detection is accurate, the system performance at the patient or slide level requires further validation to ensure robustness in real-world scenarios.

11.2. CONCLUSION

In this thesis, we successfully developed an automated digital microscope, the Schistoscope, which matches traditional microscopy in diagnostic accuracy, usability, and operational feasibility for detecting *S. haematobium* and intestinal helminth eggs in resource-limited settings. Our advancements include a whole slide imaging system with the perturb and observe (P&O) autofocusing algorithm, optimized whole slide scanning procedures, and deep learning-based AI detection models,

significantly improving diagnostic accuracy and speed. The integration of Edge AI with deep learning-based diagnostic frameworks has resulted in high sensitivity, specificity, and user acceptability, enabling reliable field deployment and effective performance on both fresh and banked urine samples.

11.3. FUTURE DIRECTION

Future iterations of the automated digital microscope (the Schistoscope) should focus on several key areas:

- **Hardware and Software Refinement:** Address mechanical issues such as backlash to improve autofocus consistency.
- **AI Model Optimization:** Enhance the ability to distinguish between eggs and artifacts by expanding training data sets to cover more environmental conditions and complexities. This could involve refining neural network architectures or developing new algorithms to deal with complex image conditions.
- **Dataset Expansion:** Increase dataset diversity to improve model generalization across various field conditions.
- **Broader Application:** Explore the potential of the schistoscope for diagnosing other parasitic infections, thereby amplifying its impact on global health.
- **Field Validation:** Conduct extensive field trials in diverse settings to validate the robustness, usability, and acceptance of the system among local healthcare workers.
- **Energy Efficiency:** Improve by integrating alternative power solutions, such as solar energy, to extend applicability to remote locations.
- **Local Production and Distribution:** Develop partnerships to facilitate local manufacturing and distribution, with the aim of reducing costs and increasing availability.
- **Cloud Integration:** Implement cloud-based data storage and analysis systems to support large-scale public health applications.
- **User Engagement:** Continue to involve local stakeholders in the design and implementation process to ensure the Schistoscope meets real-world needs through an iterative development approach.

These enhancements could establish the Schistoscope as a benchmark for diagnostic tools targeting neglected tropical diseases in resource-limited environments, significantly contributing to global health initiatives.

BIBLIOGRAPHY

[1] I. Abdulwahab, A. A. Olaniyan, U. Musa, and O. Ajayi. “Optimization of a droop controlled micro-grid using grasshopper optimization algorithm”. In: *Zaria J.* 10.1 (2021), p. 65.

[2] K. O. Abosalif, A. A. Ahmed, I. M. Shammat, A. S. Aljafari, A. A. Afifi, and C. J. Shiff. “A Comparative Study of Three Conventional Methods for Diagnosis of Urinary Schistosomiasis”. In: *Journal of The Faculty of Science and Technology* 6 (2019), pp. 48–61. doi: 10.52981/jfst.vi6.603.

[3] D. D. Acula, C. P. L. Buico, G. U. Cruzada, M. K. C. Encelan, and C. Y. G. Rivera. “Soil transmitted helminth egg detection and classification in fecal smear images using faster region-based convolutional neural network with residual network-50”. In: *International Conference on Green Energy, Computing and Intelligent Technology (GEn-CITy 2023)*. Vol. 2023. 2023, pp. 284–291. doi: 10.1049/icp.2023.1793.

[4] A. F. Adenowo, B. E. Oyinloye, B. I. Ogunyinka, and A. P. Kappo. “Impact of human schistosomiasis in sub-Saharan Africa”. In: *Brazilian Journal of Infectious Diseases* 19.2 (2015), pp. 196–205. doi: j.bjid.2014.11.004.

[5] M. O. Afolabi, A. Adebiyi, J. Cano, B. Sartorius, B. Greenwood, O. Johnson, and O. Wariri. “Prevalence and distribution pattern of malaria and soil-transmitted helminth co-endemicity in sub-Saharan Africa, 2000–2018: A geospatial analysis”. In: *PLoS Neglected Tropical Diseases* 16.9 (2022), e0010321. doi: 10.1371/journal.pntd.0010321.

[6] T. E. Agbana, J. C. Diehl, F. van Pul, S. M. Khan, V. Patlan, M. Verhaegen, and G. Vdovin. “Imaging & Identification of Malaria Parasites Using Cellphone Microscope with a Ball Lens”. In: *PLoS ONE* 13 (2018), e0205020. doi: 10.1371/journal.pone.0205020.

[7] T. Agbana, G. Y. Van, O. Oladepo, G. Vdovin, W. Oyibo, and J. C. Diehl. “Schistoscope: Towards a locally producible smart diagnostic device for Schistosomiasis in Nigeria”. In: *2019 IEEE Global Humanitarian Technology Conference (GHTC)*. Seattle, WA, USA, 2019, pp. 1–8. doi: 10.1109/GHTC46095.2019.9033049.

[8] T. Agbana, P. Nijman, M. Hoeber, D. van Grootheest, A. van Diepen, L. van Lieshout, J. C. Diehl, M. Verhaegen, and G. Vdovine. “Detection of Schistosoma haematobium using lensless imaging and flow cytometry, a proof of principle study”. In: *Proceedings of the Optical Diagnostics and Sensing XX: Toward Point-of-Care Diagnostics*. Vol. 11247. 2020, 112470F. doi: 10.1117/12.2545220.

[9] S. Agrebi and A. Larbi. “Use of artificial intelligence in infectious diseases”. In: *Artificial Intelligence in Precision Health*. Academic Press, 2020, pp. 415–438. isbn: 978-0-12-817133-2. doi: 10.1016/B978-0-12-817133-2.00018-5.

[10] H. Akaike. “A new look at the statistical model identification”. In: *IEEE Transactions on Automatic Control* 19.6 (1974), pp. 716–723. doi: 10.1109/TAC.1974.1100705.

[11] T. Aidukas, R. Eckert, A. R. Harvey, L. Waller, and P. C. Konda. “Low-cost, sub-micron resolution, wide-field computational microscopy using opensource hardware”. In: *Scientific Reports* 9 (2019), p. 7457. doi: 10.1038/s41598-019-43845-9.

[12] S. Aksoy, P. Buscher, M. Lehane, P. Solano, and J. Van Den Abbeele. “Human African trypanosomiasis control: Achievements and challenges”. In: *PLoS Neglected Tropical Diseases* 11.4 (2017), e0005454. doi: 10.1371/journal.pntd.0005454.

[13] O. Ally, B. N. Kanoi, L. Ochola, S. G. Nyanjom, C. Shiluli, G. Misinzo, and J. Gitaka. “Schistosomiasis diagnosis: Challenges and opportunities for elimination”. In: *PLOS Neglected Tropical Diseases* 18.7 (2024), e0012282. doi: 10.1371/journal.pntd.0012282.

[14] G. A. Amuga, O. J. Nebe, F. O. Nduka, N. N., D. A. Dakul, S. Isiyaku, E. Ngige, S. Jibrin, S. M. Jacob, I. A. Nwoye, U. Nwankwo, R. Urude, S. M. Aliyu, A. Garba, W. Adamani, C. O. Nwosu, I. A. Anagbogu, R. Dixon, A. clark, and G. O. Adeoye. “Schistosomiasis: epidemiological factors enhancing transmission in Nigeria”. In: *Global Research Journal of Public Health and Epidemiology* 8.7 (2020), pp. 023–032.

[15] S. Y. Audee, M. B. Muâzu, S. Man-Yahaya, Z. Haruna, A. T. Salawudeen, and P. Oyibo. “Development of a dynamic cuckoo search algorithm”. In: *Covenant Journal of Informatics and Communication Technology* 7.2 (2019).

[16] O. P. Aula, D. P. McManus, M. K. Jones, and C. A. Gordon. “Schistosomiasis with a focus on Africa”. In: *Tropical Medicine and Infectious Disease* 6.3 (2021), p. 109. doi: 10.3390/tropicalmed603010

[17] A. Alva, C. Cangalaya, M. Quiliano, C. Krebs, R. H. Gilman, P. Sheen, and M. Zimic. “Mathematical algorithm for the automatic recognition of intestinal parasites”. In: *PLoS ONE* 12.4 (2017), e0175646. doi: 10.1371/journal.pone.0175646.

[18] V. Amato Neto, R. Campos, P. L. Pinto, L. Matsubara, L. M. Braz, A. Miyamoto, R. Foster, S. A. do Nascimento, H. B. de Souza, and A. A. Moreira. “Evaluation of the usefulness of the Coprotest for parasitologic examination of feces”. In: *Rev. Hosp. Clin.* 44.4 (1989), pp. 153–5.

[19] M. Armstrong, A. R. Harris, M. V. D’Ambrosio, J. T. Coulibaly, S. Essien-Baidoo, R. K. D. Ephraim, J. R. Andrews, I. I. Bogoch, and D. A. Fletcher. “Point-of-care sample preparation and automated quantitative detection of schistosoma haematobium using mobile phone microscopy”. In: *American Journal of Tropical Medicine and Hygiene* 106.5 (2022), pp. 1442–1449. doi: 10.4269/ajtmh.21-1071.

[20] L. R. Ash and T. C. Orihel. *Atlas of Human Parasitology*. 5th. American Society of clinical pathologists, 2007. isbn: 978-0891891673.

[21] D. Avci and A. Varol. “An expert diagnosis system for classification of human parasite eggs based on multi-class SVM”. In: *Expert Systems with Applications* 36.1 (2009), pp. 43–48. doi: 10.1016/j.eswa.2007.09.012.

[22] J. Balsam, M. Ossandon, H. A. Bruck, I. Lubensky, and A. Rasooly. “Low-cost technologies for medical diagnostics in low-resource settings”. In: *Expert opinion on medical diagnostics* 7.3 (2013), pp. 243–255. doi: 10.1517/17530059.2013.767796.

[23] C. C. Bass. “The diagnosis of hookworm infection with special reference to the examination of feces for eggs of intestinal parasites”. In: *Arch Diag* 3 (1910), pp. 231–236.

[24] M. Bengtson, A. Onasanya, P. Oyibo, B. Meulah, K. T. Samenjo, I. Braakman, W. Oyibo, and J. C. Diehl. “A usability study of an innovative optical device for the diagnosis of schistosomiasis in Nigeria”. In: *2022 IEEE Global Humanitarian Technology Conference (GHTC)*. Santa Clara, CA, USA: IEEE, 2022, pp. 17–22. doi: 10.1109/GHTC55712.2022.9911019.

[25] J. Bethony, S. Brooker, M. Albonico, S. M. Geiger, A. Loukas, D. Diemert, and P. J. Hotez. “Soil-transmitted helminth infections: ascariasis, trichuriasis, and hookworm”. In: *The lancet* 367.9521 (2006), pp. 1521–1532. doi: 10.1016/S0140-6736(06)68653-4.

[26] Z. Bian, C. Guo, S. Jiang, J. Zhu, R. Wang, P. Song, Z. Zhang, K. Hoshino, and G. Zheng. “Autofocusing technologies for whole slide imaging and automated microscopy”. In: *Journal of Biophotonics* 13.12 (2020), e202000227. doi: 10.1002/jbio.202000227.

[27] C. M. Bishop. *Pattern Recognition and Machine Learning*. Springer, 2006. isbn: 978-0-387-31073-2.

[28] F. R. Boddeke, L. J. Van Vliet, and I. T. Young. “Calibration of the automated z-axis of a microscope using focus functions”. In: *Journal of Microscopy* 186.3 (1997), pp. 270–274. doi: 10.1046/j.1365-2818.1997.2060766.x.

[29] I. I. Bogoch, J. R. Andrews, B. Speich, J. Utzinger, S. M. Ame, S. M. Ali, and J. Keiser. “Mobile phone microscopy for the diagnosis of soil-transmitted helminth infections: A proof-of-concept study”. In: *The American Journal of Tropical Medicine and Hygiene* 88.4 (2013), pp. 626–629. doi: 10.4269/ajtmh.12-0742.

[30] I. I. Bogoch, J. T. Coulibaly, J. R. Andrews, B. Speich, J. Keiser, J. R. Stothard, E. K. N’goran, and J. Utzinger. “Evaluation of portable microscopic devices for the diagnosis of Schistosoma and soil-transmitted helminth infection”. In: *Parasitology* 141.14 (2014), pp. 1811–1818. doi: 10.1017/S0031182014000432.

[31] I. I. Bogoch, H. C. Koydemir, D. Tseng, R. K. D. Ephraim, E. Duah, J. Tee, J. R. Andrews, and A. Ozcan. “Evaluation of a mobile phone-based microscope for screening of Schistosoma haematobium infection in rural Ghana”. In: *American Journal of Tropical Medicine and Hygiene* 96.6 (2017), pp. 1468–1471. doi: 10.4269/ajtmh.16-0912.

[32] I. I. Bogoch, J. Lundin, N. C. Lo, and J. R. Andrews. “Mobile phone and handheld microscopes for public health applications”. In: *The Lancet Public Health* 2.8 (2017), e355. doi: 10.1016/S2468-2667(17)30120-2.

[33] F. Bosch, M. S. Palmeirim, S. M. Ali, S. M. Ame, J. Hattendorf, and J. Keiser. “Diagnosis of soil-transmitted helminths using the Kato-Katz technique: What is the influence of stirring, storage time and storage temperature on stool sample egg counts?” In: *PLoS Neglected Tropical Diseases* 15.1 (2021), e0009032. doi: 10.1371/journal.pntd.0009032.

[34] I. Braakman. “Improving an Optical Diagnostics Device for Schistosomiasis”. MA thesis. Delft, The Netherlands: Delft University of Technology, 2021.

[35] J. F. Brenner, B. S. Dew, J. B. Horton, T. King, P. W. Neurath, and W. D. Selles. “An automated microscope for cytologic research a preliminary evaluation”. In: *Journal of Histochemistry & Cytochemistry* 24.1 (1976), pp. 100–111. doi: 10.1177/24.1.1254907.

[36] R. Brink. “A simple McMaster egg counting procedure for trichostrongylid eggs in cattle faeces”. In: *Tijdschr. Diergeneeskd.* 96.13 (1971), pp. 859–862.

[37] J. Brooks. *COCO Annotator*. GitHub repository. 2019. url: https://github.com/jsbroks/coco-annotator/ (visited on 12/18/2021).

[38] J. S. Brownstein, B. Rader, C. M. Astley, and H. Tian. “Advances in Artificial Intelligence for infectious-disease surveillance”. In: *New England Journal of Medicine* 388.17 (2023), pp. 1597–1607. doi: 10.1056/NEJMra2107472.

[39] B. Bruun and J. Aagaard-Hansen. *The social context of schistosomiasis and its control: an introduction and annotated bibliography*. World Health Organization, 2008. isbn: 9789241597180.

[40] J. M. Bruun, C. M. Kapel, and J. M. Carstensen. “Detection and classification of parasite eggs for use in helminthic therapy”. In: *2012 9th IEEE International Symposium on Biomedical Imaging (ISBI)*. Barcelona, Spain, 2012, pp. 1627–1630. doi: 10.1109/ISBI.2012.6235888.

[41] A. L. Bustinduy, B. Randriansolo, A. S. Sturt, S. A. Kayuni, P. D. C. Leustcher, B. L. Webster, L. V. Lieshout, J. R. Stothard, H. Feldmeier, and M. Gyapong. “An update on female and male genital schistosomiasis and a call to integrate efforts to escalate diagnosis, treatment and awareness in endemic and non-endemic settings: the time is now”. In: *Advances in Parasitology* 115 (2022), pp. 1–44. doi: 10.1016/bs.apar.2021.12.003.

[42] A. Cable, J. Wollenzin, R. Johnstone, K. Gossage, J. S. Brooker, J. Mills, J. Jiang, and D. Hillmann. “Microscopy system with autofocus adjustment by low-coherence interferometry”. Pat. US9869852B2. 2018.

[43] A. Caetano, C. Santana, and R. A. de Lima. “Diagnostic support of parasitic infections with an AI-powered microscope”. In: *Research on Biomedical Engineering* 39.3 (2023), pp. 561–572. doi: 10.1007/s42600-023-00288-6.

[44] R. A. Campbell, R. W. Eifert, and G. C. Turner. “Openstage: A low-cost motorized microscope stage with sub-micron positioning accuracy”. In: *PLoS ONE* 9.2 (2014), e88977. doi: 10.1371/journal.pone.0088977.

[45] Centers for Disease Control and Prevention. *CDC-Schistosomiasis*. 2022. url: https://www.cdc.gov/parasites/schistosomia index.html (visited on 02/12/2022).

[46] G. Chaia, A. B. Q. Chaia, J. McAullife, N. Katz, and D. Gasper. "Coprological diagnosis of schistosomiasis. II. Comparative study of quantitative methods". In: *Rev. Inst. Med. Trop. São Paulo* 10.6 (1968).

[47] A. M. Chagas, L. L. Prieto-Godino, A. B. Arrenberg, and T. Baden. "The €100 Lab: A 3D-Printable Open-Source Platform for Fluorescence Microscopy, Optogenetics, and Accurate Temperature Control during Behaviour of Zebrafish, Drosophila, and Caenorhabditis Elegans". In: *PLoS Biology* 15.7 (2017), e2002702. doi: 10.1371/journal.pbio.2002702.

[48] L.-C. Chen, G. Papandreou, F. Schroff, and H. Adam. *Rethinking atrous convolution for semantic image segmentation*. preprint. 2017. doi: 10.48550/arXiv.1706.05587. arXiv: 1706.05587.

[49] P. H. C. Chen, K. Gadepalli, R. MacDonald, Y. Liu, S. Kadowaki, K. Nagpal, T. Kohlberger, J. Dean, G. S. Corrado, J. D. Hipp, C. H. Mermel, and M. C. Stumpe. "An augmented reality microscope with real-time artificial intelligence integration for cancer diagnosis". In: *Nature Medicine* 25.9 (2019), pp. 1453–1457. doi: 10.1038/s41591-019-0539-7.

[50] P. M. Z. Coelho, A. D. Jurberg, Á. A. Oliveira, and N. Katz. "Use of a saline gradient for the diagnosis of schistosomiasis". In: *Mem. Inst. Oswaldo Cruz* 104.5 (Aug. 2009), pp. 720–723. doi: 10.1590/S0074-02762009000500010.

[51] P. A. Collender, A. E. Kirby, D. G. Addiss, M. C. Freeman, and J. V. Remais. "Methods for quantification of soil-transmitted helminths in environmental media: current techniques and recent advances". In: *Trends Parasitol.* 31.12 (2015), pp. 625–639. doi: 10.1016/j.pt.2015.08.007.

[52] D. G. Colley, A. L. Bustinduy, W. E. Secor, and C. H. King. "Human schistosomiasis". In: *The Lancet* 383.9936 (2014), pp. 2253–2264. doi: 10.1016/S0140-6736(13)61949-2.

[53] J. T. Collins, J. Knapper, J. Stirling, J. Mduda, C. Mkindi, V. Mayagaya, G. A. Mwakajinga, P. T. Nyakyi, V. L. Sanga, D. Carbery, L. White, S. Dale, Z. J. Lim, J. J. Baumberg, P. Cicuta, S. McDermott, B. Vodenicharski, and R. Bowman. "Robotic microscopy for everyone: the OpenFlexure microscope". In: *Biomed. Opt. Express* 11.5 (May 2020), pp. 2447–2460. doi: 10.1364/BOE.385729.

[54] I. R. Cooke, C. J. Laing, L. V. White, S. J. Wakes, and S. J. Sowerby. “Analysis of menisci formed on cones for single field of view parasite egg microscopy”. In: *J. Microsc.* 257.2 (2015), pp. 133–141. doi: 10.1111/jmi.12192.

[55] P. L. A. M. Corstjens, C. J. de Dood, S. Knopp, M. N. Clements, G. Ortu, I. Umulisa, E. Ruberanziza, U. Wittmann, T. Kariuki, P. LoVerde, W. E. Secor, L. Atkins, S. Kinung’hi, S. Binder, C. H. Campbell Jr., D. G. Colley, and G. J. van Dam. “Circulating Anodic Antigen (CAA): a highly sensitive diagnostic biomarker to detect active Schistosoma infections—improvement and use during SCORE”. In: *The American Journal of Tropical Medicine and Hygiene* 103.1 Suppl (2020), pp. 50–57. doi: 10.4269/ajtmh.19-0819.

[56] J. T. Coulibaly, M. Ouattara, M. V. D’Ambrosio, D. A. Fletcher, J. Keiser, J. Utzinger, E. K. N’Goran, J. R. Andrews, and I. I. Bogoch. “Accuracy of mobile phone and handheld light microscopy for the diagnosis of schistosomiasis and intestinal protozoa infections in Côte d’Ivoire”. In: *PLoS Neglected Tropical Diseases* 10.6 (2016), e0004768. doi: 10.1371/journal.pntd.0004768.

[57] J. T. Coulibaly, K. D. Silue, M. Armstrong, M. Díaz de León Derby, M. V. D’Ambrosio, D. A. Fletcher, J. Keiser, K. Fisher, J. R. Andrews, and I. I. Bogoch. “High Sensitivity of Mobile Phone Microscopy Screening for Schistosoma haematobium in Azaguié, Côte d’Ivoire”. In: *The American Journal of Tropical Medicine and Hygiene* 108.1 (2023), p. 41. doi: 10.4269/ajtmh.22-0527.

[58] P. D. Cox and A. C. Todd. “Survey of gastrointestinal parasitism in Wisconsin dairy cattle”. In: *J. Am. Vet. Med. Assoc.* 141.6 (1962), pp. 706–709.

[59] G. Cringoli, L. Rinaldi, M. P. Maurelli, and J. Utzinger. “FLOTAC: new multivalent techniques for qualitative and quantitative copromicroscopic diagnosis of parasites in animals and humans”. In: *Nat. Protoc.* 5.3 (2010), pp. 503–515. doi: 10.1038/nprot.2009.235.

[60] G. Cringoli, L. Rinaldi, M. Albonico, R. Bergquist, and J. Utzinger. “Geospatial (s) tools: integration of advanced epidemiological sampling and novel diagnostics”. In: *Geospatial Health* 7.2 (2013), pp. 399–404. doi: 10.4081/gh.2013.97.

[61] N. Cure-Bolt, F. Perez, L. A. Broadfield, B. Levecke, P. Hu, J. Oleynick, M. Beltrán, P. Ward, and L. Stuyver. “Artificial intelligence-based digital pathology for the detection and quantification of soil-transmitted helminths eggs”. In: *PLOS Neglected Tropical Diseases* 18.9 (2024), e0012492. doi: 10.1371/journal.pntd.0012492.

[62] J. S. Cybulski, J. Clements, and M. Prakash. “Foldscope: Origami-based paper microscope”. In: *PLoS ONE* 9 (2014), e98781. doi: 10.1371/journal.pone.0098781.

[63] E. Dacal, D. Bermejo-Peláez, L. Lin, E. Álamo, D. Cuadrado, Á. Martínez, A. Mousa, M. Postigo, A. Soto, E. Sukosd, A. Vladimirov, C. Mwandawiro, P. Gichuki, N. A. Williams, J. Muñoz, S. Kepha, and M. Luengo-Oroz. “Mobile microscopy and telemedicine platform assisted by deep learning for the quantification of Trichuris trichiura infection”. In: *PLoS neglected tropical diseases* 15.9 (2021). doi: 10.1371/journal.pntd.0009677.

[64] T. Rai Dastidar. “Automated focus distance estimation for digital microscopy using deep convolutional neural networks”. In: *2019 IEEE/CVF Conference on Computer Vision and Pattern Recognition Workshops (CVPRW)*. Long Beach, CA, USA, 2019, pp. 1049–1056. doi: 10.1109/CVPRW.2019.00137.

[65] T. R. Dastidar and R. Ethirajan. “Whole slide imaging system using deep learning-based automated focusing”. In: *Biomedical Optics Express* 11.1 (2020), pp. 480–491. doi: 10.1364/BOE.379780.

[66] J. C. Dejon-Agobé, Y. J. Honkpehedji, J. F. Zinsou, J. R. Edoa, B. R. Adégbitè, A. Mangaboula, S. T. Agnandji, G. Mombo-Ngoma, M. Ramharter, P. G. Kremsner, B. Lell, M. P. Grobusch, and A. A. Adegnika. “Epidemiology of schistosomiasis and soil-transmitted helminth coinfections among schoolchildren living in Lambaréné, Gabon”. In: *The American Journal of Tropical Medicine and Hygiene* 103.1 (2020), p. 325. doi: 10.4269/ajtmh.19-0835.

[67] K. E. delas Peñas, E. A. Villacorte, P. T. Rivera, and P. C. Naval. “Automated Detection of Helminth Eggs in Stool Samples Using Convolutional Neural Networks”. In: *2020 IEEE REGION 10 CONFERENCE (TENCON)*. Osaka, Japan, 2020, pp. 750–755. doi: 10.1109/TENCON50793.2020.9293746.

[68] J. C. Diehl, P. Oyibo, T. Agbana, S. Jujjavarapu, G. Van, G. Vdovin, and W. Oyibo. “Schistoscope: Smartphone versus Raspberry Pi based low-cost diagnostic device for urinary Schistosomiasis”. In: *Proceedings of the 2020 IEEE Global Humanitarian Technology Conference (GHTC)*. Seattle, WA, USA, 2020, pp. 1–8. doi: 10.1109/GHTC46280.2020.9342871.

[69] N. Dimitriou, O. Arandjelović, and P. D. Caie. “Deep learning for whole slide image analysis: An overview”. In: *Frontiers in Medicine* 6 (2019). doi: 10.3389/fmed.2019.00264.

[70] R. T. Dong, U. Rashid, and J. Zeineh. “System and method for generating digital images of a microscope slide”. Pat. US20050089208A1. 2005.

[71] A. R. Dopp, K. E. Parisi, S. A. Munson, and A. R. Lyon. “A glossary of user-centered design strategies for implementation experts”. In: *Translational Behavioral Medicine* 9.6 (Nov. 2019), pp. 1057–1064. doi: 10.1093/tbm/iby119.

[72] K. Dunning and J. R. Stothard. “From the McArthur to the millennium health microscope (MHM): future developments in microscope miniaturization for international health”. In: *Microsc Today* 15.2 (2007), pp. 18–21.

[73] X. Du, L. Liu, X. Wang, G. Ni, J. Zhang, R. Hao, J. Liu, and Y. Liu. “Automatic classification of cells in microscopic fecal images using convolutional neural networks”. In: *Biosci. Rep.* 39.4 (2019). doi: 10.1042/BSR20182100.

[74] M. Everingham, L. Van Gool, C. K. I. Williams, J. Winn, and A. Zisserman. “The Pascal visual object classes (VOC) challenge”. In: *International Journal of Computer Vision* 88.2 (2010), pp. 303–338. doi: 10.1007/s11263-009-0275-4.

[75] T. G. Egwang and J. O. Slocombe. “Evaluation of the Cornell-Wisconsin centrifugal flotation technique for recovering trichostrongylid eggs from bovine feces”. In: *Can. J. Comp. Med.* 46.2 (1982), pp. 133–137.

[76] R. K. Ephraim, E. Duah, J. R. Andrews, and I. I. Bogoch. “Ultra-low-cost urine filtration for Schistosoma haematobium diagnosis: a proof-of-concept study”. In: *American Journal of Tropical Medicine and Hygiene* 91.3 (Sept. 2014), pp. 544–546. doi: 10.4269/ajtmh.14-0221.

[77] R. K. D. Ephraim, E. Duah, J. S. Cybulski, M. Prakash, M. V. D’Ambrosio, D. A. Fletcher, J. Keiser, J. R. Andrews, and I. I. Bogoch. “Diagnosis of Schistosoma haematobium infection with a mobile phone-mounted Foldscope and a reversed-lens CellScope in Ghana”. In: *American Journal of Tropical Medicine and Hygiene* 92.6 (2015), pp. 1253–1256. doi: 10.4269/ajtmh.14-0741.

[78] J. Frean. “Microscopic images transmitted by mobile cameraphone”. In: *Trans. R. Soc. Trop. Med. Hyg.* 101.10 (2007), pp. 1053–1053. doi: 10.1016/j.trstmh.2007.06.008.

[79] M. D. French, D. Evans, F. M. Fleming, W. E. Secor, N. Biritwum, B. S. J., A. Bustinduy, A. Gouvras, N. Kabatereine, C. H. King, M. Rebollo Polo, J. Reinhard-Rupp, D. Rollinson, L. A. Tchuem Tchuenté, J. Utzinger, J. Waltz, and Y. Zhang. “Schistosomiasis in Africa: Improving strategies for long-term and sustainable morbidity control”. In: *PLoS neglected tropical diseases* 12.6 (2018). doi: 10.1371/journal.pntd.0006484.

[80] L. S. Garcia, M. Arrowood, E. Kokoskin, G. P. Paltridge, D. R. Pillai, G. W. Procop, N. Ryan, R. Y. Shimizu, and G. Visvesvara. “Laboratory diagnosis of parasites from the gastrointestinal tract”. In: *Clin. Microbiol. Rev.* 31.1 (2018). doi: 10.1128/CMR.00025-17.

[81] J. M. Geusebroek, F. Cornelissen, A. W. Smeulders, and H. Geerts. “Robust autofocusing in microscopy”. In: *Cytometry* 39.1 (2000), pp. 1–9. doi: 10.1002/(SICI)1097-0320(20000101)39:1<1::AID-CYTO2>3.0.CO;2-J.

[82] J. R. Gilbertson, J. Ho, L. Anthony, D. M. Jukic, Y. Yagi, and A. V. Parwani. “Primary histologic diagnosis using automated whole slide imaging: A validation study”. In: *BMC Clinical Pathology* 6 (2006), pp. 1–19. doi: 10.1186/1472-6890-6-4.

[83] H. M. Gordon and H. V. Whitlock. “A new technique for counting nematode eggs in sheep faeces”. In: *J. Counc. Sci. Ind. Res.* 12.1 (1939), pp. 50–52.

[84] Z. Grier, M. F. Soddu, N. Kenyatta, S. A. Odame, J. Sanders, L. Wright, and F. Anselmi. “A low-cost do-it-yourself microscope kit for hands-on science education”. In: *Proceedings of the Optics Education and Outreach V*. Vol. 10741. International Society for Optics and Photonics. San Diego, California, United States, 2018, 107410K. doi: 10.1117/12.2320655.

[85] B. Gryseels, K. Polman, J. Clerinx, and L. Kestens. “Human schistosomiasis”. In: *The Lancet* 368.9541 (2006), pp. 1106–1118. doi: 10.1016/S0140-6736(06)69440-3.

[86] K. Guo, J. Liao, Z. Bian, X. Heng, and G. Zheng. “InstantScope: A low-cost whole slide imaging system with instant focal plane detection”. In: *Biomedical Optics Express* 6.9 (2015), pp. 3210–3216. doi: 10.1364/BOE.6.003210.

[87] C. Guo, Z. Bian, S. Jiang, M. Murphy, J. Zhu, R. Wang, P. Song, X. Shao, Y. Zhang, and G. Zheng. “OpenWSI: A low-cost, high-throughput whole slide imaging system via single-frame autofocusing and open-source hardware”. In: *Optics Letters* 45.1 (2019), pp. 260–263. doi: 10.1364/OL.45.000260.

[88] T. W. Gyorkos, M. Ramsan, A. Foum, and I. S. Khamis. “Efficacy of new low-cost filtration device for recovering Schistosoma haematobium eggs from urine”. In: *Journal of Clinical Microbiology* 39.7 (July 2001), pp. 2681–2682. doi: 10.1128/JCM.39.7.2681-2682.2001.

[89] P. Hagemann. “Manual of Basic Techniques for a Health Laboratory”. In: *Clinical Chemistry* 49 (2003), pp. 1712–1713.

[90] Z. Haruna, M. B. Mu'azu, P. Oyibo, and S. A. Tijani. "Development of an optimal path planning using elite opposition based bat algorithm for a mobile robot". In: *Yanbu Journal of Engineering and Science* 16.1 (2021), pp. 1–9. doi: doi.org/10.53370/001c.24338.

[91] M. O. K. Hassan and K. M. Al-Hity. "Computer-aided diagnosis of schistosomiasis: automated schistosoma egg detection". In: *Journal of Clinical Engineering* 37.1 (2012), pp. 29–34. doi: 10.1097/JCE.0b013e31823fda36.

[92] S. A. Henriksen and K. Aagaard. "A simple flotation and McMaster method (author's transl)". In: *Nord. Vet. Med.* 28.7–8 (1976), p. 392.

[93] P. T. Hoekstra, G. J. van Dam, and L. van Lieshout. "Context-specific procedures for the diagnosis of human schistosomiasis – a mini review". In: *Frontiers in Tropical Diseases* 2 (2021), p. 722438. doi: 10.3389/fitd.2021.722438.

[94] W. A. Hoffman, J. A. Pons, and J. L. Janer. "The sedimentation-concentration method in schistosomiasis mansoni". In: *Puerto Rico Journal of Public Health and Tropical Medicine* 9.3 (1934), pp. 283–291.

[95] O. Holmström, N. Linder, M. Lundin, H. Moilanen, A. Suutala, R. Turkki, H. Joensuu, J. Isola, V. Diwan, and J. Lundin. "Quantification of estrogen receptor-alpha expression in human breast carcinomas with a miniaturized, low-cost digital microscope: a comparison with a high-end whole slide-scanner". In: *PloS ONE* 10.12 (2015), e0144688. doi: 10.1371/journal.pone.0144688.

[96] O. Holmström, N. Linder, B. Ngasala, A. Mårtensson, E. Linder, M. Lundin, H. Moilanen, A. Suutala, V. Diwan, and J. Lundin. "Point-of-care mobile digital microscopy and deep learning for the detection of soil-transmitted helminths and *Schistosoma haematobium*". en. In: *Global Health Action* 10.sup3 (June 2017), p. 1337325. doi: 10.1080/16549716.2017.1337325.

[97] P. Hotez. "Hookworm and poverty". In: *Ann. N. Y. Acad. Sci.* 1136.1 (2008), pp. 38–44. doi: 10.1196/annals.1425.000.

[98] A. G. Howard, M. Zhu, B. Chen, D. Kalenichenko, W. Wang, T. Weyand, M. Andreetto, and H. Adam. *MobileNets: efficient convolutional neural networks for mobile vision applications*. preprint. 2017. doi: 10.48550/arXiv.1704.04861. arXiv: 1704.04861.

[99] Y. Huo, J. Zhang, X. Du, X. Wang, J. Liu, and L. Liu. “Recognition of parasite eggs in microscopic medical images based on YOLOv5”. In: *2021 5th Asian Conference on Artificial Intelligence Technology (ACAIT)*. Haikou, China, 2021, pp. 123–127. doi: 10.1109/ACAIT53529.2021.9731120.

[100] International Organization for Standardization. *ISO 12233:2017*. 2017. url: https://www.iso.org/cms/render/live/en/sites/isoorg/contents/data/standard/07/16/71696.html (visited on 03/03/2022).

[101] K. Jaromin-Gleń, T. Kłapeć, G. Łagód, J. Karamon, J. Malicki, A. Skowrońska, and A. Bieganowski. “Division of methods for counting helminths’ eggs and the problem of efficiency of these methods”. In: *Ann Agric Env. Med* 24.1 (2017), pp. 1–7. doi: 10.5604/12321966.1233891.

[102] S. Jiang, J. Liao, Z. Bian, K. Guo, Y. Zhang, and G. Zheng. “Transform- and multi-domain deep learning for single-frame rapid autofocusing in whole slide imaging”. In: *Biomedical Optics Express* 9.4 (2018), pp. 1601–1612. doi: 10.1364/BOE.9.001601.

[103] S. Jiang, Z. Bian, X. Huang, P. Song, H. Zhang, Y. Zhang, and G. Zheng. “Rapid and robust whole slide imaging based on LED-array illumination and color-multiplexed single-shot autofocusing”. In: *Quantitative Imaging in Medicine and Surgery* 9.5 (2019), pp. 823–831. doi: 10.21037/qims.2019.05.04.

[104] B. Jiménez, C. Maya, G. Velásquez, F. Torner, F. Arambula, J. Barrios, and M. Velasco. “Identification and quantification of pathogenic helminth eggs using a digital image system”. In: *Experimental Parasitology* 166 (2016), pp. 164–172. doi: 10.1016/j.exppara.2016.04.016.

[105] S. R. Jones, S. Carley, and M. Harrison. “An introduction to power and sample size estimation”. In: *Emergency Medicine Journal* 20.5 (2003), pp. 453–458. doi: 10.1136/emj.20.5.453.

[106] P. M. Jourdan, P. H. L. Lamberton, A. Fenwick, and D. G. Addiss. “Soil-transmitted helminth infections”. In: *The Lancet* 391.10117 (2018), pp. 252–265. doi: 10.1016/S0140-6736(17)31930-X.

[107] S. Jujjavarapu. “Automating the Diagnosis and Quantification of Urinary Schistosomiasis”. MA thesis. Delft, The Netherlands: Delft University of Technology, 2020.

[108] K. Kato. “Comparative examinations”. In: *Jpn J Parasitol* 3 (1954), p. 35.

[109] K. Kato. “A correct application of the thick-smear technique with cellophane paper cover. A pamphlet. 9p., 1960 (In Japanese)”. In: *Jpn. J Med Sci Biol* 19.1 (1966), pp. 59–64.

[110] N. Katz, P. M. Z. Coelho, and J. Pellegrino. “Evaluation of Kato’s quantitative method through the recovery of Schistosoma mansoni eggs added to human feces”. In: *J. Parasitol.* 56.5 (1970).

[111] N. Katz, A. Chaves, and J. Pellegrino. “A simple device for quantitative stool thick-smear technique in Schistosomiasis mansoni”. In: *Rev. Inst. Med. Trop. Sao Paulo* 14.6 (1972), pp. 397–400.

[112] M. Kavya and S. Jayalalitha. “Developments in perturb and observe algorithm for maximum power point tracking in photo voltaic panel: A review”. In: *Archives of Computational Methods in Engineering* 28.4 (2021), pp. 2447–2457. doi: 10.1007/s11831-020-09461-x.

[113] D. Keller, J. Rothen, J.-P. Dangy, C. Saner, C. Daubenberger, F. Allan, S. M. Ame, S. M. Ali, F. Kabole, J. Hattendorf, D. Rollinson, R. Seyfarth, and S. Knopp. “Performance of a real-time PCR approach for diagnosing Schistosoma haematobium infections of different intensity in urine samples from Zanzibar”. In: *Infectious Diseases of Poverty* 9.1 (Sept. 2020), p. 128. doi: 10.1186/s40249-020-00726-y.

[114] H. M. Kenguele, A. A. Adegnika, A. M. Nkoma, U. Ateba-Ngoa, M. Mbong, J. Zinsou, B. Lell, and J. J. Verweij. “Impact of short-time urine freezing on the sensitivity of an established Schistosoma real-time PCR assay”. In: *American Journal of Tropical Medicine and Hygiene* 90.6 (2014), pp. 1153–1155. doi: 10.4269/ajtmh.14-0005.

[115] N. A. A. Khairudin, C. C. Lim, A. S. A. Nasir, and Z. Mohamed. “Efficient Classification Techniques in Classifying Human Intestinal Parasite Ova”. In: *Journal of Telecommunication, Electronic and Computer Engineering (JTEC)* 14.3 (2022), pp. 17–23. doi: 10.54554/jtec.2022.14.03.003.

[116] A. Kitvimonrat, N. Hongcharoen, S. Marukatat, and S. Watcharabutsarakham. “Automatic Detection and Characterization of Parasite Eggs using Deep Learning Methods”. In: *2020 17th International Conference on Electrical Engineering/Electronics, Computer, Telecommunications and Information Technology (ECTI-CON)*. 2020, pp. 153–156.

[117] T. Kohlberger, Y. Liu, M. Moran, P. H. C. Chen, T. Brown, J. D. Hipp, C. H. Mermel, and M. C. Stumpe. “Whole-slide image focus quality: Automatic assessment and impact on AI cancer detection”. In: *Journal of Pathology Informatics* 10.1 (2019), p. 39. doi: 10.4103/jpi.jpi_11_19.

[118] C. Kokaliaris, A. Garba, M. Matuska, R. N. Bronzan, D. G. Colley, A. M. Dorkenoo, U. F. Ekpo, F. M. Fleming, M. D. French, A. Kabore, J. B. Mbonigaba, N. Midzi, P. N. M. Mwinzi, E. K. N'Goran, M. R. Polo, M. Sacko, L.-A. Tchuem Tchuenté, E. M. Tukahebwa, P. A. Uvon, G. Yang, L. Wiesner, Y. Zhang, J. Utzinger, and P. Vounatsou. "Effect of preventive chemotherapy with praziquantel on schistosomiasis among school-aged children in sub-Saharan Africa: a spatiotemporal modelling study". In: *The Lancet Infectious Diseases* 22.1 (Jan. 2022), pp. 136–149. doi: 10.1016/S1473-3099(21)00090-6.

[119] Y. Komiya and A. Kobayashi. "Evaluation of Kato's thick smear technic with a cellophane cover for helminth eggs in feces". In: *Jpn. J. Med. Sci. Biol.* 19.1 (1966), pp. 59–64.

[120] K. C. Kosinski, K. M. Bosompem, M. J. Stadecker, A. D. Wagner, J. Plummer, J. L. Durant, and D. M. Gute. "Diagnostic accuracy of urine filtration and dipstick tests for Schistosoma haematobium infection in a lightly infected population of Ghanaian school children". In: *Acta Tropica* 118.2 (2011), pp. 123–127. doi: 10.1016/j.actatropica.2011.02.006.

[121] H. C. Koydemir, J. T. Coulibaly, D. Tseng, I. I. Bogoch, and A. Ozcan. "Design and validation of a wide-field mobile phone microscope for the diagnosis of schistosomiasis". In: *Travel medicine and infectious disease* 30 (2019), pp. 128–129. doi: 10.1016/j.tmaid.2018.12.001.

[122] R. J. Kreindler. "The Nm1 (Newton Microscopes): Part 2 of 2". In: *-Depth Exam. Comp. Folded-Opt. Des. Micscape Mag.* (2013).

[123] K. Kura, R. J. Hardwick, J. E. Truscott, J. Toor, T. D. Hollingsworth, and R. M. Anderson. "The impact of mass drug administration on Schistosoma haematobium infection: what is required to achieve morbidity control and elimination?" In: *Parasites & Vectors* 13.1 (2020), pp. 1–10. doi: 10.1186/s13071-020-04329-y.

[124] A. W. Kushniruk and V. L. Patel. "Cognitive and usability engineering methods for the evaluation of clinical information systems". In: *Journal of Biomedical Informatics* 37.1 (2004), pp. 56–76. doi: 10.1016/j.jbi.2004.01.003.

[125] M. Layrisse, C. Martínez-Torres, and H. Ferrer-Farias. "A simple volumetric device for preparing stool samples in the cellophane thick-smear technique". In: *Am. J. Trop. Med. Hyg.* 18.4 (1969), pp. 553–554.

[126] C.-C. Lee, P.-J. Huang, Y.-M. Yeh, P.-H. Li, C.-H. Chiu, W.-H. Cheng, and P. Tang. "Helminth egg analysis platform (HEAP): An opened platform for microscopic helminth egg identification and quantification based on the integration of deep learning architectures".

In: *Journal of Microbiology, Immunology and Infection* 55.3 (2022), pp. 395–404. doi: 10.1016/j.jmii.2021.07.014.

[127] L. Le and M. H. Hsieh. “Diagnosing urogenital schistosomiasis: Dealing with diminishing returns”. In: *Trends in Parasitology* 33.5 (2017), pp. 378–387. doi: 10.1016/j.pt.2016.12.009.

[128] J. Liao, Z. Wang, Z. Zhang, Z. Bian, K. Guo, A. Nambiar, Y. Jiang, S. Jiang, J. Zhong, M. Choma, and G. Zheng. “Dual light-emitting diode-based multichannel microscopy for whole-slide multiplane, multispectral and phase imaging”. In: *Journal of Biophotonics* 11.2 (2017), e201700075. doi: 10.1002/jbio.201700075.

[129] J. Liao, Y. Jiang, Z. Bian, B. Mahrou, A. Nambiar, A. W. Magsam, K. Guo, S. Wang, Y. K. Cho, and G. Zheng. “Rapid focus map surveying for whole slide imaging with continuous sample motion”. In: *Optics Letters* 42.17 (2017), pp. 3379–3382. doi: 10.1364/OL.42.003379.

[130] J. Liao, S. Jiang, Z. Zhang, K. Guo, Z. Bian, Y. Jiang, J. Zhong, and G. Zheng. “Terapixel hyperspectral whole-slide imaging via slit-array detection and projection”. In: *Journal of Biomedical Optics* 23.6 (2018), p. 066503. doi: 10.1117/1.JBO.23.6.066503.

[131] J. Liao, X. Chen, G. Ding, P. Dong, H. Ye, H. Wang, Y. Zhang, and J. Yao. “Deep learning-based single-shot autofocus method for digital microscopy”. In: *Biomedical Optics Express* 13.1 (2022), pp. 314–327. doi: 10.1364/BOE.446928.

[132] I. O. Libouga, L. Bitjoka, D. L. L. Gwet, O. Boukar, and A. M. N. Nlôga. “A supervised U-Net based color image semantic segmentation for detection & classification of human intestinal parasites”. In: *e-Prime - Advances in Electrical Engineering, Electronics and Energy* 2 (2022), p. 100069. doi: 10.1016/j.prime.2022.100069.

[133] C. C. Lim, N. A. A. Khairudin, S. W. Loke, A. S. A. Nasir, Y. F. Chong, and Z. Mohamed. “Comparison of Human Intestinal Parasite Ova Segmentation Using Machine Learning and Deep Learning Techniques”. In: *Applied Sciences* 12.15 (2022), p. 7542. doi: 10.3390/app12157542.

[134] E. Linder, A. Grote, S. Varjo, N. Linder, M. Lebbad, M. Lundin, V. Diwan, J. Hannuksela, and J. Lundin. “On-chip imaging of Schistosoma haematobium eggs in urine for diagnosis by computer vision”. In: *PLoS Neglected Tropical Diseases* 7.12 (2013), e2547. doi: 10.1371/journal.pntd.0002547.

[135] T.-Y. Lin, M. Maire, S. Belongie, J. Hays, P. Perona, D. Ramanan, P. Dollár, and C. L. Zitnick. “Microsoft COCO: Common Objects in Context”. In: *Computer Vision – ECCV 2014*. Vol. 8693. Zurich, Switzerland: Springer International Publishing, 2014, pp. 740–755. isbn: 978-3-319-10601-4 978-3-319-10602-1. doi: 10.1007/978-3-319-10602-1_48.

[136] T.-Y. Lin, P. Goyal, R. Girshick, K. He, and P. Dollár. “Focal Loss for Dense Object Detection”. In: *2017 IEEE International Conference on Computer Vision (ICCV)*. Venice, Italy, 2017, pp. 2999–3007. doi: 10.1109/ICCV.2017.324.

[137] L. Lin, D. Bermejo-Peláez, D. Capellán-Martín, D. Cuadrado, C. Rodríguez, L. García, N. Díez, R. Tomé, M. Postigo, M. J. Ledesma-Carbayo, and M. Luengo-Oroz. “Combining collective and artificial intelligence for global health diseases diagnosis using crowdsourced annotated medical images”. In: *2021 43rd Annual International Conference of the IEEE Engineering in Medicine & Biology Society (EMBC)*. Mexico, 2021, pp. 3344–3348. doi: 10.1109/EMBC46164.2021.9630868.

[138] Y. Liron, Y. Paran, N. G. Zatorsky, B. Geiger, and Z. Kam. “Laser autofocusing system for high-resolution cell biological imaging”. In: *Journal of Microscopy* 221.2 (2006), pp. 145–151. doi: 10.1111/j.1365-2818.2006.01550.x.

[139] L. Liu, H. Lei, J. Zhang, Y. Yuan, Z. Zhang, J. Liu, Y. Xie, G. Ni, and Y. Liu. “Automatic identification of human erythrocytes in microscopic fecal specimens”. In: *J. Med. Syst.* 39.11 (2015), p. 146. doi: 10.1007/s10916-015-0334-z.

[140] Z. Li, H. Gong, W. Zhang, L. Chen, J. Tao, L. Song, and Z. Wu. “A robust and automatic method for human parasite egg recognition in microscopic images”. In: *Parasitol. Res.* 114.10 (2015), pp. 3807–3813. doi: 10.1007/s00436-015-4611-z.

[141] Y. Li, R. Zheng, Y. Wu, K. Chu, Q. Xu, M. Sun, and Z. J. Smith. “A low-cost, automated parasite diagnostic system via a portable, robotic microscope and deep learning”. In: *J. Biophotonics* 12.9 (2019), e201800410. doi: 10.1002/jbio.201800410.

[142] H. Li, H. Soto-Montoya, M. Voisin, L. Valenzuela, and M. Prakash. *Octopi: Open configurable high-throughput imaging platform for infectious disease diagnosis in the field*. preprint. 2019. doi: 10.1101/684423. BioRxiv: 684423.

[143] Q. Li, S. Li, X. Liu, Z. He, T. Wang, Y. Xu, H. Guan, R. Chen, S. Qi, and F. Wang. “FecalNet: Automated detection of visible components in human feces using deep learning”. In: *Med. Phys.* 47.9 (2020), pp. 4212–4222. doi: 10.1002/mp.14352.

[144] A. D. Long. *Malaria: Obstacles and Opportunities*. Washington, DC, USA: Agency for International Development, 1991.

[145] P. T. LoVerde. "Schistosomiasis". In: *Digenetic Trematodes*. Springer International Publishing, 2024, pp. 75–105. isbn: 978-3-031-60121-7. doi: 10.1007/978-3-031-60121-7_3.

[146] J. Lundin, A. Suutala, O. Holmström, S. Henriksson, S. Valkamo, H. Kaingu, F. Kinyua, M. Muinde, M. Lundin, and V. Diwan. "Diagnosis of soil-transmitted helminth infections with digital mobile microscopy and artificial intelligence in a resource-limited setting". In: *PLOS Neglected Tropical Diseases* 18.4 (2024), e0012041. doi: 10.1371/journal.pntd.0012041.

[147] A. O. Lutz. "Schistosomum mansoni e a schistosomatose segundo observações feitas no Brasil". In: *Mem. Inst. Oswaldo Cruz* 11.1 (1919), pp. 121–155. doi: 10.1590/S0074-02761919000100006.

[148] Q. Lu, G. Liu, C. Xiao, C. Hu, S. Zhang, R. X. Xu, K. Chu, and Q. Xu. "A modular, open-source, slide-scanning microscope for diagnostic applications in resource-constrained settings". In: *PloS ONE* 13.3 (2018), e0194063. doi: 10.1371/journal.pone.0194063.

[149] D. Machin, M. J. Campbell, S. B. Tan, and S. H. Tan. *Sample size tables for clinical studies*. 3rd. John Wiley Sons, 2011. isbn: 9781444357967.

[150] A. S. Mahdi, A. K. Mahamad, S. Saon, T. Tuwoso, H. Elmunsyah, and S. W. Mudjanarko. "Maximum power point tracking using perturb and observe, fuzzy logic and ANFIS". In: *SN Applied Sciences* 2.1 (2019), p. 89. doi: 10.1007/s42452-019-1886-1.

[151] L. Makau-Barasa, L. Assefa, M. Aderogba, D. Bell, J. Solomon, R. O. Urude, O. J. Nebe, J. A-Enegela, J. G. Damen, S. Popoola, J. C. Diehl, G. Vdovine, and T. Agbana. "Performance evaluation of the AiDx multi-diagnostic automated microscope for the detection of schistosomiasis in Abuja, Nigeria". In: *Scientific Reports* 13.1 (Sept. 2023), p. 14833. doi: 10.1038/s41598-023-42049-6.

[152] J. Maldonado and J. Acosta-Matienzo. "A Comparison of fecal examination procedures in the diagnosis of schistosomiasis mansoni". In: *Exp. Parasitol.* 2.3 (1953), pp. 294–310. doi: 10.1016/0014-4894(53)90040-X.

[153] M. M. Manser, A. C. S. Saez, and P. L. Chiodini. "Faecal parasitology: concentration methodology needs to be better standardised". In: *PLoS Negl. Trop. Dis.* 10.4 (2016), e0004579. doi: 10.1371/journal.pntd.0004579.

[154] L. K. Martin and P. C. Beaver. "Evaluation of Kato thick-smear technique for quantitative diagnosis of helminth infections". In: *Am. J. Trop. Med. Hyg.* 17.3 (1968), pp. 382–391. doi: 10.4269/ajtmh.1968.17.382.

[155] C. Massone, H. P. Soyer, G. P. Lozzi, A. Di Stefani, B. Leinweber, G. Gabler, M. Asgari, R. Boldrini, L. Bugatti, V. Canzonieri, G. Ferrara, K. Kodama, D. Mehregan, F. Rongioletti, S. A. Janjua, V. Mashayekhi, I. Vassilaki, B. Zelger, B. Žgavec, and H. Kerl. "Feasibility and diagnostic agreement in teledermatopathology using a virtual slide system". In: *Human Pathology* 38.4 (2007), pp. 546–554. doi: 10.1016/j.humpath.2006.10.006.

[156] J. M. Mateos-Pérez, R. Redondo, R. Nava, J. C. Valdiviezo, G. Cristóbal, B. Escalante-Ramírez, M. J. Ruiz-Serrano, J. Pascau, and M. Desco. "Comparative evaluation of autofocus algorithms for a real-time system for automatic detection of Mycobacterium tuberculosis". In: *Cytometry Part A* 81A.3 (2012), pp. 213–221. doi: 10.1002/cyto.a.22020.

[157] M. L. McHugh. "Interrater reliability: the kappa statistic". In: *Biochemia Medica (Zagreb)* 22.3 (2012), pp. 276–282.

[158] R. R. McKay, V. A. Baxi, and M. C. Montalto. "The accuracy of dynamic predictive autofocusing for whole slide imaging". In: *Journal of Pathology Informatics* 2.1 (2011), p. 38. doi: 10.4103/2153-3539.84231.

[159] D. P. McManus, D. W. Dunne, M. Sacko, J. Utzinger, B. J. Vennervald, and X. N. Zhou. "Schistosomiasis". In: *Nature Reviews Disease Primers* 4.1 (2018), p. 13. doi: 10.1038/s41572-018-0013-8.

[160] C. R. Mendes, A. T. Teixeira, R. A. Pereira, and L. C. Dias. "A Comparative Study Of The Parasitological Techniques: Kato-katz And Coprotest". In: *Rev. Soc. Bras. Med. Trop.* 38.2 (2005), pp. 178–180. doi: 10.1590/s0037-86822005000200010.

[161] B. Meulah, P. Oyibo, M. Bengtson, T. Agbana, R. A. L. Lontchi, A. A. Adegnika, W. Oyibo, C. H. Hokke, J. C. Diehl, and L. v. Lieshout. "Performance Evaluation of the Schistoscope 5.0 for (Semi-)automated Digital Detection and Quantification of Schistosoma haematobium Eggs in Urine: A Field-based Study in Nigeria". In: *The American Journal of Tropical Medicine and Hygiene* 107.5 (2022). doi: 10.4269/ajtmh.22-0276.

[162] B. Meulah, M. Bengtson, L. Van Lieshout, C. H. Hokke, A. Kreidenweiss, J. C. Diehl, A. A. Adegnika, and T. E. Agbana. "A Review on Innovative Optical Devices for the Diagnosis of Human Soil-Transmitted Helminthiasis and Schistosomiasis: From Research and Development to Commercialization". In: *Parasitology* 150.2 (2023), pp. 137–149. doi: 10.1017/S0031182022001664.

[163] B. Meulah, P. Oyibo, P. T. Hoekstra, P. A. N. Moure, M. N. Maloum, R. A. Laclong-Lontchi, Y. J. Honkpehedji, M. Bengtson, C. Hokke, P. L. A. M. Corstjens, T. Agbana, J. C. Diehl, A. A. Adegnika, and L. v. Lieshout. "Validation of artificial intelligence-based digital microscopy for automated detection of Schistosoma haematobium eggs in urine in Gabon". In: *PLoS neglected tropical diseases* 18.2 (2024). doi: 10.1371/journal.pntd.0011967.

[164] S. Minaee, R. Kafieh, M. Sonka, S. Yazdani, and G. J. Soufi. "Deep-COVID: predicting COVID-19 from chest X-ray images using deep transfer learning". In: *Medical Image Analysis* 65 (2020), p. 101794. doi: 10.1016/j.media.2020.101794.

[165] J. J. Mines. "Modifications of the McMaster worm egg counting method". In: *Aust. Vet. J.* 53.7 (1977), pp. 342–343. doi: 10.1111/j.1751-0813.1977.tb00247.x.

[166] T. M. Mitchell. *Machine Learning*. New York: McGraw-Hill, 1997.

[167] A. Montresor, D. Mupfasoni, A. Mikhailov, P. Mwinzi, A. Lucianez, M. Jamsheed, E. Gasimov, S. Warusavithana, A. Yajima, Z. Bisoffi, D. Buonfrate, P. Steinmann, J. Utzinger, B. Levecke, J. Vlaminck, P. Cools, J. Vercruysse, G. Cringoli, L. Rinaldi, B. Blouin, and T. W. Gyorkos. "The global progress of soil-transmitted helminthiases control in 2020 and World Health Organization targets for 2030". In: *PLoS neglected tropical diseases* 14.8 (2020), e0008505. doi: 10.1371/journal.pntd.0008505.

[168] R. H. Mnkugwe, O. S. Minzi, S. M. Kinungohi, A. A. Kamuhabwa, and E. Aklillu. "Efficacy and safety of praziquantel for treatment of schistosoma mansoni infection among school children in Tanzania". In: *Pathogens* 9.1 (2019), p. 28. doi: 10.3390/pathogens9010028.

[169] U. K. Mustafa, K. S. Kreppel, J. Brinkel, and E. Sauli. "Digital Technologies to Enhance Infectious Disease Surveillance in Tanzania: A Scoping Review". In: *Healthcare* 11.4 (2023), p. 470. doi: 10.3390/healthcare11040470.

[170] K. M. Naing, S. Boonsang, S. Chuwongin, V. Kittichai, T. Tongloy, S. Prommongkol, P. Dekumyoy, and D. Watthanakulpanich. "Automatic recognition of parasitic products in stool examination using object detection approach". In: *PeerJ Computer Science* 8 (2022), e1065. doi: 10.7717/peerj-cs.1065.

[171] Y. H. Nai, B. W. Teo, N. L. Tan, S. O'Doherty, M. C. Stephenson, Y. L. Thian, E. Chiong, and A. Reilhac. "Comparison of metrics for the evaluation of medical segmentations using prostate MRI dataset". In: *Computers in Biology and Medicine* 134 (2021), p. 104497. doi: 10.1016/j.compbiomed.2021.104497.

[172] R. Nakasi, E. R. Aliija, and J. Nakatumba. “A Poster on Intestinal Parasite Detection in Stool Sample Using AlexNet and GoogleNet Architectures”. In: *Proceedings of the 4th ACM SIGCAS Conference on Computing and Sustainable Societies*. COMPASS ’21. New York, NY, USA: Association for Computing Machinery, 2021, pp. 389–395. isbn: 978-1-4503-8453-7. doi: 10.1145/3460112.3472309.

[173] R. Ngakhushi, R. Kaiti, S. Bhattarai, and G. Shrestha. “Prevalence of myopia and binocular vision dysfunctions in microscopists”. In: *International Eye Science* 18 (2018), pp. 1180–1183. doi: 10.3980/j.issn.1672-5123.2018.7.03.

[174] M. Mbong Ngwese, G. Prince Manouana, P. A. Nguema Moure, M. Ramharter, M. Esen, and A. A. Adégnika. “Diagnostic Techniques of Soil-Transmitted Helminths: Impact on Control Measures”. In: *Trop. Med. Infect. Dis.* 5.2 (2020), p. 93. doi: 10.3390/tropicalmed50

[175] B. B. Obeng, Y. A. Aryeetey, C. J. de Dood, A. S. Amoah, I. A. Larbi, A. M. Deelder, M. Yazdanbakhsh, F. C. Hartgers, D. A. Boakye, J. J. Verweij, G. J. van Dam, and L. van Lieshout. “Application of a circulating-cathodic-antigen (CCA) strip test and real-time PCR, in comparison with microscopy, for the detection of Schistosoma haematobium in urine samples from Ghana”. In: *Annals of Tropical Medicine and Parasitology* 102.7 (2008), pp. 625–633. doi: 10.1179/136485908X337490.

[176] B. A. S. Oliveira, J. M. P. Moreira, P. R. S. Coelho, D. A. Negrão-Corrêa, S. M. Geiger, and F. G. Guimarães. “Automated diagnosis of schistosomiasis by using faster R-CNN for egg detection in microscopy images prepared by the Kato–Katz technique”. In: *Neural Computing and Applications* 34.11 (2022), pp. 9025–9042. doi: 10.1007/s00521-022-06924-z.

[177] I. B. Oluchi, E. A. Adedokun, M. B. Mua’zu, N. Salifu, and P. Oyibo. “Development of a Nigeria vehicle license plate detection system”. In: *Applications of Modelling and Simulation* 3.3 (2019), pp. 188–195.

[178] W. P. O’Meara, M. Barcus, C. Wongsrichanalai, S. Muth, J. D. Maguire, R. G. Jordan, W. R. Prescott, and F. E. McKenzie. “Reader technique as a source of variability in determining malaria parasite density by microscopy”. In: *Malaria Journal* 5 (2006), pp. 1–7. doi: 10.1186/1475-2875-5-118.

[179] W. P. O’Meara, J. N. Mangeni, R. Steketee, and B. Greenwood. “Changes in the burden of malaria in sub-Saharan Africa”. In: *The Lancet Infectious Diseases* 10.8 (2010), pp. 545–555. doi: 10.1016/S1473-3099(10)70096-7.

[180] A. Onasanya, M. Keshinro, O. Oladepo, J. V. Engelen, and J. C. Diehl. “A Stakeholder Analysis of Schistosomiasis Diagnostic Landscape in South-West Nigeria: Insights for Diagnostics Co-creation”. In: *Frontiers in Public Health* 8 (2020). doi: 10.3389/fpubh.2020.564381.

[181] A. Onasanya, M. Bengtson, L. de Goeje, J. Van Engelen, J. C. Diehl, and L. van Lieshout. “Developing inclusive digital health diagnostic for schistosomiasis: a need for guidance via target product profiles”. In: *Frontiers in Parasitology* 2 (2023). doi: 10.3389/fpara.2023.1255848.

[182] A. Onasanya, M. Bengtson, T. Agbana, O. Oladunni, J. van Engelen, O. Oladepo, and J. C. Diehl. “Towards Inclusive Diagnostics for Neglected Tropical Diseases: User Experience of a New Digital Diagnostic Device in Low-Income Settings”. In: *Tropical Medicine and Infectious Disease* 8.3 (2023), p. 176. doi: 10.3390/tropicalmed8030176.

[183] P. O. Oyibo, O. Ajayi, I. Abubakar, M. T. Abdulwahab, and O. A. S. “Development of Power Line Detection Algorithm using Frangi Filter and First-Order Derivative of Gaussian”. In: *Zaria Journal of Electrical Engineering Technology* 8.1 (2019).

[184] P. Oyibo, S. Jujjavarapu, B. Meulah, T. Agbana, I. Braakman, A. van Diepen, M. Bengtson, L. van Lieshout, W. Oyibo, G. Vdovine, and J. C. Diehl. “Schistoscope: An Automated Microscope with Artificial Intelligence for Detection of Schistosoma haematobium Eggs in Resource-Limited Settings”. In: *Micromachines* 13.5 (2022), p. 643. doi: 10.3390/mi13050643.

[185] P. Oyibo, B. Meulah, M. Bengtson, L. van Lieshout, W. Oyibo, J. C. Diehl, G. Vdovine, and T. Agbana. “Two-stage automated diagnosis framework for urogenital schistosomiasis in microscopy images from low-resource settings”. In: *Journal of Medical Imaging* 10.4 (2023), pp. 044005–044005. doi: 10.1117/1.JMI.10.4.044005.

[186] P. Oyibo, T. Agbana, L. van Lieshout, W. Oyibo, J. C. Diehl, and G. Vdovine. “An automated slide scanning system for membrane filter imaging in diagnosis of urogenital schistosomiasis”. In: *Journal of Microscopy* 294.1 (2024), pp. 52–61. doi: 10.1111/jmi.13269.

[187] P. Oyibo, P. Brynolfsson, and E. Spezi. “Integrating Radiomic Image Analysis in the Hero Imaging Platform”. In: *Proceedings of the Cardiff University School of Engineering Research Conference 2024*. Cardiff, United Kingdom: Cardiff University Press, 2024. doi: 10.18573/conf3.g.

[188] P. Oyibo, B. Meulah, T. Agbana, L. van Lieshout, W. Oyibo, G. Vdovin, and J. C. Diehl. “Deep learning-based automated detection and multiclass classification of soil-transmitted helminths and Schistosoma mansoni eggs in fecal smear images”. In: *Scientific Reports* 15.1 (2025), p. 21495. doi: 10.1038/s41598-025-02755-9.

[189] P. Oyibo, K. W. Kim, S. Hargreaves, P. Wheeler, O. Woodley, T. Rackley, M. Evans, and E. Spezi. “3D DeepLab-based automated GTV segmentation in head and neck cancer using PET/CT imaging”. In: *Radiotherapy and Oncology* 206.1 (2025), S2536–S2538. doi: 10.1016/S0167-8140(25)01892-4.

[190] C. Panagiotakis and A. Argyros. “Region-based fitting of overlapping ellipses and its application to cells segmentation”. In: *Image and Vision Computing* 93 (2020), p. 103810. doi: 10.1016/j.imavis.2019.09.001.

[191] A. Paszke, S. Gross, F. Massa, A. Lerer, J. Bradbury, G. Chanan, T. Killeen, Z. Lin, N. Gimelshein, L. Antiga, A. Desmaison, A. Köpf, E. Yang, Z. DeVito, M. Raison, A. Tejani, S. Chilamkurthy, B. Steiner, L. Fang, J. Bai, and S. Chintala. “Pytorch: an imperative style, high-performance deep learning library”. In: *Proceedings of the 33rd International Conference on Neural Information Processing Systems*. Vol. 32. Vancouver, Canada: Curran Associates Inc., 2019, pp. 8026–803.

[192] A. Z. Peixinho, S. B. Martins, J. E. Vargas, A. X. Falcao, J. F. Gomes, and C. T. Suzuki. “Diagnosis of human intestinal parasites by deep learning”. In: *Computational Vision and Medical Image Processing V: Proceedings of the 5th Eccomas Thematic Conference on Computational Vision and Medical Image Processing (VipIMAGE 2015)*. Tenerife, Spain, 2015, p. 107. doi: 10.1201/b19241-19.

[193] A. Pereckiene, V. Kaziūnaite, A. Vysniauskas, S. Petkevicius, A. Malakauskas, M. Sarkūnas, and M. A. Taylor. “A comparison of modifications of the McMaster method for the enumeration of Ascaris suum eggs in pig faecal samples”. In: *Vet. Parasitol.* 149.1–2 (2007), pp. 111–116. doi: 10.1016/j.vetpar.2007.04.014.

[194] H. Pinkard, Z. Phillips, A. Babakhani, D. A. Fletcher, and L. Waller. “Deep learning for single-shot autofocus microscopy”. In: *Optica* 6.6 (2019), pp. 794–797. doi: 10.1364/OPTICA.6.000794.

[195] A. Pinto-Almeida, T. Mendes, R. N. de Oliveira, S. A. P. Corrêa, S. M. Allegretti, S. Belo, A. Tomás, F. F. Anibal, E. Carrilho, and A. Afonso. “Morphological characteristics of Schistosoma mansoni PZQ-resistant and -susceptible strains are different in presence

of Praziquantel". In: *Frontiers in Microbiology* 7 (2016), p. 00594. doi: 10.3389/fmicb.2016.00594.

[196] I. Prieto-Egido, A. González-Escalada, V. García-Giganto, and A. Martínez-Fernández. "Design of New Procedures for Diagnosing Prevalent Diseases Using a Low-Cost Telemicroscopy System". In: *Telemedicine Journal and e-Health* 22.11 (2016), pp. 952–959. doi: 10.1089/tmj.2015.0239.

[197] S. Jaya Sundar Rajasekar, G. Jaswal, V. Perumal, S. Ravi, and V. Dutt. "Parasite.ai – An Automated Parasitic Egg Detection Model from Microscopic Images of Fecal Smears using Deep Learning Techniques". In: *2023 International Conference on Advances in Computing, Communication and Applied Informatics (ACCAI)*. Chennai, India, 2023, pp. 1–9. doi: 10.1109/ACCAI58221.2023.10200869.

[198] J. Rajchgot, J. T. Coulibaly, J. Keiser, J. Utzinger, N. C. Lo, M. K. Mondry, J. R. Andrews, and I. I. Bogoch. "Mobile-phone and handheld microscopy for neglected tropical diseases". In: *PLoS Neglected Tropical Diseases* 11.7 (2017), e0005550. doi: 10.1371/journal.pntd.0005550.

[199] N. Rajeshwori, K. Raju, B. Sanjeev, and S. B. Gulshan. "Prevalence of myopia and binocular vision dysfunctions in microscopists". In: *International Eye Science* 18.7 (2018), pp. 1180–1183. doi: 10.3980/j.issn.1672-5123.2018.7.03.

[200] M. H. Rashid, M. A. Stevenson, S. Waenga, G. Mirams, A. J. D. Campbell, J. L. Vaughan, and A. Jabbar. "Comparison of McMaster and FECPAK G2 methods for counting nematode eggs in the faeces of alpacas". In: *Parasit. Vectors* 11.1 (2018), p. 278. doi: 10.1186/s13071-018-2861-1.

[201] J. P. Raynaud, J. C. Leroy, M. Virat, and J. A. Nicolas. "A polyvalent egg count technique by dilution and sedimentation in water, flotation in a high sd solution (DSF) and counting in Mac Master slide. Note 1-Interest, justification and description". In: *Rev. Med. Veterinaire* (1979).

[202] R. Redondo, G. Bueno, J. C. Valdiviezo, R. Nava, G. Cristóbal, O. Déniz, M. García-Rojo, J. Salido, M. d. M. Fernández, J. Vidal, and B. Escalante-Ramírez. "Autofocus evaluation for brightfield microscopy pathology". In: *Journal of Biomedical Optics* 17.3 (2012), pp. 036008–036008. doi: 10.1117/1.JBO.17.3.036008.

[203] G. Reinheimer. "Arrangement for automatically focussing an optical instrument". Pat. US3721827A. 1973.

[204] V. Renjith, R. Yesodharan, J. A. Noronha, E. Ladd, and A. George. “Qualitative Methods in Health Care Research”. In: *International Journal of Preventive Medicine* 12 (Feb. 2021), p. 20. doi: 10.4103/ijpvm.IJPVM_321_19.

[205] F. Richards Jr, J. Sullivan, E. Ruiz-Tiben, M. Eberhard, and H. Bishop. “Effect of praziquantel on the eggs of Schistosoma mansoni, with a note on the implications for managing central nervous system schistosomiasis”. In: *Annals of Tropical Medicine and Parasitology* 83.5 (1989), pp. 465–472. doi: 10.1080/00034983.1989.11812373.

[206] M. Roder, L. A. Passos, L. C. F. Ribeiro, B. C. Benato, A. X. Falcão, and J. P. Papa. “Intestinal Parasites Classification Using Deep Belief Networks”. In: *International Conference on Artificial Intelligence and Soft Computing*. Vol. 12415. Springer. Zakopane, Poland, 2020, pp. 242–251. doi: 10.1007/978-3-030-61401-0_23.

[207] O. Ronneberger, P. Fischer, and T. Brox. “U-net: convolutional networks for biomedical image segmentation”. In: *Medical Image Computing and Computer-Assisted Intervention – MICCAI 2015*. Vol. 9351. Munich, Germany, 2015, pp. 234–241. doi: 10.1007/978-3-319-24574-4_28.

[208] W. B. Rowan and A. L. Gram. “Quantitative recovery of helminth eggs from relatively large samples of feces and sewage”. In: *J. Parasitol.* 45.6 (1959), pp. 615–622.

[209] L. S. Ritchie. “An ether sedimentation technique for routine stool examinations”. In: *Bull. U. S. Army Med. Dep.* 8.4 (1948).

[210] L. S. Ritchie and L. A. Berrios-Duran. “A simple procedure for recovering schistosome eggs in mass from tissues”. In: *J. Parasitol.* 47.3 (1961), pp. 363–365.

[211] Y. Rivenson, Z. Göröcs, H. Günaydin, Y. Zhang, H. Wang, and A. Ozcan. “Deep learning microscopy”. In: *Optica* 4.11 (2017), pp. 1437–1443. doi: 10.1364/OPTICA.4.001437.

[212] M. J. Russell and T. S. Douglas. “Evaluation of autofocus algorithms for tuberculosis microscopy”. In: *29th Annual International Conference of the IEEE Engineering in Medicine and Biology Society*. Lyon, France, 2007, pp. 3489–3492. doi: 10.1109/IEMBS.2007.4353082.

[213] M. A. Saeed and A. Jabbar. “Smart diagnosis of parasitic diseases by use of smartphones”. In: *Journal of Clinical Microbiology* 56.1 (2018), e01469–17. doi: 10.1128/JCM.01469-17.

[214] G. Sengul. “Classification of parasite egg cells using gray level cooccurence matrix and kNN”. In: *Biomedical Research* 27.3 (2016), pp. 829–834.

[215] S. Shenoy, A. K. Rajan, M. Rashid, V. P. Chandran, P. G. Poojari, V. Kunhikatta, D. Acharya, S. Nair, M. Varma, and G. Thunga. “Artificial intelligence in differentiating tropical infections: A step ahead”. In: *PLoS Neglected Tropical Diseases* 16.6 (2022), e0010455. doi: 10.1371/journal.pntd.0010455.

[216] J. S. Silfies, E. G. Lieser, S. A. Schwartz, and M. W. Davidson. *Nikon Perfect Focus System (PFS)*. 2024. url: https://www.microscopyu.com/tutorials/the-nikon-perfect-focus-system-pfs (visited on 08/04/2024).

[217] A. Silumbwe, J. M. Zulu, H. Halwindi, C. Jacobs, J. Zgambo, R. Dambe, M. Chola, G. Chongwe, and C. Michelo. “A systematic review of factors that shape implementation of mass drug administration for lymphatic filariasis in sub-Saharan Africa”. In: *BMC Public Health* 17.1 (2017), p. 484. doi: 10.1186/s12889-017-4414-5.

[218] V. Silva-Moraes, L. M. Shollenberger, L. M. V. Siqueira, W. Castro-Borges, D. A. Harn, R. F. Q. E. Grenfell, A. L. T. Rabello, and P. M. Z. Coelho. “Diagnosis of Schistosoma mansoni infections: what are the choices in Brazilian low-endemic areas?” In: *Mem. Inst. Oswaldo Cruz* 114 (2019), e180478. doi: 10.1590/0074-02760180478.

[219] L. Silvestri, M. C. Müllenbroich, I. Costantini, A. P. D. Giovanna, L. Sacconi, and F. S. Pavone. *RAPID: Real-time image-based autofocus for all wide-field optical microscopy systems*. preprint. 2017. doi: 10.1101/170555. bioRxiv: 170555.

[220] Sithu3. *PyTorch-ONNX-TFLite*. GitHub repository. 2021. url: https://github.com/sithu31296/PyTorch-ONNX-TFLite (visited on 08/04/2023).

[221] M. Sluiter, A. Onasanya, O. Oladepo, J. van Engelen, M. Keshinro, and T. Agbana. “Target product profiles for devices to diagnose urinary schistosomiasis in Nigeria”. In: *2020 IEEE Global Humanitarian Technology Conference (GHTC)*. Seattle, WA, USA, 2020, pp. 1–8. doi: 10.1109/GHTC46280.2020.9342953.

[222] F. A. Soares, A. D. N. Benitez, B. M. D. Santos, S. H. N. Loiola, S. L. Rosa, W. B. Nagata, S. V. Inácio, C. T. N. Suzuki, K. D. S. Bresciani, A. X. Falcão, and J. F. Gomes. “A historical review of the techniques of recovery of parasites for their detection in human stools”. In: *Rev. Soc. Bras. Med. Trop.* 53 (2020). doi: 10.1590/0037-8682-0535-2019.

[223] I. Söderberg, B. Calissendorff, S. Elofsson, B. Knave, and K. G. Nyman. “Investigation of visual strain experienced by microscope operators at an electronics plant”. In: *Applied Ergonomics* 14.4 (1983), pp. 297–305. doi: 10.1016/0003-6870(83)90010-8.

[224] A. A. Souza, C. Ducker, D. Argaw, J. D. King, A. W. Solomon, M. A. Biamonte, R. N. Coler, I. Cruz, V. Lejon, B. Levecke, F. K. Marchini, M. Marks, P. Millet, S. M. Njenga, R. Noordin, R. Paulussen, E. Sreekumar, and P. J. Lammie. "Diagnostics and the neglected tropical diseases roadmap: setting the agenda for 2030". In: *Transactions of the Royal Society of Tropical Medicine and Hygiene* 115.2 (2021), pp. 129–135. doi: 10.1093/trstmh/traa118.

[225] S. J. Sowerby, J. A. Crump, M. C. Johnstone, K. L. Krause, and P. C. Hill. "Smartphone microscopy of parasite eggs accumulated into a single field of view". In: *The American Journal of Tropical Medicine and Hygiene* 94.1 (2016), pp. 227–230. doi: 10.4269/ajtmh.15-0427.

[226] P. Steinmann, J. Keiser, R. Bos, M. Tanner, and J. Utzinger. "Schistosomiasis and water resources development: systematic review, meta-analysis, and estimates of people at risk". In: *The Lancet infectious diseases* 6.7 (2006), pp. 411–425. doi: 10.1016/S1473-3099(06)70521-7.

[227] J. R. Stothard, N. B. Kabatereine, E. M. Tukahebwa, F. Kazibwe, W. Mathieson, J. P. Webster, and A. Fenwick. "Field evaluation of the Meade Readiview handheld microscope for diagnosis of intestinal schistosomiasis in Ugandan school children". In: *Am. J. Trop. Med. Hyg.* 73.5 (2005), pp. 949–955. doi: 10.4269/ajtmh.2005.73.949.

[228] J. R. Stothard, B. Nabatte, J. C. Sousa-Figueiredo, and N. B. Kabatereine. "Towards malaria microscopy at the point-of-contact: an assessment of the diagnostic performance of the Newton Nm1 microscope in Uganda". In: *Parasitology* 141.14 (2014), p. 1819. doi: 10.1017/S0031182014000833.

[229] L. J. Stuyver and B. Levecke. "The role of diagnostic technologies to measure progress toward WHO 2030 targets for soil-transmitted helminth control programs". In: *PLoS Neglected Tropical Diseases* 15.6 (2021). doi: 10.1371/journal.pntd.0009422.

[230] S. Sukas, B. Van Dorst, A. Kryj, O. Lagatie, W. De Malsche, and L. J. Stuyver. "Development of a Lab-on-a-Disk Platform with Digital Imaging for Identification and Counting of Parasite Eggs in Human and Animal Stool". In: *Micromachines* 10.12 (2019), p. 852. doi: 10.3390/mi10120852.

[231] C. T. Suzuki, J. F. Gomes, A. X. Falcao, J. P. Papa, and S. Hoshino-Shimizu. "Automatic segmentation and classification of human intestinal parasites from microscopy images". In: *IEEE Trans. Biomed. Eng.* 60.3 (2012), pp. 803–812. doi: 10.1109/TBME.2012.2187204.

[232] N. A. Switz, M. V. D'Ambrosio, and D. A. Fletcher. "Low-cost mobile phone microscopy with a reversed mobile phone camera lens". In: *PLoS ONE* 9.5 (2014), e95330. doi: 10.1371/journal.pone.0095330.

[233] M. Tan, R. Pang, and Q. V. Le. "EfficientDet: Scalable and Efficient Object Detection". In: *Proceedings of the IEEE/CVF Conference on Computer Vision and Pattern Recognition (CVPR)*. Seattle, WA, USA, 2020, pp. 10781–10790. doi: 10.1109/CVPR42600.2020.01079.

[234] B. S. Tchinda, M. Noubom, D. Tchiotsop, V. Louis-Dorr, and D. Wolf. "Towards an automated medical diagnosis system for intestinal parasitosis". In: *Inform. Med. Unlocked* 13 (2018), pp. 101–111. doi: 10.1016/j.imu.2019.100238.

[235] W. Telemann. "Eine methode zur erleichterung der auffindung von parasiteneiern in den faeces". In: *DMW-Dtsch. Med. Wochenschr.* 34.35 (1908), pp. 1510–1511. doi: 10.1055/s-0028-1135692.

[236] R. Tello, A. Terashima, L. A. Marcos, J. Machicado, M. Canales, and E. Gotuzzo. "Highly effective and inexpensive parasitological technique for diagnosis of intestinal parasites in developing countries: spontaneous sedimentation technique in tube". In: *Int J Infect Dis* 16.6 (2012), e414–e416. doi: 10.1016/j.ijid.2011.12.017.

[237] S. A. L. Thétiot-Laurent, J. Boissier, A. Robert, and B. Meunier. "Schistosomiasis Chemotherapy". In: *Angewandte Chemie International Edition* 52.31 (2013), pp. 7936–7956. doi: 10.1002/anie.201208390.

[238] B. Tilahun, K. D. Gashu, Z. A. Mekonnen, B. F. Endehabtu, and D. A. Angaw. "Mapping the role of digital health technologies in the case detection, management, and treatment outcomes of neglected tropical diseases: a scoping review". In: *Tropical Medicine and Health* 49 (2021), pp. 1–10. doi: 10.1186/s41182-020-00285-7.

[239] H. R. Tizhoosh and L. Pantanowitz. "Artificial intelligence and digital pathology: Challenges and opportunities". In: *Journal of Pathology Informatics* 9.1 (2018), p. 38. doi: 10.4103/jpi.jpi_53_18.

[240] C. J. Tuijn, B. J. Hoefman, H. Van Beijma, L. Oskam, and N. Chevrollier. "Data and image transfer using mobile phones to strengthen microscopy-based diagnostic services in low and middle income country laboratories". In: *PLoS ONE* 6.12 (2011), e28348. doi: 10.1371/journal.pone.0028348.

[241] A. Umar, M. B. Muazu, U. D. Aliyu, U. Musa, Z. Haruna, and P. O. Oyibo. “Position and trajectory tracking control for the ball and plate system using mixed sensitivity problem”. In: *Covenant Journal of Informatics and Communication Technology* 6.1 (2018).

[242] UNAIDS. *No more neglect—female genital schistosomiasis and HIV—integrating sexual and reproductive health interventions to improve women’s lives*. 2019. url: https://www.unaids.org/en/resources/documents/2019/female_genital_schistosomiasis_and_hiv (visited on 10/11/2023).

[243] J. Utzinger, G. Raso, S. Brooker, D. De Savigny, M. Tanner, N. Ornbjerg, B. H. Singer, and E. K. N’goran. “Schistosomiasis and neglected tropical diseases: towards integrated and sustainable control and a word of caution”. In: *Parasitology* 136.13 (2009), pp. 1859–1874. doi: 10.1017/S0031182009991600.

[244] J. Utzinger, S. L. Becker, L. Van Lieshout, G. J. Van Dam, and S. Knopp. “New diagnostic tools in schistosomiasis”. In: *Clinical microbiology and infection* 21.6 (2015), pp. 529–542. doi: 10.1016/j.cmi.2015.03.014.

[245] G. Y. Van, A. Onasanya, J. van Engelen, O. Oladepo, and J. C. Diehl. “Improving Access to Diagnostics for Schistosomiasis Case Management in Oyo State Nigeria: Barriers and Opportunities”. In: *Diagnostics* 10.5 (2020), p. 328. doi: 10.3390/diagnostics1005032

[246] A. Vasiman, J. R. Stothard, and I. I. Bogoch. “Mobile phone devices and handheld microscopes as diagnostic platforms for malaria and neglected tropical diseases (NTDs) in low-resource settings: a systematic review, historical perspective and future outlook”. In: *Advances in Parasitology* 103 (2019), pp. 151–173. doi: 10.1016/bs.apar.2018.09.001.

[247] N. Q. Viet, D. T. ThanhTuyen, and T. H. Hoang. “Parasite worm egg automatic detection in microscopy stool image based on Faster R-CNN”. In: *Proceedings of the 3rd International Conference on Machine Learning and Soft Computing*. New York, NY, USA: Association for Computing Machinery, 2019, pp. 197–202. isbn: 978-1-4503-6612-0. doi: 10.1145/3310986.3311014.

[248] N. V. Vinkeles Melchers, G. J. van Dam, D. Shaproski, A. I. Kahama, E. A. Brienen, B. J. Vennervald, and L. van Lieshout. “Diagnostic performance of Schistosoma real-time PCR in urine samples from Kenyan children infected with Schistosoma haematobium: day-to-day variation and follow-up after praziquantel treatment”. In: *PLoS Neglected Tropical Diseases* 8.4 (2014), e2807. doi: 10.1371/journal.pntd.0002807.

[249] T. Virág, A. László, B. Molnár, A. Tagscherer, and V. S. Varga. “Focusing method for the high-speed digitalisation of microscope slides and slide displacing device, focusing optics, and optical rangefinder”. Pat. US7663078B2. 2010.

[250] T. Vos, S. S. Lim, C. Abbafati, K. M. Abbas, M. Abbasi, M. Abbasifard, M. Abbasi-Kangevari, H. Abbastabar, and F. Abd-Allah. “Global burden of 369 diseases and injuries in 204 countries and territories, 1990–2019: a systematic analysis for the Global Burden of Disease Study 2019”. In: *The Lancet* 396.10285 (2020), pp. 1204–1222. doi: 10.1016/S0140-6736(20)30925-9.

[251] P. Ward, P. Dahlberg, O. Lagatie, J. Larsson, A. Tynong, J. Vlaminck, M. Zumpe, S. Ame, M. Ayana, V. Khieu, Z. Mekonnen, M. Odiere, T. Yohannes, S. V. Hoecke, B. Levecke, and L. J. Stuyver. “Affordable artificial intelligence-based digital pathology for neglected tropical diseases: A proof-of-concept for the detection of soil-transmitted helminths and Schistosoma mansoni eggs in Kato-Katz stool thick smears”. In: *PLoS neglected tropical diseases* 16.6 (2022), e0010500. doi: 10.1371/journal.pntd.0010500.

[252] P. Ward, T. Yohannes, M. Ayanna, G. Jonsson-Glans, O. Lagatie, M. Zumpe, A. Tynnong, P. Dahlberg, M. Odiere, V. Khieu, Z. Mekonnen, M. Odiere, T. Yohannes, S. V. Hoecke, B. Levecke, and L. J. Stuyver. *AI4NTD KK2.0 P1.5 STH & SCHm Dataset*. Kaggle repository. 2022. doi: 10.34740/KAGGLE/DS/1896823.

[253] P. Ward, B. Levecke, and S. Ajjampur. “Harnessing artificial intelligence microscopy to improve diagnostics for soil-transmitted helminthiasis and schistosomiasis: a review of recent advances and future pathways”. In: *Current Opinion in Infectious Diseases* 37.5 (2024), pp. 376–384. doi: 10.1097/QCO.0000000000001048.

[254] X. Wang, L. Liu, X. Du, J. Zhang, J. Liu, G. Ni, R. Hao, and Y. Liu. “Leukocyte recognition in human fecal samples using texture features”. In: *J. Opt. Soc. Am. A* 35.11 (2018), pp. 1941–1948. doi: 10.1364/JOSAA.35.001941.

[255] W. Wang, M. Si, F. Chen, H. Liu, and X. Jiang. “Study on recognition method of label-free red and white cell using fecal microscopic image”. In: *Proceedings of the 2018 6th International Conference on Bioinformatics and Computational Biology*. Chengdu, China, 2018, pp. 95–100. doi: 10.1145/3194480.3198909.

[256] J. P. Webster, D. H. Molyneux, P. J. Hotez, and A. Fenwick. “The contribution of mass drug administration to global health: past, present and future”. In: *Phil. Trans. R. Soc. B* 369.1645 (2014), p. 20130434. doi: 10.1098/rstb.2013.0434.

[257] K. G. Weerakoon, G. N. Gobert, P. Cai, and D. P. McManus. “Advances in the diagnosis of human schistosomiasis”. In: *Clin Microbiol Rev* 28.4 (2015), pp. 939–967. doi: 10.1128/CMR.00137-14.

[258] K. G. Weerakoon, C. A. Gordon, and D. P. McManus. “DNA diagnostics for schistosomiasis control”. In: *Trop Med Infect Dis* 3.3 (2018), pp. 1–20. doi: 10.3390/tropicalmed3030081.

[259] M. J. van der Werf, S. J. de Vlas, S. Brooker, C. W. Looman, N. J. Nagelkerke, J. D. Habbema, and D. Engels. “Quantification of clinical morbidity associated with schistosome infection in sub-Saharan Africa”. In: *Acta Tropica* 86.2-3 (2003), pp. 125–139. doi: 10.1016/s0001-706x(03)00029-9.

[260] H. V. Whitlock. “Some modifications of the McMaster helminth egg-counting technique and apparatus”. In: *J. Counc. Sci. Ind. Res. Aust.* 21.3 (1948), pp. 177–180.

[261] World Health Organization. *Prevention and control of schistosomiasis and soil-transmitted helminthiasis: report of a WHO expert committee*. World Health Organization, 2002. isbn: 9241209127. url: https://iris.who.int/handle/10665/42588.

[262] World Health Organization. *Accelerating work to overcome the global impact of neglected tropical diseases: a roadmap for implementation: executive summary*. World Health Organization, 2012. url: https://iris.who.int/handle/10665/338712.

[263] World Health Organization. *Ending the Neglect to Attain the Sustainable Development Goals—A Road Map for Neglected Tropical Diseases 2021–2030*. World Health Organization, 2020. isbn: 9789240010352. url: https://iris.who.int/handle/10665/338565.

[264] World Health Organization. *Global health estimates: leading causes of death*. 2020. url: https://www.who.int/data/gho/data/themes/mortality-and-global-health-estimates/ghe-leading-causes-of-death (visited on 10/11/2023).

[265] World Health Organization. *2030 targets for soil-transmitted helminthiases control programmes*. World Health Organization, 2020. isbn: 9789240000315. url: https://iris.who.int/handle/10665/330611.

[266] World Health Organization. *WHO | World Health Organization*. 2020. url: http://www.who.int/neglected_diseases/diseases/en/ (visited on 04/23/2020).

[267] World Health Organization. *Report of the first meeting of the WHO Diagnostic Technical Advisory Group for Neglected Tropical Diseases Geneva, 30-31 October 2019*. World Health Organization, 2020. isbn: 9789240003590. url: https://iris.who.int/handle/10665/331954.

[268] World Health Organization. *Diagnostic target product profiles for monitoring, evaluation and surveillance of schistosomiasis control programmes*. World Health Organization, 2021. isbn: 9789240031104. url: https://iris.who.int/handle/10665/344813.

[269] World Health Organization. *Diagnostic target product profile for monitoring and evaluation of soil-transmitted helminth control programmes*. World Health Organization, 2021. isbn: 9789240031227. url: https://iris.who.int/handle/10665/342539.

[270] World Health Organization. *Ending the Neglect to Attain the Sustainable Development Goals: A Global Strategy on Water, Sanitation and Hygiene to Combat Neglected Tropical Diseases, 2021–2030*. World Health Organization, 2021. isbn: 9789240022782. url: https://iris.who.int/handle/10665/340240.

[271] World Health Organization. *Public consultation: Target Product Profiles for diagnostic tests to meet Schistosomiasis and soil-transmitted Helminth programme needs*. 2021. url: https://www.who.int/news-room/articles-detail/public-consultation-target-product-profiles-for-diagnostic-tests-to-meet-schistosomiasis-and-soil-transmitted-helminth-programme-needs (visited on 03/17/2022).

[272] World Health Organization. *WHO guideline on control and elimination of human schistosomiasis*. World Health Organization, 2022. isbn: 9789240041608. url: https://iris.who.int/handle/10665/351856.

[273] World Health Organization. “34th meeting of the International Task Force for Disease Eradication, 34ˆè reunion du Groupe spécial international pour l’éradication des maladies, 19–20 Septembre 2022”. In: *Weekly Epidemiological Record* 98.04 (2022), pp. 41–50. url: https://iris.who.int/handle/10665/365721.

[274] World Health Organization. “Schistosomiasis and soil-transmitted helminthiases: progress report, 2021”. In: *Weekly Epidemiological Record* 97.48 (2022), pp. 621–632. url: https://www.who.int/publications/i/item/who-wer9748-621-632.

[275] World Health Organization. *Soil-transmitted helminth infections*. Aug. 2023. url: https://www.who.int/news-room/fact-sheets/detail/soil-transmitted-helminth-infections (visited on 09/26/2024).

[276] World Health Organisation. *Strengthening diagnostic capacity*. 2023. url: https://www.eliminateschisto.org/news-events/news/world-health-assembly-resolution-on-strengthening-diagnostics-capacity (visited on 07/17/2023).

[277] World Health Organisation. *Neglected tropical diseases – GLOBAL*. 2024. url: https://www.who.int/health-topics/neglected-tropical-diseases#tab=tab_1 (visited on 11/02/2024).

[278] World Health Organisation. *Schistosomiasis*. 2024. url: https://www.who.int/news-room/fact-sheets/detail/schistosomiasis (visited on 09/26/2024).

[279] R. E. Wiegand, W. E. Secor, F. M. Fleming, M. D. French, C. H. King, A. K. Deol, S. P. Montgomery, D. Evans, J. Utzinger, P. Vounatsou, and S. J. de Vlas. "Associations between infection intensity categories and morbidity prevalence in school-age children are much stronger for Schistosoma haematobium than for S. mansoni". In: *PLoS Neglected Tropical Diseases* 15.5 (2021), e0009444. doi: 10.1371/journal.pntd.0009444.

[280] R. E. Wiegand, W. E. Secor, F. M. Fleming, M. D. French, C. H. King, S. P. Montgomery, D. Evans, J. Utzinger, P. Vounatsou, and S. J. de Vlas. "Control and elimination of schistosomiasis as a public health problem: thresholds fail to differentiate schistosomiasis morbidity prevalence in children". In: *Open Forum Infectious Diseases* 8.7 (2021), ofab179. doi: 10.1093/ofid/ofab179.

[281] H. H. Willis. "A simple levitation method for the detection of hookworm ova". In: *Med. J. Aust.* 2.18 (1921). doi: 10.5694/j.1326-5377.1921.tb60654.x.

[282] S. Y. Wu, N. Dugan, and B. M. Hennelly. "Investigation of autofocus algorithms for brightfield microscopy of unstained cells". In: *Proceedings of SPIE – The International Society for Optical Engineering*. Vol. 9131. Brussels, Belgium, 2014, 91310T. doi: 10.1117/12.2051944.

[283] Y. Xiao, Y. Lu, M. Hsieh, J. Liao, and P. K. Wong. "A microfiltration device for urogenital schistosomiasis diagnostics". In: *PLoS ONE* 11.4 (2016), e0154640. doi: 10.1371/journal.pone.0154640.

[284] E. Xie, W. Wang, W. Wang, M. Ding, C. Shen, and P. Luo. “Segmenting transparent objects in the wild”. In: *Computer Vision – ECCV 2020*. Vol. 12358. Glasgow, United Kingdom, 2020, pp. 696–711. doi: 10.1007/978-3-030-58601-0_41.

[285] Y. S. Yang, D. K. Park, H. C. Kim, M. H. Choi, and J. Y. Chai. “Automatic identification of human helminth eggs on microscopic fecal specimens using digital image processing and an artificial neural network”. In: *IEEE Transactions on Biomedical Engineering* 48.6 (2001), pp. 718–730. doi: 10.1109/10.923789.

[286] A. Yang, N. Bakhtari, L. Langdon-Embry, E. Redwood, S. G. Lapierre, P. Rakotomanga, A. Rafalimanantsoa, J. D. D. Santos, I. Vigan-Womas, A. M. Knoblauch, and L. A. Marcos. “Kankanet: An artificial neural network-based object detection smartphone application and mobile microscope as a point-of-care diagnostic aid for soil-transmitted helminthiases”. In: *PLoS neglected tropical diseases* 13.8 (2019), e0007577. doi: 10.1371/journal.pntd.0007577.

[287] C. Yohana, J. S. Bakuza, S. M. Kinung, B. A. Nyundo, and P. F. Rambau. “The trend of schistosomiasis related bladder cancer in the lake zone, Tanzania: a retrospective review over 10 years period”. In: *Infect Agent Cancer* 18.10 (2023), pp. 1–10. doi: 10.1186/s13027-023-00491-1.

[288] K. H. Young, S. L. Bullock, D. M. Melvin, and C. L. Spruill. “Ethyl acetate as a substitute for diethyl ether in the formalin-ether sedimentation technique”. In: *J. Clin. Microbiol.* 10.6 (1979), pp. 852–853. doi: 10.1128/jcm.10.6.852-853.1979.

[289] J. Zhang, Y. Lin, Y. Liu, Z. Li, Z. Li, S. Hu, Z. Liu, D. Lin, and Z. Wu. “Cascaded-Automatic Segmentation for Schistosoma japonicum eggs in images of fecal samples”. In: *Comput. Biol. Med.* 52 (2014), pp. 18–27. doi: 10.1016/j.compbiomed.2014.05.012.

[290] H. Zhu, S. O. Isikman, O. Mudanyali, A. Greenbaum, and A. Ozcan. “Optical imaging techniques for point-of-care diagnostics”. In: *Lab on a Chip* 13.1 (2013), pp. 51–67. doi: 10.1039/c2lc40864c.

ACKNOWLEDGEMENTS

I am deeply grateful to everyone who has supported me throughout the journey of completing this PhD thesis. First and foremost, I would like to extend my sincere appreciation to my supervisors, Prof. Gleb Vdovine, Prof. J.C. Diehl, Prof. Wellington Oyibo, and Dr. Tope Agbana. Your invaluable guidance, constructive feedback, and continuous encouragement have been instrumental in shaping both my research and academic growth. Your expertise and insights have had a profound impact on my development as a scholar.

I also wish to express my heartfelt thanks to the INSPiRED team at Delft University of Technology, University of Lagos, Leiden University Medical Center, University of Ibadan, and the Centre de Recherches Médicales de Lambaréné (CERMEL). The collaboration, stimulating discussions, and technical support provided by these institutions greatly enriched my research and learning experience. A special thank you to Prof. Lisette van Lieshout, Dr. Michel Bengtson, and Dr. Pytsje Hoekstra for their mentorship, which was critical in the development of the Schistoscope and other key aspects of my work. I would also like to thank my fellow PhD candidates, Dr. Brice Meulah and Dr. Adeola Onasanya, for their camaraderie and support throughout this journey.

To the research participants, field collaborators, and healthcare professionals involved in the validation studies, your contributions were essential to the success of this project. I am also profoundly grateful to the Neglected Tropical Disease team from the Federal Ministry of Health, Abuja, and the Federal Capital Territory Administration (FCTA) Public Health Department, Abuja, Nigeria, as well as the administrative and technical staff from CERMEL in Gabon, who provided the infrastructure and support necessary for the completion of this research.

I would like to acknowledge the administrative support provided by Erica and Francy at DCSC, and Mascha from the 3me Graduate School. Their assistance has been invaluable throughout my PhD journey.

Many thanks to the Delft Global Initiative team and my fellow Delft Global fellows for their guidance and support. I am also grateful to G-Young, Satya, and Karl for their friendship and support during my time in Delft. I would also like to thank my line manager at Cardiff University, Prof. Emiliano Spezi, as well as my colleagues in the LIDA and IPOCH research groups for their love and encouragement.

I owe an immense debt of gratitude to my family for their unwavering love, support, and encouragement. To my parents, Engr. and Mrs.

J.E. Oyibo, thank you for your constant care, prayers, and belief in me. To my wife, Seun, your patience, understanding, and faith in me have been an unshakeable source of strength. To my siblings — Victory, Onos, Success, and Knightess — thank you for your constant support and inspiration. To my mother-in-law, Dr. Febisola Owolabi, your support and encouragement have meant the world to me.

Finally, I would like to acknowledge the financial support from the Dutch Research Council (NWO-WOTRO), which made this research possible. This thesis is a testament to the collective efforts of all who have contributed, both directly and indirectly, to my academic and personal growth. Thank you all.

CURRICULUM VITæ

PERSONAL STATEMENT

As a dedicated Artificial Intelligence researcher, I am passionate about harnessing technology to tackle critical global health challenges. My career is defined by a strong commitment to developing innovative diagnostic tools—particularly in medical image processing, radiomics, and automated diagnostic systems—to enhance healthcare accessibility and diagnostic accuracy across both resource-limited and advanced clinical settings.

Driven by curiosity and a desire to create meaningful impact, my work focuses on integrating computer vision, radiomics, and AI with medical technologies. I thrive in interdisciplinary environments, collaborating with clinicians, public health institutions, engineering teams, and government agencies. My overarching goal is to bridge the gap between advanced technological innovation and real-world healthcare needs, contributing to solutions that save lives and improve health outcomes on a global scale.

KEY RESEARCH AND INNOVATION

As a Research Associate at Cardiff University within the Life Imaging and Data Analytics Group, my work centres on developing advanced AI-driven tools to support cancer diagnosis and treatment planning. Currently, I am working on a Cancer Research UK-funded project focused on deriving novel, non-invasive radiomic and AI-based classifiers to characterise the molecular behaviour of rectal cancer and predict its response to radiotherapy. I am applying machine learning techniques, to build predictive radiomics signatures associated with clinical outcomes. The ultimate aim is to deliver novel, less invasive diagnostic tools that better predict radiotherapy responses, particularly in rectal cancer, thus improving personalised treatment planning.

One of my recent projects addressed the auto-segmentation of Gross Tumour Volume (GTV) in Head and Neck Cancer (HNC). This work tackled the limitations of manual contouring in radiotherapy planning by improving accuracy, consistency, and efficiency. We developed a novel approach to automatically segment GTV from PET/CT images and evaluated its performance against both expert-defined contours and ATLAAS—a machine learning model trained on simulated and phantom-based PET

images. The method offers promising advancements for precision in radiotherapy.

In parallel, I led the development and validation of multimodality quantitative medical image analysis software for oncology. A key achievement was the creation of the SPAARC-Hero node, which integrates IBSI-compliant radiomics into the Hero Imaging platform. This tool enhances reproducibility in radiomics research and improves accessibility by removing the need for programming expertise. The SPAARC-Hero node was featured at the ESTRO 2024 Conference in Glasgow, highlighting its clinical relevance and impact.

Prior to this, during my PhD at Delft University of Technology, I spearheaded research on AI-based digital microscopes for the detection of parasitic diseases in Sub-Saharan Africa. This work aimed to address diagnostic gaps in low-resource settings by using AI to automate parasite detection, supporting more effective disease surveillance and contributing to global health equity.

TECHNICAL EXPERTISE

My technical proficiency spans a broad spectrum of skills critical to the development of intelligent diagnostic tools:

- **Computer Vision & Machine Learning:** Advanced algorithms for image segmentation, object recognition, and predictive modelling.
- **Radiomics & Medical Image Processing:** Development of non-invasive classifiers and predictive radiomics signatures to improve treatment outcomes.
- **Optimization Algorithms:** Enhancing the efficiency and accuracy of diagnostic systems.
- **Programming Languages:** Proficient in Python, MATLAB, R, and C++.
- **Medical Imaging Software:** Extensive hands-on experience with MIM, Velocity, and the Hero Imaging platform, coupled with in-depth knowledge of DICOM standards for efficient medical image management and analysis.
- **CAD Design Tools:** Skilled in SolidWorks and Fusion 360 for device design.

LEADERSHIP AND COLLABORATION

Collaboration has been at the heart of my professional journey. I have successfully coordinated multidisciplinary teams, fostering partnerships

between academia, healthcare professionals, and international organisations. My role often involves translating complex technical concepts into actionable insights for diverse audiences, ensuring that technological advancements are both innovative and practically applicable. Additionally, mentorship from leading experts at both Cardiff and Delft has profoundly shaped my career, reinforcing my commitment to fostering a culture of scientific excellence and collaboration.

EDUCATION AND CONTINUOUS DEVELOPMENT

My academic path reflects a strong foundation in control engineering and systems science, culminating in a PhD in Systems and Control Engineering from Delft University of Technology. I also hold a Master's and Bachelor's degree in Control and Electrical Engineering, respectively, from Ahmadu Bello University, Zaria. In pursuit of continuous learning, I have completed certifications in data science and advanced statistical analysis. Recently, I completed the Cardiff Education Fellowship Academy and am on the path to obtaining the Associate Fellowship of the Higher Education Academy (AFHEA). This recognition highlights my commitment to professional growth and academic excellence.

AWARDS AND GRANTS

In 2021, I received a €2,400 Delft Global Support Fund grant to support the field validation of the Schistoscope for the diagnosis of urinary schistosomiasis in Nigeria. In 2024, I was endorsed by UK Research and Innovation (UKRI) under the Global Talent Visa route, in recognition of my research leadership and potential to advance the UK's scientific community in AI for medical imaging. In 2025, I was awarded an EPSRC Impact Acceleration Account (IAA) grant of £18,773 to lead the project "Accelerating Innovation and Expanding Worldwide the Footprint of Cardiff University SPAARC Radiomics for Medical Image Analysis." This initiative supports the clinical and commercial translation of SPAARC radiomics tools, reinforcing Cardiff University's global influence in AI-enabled medical diagnostics.

FUTURE VISION

I intend to leverage my skills and experience to advance global healthcare priorities, including early cancer detection, personalised medicine, and enhanced diagnostic accuracy. By fostering collaborations with academic institutions, NGOs, and industry partners, I aim to bridge the gap between cutting-edge research and real-world clinical applications. My goal is to drive healthcare innovation that delivers meaningful impact across both developing and developed regions.

LIST OF PUBLICATIONS

16. P. Oyibo, K. W. Kim, S. Hargreaves, P. Wheeler, O. Woodley, T. Rackley, M. Evans, and E. Spezi. "3D DeepLab-based automated GTV segmentation in head and neck cancer using PET/CT imaging". In: *Radiotherapy and Oncology* 206.1 (2025), S2536–S2538. doi: 10.1016/S0167-8140(25)01892-4

15. P. Oyibo, B. Meulah, T. Agbana, L. van Lieshout, W. Oyibo, G. Vdovin, and J. C. Diehl. "Deep learning-based automated detection and multiclass classification of soil-transmitted helminths and Schistosoma mansoni eggs in fecal smear images". In: *Scientific Reports* 15.1 (2025), p. 21495. doi: 10.1038/s41598-025-02755-9

14. P. Oyibo, P. Brynolfsson, and E. Spezi. "Integrating Radiomic Image Analysis in the Hero Imaging Platform". In: *Proceedings of the Cardiff University School of Engineering Research Conference 2024*. Cardiff, United Kingdom: Cardiff University Press, 2024. doi: 10.18573/conf3.g

13. P. Oyibo, T. Agbana, L. van Lieshout, W. Oyibo, J. C. Diehl, and G. Vdovine. "An automated slide scanning system for membrane filter imaging in diagnosis of urogenital schistosomiasis". In: *Journal of Microscopy* 294.1 (2024), pp. 52–61. doi: 10.1111/jmi.13269

12. B. Meulah, P. Oyibo, P. T. Hoekstra, P. A. N. Moure, M. N. Maloum, R. A. Laclong-Lontchi, Y. J. Honkpehedji, M. Bengtson, C. Hokke, P. L. A. M. Corstjens, T. Agbana, J. C. Diehl, A. A. Adegnika, and L. v. Lieshout. "Validation of artificial intelligence-based digital microscopy for automated detection of Schistosoma haematobium eggs in urine in Gabon". In: *PLoS neglected tropical diseases* 18.2 (2024). doi: 10.1371/journal.pntd.0011967

11. P. Oyibo, B. Meulah, M. Bengtson, L. van Lieshout, W. Oyibo, J. C. Diehl, G. Vdovine, and T. Agbana. "Two-stage automated diagnosis framework for urogenital schistosomiasis in microscopy images from low-resource settings". In: *Journal of Medical Imaging* 10.4 (2023), pp. 044005–044005. doi: 10.1117/1.JMI.10.4.044005

10. B. Meulah, P. Oyibo, M. Bengtson, T. Agbana, R. A. L. Lontchi, A. A. Adegnika, W. Oyibo, C. H. Hokke, J. C. Diehl, and L. v. Lieshout. "Performance Evaluation of the Schistoscope 5.0 for (Semi-)automated Digital Detection and Quantification of Schistosoma haematobium Eggs in Urine: A Field-based Study in Nigeria". In: *The American Journal of Tropical Medicine and Hygiene* 107.5 (2022). doi: 10.4269/ajtmh.22-0276

9. M. Bengtson, A. Onasanya, P. Oyibo, B. Meulah, K. T. Samenjo, I. Braakman, W. Oyibo, and J. C. Diehl. “A usability study of an innovative optical device for the diagnosis of schistosomiasis in Nigeria”. In: *2022 IEEE Global Humanitarian Technology Conference (GHTC)*. Santa Clara, CA, USA: IEEE, 2022, pp. 17–22. doi: 10.1109/GHTC55712.2022.9911019

8. P. Oyibo, S. Jujjavarapu, B. Meulah, T. Agbana, I. Braakman, A. van Diepen, M. Bengtson, L. van Lieshout, W. Oyibo, G. Vdovine, and J. C. Diehl. “Schistoscope: An Automated Microscope with Artificial Intelligence for Detection of Schistosoma haematobium Eggs in Resource-Limited Settings”. In: *Micromachines* 13.5 (2022), p. 643. doi: 10.3390/mi13050643

7. J. C. Diehl, P. Oyibo, T. Agbana, S. Jujjavarapu, G. Van, G. Vdovin, and W. Oyibo. “Schistoscope: Smartphone versus Raspberry Pi based low-cost diagnostic device for urinary Schistosomiasis”. In: *Proceedings of the 2020 IEEE Global Humanitarian Technology Conference (GHTC)*. Seattle, WA, USA, 2020, pp. 1–8. doi: 10.1109/GHTC46280.2020.9342871

6. Z. Haruna, M. B. Mu’azu, P. Oyibo, and S. A. Tijani. “Development of an optimal path planning using elite opposition based bat algorithm for a mobile robot”. In: *Yanbu Journal of Engineering and Science* 16.1 (2021), pp. 1–9. doi: doi.org/10.53370/001c.24338

5. I. Abdulwahab, A. A. Olaniyan, U. Musa, and O. Ajayi. “Optimization of a droop controlled micro-grid using grasshopper optimization algorithm”. In: *Zaria J.* 10.1 (2021), p. 65

4. S. Y. Audee, M. B. Muâzu, S. Man-Yahaya, Z. Haruna, A. T. Salawudeen, and P. Oyibo. “Development of a dynamic cuckoo search algorithm”. In: *Covenant Journal of Informatics and Communication Technology* 7.2 (2019)

3. I. B. Oluchi, E. A. Adedokun, M. B. Mua’zu, N. Salifu, and P. Oyibo. “Development of a Nigeria vehicle license plate detection system”. In: *Applications of Modelling and Simulation* 3.3 (2019), pp. 188–195

2. P. O. Oyibo, O. Ajayi, I. Abubakar, M. T. Abdulwahab, and O. A. S. “Development of Power Line Detection Algorithm using Frangi Filter and First-Order Derivative of Gaussian”. In: *Zaria Journal of Electrical Engineering Technology* 8.1 (2019)

1. A. Umar, M. B. Muazu, U. D. Aliyu, U. Musa, Z. Haruna, and P. O. Oyibo. “Position and trajectory tracking control for the ball and plate system using mixed sensitivity problem”. In: *Covenant Journal of Informatics and Communication Technology* 6.1 (2018)

About the Author

Prosper Obaro Oyibo is an Artificial Intelligence researcher and systems engineer with a strong passion for leveraging technology to address global health challenges. He holds a B.Eng. in Electrical Engineering (2014) and an M.Sc. in Control Engineering (2017) from Ahmadu Bello University, Zaria, Nigeria, and is completing his PhD in Systems and Control Engineering at Delft University of Technology in the Netherlands.

During his PhD, Prosper led the development of the ***Schistoscope*** – a low-cost, AI-powered digital microscope designed to automate the detection of schistosomiasis and soil-transmitted helminth infections in resource-limited settings. His work combines deep learning, digital microscopy, embedded systems, and user-centred design, and has been field-tested in Nigeria and Gabon to support disease control and promote health equity.

Prosper currently works as a Research Associate at Cardiff University's Life Imaging and Data Analytics Group, where he focuses on AI-driven radiomics for cancer diagnosis and treatment planning. His research includes developing predictive models for rectal cancer response to radiotherapy and automating tumour segmentation in Head and Neck Cancer using PET/CT imaging.

His innovations have been featured at leading conferences such as ESTRO and supported by prestigious grants, including an EPSRC Impact Acceleration Account award and a UKRI Global Talent endorsement. With a commitment to translational research and interdisciplinary collaboration, Prosper is dedicated to bridging the gap between cutting-edge AI technologies and real-world clinical needs – delivering scalable, impactful solutions for global healthcare.